

# Six new species of *Aspidophorodon* Verma, 1967 (Hemiptera, Aphididae, Aphidinae) from China

Ying Xu<sup>1,3</sup>, Li-Yun Jiang<sup>1</sup>, Jing Chen<sup>1</sup>,  
Bakhtiyor Rustamovich Kholmatov<sup>2</sup>, Ge-Xia Qiao<sup>1,3</sup>

**1** Key Laboratory of Zoological Systematics and Evolution, Institute of Zoology, Chinese Academy of Sciences, No. 1-5 Beichen West Road, Chaoyang District, Beijing 100101, China **2** Institute of Zoology, Academy of Sciences Republic of Uzbekistan, Bagishamol Str., 232b, Tashkent 100053, Uzbekistan **3** College of Life Science, University of Chinese Academy of Sciences, No. 19, Yuquan Road, Shijingshan District, Beijing 100049, China

Corresponding authors: Li-Yun Jiang ([jiangliyun@ioz.ac.cn](mailto:jiangliyun@ioz.ac.cn)), Ge-Xia Qiao ([qiaogx@ioz.ac.cn](mailto:qiaogx@ioz.ac.cn))

Academic editor: Colin Favret | Received 12 November 2021 | Accepted 18 May 2022 | Published 16 June 2022

<http://zoobank.org/27BB738A-103E-4081-BF66-44F645E207A4>

**Citation:** Xu Y, Jiang L-Y, Chen J, Kholmatov BR, Qiao G-X (2022) Six new species of *Aspidophorodon* Verma, 1967 (Hemiptera, Aphididae, Aphidinae) from China. ZooKeys 1106: 1–55. <https://doi.org/10.3897/zookeys.1106.77912>

## Abstract

The genus *Aspidophorodon* Verma is presented, including six new species from China, namely *Aspidophorodon capitatum* Qiao & Xu, **sp. nov.**, *Aspidophorodon longicornutum* Qiao & Xu, **sp. nov.**, *Aspidophorodon reticulatum* Qiao & Xu, **sp. nov.**, *Aspidophorodon furcatum* Qiao & Xu, **sp. nov.**, *Aspidophorodon longirostre* Qiao & Xu, **sp. nov.**, and *Aspidophorodon obtusirostre* Qiao & Xu, **sp. nov.** *Aspidophorodon cornuatum* Qiao, 2015 is considered as a junior synonym of *Aspidophorodon longituberculatum* (Zhang, Zhong & Zhang, 1992), **syn. nov.** Two species, *Aspidophorodon harvense* Verma and *Aspidophorodon indicum* (David, Rajasingh & Narayanan) are recorded for the first time in China. The genus is mainly distributed in East Asia and is represented by 15 species in the world, of which 12 are found in China. Keys to the species of *Aspidophorodon* are given.

## Keywords

DNA barcode, key, new record, new synonym, NJ tree, *Salix*

## Table of contents

Introduction.....	2
Materials and methods .....	3
Morphological description .....	3
DNA barcoding .....	3
Specimen depositories .....	4
Taxonomy .....	4
<i>Aspidophorodon</i> Verma, 1967 .....	4
Subgenus <i>Aspidophorodon</i> Verma, 1967 .....	5
Key to the species of <i>Aspidophorodon</i> ( <i>Aspidophorodon</i> ) (based on apterous viviparous females) .....	6
<i>Aspidophorodon capitatum</i> Qiao & Xu, sp. nov. ....	7
<i>Aspidophorodon harvense</i> Verma, 1967 .....	14
<i>Aspidophorodon longicornutum</i> Qiao & Xu, sp. nov. ....	17
<i>Aspidophorodon musaicum</i> Qiao, 2015.....	21
<i>Aspidophorodon obtusum</i> Qiao, 2015 .....	21
<i>Aspidophorodon reticulatum</i> Qiao & Xu, sp. nov. ....	21
<i>Aspidophorodon salicis</i> Miyazaki, 1971 .....	25
Subgenus <i>Eoessigia</i> David, Rajasingh & Narayanan, 1972 .....	26
Key to species of subgenus <i>Eoessigia</i> (based on apterous female viviparous).....	26
<i>Aspidophorodon</i> ( <i>Eoessigia</i> ) <i>furcatum</i> Qiao & Xu, sp. nov. ....	27
<i>Aspidophorodon</i> ( <i>Eoessigia</i> ) <i>indicum</i> (David, Rajasingh & Narayanan, 1972).....	33
<i>Aspidophorodon</i> ( <i>Eoessigia</i> ) <i>longicauda</i> (Richards, 1963) .....	37
<i>Aspidophorodon</i> ( <i>Eoessigia</i> ) <i>longirostre</i> Qiao & Xu, sp. nov. ....	37
<i>Aspidophorodon</i> ( <i>Eoessigia</i> ) <i>longituberculatum</i> (Zhang, Zhong & Zhang, 1992) ....	44
<i>Aspidophorodon</i> ( <i>Eoessigia</i> ) <i>sorbi</i> (Chakrabarti & Maity, 1984).....	46
<i>Aspidophorodon</i> ( <i>Eoessigia</i> ) <i>obtusirostre</i> Qiao & Xu, sp. nov. ....	46
<i>Aspidophorodon</i> ( <i>Eoessigia</i> ) <i>vera</i> Stekolshchikov & Novgorodova, 2010.....	52
DNA barcoding .....	52
Discussion.....	53
Acknowledgements.....	54
References .....	54

## Introduction

*Aspidophorodon* is a genus of Macrosiphini (Hemiptera: Aphididae: Aphidinae) with two subgenera, the nominate subgenus and subgenus *Eoessigia* (Favret 2022), mostly feeding on plants of Salicaceae and Rosaceae (Blackman and Eastop 2006). The taxonomy of *Aspidophorodon* was last revised by Chen et al. (2015) with ten species, namely *A. cornuatum* Qiao, *A. harvense* Verma, *A. musaicum* Qiao, *A. obtusum* Qiao, *A. salicis* Miyazaki, *A. (Eoessigia) indicum* (David, Rajasingh & Narayanan), *A. (Eoessigia) longicauda* (Richards), *A. (Eoessigia) longituberculatum* (Zhang, Zhong

& Zhang), *A. (Eoessigia) sorbi* (Chakrabarti & Maity), and *A. (Eoessigia) vera* Stekolshchikov & Novgorodova.

The genus is distinguished from others as follows: head with three processes on frons; dorsum of body variously decorated with wrinkles, irregular polygonal reticulations, oval or semicircular sculptures, small papillate tubercles; siphunculus long and spoon-shaped, broad at base, slightly swollen distally, without flange. After examining specimens of this genus from China, six new species are here described. In addition, *Aspidophorodon cornuatum* Qiao, 2015 is regarded as a junior synonym of *Aspidophorodon longituberculatum* (Zhang, Zhong & Zhang, 1992), syn. nov. Two species, *Aspidophorodon harvense* Verma and *Aspidophorodon indicum* (David, Rajasingh & Narayanan) are recorded in China for the first time.

## Materials and methods

### Morphological description

Aphid terminology in this paper generally follows that of Chen et al. (2015). The unit of measurement is millimeters (mm). In this paper, the following abbreviations are used:

<b>Ant. I, II, III, IV, V, VI</b>	antennal segments I, II, III, IV, V, VI;
<b>Ant. IVb, Vb, VIb</b>	base of segment IV, V or VI, respectively;
<b>PT</b>	processus terminalis;
<b>Ant. III BD</b>	basal diameter of antennal segment III;
<b>URS</b>	ultimate rostral segment;
<b>BW URS</b>	basal width of ultimate rostral segment;
<b>MW hind tibia</b>	mid-width of hind tibia;
<b>2HT</b>	second hind tarsal segment;
<b>SIPH</b>	siphunculus;
<b>BW SIPH</b>	basal width of siphunculus;
<b>MW SIPH</b>	mid-width of siphunculus;
<b>DW SIPH</b>	distal width of siphunculus;
<b>BW Cauda</b>	basal width of cauda.

### DNA barcoding

The DNA barcodes of twenty-six samples of *Aspidophorodon* were obtained, including the six new species and seven known species. The aphid samples used in this research and voucher information are listed in Table 1.

The methods of extracting DNA and PCR thermal regime followed those of Chen et al. (2015). Sequences were assembled by SeqMan II (DNASTar, Inc., Madison, WI, USA) with inspection and manual editing, and then were examined using BLAST to confirm the sequences were highly similar to aphid species. All sequences were deposited in GenBank (Table 1). Multiple alignments were performed with ClustalW (Thompson et al. 1994)

**Table 1.** Voucher and GenBank accession numbers for aphid samples used in the molecular analyses.

Species	Voucher number	Collection locality	Host plant	COI
<i>A. capitatum</i> Qiao & Xu, sp. nov.	49120	China: Tibet (Bomi)	<i>Salix</i> sp.	OK668442
<i>A. capitatum</i> Qiao & Xu, sp. nov.	51730	China: Tibet (Bomi)	<i>Salix</i> sp.	OK668446
<i>A. furcatum</i> Qiao & Xu, sp. nov.	45884	China: Sichuan (Minya Konka)	<i>Salix</i> sp.	OK668438
<i>A. furcatum</i> Qiao & Xu, sp. nov.	45911	China: Sichuan (Minya Konka)	<i>Salix</i> sp.	OK668439
<i>A. harvensis</i> Verma	45942	China: Sichuan (Ganzi)	<i>Spiraea</i> sp.	OK668440
<i>A. indicum</i> (David, Rajasingh & Narayanan)	52024	China: Tibet (Jilong)	<i>Cotoneaster</i> sp.	OK668434
<i>A. indicum</i> (David, Rajasingh & Narayanan)	52044	China: Tibet (Jilong)	<i>Cotoneaster</i> sp.	OK668447
<i>A. longicauda</i> (Richards)	CNC#HEM114051	Canada	Unknown	KR031700.1*
<i>A. longicauda</i> (Richards)	CNC#HEM057620	Canada	Unknown	KR038732.1*
<i>A. longicauda</i> (Richards)	CNC#HEM114048	Canada	Unknown	KR038867.1*
<i>A. longicauda</i> (Richards)	CNC#HEM057547	Canada	Unknown	KR042463.1*
<i>A. longicauda</i> (Richards)	CNC#HEM057563	Canada	Unknown	KR045217.1*
<i>A. longicornutum</i> Qiao & Xu, sp. nov.	41008	China: Shaanxi (Ankang)	<i>Salix</i> sp.	OK668436
<i>A. longicornutum</i> Qiao & Xu, sp. nov.	41027	China: Shaanxi (Ankang)	Unknown	OK668437
<i>A. longirostre</i> Qiao & Xu, sp. nov.	15089	China: Sichuan (Baoping)	<i>Salix</i> sp.	OK668432
<i>A. cornuatum</i> (Qiao), 2015, syn. nov.	25908	China: Tibet (Yadong)	<i>Salix cupularis</i>	KJ374724*
<i>A. cornuatum</i> (Qiao), 2015, syn. nov.	51707	China: Tibet (Bomi)	<i>Salix</i> sp.	OK668444
<i>A. longituberculatum</i> (Zhang, Zhong & Zhang, 1992)	51707 al.	China: Tibet (Bomi)	<i>Salix</i> sp.	OK668445
<i>A. musaicum</i> Qiao	17257	China: Sichuan (Meigu)	Unknown	KJ374722*
<i>A. obtusum</i> Qiao	22562	China: Sichuan (Minya Konka)	<i>Salix</i> sp.	KJ374723*
<i>A. obtusum</i> Qiao	47777	China: Sichuan (Minya Konka)	<i>Cotoneaster</i> sp.	OK668441
<i>A. reticulatum</i> Qiao & Xu, sp. nov.	37265	China: Tibet (Cuona)	<i>Salix cupularis</i>	OK668435
<i>A. salicis</i> Miyazaki	15038	China: Sichuan (Baoping)	<i>Salix</i> sp.	KT221040*
<i>A. salicis</i> Miyazaki	49999	China: Beijing	<i>Salix</i> sp.	OK668443
<i>A. salicis</i> Miyazaki	23167	China: Sichuan (Leshan)	<i>Salix</i> sp.	KT221041*
<i>A. obtusirostre</i> Qiao & Xu, sp. nov.	35918	China: Beijing (Mt. Dongling)	Unknown	OK668433

\*Sequences downloaded from GenBank.

and then verified manually. Pairwise genetic distances and Neighbor-joining (NJ) tree for COI gene were estimated using MEGA7 (Kumar et al. 2016) under Kimura's two-parameter (K2P) model (Kimura 1980). Bootstrap analyses were performed with 1000 replicates.

## Specimen depositories

The holotypes and some paratypes of six new species and other specimens examined are deposited in the National Animal Collection Resource Center, Institute of Zoology, Chinese Academy of Sciences, Beijing, China (unmarked in the text). The other paratypes of new species are deposited in the Natural History Museum, London, UK (NHMUK, marked in the text).

## Taxonomy

### *Aspidophorodon* Verma, 1967

*Aspidophorodon* Verma 1967: 507. Type species: *Aspidophorodon harvensis* Verma 1967; by original designation. Miyazaki 1971: 183; Eastop and Hille Ris Lambers 1976:

95; Remaudière and Remaudière 1997: 73; Zhang et al. 1999: 349; Blackman and Eastop 2006: 1098; Stekolshchikov and Novgorodova 2010: 44; Nieto Nafria et al. 2011: 145; Chen et al. 2015: 557.

*Indotuberoaphis* Chakrabarti & Maity 1984: 198. Type species: *Indotuberoaphis sorbi* Chakrabarti & Maity 1984; by original designation.

*Margituberculatus* Zhang, Zhong & Zhang 1992: 381. Type species: *Margituberculatus longituberculatum* Zhang, Zhong & Zhang 1992; by original designation.

*Raychaudhuriella* Chakrabarti 1978: 355. Type species: *Raychaudhuriella myzaphoides* Chakrabarti 1978: 357; by original designation.

**Generic diagnosis.** Head with three processes on frons; median frontal tubercle in apterae distinctly protuberant, hemispherical, rectangular, or forked, sometimes with a depression at the middle; antennal tubercles undeveloped, but each with a cylindrical, finger-shaped, or long horn-shaped process at inner apex, the process higher or lower than median frontal tubercle in apterae. Body dorsum with various markings in apterous viviparous females: wrinkles, irregular polygonal reticulations, oval or semicircular sculptures, or small papillate tubercles. Antennae 4- or 5-segmented (rarely 6-segmented) in apterae, 5- or 6-segmented in alatae. Ant. I usually rounded or projected to short cylindrical at inner apex. Secondary rhinaria present on antennal segments III–V in alatae. SIPH spoon-shaped, broad at base, thin at the middle, slightly swollen distally, obliquely truncated at tip, without flange. Cauda tongue-shaped or elongate conical, slightly constricted near the middle, sometimes with a constriction at base, with 4–5 setae, rarely 6–11.

**Distribution.** Canada, China, India, Japan, Russia (Sakhalin, the Altai Republic, and the Kuril Islands), and Kashmir region.

**Host plants.** Rosaceae (*Cotoneaster*, *Potentilla*, *Sorbus*, *Spiraea*), and Salicaceae (*Salix*), rarely on Polygonaceae (*Polygonum*).

**Comments.** The genus *Aspidophorodon* includes two subgenera, the nominate subgenus and subgenus *Eoessigia*. The most important difference between the two subgenera is the presence of at least one spinal process on abdominal tergite VIII in *Aspidophorodon* (*Eoessigia*), whereas no such spinal process is found on members of the nominate subgenus. See Chen et al. (2015) for a key to subgenera.

### **Subgenus *Aspidophorodon* Verma, 1967**

*Aspidophorodon* Verma 1967: 507. Type species: *Aspidophorodon harvense* Verma 1967; by original designation.

*Aspidophorodon* (*Aspidophorodon*) Verma: Remaudière and Remaudière 1997: 73; Stekolshchikov and Novgorodova 2010: 44; Nieto Nafria et al. 2011: 145; Chen et al. 2015: 557.

**Comments.** Spinal processes on body dorsum absent, and marginal processes present or absent on thoracic nota and abdominal tergites I–IV in apterae. Median frontal tubercle protuberant, hemispherical, rectangular, sometimes with a depression at the

middle in apterae. Antennae 4- or 5-segmented in apterae. Cauda tongue-shaped with 4 or 5 setae, sometimes with 6 setae.

The nominate subgenus contains seven species, including three new species. *Aspidophorodon harvense* Verma is first recorded in China. This subgenus is mainly distributed in eastern Asia.

### Key to the species of *Aspidophorodon* (*Aspidophorodon*) (based on apterous viviparous females)

- 1 Marginal processes on thoracic nota and abdominal tergites absent ..... 2
- Marginal processes on thoracic nota and abdominal tergites present ..... 5
- 2 Head with three inconspicuous processes on frons, median frontal tubercle moderately protuberant; antennal tubercles each with an inconspicuous process at inner apex; Ant. I rounded at inner apex; body dorsum scabrous with many small papillate tubercles; body dorsal setae extremely thick long and capitate, on swollen setal tubercles ..... ***A. capitatum* Qiao & Xu, sp. nov.**
- Head with three developed processes on frons, median frontal tubercle rectangular or hemispherical; antennal tubercles each with a short cylindrical or horn-shaped process at inner apex; Ant. I projected at inner apex; body dorsum with reticulations, without small papillate tubercles; body dorsal setae short and thin, blunt or pointed at apices, on normal setal tubercles ..... 3
- 3 Median frontal tubercle with a depression at the middle; process at inner apex of antennal tubercle as high as median frontal tubercle .... ***A. salicis* Miyazaki**
- Median frontal tubercle without a depression at the middle; process at inner apex of antennal tubercle much higher than median frontal tubercle ..... 4
- 4 Antennal tubercles each with a long horn-shaped process at inner apex, 2.40–2.50 × as long as its basal width; body dorsum with distinctly oval and polygonal reticulations ..... ***A. harvense* Verma**
- Antennal tubercles each with a cylindrical process at inner apex, 1.82–2.04 × as long as its basal width; body dorsum with reticulations consisting of small triangles arranged in polygons ..... ***A. reticulatum* Qiao & Xu, sp. nov.**
- 5 Antennal tubercles each with a short cylindrical process at inner apex, the process lower than median frontal tubercle; marginal processes on meso- and metanotum and abdominal tergites I–IV distinctly long and horn-shaped ..... ***A. longicornutum* Qiao & Xu, sp. nov.**
- Antennal tubercles each with a cylindrical process at inner apex, the process higher than median frontal tubercle; marginal processes on thoracic nota and abdominal tergites I–IV cylindrical ..... 6
- 6 Abdominal tergites with irregular polygonal mosaic-like markings; marginal processes on thoracic nota and abdominal tergites I–IV long and tapered ..... ***A. musaicum* Qiao**
- Abdominal tergites with reticulations formed by small irregular oval markings; marginal processes on thoracic nota and abdominal tergites I–IV cylindrical, with obtuse apices ..... ***A. obtusum* Qiao**

***Aspidophorodon capitatum* Qiao & Xu, sp. nov.**

<http://zoobank.org/101581BE-83AD-4F7B-9C28-BEB8F727838F>

Figs 1–2, 21A, Table 2

**Specimens examined.** *Holotype*: apterous viviparous female, CHINA, Tibet (Bomi County, 30.15°N, 94.99°E, altitude 2160 m), 01.IX.2020, No. 49120-1-1-2, on *Salix* sp., coll. Y. Xu. *Paratypes*: one apterous viviparous female (slide), No. 49120-1-1-1, one apterous viviparous female (COI: OK668442), and four fourth instar apterous nymphs, with the same collection data as holotype; one apterous viviparous female, 26.VI.2021, No. 51696-1-1, on *Salix* sp., coll. Y. Xu; one apterous viviparous female (slide) and one apterous viviparous female (COI: OK668446), 29.VI.2021, No. 51730-1-2, on *Salix* sp., coll. Y. Xu; one apterous viviparous female, No. 49120-1-2 (NHMUK), with the same collection data as holotype.

**Diagnosis.** Dorsum of body densely covered with small papillate tubercles; median frontal tubercle moderately protuberant, with a shallow depression at the middle; antennal tubercles each with an inconspicuous process at inner apex lower than median frontal tubercle; dorsal setae of body distinctly long, thick, capitate, on swollen setal tubercles.

**Description.** Apterous viviparous females: body elongated oval (Fig. 2A), yellowish white in life (Fig. 21A).

**Mounted specimens.** Body pale; head, compound eyes, Ant. IV, distal part of rostrum, legs, setal tubercles, distal part of SIPH, cauda and anal plate pale brown; tarsi brown. Thoracic nota and abdominal tergites I–IV each with one pair of spinal and one pair of pleural sclerites, tergites V–VII each with one pair of spinal sclerites, those sclerites pale brown in color; tergite VIII with a pale brown band (Figs 1C, 2A); other parts pale in color. See Table 2 for general measurements.

**Head.** Ocular tubercles small. Dorsum of head densely covered with small papillate tubercles (Figs 1A, 2B), venter with wrinkles and sparse small papillate tubercles. Median frontal tubercle moderately protuberant, with a shallow depression at the middle (Figs 1A, 2B), with one pair of long capitate setae on venter. Antennal tubercles undeveloped, each with an inconspicuous process at inner apex, lower than median frontal tubercle, each process with a long capitate seta at apex (Figs 1A, 2B). Dorsal setae of head extremely long, thick, capitate, on swollen setal tubercles which are covered with sparsely small papillae. Head with one pair of cephalic setae, one pair of dorsal setae between antennae, and two pairs of dorsal setae between compound eyes arranged transversely (Figs 1A, 2B). Antennae 4-segmented, Ant. I–II with wrinkles, Ant. III–IV slightly imbricated; Ant. I rounded at inner apex (Figs 1B, 2C). Antennal setae long, thick and capitate on Ant. I–II, short and blunt on Ant. III–IV; Ant. I–IV with 3, 1-2, 1-2, 2 (base) +0-1 (PT) setae, respectively; apex of PT with two or three setae. Primary rhinaria not ciliated. Rostrum reaching mid-coxae, URS wedge-shaped (Figs 1D, 2D), with three pairs of primary setae, without accessory setae.

**Thorax.** Pronotum densely covered with small papillate tubercles, meso- and metanotum with small papillate tubercles, distinctly developed on marginal area. Dorsal setae of thorax extremely long, thick, capitate, on swollen setal tubercles which are

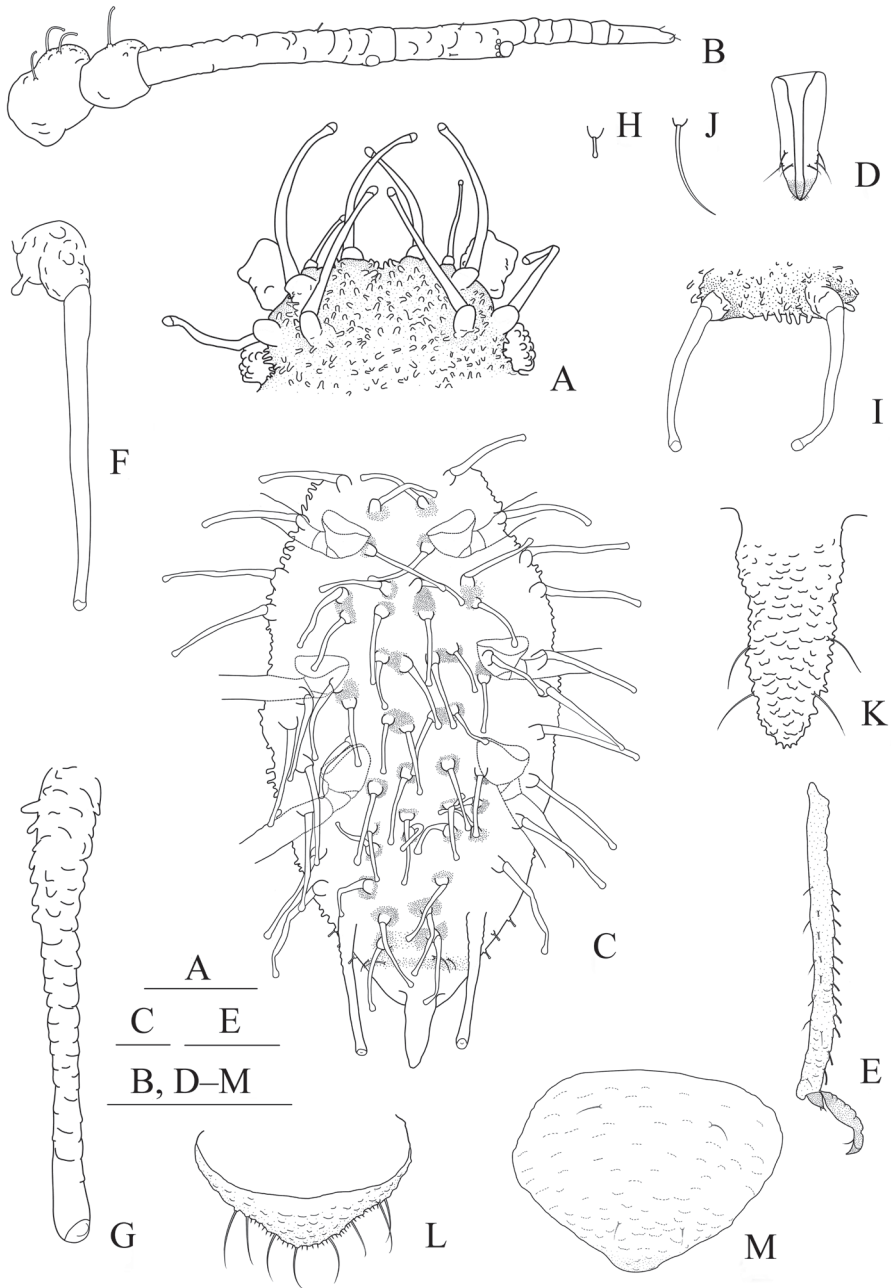


**Figure 1.** *Aspidophorodon capitatum* Qiao & Xu, sp. nov. Apterous viviparous female **A** dorsal view of head **B** antenna **C** dorsal view of thorax and abdomen **D** ultimate rostral segment **E** hind tibia and tarsi **F** marginal seta of abdominal tergite I **G** siphunculus **H** marginal seta of abdominal tergite V **I** spinal setae of abdominal tergite VII **J** spinal seta of abdominal tergite VIII **K** cauda **L** anal plate **M** genital plate. Scale bars: 0.10 mm.

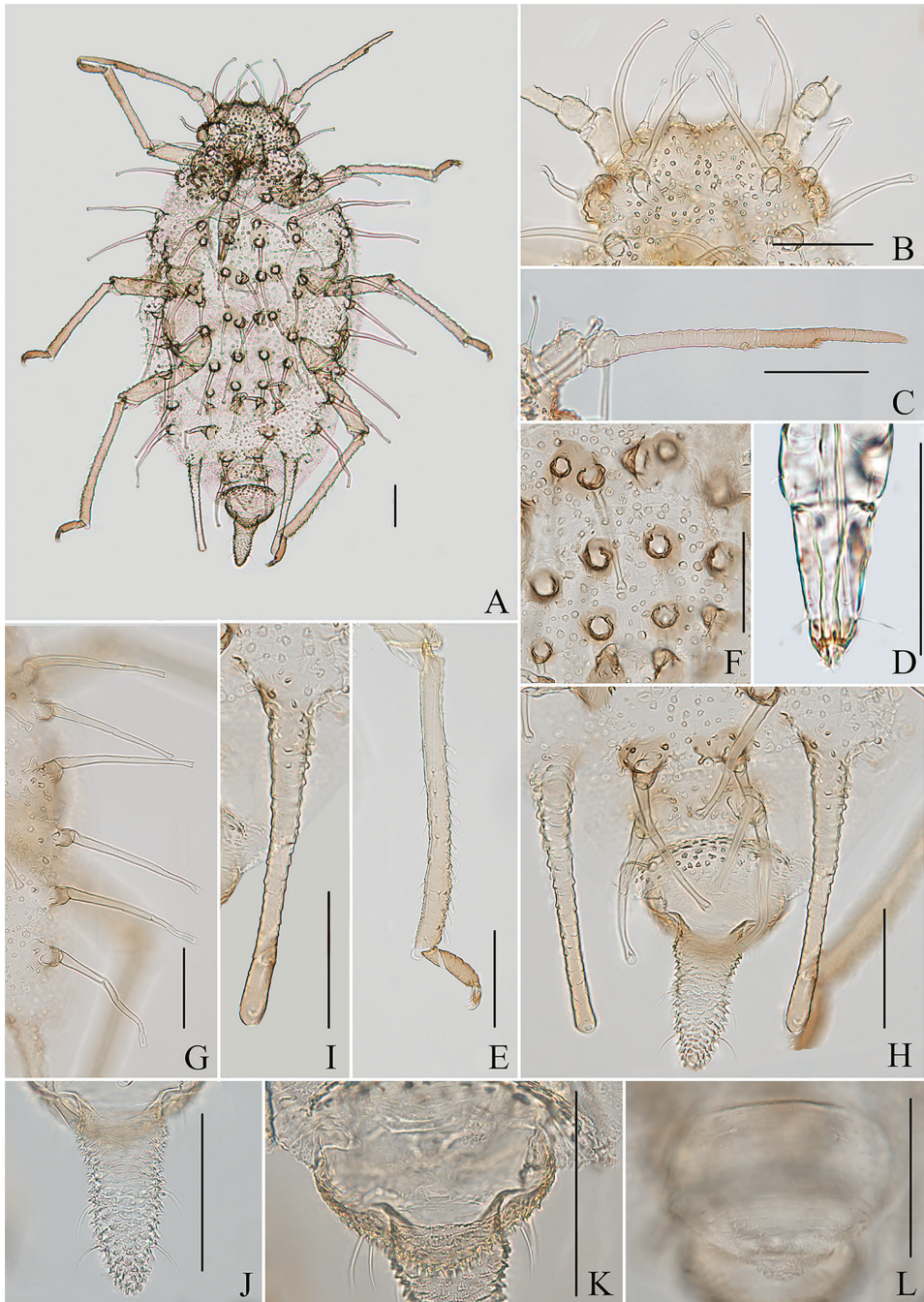


**Figure 2.** *Aspidophorodon capitatum* Qiao & Xu, sp. nov. Apterous viviparous female **A** dorsal view of body **B** dorsal view of head **C** antenna **D** ultimate rostral segment **E** hind tibia and tarsi **F** papillated tubercles at seta-basal of abdominal tergites **G** marginal setae of metanotum and abdominal tergites I–IV **H** dorsal view of abdominal tergites VI–VIII **I** siphunculus **J** cauda **K** anal plate **L** genital plate. Scale bars: 0.10 mm.

Table 2. Morphometric data about species of the nominate subgenus (in mm).

Parts	<i>A. capitatum</i> Qiao & Xu, sp. nov.		<i>A. harvense</i> Verma		<i>A. longicornutum</i> Qiao & Xu, sp. nov.		<i>A. reticulatum</i> Qiao & Xu, sp. nov.	
	Apterous viviparous female (n = 4)	4 <sup>th</sup> apterous nymph (n = 4)	Apterous viviparous female (n = 2)	Alate viviparous female (n = 1)	Apterous viviparous female (n = 7)	Apterous viviparous female (n = 2)	Apterous viviparous female (n = 7)	Apterous viviparous female (n = 2)
Length (mm)								
Body length	1.001–1.104	0.817–0.894	2.147–2.238	1.884	0.899–1.079	1.743–1.753		
Body width	0.448–0.540	0.408–0.497	0.966–1.091	0.741	0.382–0.467	0.908–0.940		
Antennae	0.362–0.374	0.324–0.338	0.806–0.828	1.034	0.330–0.422	0.569–0.537		
Ant. I	0.051–0.053	0.048–0.051	0.086–0.088	0.080	0.046–0.055	0.062–0.067		
Ant. II	0.036–0.038	0.032–0.038	0.062–0.070	0.067	0.033–0.039	0.044–0.048		
Ant. III	0.130–0.144	0.102–0.119	0.293–0.324	0.326	0.125–0.178	0.170–0.181		
Ant. IV	/	/	0.145–0.161	0.152	/	0.101–0.103		
Ant. IVb	0.060–0.067	0.057–0.066	/	/	0.061–0.081	/		
Ant. V	/	/	/	0.188	/	/		
Ant. Vb	/	/	0.107	/	/	0.082–0.084		
Ant. V/b	/	/	/	0.113	/	/		
PT	0.081–0.084	0.071–0.083	0.094–0.097	0.108	0.064–0.075	0.097–0.104		
URS	0.076–0.079	0.074–0.083	0.082–0.092	0.082	0.084–0.095	0.124–0.128		
Hind femur	0.164–0.170	0.123–0.145	0.394–0.410	0.48	0.144–0.178	0.288–0.290		
Hind tibia	0.327–0.334	0.272–0.299	0.724–0.765	0.974	0.255–0.315	0.540–0.560		
2HT	0.058–0.061	0.059–0.065	0.114–0.119	0.122	0.056–0.067	0.080–0.082		
SIPH	0.226–0.257	0.175–0.203	0.362–0.381	0.269	0.244–0.331	0.256–0.263		
BW SIPH	0.029–0.031	0.032–0.044	0.064–0.069	0.036	0.036–0.049	0.047–0.049		
MW SIPH	0.014–0.015	0.014–0.016	0.042–0.049	0.026	0.012–0.014	0.028–0.030		
DW SIPH	0.019–0.020	0.017–0.018	0.031–0.035	0.035	0.016–0.018	0.028–0.032		
Cauda	0.126–0.136	/	0.190	0.134	0.086–0.112	0.149–0.162		
BW Cauda	0.071–0.078	/	0.110–0.117	0.090	0.045–0.057	0.097–0.103		
MW Cauda	/	/	0.082–0.086	0.046	0.032–0.037	0.062–0.063		
Ant. IIIBD	0.018–0.020	0.021	0.033–0.037	0.033	0.017–0.022	0.025–0.026		
Widest width of hind femur	0.045–0.048	0.044–0.050	0.076–0.078	0.067	0.036–0.045	0.062–0.068		
MW hind tibia	0.022–0.024	0.028–0.032	0.039–0.041	0.034	0.019–0.021	0.036		
Cephalic setae	0.124–0.132	0.075–0.084	0.020–0.023	0.023	0.022–0.033	0.024		
Dorsal setae of head	/	/	0.006–0.008	0.013	/	0.023–0.024		
Dorsal setae of head between antenna	0.157–0.161	0.105–0.119	/	/	0.021–0.030	/		
Dorsal setae of head between compound eyes	0.139–0.175	0.076–0.111	/	/	0.029–0.034	/		

Parts	<i>A. capitatum</i> Qiao & Xu, sp. nov.				<i>A. harvense</i> Verma				<i>A. longicornutum</i> Qiao & Xu, sp. nov.		<i>A. reticulatum</i> Qiao & Xu, sp. nov.	
	Apterous viviparous female (n = 4)	4 <sup>th</sup> apterous nymph (n = 4)	Apterous viviparous female (n = 2)	Alate viviparous female (n = 1)	Apterous viviparous female (n = 7)	Apterous viviparous female (n = 2)	Alate viviparous female (n = 1)	Apterous viviparous female (n = 7)	Apterous viviparous female (n = 2)	Apterous viviparous female (n = 2)		
Length (mm)												
Marginal setae on Tergite I	0.193-0.198	0.118-0.129	0.006-0.010	0.014	0.026-0.033	0.014-0.016						
Spinal setae on Tergite VIII	0.018-0.021	0.013-0.019	0.019-0.025	0.031	0.027-0.035	0.025-0.028						
Setae on Ant. III	0.008-0.010	0.005-0.007	0.006-0.007	0.011	/	0.010-0.012						
Setae on hind tibia	0.017-0.019	0.028-0.036	0.016-0.017	0.021	0.014-0.02	0.054-0.056						
Processes on antennal tubercle	/	/	0.110-0.120	0.019	0.015-0.026	0.051-0.056						
Marginal process on mesonotum	/	/	/	/	0.268-0.325	/						
Marginal process on metanotum	/	/	/	/	0.244-0.286	/						
Marginal process on Tergite I	/	/	/	/	0.211-0.26	/						
Marginal process on Tergite II	/	/	/	/	0.224-0.265	/						
Marginal process on Tergite III	/	/	/	/	0.233-0.288	/						
Marginal process on Tergite IV	/	/	/	/	0.234-0.309	/						
Body length / Body width	2.00-2.23	1.80-2.08	2.05-2.22	2.54	2.23-2.81	1.85-1.93						
Whole antennae / Body	0.33-0.37	0.37-0.41	0.36-0.39	0.55	0.34-0.40	0.33						
Hind femur / Ant. III	1.18-1.27	1.10-1.42	1.22-1.40	1.47	1.00-1.21	1.60-1.69						
Hind tibia / Body	0.30-0.33	0.30-0.37	0.32-0.36	0.52	0.28-0.30	0.31-0.32						
Ant. I / Ant. III	0.35-0.41	0.43-0.50	0.27-0.29	0.25	0.29-0.38	0.37						
Ant. II / Ant. III	0.26-0.29	0.27-0.36	0.21-0.22	0.21	0.21-0.27	0.24-0.28						
Ant. IV / Ant. III	/	/	0.45-0.55	0.47	/	0.56-0.61						
Ant. VI / Ant. III	/	/	/	0.58	/	/						
Ant. IVb, Vb or VIb / Ant. III	0.42-0.52	0.52-0.59	0.33-0.37	0.35	0.43-0.49	0.46-0.48						
PT / Ant. III	0.56-0.65	0.62-0.81	0.29-0.33	0.33	0.40-0.52	0.54-0.61						
PT / Ant. IVb, Vb or VIb	1.25-1.38	1.08-1.43	0.88-0.91	0.96	0.88-1.09	1.16-1.27						
URS / BW URS	2.03-2.05	1.95-2.36	1.39-1.63	1.55	2.37-2.85	2.70-2.72						
URS / 2HT	1.28-1.32	1.20-1.41	0.69-0.81	0.67	1.31-1.59	1.51-1.61						
SIPH / Body	0.22-0.26	0.21-0.24	0.16-0.17	0.14	0.27-0.31	0.15						
SIPH / Cauda	1.66-1.88	/	1.91-2.01	2.01	2.64-3.07	1.58-1.77						
SIPH / BW SIPH	7.29-8.86	3.98-5.88	5.22-5.66	7.47	6.10-7.15	5.22-5.66						
SIPH / MW SIPH	16.14-17.13	11.67-12.69	7.78-8.62	10.35	20.00-24.31	8.74-9.14						
SIPH / DW SIPH	11.85-12.85	10.29-11.29	10.34-12.29	7.69	13.56-19.47	8.23-9.14						
Cauda / BW Cauda	1.75-1.92	/	1.62-1.73	1.49	1.78-2.24	1.53-1.57						
Cephalic setae / Ant. IIIBD	6.30-6.89	3.75-4.00	0.61-0.62	0.7	1.22-1.71	0.92-0.98						
Marginal setae on Tergite I / Ant. III BD	9.76-10.78	5.62-6.40	0.18-0.27	0.42	1.24-1.29	0.54-0.66						

Parts	<i>A. capitatum</i> Qiao & Xu, sp. nov.		<i>A. harvense</i> Verma		<i>A. longicornutum</i> Qiao & Xu, sp. nov.		<i>A. reticulatum</i> Qiao & Xu, sp. nov.	
	Apterous viviparous female (n = 4)	4 <sup>th</sup> apterous nymph (n = 4)	Apterous viviparous female (n = 2)	Alate viviparous female (n = 1)	Apterous viviparous female (n = 7)	Apterous viviparous female (n = 2)	Apterous viviparous female (n = 2)	
Ratio (times)								
Spinal setae on Tergite VIII / Ant. III BD	2.50–3.11	1.62–2.00	0.51–0.76	0.94	1.50–1.82	0.96–1.14	0.96–1.14	
Setae on Ant. III / Ant. IIIBD	0.40–0.50	0.24–0.33	0.18–0.19	0.33	/	0.43–0.46	0.43–0.46	
Setae on hind tibia / MW hind tibia	0.77–0.79	1.00–1.29	0.41–0.42	0.62	0.74–0.95	0.60–0.67	0.60–0.67	
Length of processes on antennal tubercle / its basal width	/	/	2.40–2.50	0.61	0.89–1.73	1.82–2.04	1.82–2.04	
Length of marginal process on mesonotum / its basal width	/	/	/	/	7.05–10.48	/	/	
Length of marginal process on mesonotum / SIPH	/	/	/	/	0.86–1.11	/	/	
Length of marginal process on metanotum / its basal width	/	/	/	/	6.95–9.53	/	/	
Length of marginal process on metanotum / SIPH	/	/	/	/	0.81–1.00	/	/	
Length of marginal process on Tergite I / its basal width	/	/	/	/	5.90–6.89	/	/	
Length of marginal process on Tergite I / SIPH	/	/	/	/	0.74–0.88	/	/	
Length of marginal process on Tergite II / its basal width	/	/	/	/	5.88–8.55	/	/	
Length of marginal process on Tergite II / SIPH	/	/	/	/	0.79–0.96	/	/	
Length of marginal process on Tergite III / its basal width	/	/	/	/	6.68–9.32	/	/	
Length of marginal process on Tergite III / SIPH	/	/	/	/	0.87–1.02	/	/	
Length of marginal process on Tergite IV / its basal width	/	/	/	/	6.58–8.36	/	/	
Length of marginal process on Tergite IV / SIPH	/	/	/	/	0.90–0.96	/	/	

covered with sparsely small papillae; pronotum with two pairs of spinal setae, arranged anteriorly and posteriorly, one pair of pleural and one pair of marginal setae; meso-, and metanotum with two pairs of spinal, pleural, and marginal setae, respectively (Figs 1C, 2A). Legs normal. Distal parts of femora and tibiae slightly imbricated. Setae on 2/3 distal part of femora and hind tibiae short, blunt ventrally and capitate dorsally (Figs 1E, 2E). First tarsal chaetotaxy: 3, 2, 2. Second tarsal segments with imbrications.

**Abdomen.** Abdominal tergites with small papillate tubercles (Fig. 2F), distinctly developed on marginal area. Venter of abdominal tergites III–VIII with fine spinules arranged in rows. Dorsal setae of abdomen extremely long, thick, capitate, on swollen setal tubercles which are covered with small papillae (Figs 1C, 1F, 1I, 2G); the marginal setae of tergites V–VII short, thin, and capitate (Fig. 1H), the setae on tergite VIII long and pointed (Fig. 1J); ventral setae short and pointed. Abdominal tergite I with two pairs of spinal, one pair of pleural and one pair of marginal setae, tergites II–IV each with one pair of spinal, pleural and marginal setae, tergite V with one pair of pleural and one pair of marginal setae, tergites VI–VIII with one pair of spinal and one pair of marginal setae (Figs 1C, 2A). Length of marginal setae on abdominal tergites I–IV, marginal setae on abdominal tergites V–VII, spinal and marginal setae on abdominal tergite VIII 9.65–10.78, 0.60–0.67, 2.50–3.11, 0.90–1.17 × as long as Ant. III BD, respectively. Spiracles reniform and open. SIPH long, spoon-shaped, broad at base, thin at the middle, slightly swollen distally; basal part with small papillate tubercles, other parts with imbrications, obliquely truncated at tip, without flange (Figs 1G, 2I). Cauda elongate, conical, slightly constricted at the middle, with spinulose imbrications (Figs 1K, 2J) and four setae. Anal plate semicircular, hind margin slightly protruding backwards, spinulose (Figs 1L, 3K), with 6–9 setae. Genital plate broadly round with sparse spinules in transverse rows, hind margin slightly protruding backwards (Figs 1M, 2L); with two anterior setae and two setae along the posterior margin.

**Fourth instar apterous nymph.** As in apterous viviparous females, except setae on legs long and pointed, and with a row of short and blunt setae dorsally on middle of hind tibiae.

**Etymology.** The species is named for its extremely long, thick and capitate setae, *capitatum* being the neuter form of the adjective.

**Taxonomic notes.** The new species resembles *A. harvense* Verma, but differs from it as follows: dorsum of body scabrous, with densely distributed, small, papillate tubercles (the latter: dorsum of body with irregular polygonal markings); median frontal tubercle moderately protuberant, with a shallow depression at middle, antennal tubercles each with an inconspicuous process at inner apex, lower than median frontal tubercle (the latter: median frontal tubercle hemispherical, without a depression at middle, antennal tubercles each with a long horn-shaped process at inner apex, higher than median frontal tubercle); dorsal setae of body extremely long, thick, and capitate, with swollen bases (dorsal setae of body short, thin, and blunt, with normal bases).

**Host plant.** *Salix* sp.

**Distribution.** China (Tibet).

**Biology.** The species dispersedly feeds on the undersides of leaves (Fig. 21A).

***Aspidophorodon harvense* Verma, 1967**

Figs 3–5, 21F, Table 2

*Aspidophorodon harvense* Verma 1967: 507; Eastop and Hille Ris Lambers 1976: 96; Blackman and Eastop 1994: 569.

*Aspidophorodon (Aspidophorodon) harvense* Verma: Remaudière and Remaudière 1997: 73; Stekolshchikov and Novgorodova 2010: 44; Chen et al. 2015: 558.

**Specimens examined.** Two apterous viviparous females (slides) and one apterous viviparous female (COI: OK668440), CHINA: Sichuan (Ganzi City, Minya Konka,

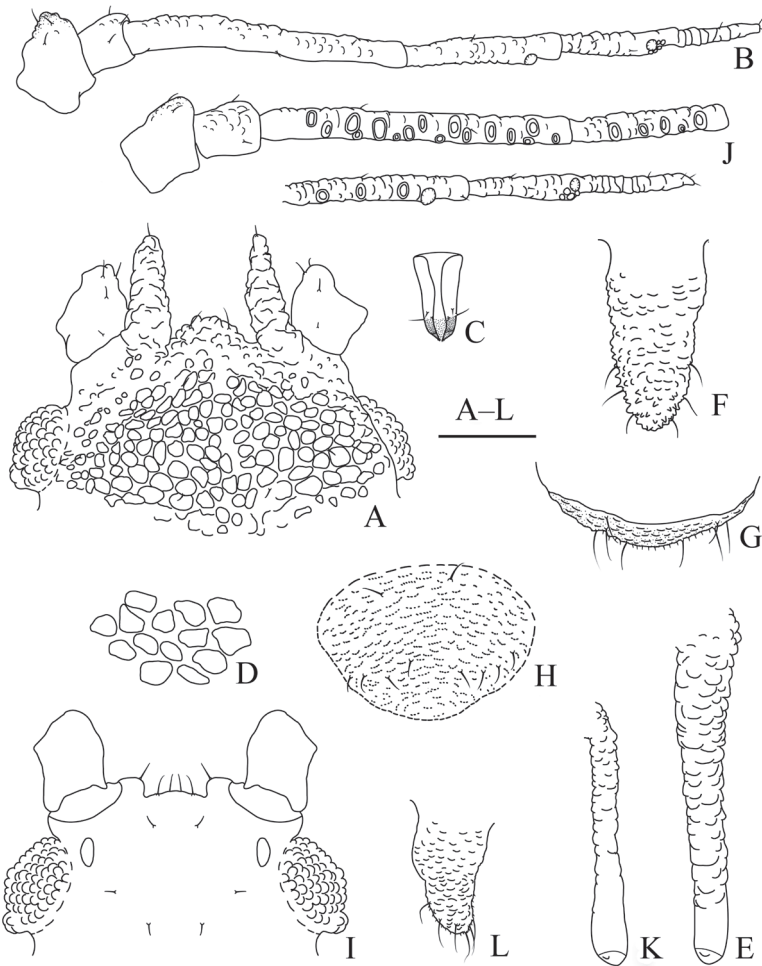


**Figure 3.** *Aspidophorodon harvense* Verma. Apterous viviparous female **A** dorsal view of head **B** antenna **C** ultimate rostral segment **D** irregular polygonal markings on abdominal tergites **E** siphunculus **F** cauda **G** anal plate **H** genital plate. Alate viviparous female **I** dorsal view of head **J** antenna **K** siphunculus **L** cauda. Scale bar: 0.10 mm.

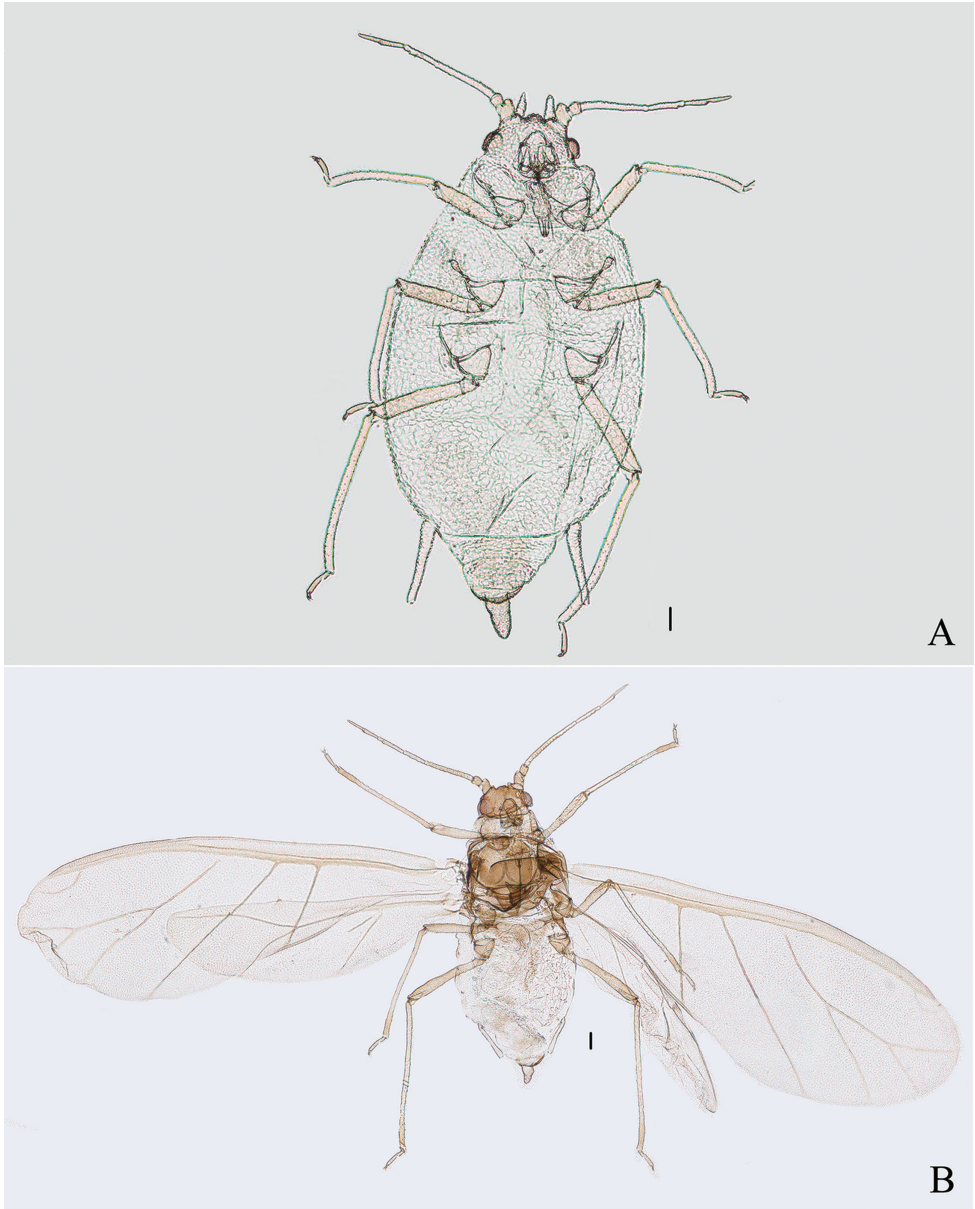


**Figure 4.** *Aspidophorodon harvensis* Verma **A** dorsal view of apterous viviparous female **B** dorsal view of alate viviparous female. Scale bar: 0.10 mm.

29.90°N, 102.03°E, altitude 4031 m), 30.VII.2019, No. 45939-1-1, No. 45942-1-1-2, on *Spiraea* sp., coll. J.F. Ji; one alate viviparous female, No. 45942-1-1-1, with the same collection data as apterous viviparous females.

**Comment.** *Aspidophoron* being neuter, the adjectival specific epithet is also neuter, so *harvensis* is revised as *harvensae*.

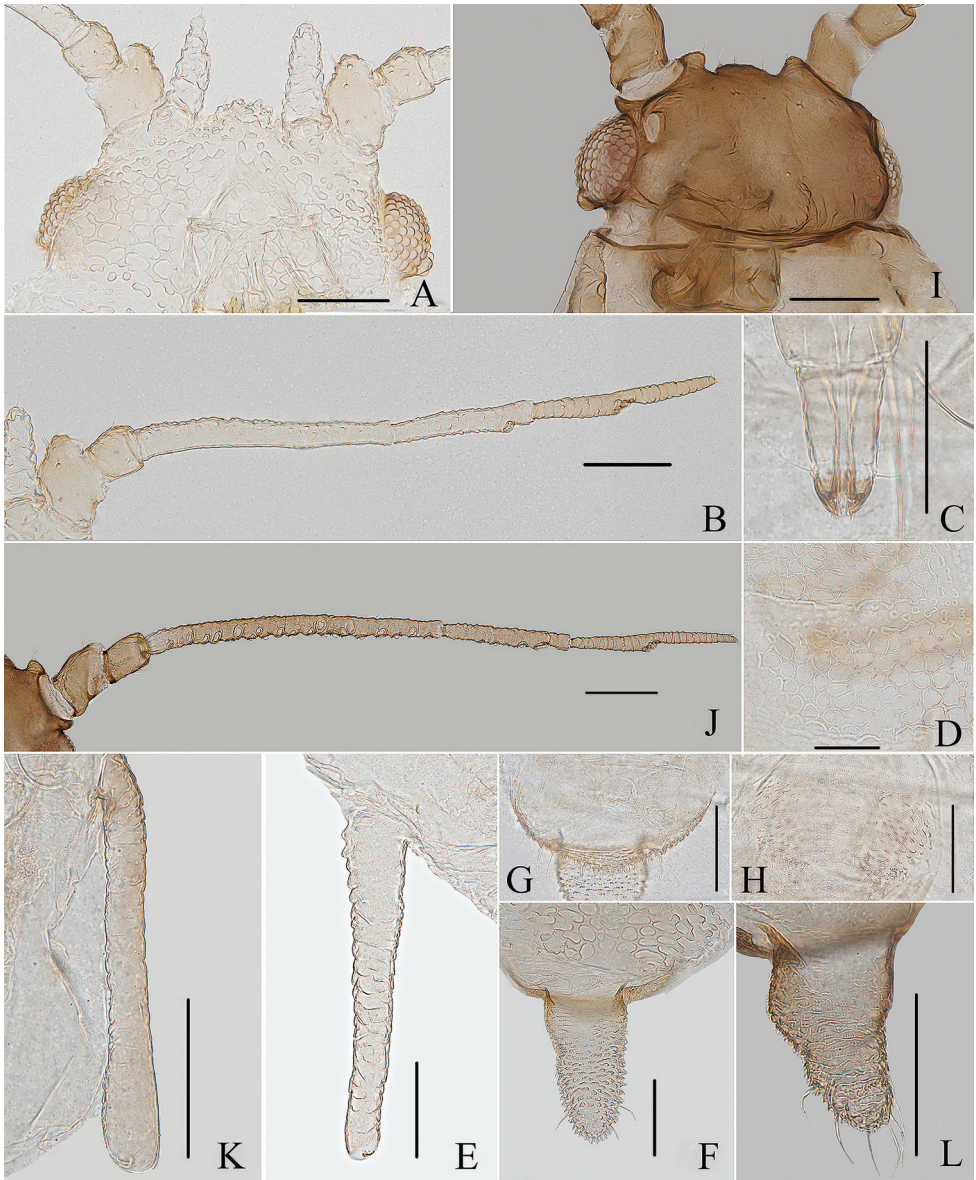


**Figure 5.** *Aspidophorodon harvense* Verma. Apterous viviparous female **A** dorsal view of head **B** antenna **C** ultimate rostral segment **D** irregular polygonal markings on abdominal tergites **E** siphunculus **F** cauda **G** anal plate **H** genital plate. Alate viviparous female **I** dorsal view of head **J** antenna **K** siphunculus **L** cauda. Scale bars: 0.10 mm.

**Host plant.** *Spiraea* sp. (Rosaceae) (Fig. 21F), however, this species was collected from *Salix* sp. in Kashmir in May (Verma 1967).

**Distribution.** China (Sichuan), Kashmir.

**Biology.** The species mostly colonizes along veins on the undersides of leaves (Verma 1967).

***Aspidophorodon longicornutum* Qiao & Xu, sp. nov.**

<http://zoobank.org/C13CA9E8-905F-44D7-B240-63268FA0691C>

Figs 6–7, Table 2

**Specimens examined.** *Holotype*: apterous viviparous female, CHINA: Shaanxi (Ankang City, 33.64°N, 109.37°E, altitude 2020 m), 16.VII.2017, No. 41008-1-1-1, on *Salix* sp., coll. H. Long and J.F. Ji. *Paratypes*: one apterous viviparous female (slide), No. 41008-1-1-2 and one apterous viviparous female (COI: OK668436), two apterous viviparous females, No. 41029-1-1, with the same collection data as holotype; one apterous viviparous female, Shaanxi (Ankang City), 15.VII.2017, host plant unknown, No. 41000-1-1, coll. H. Long and J.F. Ji; two apterous viviparous females (slides), Shaanxi (Ankang City), 16.VII.2017, No. 41027-1-1 and one apterous viviparous female (COI: OK668437), host plant unknown, coll. H. Long and J.F. Ji (NHMUK).

**Diagnosis.** Dorsum of body with oval sculptures; median frontal tubercle protuberant, hemispherical, antennal tubercles each with a short finger-shaped process at inner apex, lower than median frontal tubercle; meso-, metanotum, and abdominal tergites I–IV each with one pair of strongly imbricated and long horn-shaped marginal processes; dorsal setae of abdomen long and thick, slightly swollen at apices, with distinct setal tubercles.

**Description.** Apterous viviparous females: body elongated oval (Fig. 7A), yellowish white in life.

**Mounted specimens.** Body pale; distal part of rostrum, cauda and anal plate pale brown, other parts pale in color (Fig. 7A). See Table 2 for general measurements.

**Head.** Ocular tubercles small. Dorsum of head covered with semicircular and wavy sculptures on median area, marginal area smooth, venter with slight wrinkles (Figs 6A, 7B). Median frontal tubercle distinctly protuberant, rectangular (Figs 6A, 7B), with one pair of long, capitate setae on venter. Antennal tubercles undeveloped, each with a short finger-shaped process at inner apex, lower than median frontal tubercle (Figs 6A, 7B), each process with a long, and capitate seta at apex. Dorsal setae of head long and thick, slightly swollen at apices, with distinct setal tubercles. Head with one pair of cephalic setae, one pair of dorsal setae between antennae, and two pairs of dorsal setae between compound eyes arranged transversely. Antennae 4-segmented, Ant. I and Ant. II smooth, Ant. III–VI with slight imbrication; Ant. I slightly projected at inner apex (Figs 6B, 7C). Antennal setae long, thin and capitate on Ant. I and Ant. II, short and blunt on Ant. III and Ant. IV; Ant. I–IV with 4, 1, 0, 1 (base)+1 (PT) setae, respectively; apex of PT with two or three setae. Primary rhinaria ciliated. Rostrum reaching between mid- and hind coxae; URS wedge-shaped (Figs 6D, 7D), with three pairs of primary setae, without accessory setae.

**Thorax.** Pronotum with semicircular and wavy sculptures on spino-pleural area, marginal area with small papillate tubercles. Meso- and metanotum with oval sculptures on spinal area, pleura-marginal area with oval sculptures and small papillate tubercles. Meso- and metanotum each with one pair of strongly imbricated and long horn-shaped marginal processes (Figs 6C, 7F), each process with a short capitate seta

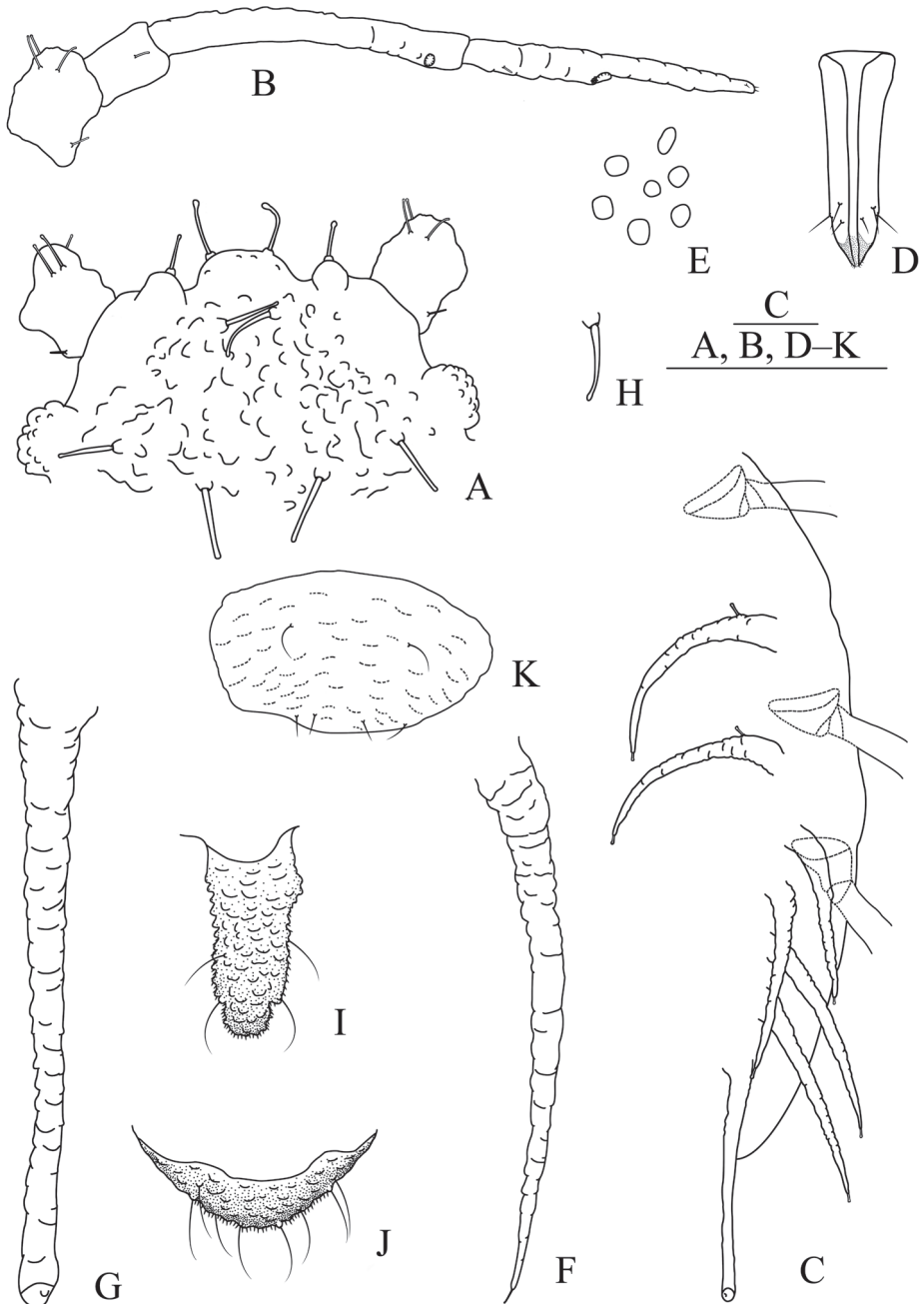


**Figure 6.** *Aspidophorodon longicornutum* Qiao & Xu sp. nov. Apterous viviparous female **A** dorsal view of head **B** antenna **C** marginal processes of thoracic nota and abdominal tergites I–IV **D** ultimate rostral segment **E** oval sculptures of abdominal tergites **F** marginal process of abdominal tergite IV **G** siphunculus **H** spinal seta of abdominal tergite VIII **I** cauda **J** anal plate **K** genital plate. Scale bars: 0.10 mm.

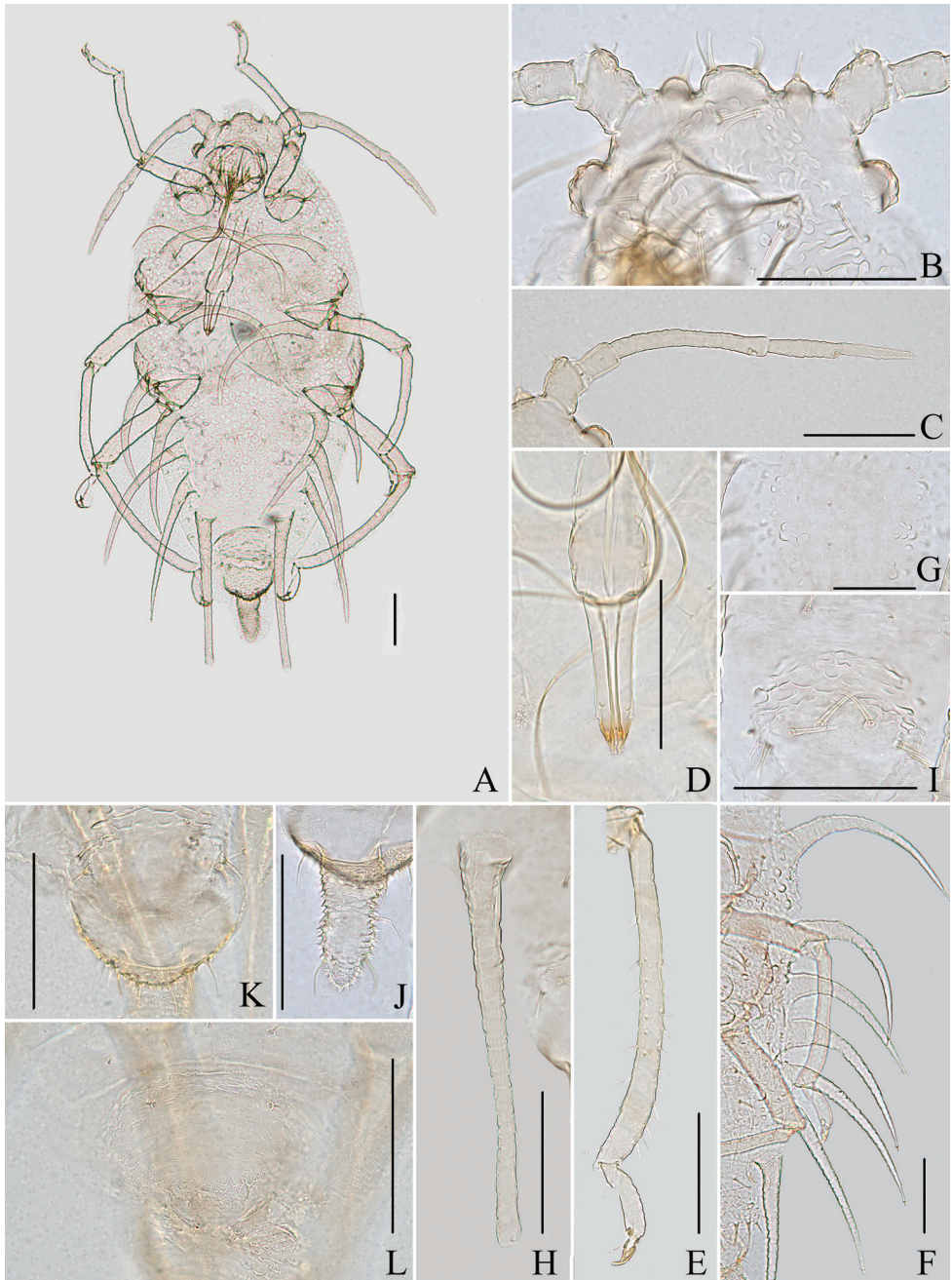


**Figure 7.** *Aspidophorodon longicornutum* Qiao & Xu, sp. nov. Apterous viviparous female **A** dorsal view of body **B** dorsal view of head **C** antenna **D** ultimate rostral segment **E** hind tibia and tarsi **F** marginal processes of thoracic nota and abdominal tergites I–IV **G** oval sculptures of abdominal tergites **H** siphunculus **I** irregular wavy sculptures of abdominal tergite VIII **J** cauda **K** anal plate **L** genital plate. Scale bars: 0.10 mm.

at apex and a short capitate seta at base. Dorsal setae of thorax long and thick, slightly swollen at apices, with distinct setal tubercles; pronotum with one pair of spinal, pleural and marginal setae, respectively, meso- and metanotum each with one pair of spinal and pleural setae. Legs normal, smooth. Setae on legs short, pointed ventrally and short, capitate dorsally. Hind tibiae with a row of short, thick, and blunt setae dorsally on middle (Fig. 7E). First tarsal chaetotaxy: 3, 2, 2. Second tarsal segments slightly imbricated.

**Abdomen.** Abdominal tergites I–VII with distinctly oval sculptures on spino-pleural area (Figs 6E, 7G), marginal area with small papillate tubercles; tergite VIII with irregular wavy sculptures (Fig. 7I). Abdominal tergites I–IV each with one pair of strongly imbricated and long horn-shaped marginal processes (Figs 6C, F, 7F), each process with a short capitate seta at apex. Dorsal setae of abdomen long and thick, slightly swollen at apices, with distinct setal tubercles (Fig. 6H); ventral setae short and pointed. Abdominal tergites I–IV each with one pair of spinal and pleural setae, tergite VII with 2–4 spino-pleural setae, tergite VIII with 7–9 setae. Spiracles reniform, open or closed, spiracular plates slightly swollen. SIPH long spoon-shaped, straight, broad at base, thin at middle, slightly swollen distally, with imbrications, obliquely truncated at tip, without flange (Figs 6G, 7H). Cauda long tongue-shaped, slightly constricted at middle, with spinulose imbrications and four setae (Figs 6I, 7J). Anal plate semicircular, spinulose (Figs 6J, 7K); with 7–12 setae. Genital plate transversely oval, with sparse spinules in transverse rows (Figs 6K, 7L); with two anterior setae and four setae along the posterior margin.

**Etymology.** The species is named for its distinctly long horn-shaped marginal processes on meso-, metanotum, and abdominal tergites I–IV; the Latin neuter adjective *cornutum* means “horned”.

**Taxonomic notes.** The new species resembles *A. longituberculatum* (Zhang, Zhong & Zhang) in meso-, metanotum and abdominal tergites I–IV each with one pair of long horn-shaped marginal processes; but differs from it as follows: antennal tubercles each with a short finger-shaped process at inner apex, lower than median tubercle (the latter: antennal tubercles each with a long horn-shaped process at inner apex and higher than median tubercle); antenna 4-segmented,  $0.35\text{--}0.40 \times$  as long as body length (the latter: antenna 5-segmented,  $0.43\text{--}0.47 \times$  as long as body length); pronotum without marginal processes, meso- and metanotum and abdominal tergites I–IV with distinctly long horn-shaped marginal processes,  $0.211\text{--}0.325$  mm, about as long as SIPH (the latter: pronotum with short conical marginal processes, meso- and metanotum and abdominal tergites I–IV with long horn-shaped marginal processes,  $0.084\text{--}0.206$  mm, shorter than SIPH); dorsal setae of body long and thick, slightly swollen at apices, with distinct bases (the latter: dorsal setae thin, short and capitate); abdominal tergite VIII with 7–9 setae (the latter: abdominal tergite VIII with two setae).

**Host plant.** *Salix* sp.

**Distribution.** China (Shaanxi).

**Biology.** The species disperses on the undersides of leaves.

***Aspidophorodon musaicum* Qiao, 2015**

*Aspidophorodon (Aspidophorodon) musaicum* Qiao: Chen et al. 2015: 557, 560.

**Specimens examined.** Two apterous viviparous females (holotype and paratype), CHINA: Sichuan (Meigu County, altitude 2600 m), 04.V.2005, No. 17257-1-4, host plant unknown, coll. X.L. Huang.

**Comment.** *Aspidophoron* being neuter, the adjectival specific epithet is also neuter, so *musaicus* is revised as *musaicum*.

**Host plant.** Unknown.

**Distribution.** China: Tibet.

**Biology.** The species colonizes the undersides of leaves of its host plant.

***Aspidophorodon obtusum* Qiao, 2015**

*Aspidophorodon (Aspidophorodon) obtusum* Qiao: Chen et al., 2015: 557,563.

**Specimens examined.** Two apterous viviparous females and four fundatrices (holotype and paratypes), CHINA: Sichuan (Luding County, Minya Konka), 16.V.2009, No. 22562-1-3-1, on *Salix* sp., coll. X.M. Su; one apterous viviparous female (slide) and one apterous viviparous (COI: OK668441), Sichuan (Luding County, Minya Konka), 30.IX.2019, No. 47777-1-2, on *Cotoneaster* sp., coll. J.F. Ji.

**Comments.** The species have been collected on *Salix cupularis* in May (Chen et al. 2015) and on *Cotoneaster* sp. in September. The population on *Cotoneaster* sp. is without marginal processes, which differs from ones on *Salix cupularis* in morphological characteristics. However, the DNA sequences of the samples from both host plants are aligned 100% and other characters are similar between the two populations; therefore, there are two different host plant morphs in this species.

*Aspidophoron* being neuter, the adjectival specific epithet is also neuter, so *obtusus* is revised as *obtusum*.

**Host plant.** *Salix cupularis*, *Cotoneaster* sp. (Rosaceae).

**Distribution.** China: Sichuan.

**Biology.** The species colonizes the undersides of leaves of its host plants (Fig. 21G). The life cycle is unknown.

***Aspidophorodon reticulatum* Qiao & Xu, sp. nov.**

<http://zoobank.org/9A45D20A-071D-4EAA-8AA9-8ED1FA4867A7>

Figs 8–9, Table 2

**Specimens examined. Holotype:** apterous viviparous female, CHINA: Tibet (Cuona County), 5.VI.2016, No. 37265-1-1, on *Salix cupularis*, coll. F. F. Niu; **Paratypes:**

one apterous viviparous female (slide) and one apterous viviparous female (COI: OK668435), No. 37265-1-2, with the same collection data as holotype.

**Diagnosis.** Dorsum of body with distinct reticulations that consist of small triangles arranged in polygons; median frontal tubercle distinctly protuberant, rectangular; antennal tubercles each with a cylindrical process at inner apex, higher than median frontal tubercle; dorsal setae of abdomen sparse and short, with small setal tubercles.

**Description.** Apterous viviparous females: body elliptical (Fig. 9A), green in life.

**Mounted specimens.** Body pale, PT, distal part of rostrum, tarsi, distal parts of SIPH, cauda, anal plate and genital plate pale brown (Fig. 9A). Thoracic nota and abdominal tergites I–VIII each with one pair of spinal sclerites, pale brown in color, other parts pale in color (Fig. 9A, F). See Table 2 for general measurements.

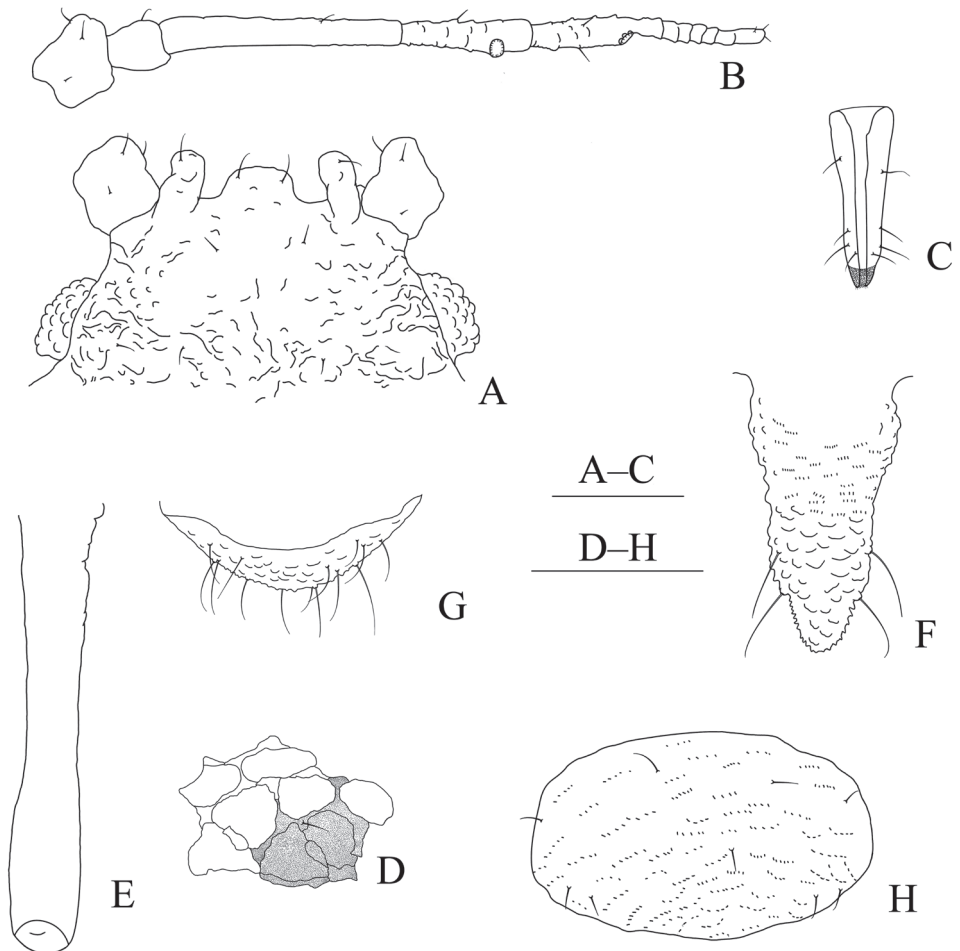


**Figure 8.** *Aspidophorodon reticulatum* Qiao & Xu, sp. nov. Apterous viviparous female **A** dorsal view of head **B** antenna **C** ultimate rostral segment **D** reticulations formed by strings of small triangles arranged in polygons on abdominal tergites **E** siphunculus **F** cauda **G** anal plate **H** genital plate. Scale bars: 0.10 mm.

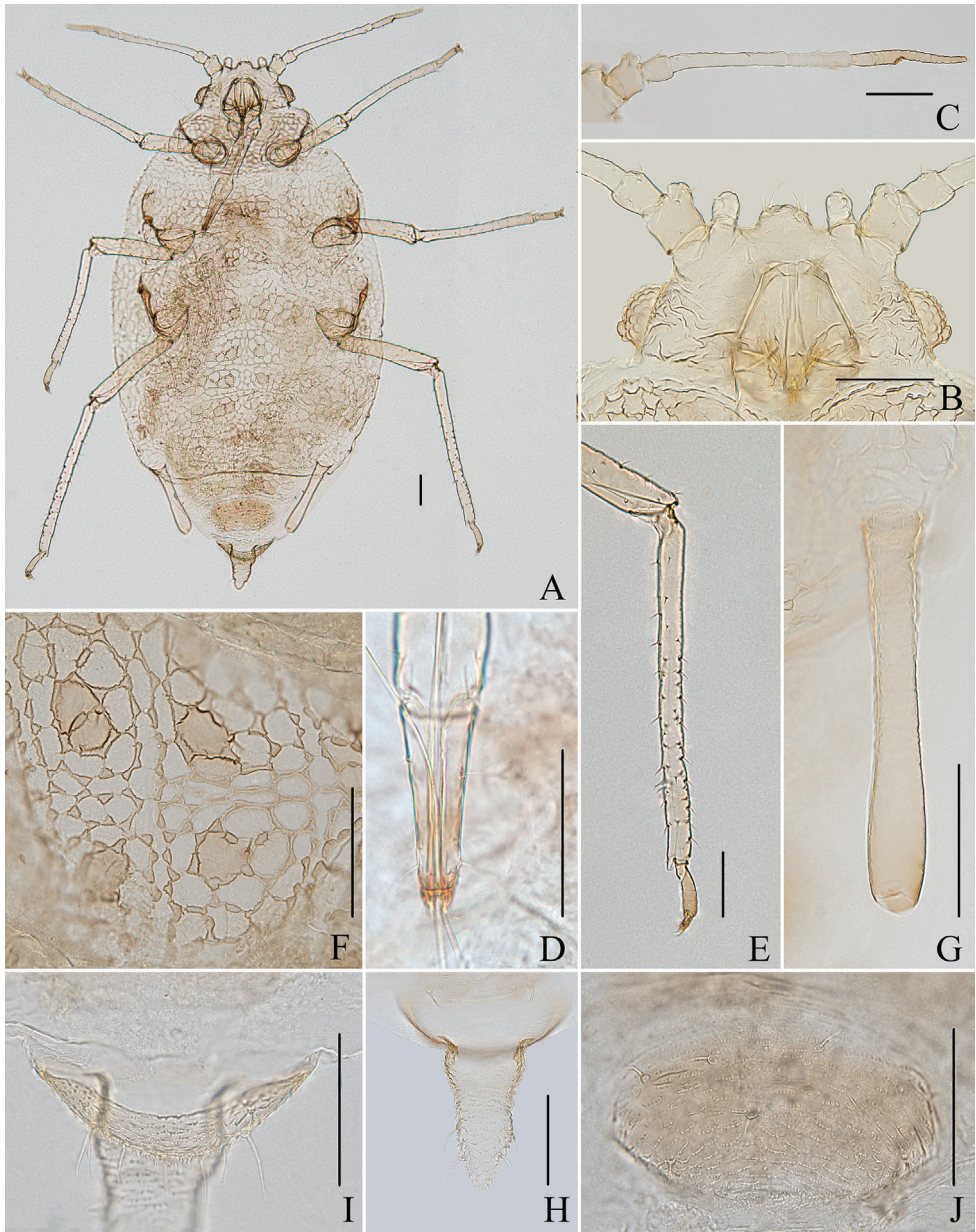


**Figure 9.** *Aspidophorodon reticulatum* Qiao & Xu, sp. nov. Apterous viviparous female **A** dorsal view of body **B** dorsal view of head **C** antenna **D** ultimate rostral segment **E** hind tibia and tarsi **F** reticulations formed by strings of small triangles arranged in polygons on abdominal tergites **G** siphunculus **H** cauda **I** anal plate **J** genital plate. Scale bars: 0.10 mm.

**Head.** Ocular tubercles small. Dorsum of head covered with wrinkles between compound eyes, anterior part with weak wrinkles (Figs 8A, 9B). Median frontal tubercle distinctly protuberant, rectangular (Figs 8A, 9B), with one pair of long and pointed setae on venter. Antennal tubercles undeveloped, each with a cylindrical, slightly wrin-

kled process at inner apex, higher than median frontal tubercle, each process with a short and pointed seta at apex (Figs 8A, 9B). Dorsal setae of head short and slightly blunt, with small setal tubercles. Head with one pair of cephalic setae, one pair of dorsal setae between antennae and two pairs of dorsal setae between compound eyes arranged transversely. Antennae 5-segmented, Ant. I–III smooth, Ant. IV–V with imbrications (Figs 8B, 9C); Ant. I slightly projected at inner apex. Antennal setae short and pointed, Ant. I–V with 3–4, 3, 1–2, 1, 1–2 (base) + 1 (PT) setae, respectively; apex of PT usually with two setae. Primary rhinaria ciliated. Rostrum reaching mid-coxae; URS wedge-shaped (Figs 8C, 9D), with two pairs of primary setae and two pairs of accessory setae.

**Thorax.** Thoracic nota with reticulations consist of small triangles arranged in polygons, those developed on pronotum. Dorsal setae of thorax short and blunt, with small setal tubercles; pronotum with two pairs of spinal setae, arranged anteriorly and posteriorly, one pair of pleural and one pair of marginal setae; meso- and metanotum each with one pair of spinal and one pair of pleural setae, two pairs of marginal setae. Legs normal, coxae and femora smooth, distal parts of tibiae imbricated. Setae on 2/3 distal part of femora and tibiae, short and pointed (Fig. 9E). First tarsal chaetotaxy: 3, 3, 2. Second tarsal segments with imbrications.

**Abdomen.** Abdominal tergites I–VII with reticulations consisting of small triangles arranged in polygons (Figs 8D, 9F). Dorsal setae of abdomen sparse, short, pointed or slightly blunt, with small setal tubercles; ventral setae short and pointed. Abdominal tergites I–III each with one pair of spinal, pleural and marginal setae; tergites IV–VII each with one pair of spinal and one pair of marginal setae; tergites VIII with one pair of spinal setae. Spiracles reniform and open, spiracular plates slightly swollen. SIPH spoon-shaped, smooth, broad at base, thin at middle, swollen distally, obliquely truncated at tip, without flange (Figs 8E, 9G). Cauda elongate conical, slightly constricted at middle, with spinulose imbrications and four setae (Figs 8F, 9H). Anal plate semi-circular, spinulose (Figs 8G, 9I), with 15–16 setae. Genital plate transversely oval, with sparse spinules in transverse rows (Figs 8H, 9J), with three or four anterior setae and four setae along the posterior margin.

**Etymology.** The species is named for the reticulations apparent on the dorsum of the body, *reticulatum* being the neuter form of the adjective.

**Taxonomic notes.** The new species resembles *A. harvense* Verma but differs from it as follows: antennal tubercles each with a cylindrical process at inner apex, 0.051–0.056mm, 1.82–2.04 × as long as its width (the latter: antennal tubercles each with a long finger-shaped process at inner apex, 0.110–0.120mm, 2.40–2.50 × as long as the basal width); dorsum of body with reticulations consist of small triangles arranged in polygons (the latter: dorsum of body with oval and irregular polygonal reticulations); URS 2.70–2.72 × as long as the basal width, 1.51–1.61 × as long as 2HT (the latter: URS 1.39–1.63 × as long as the basal width, 0.69–0.81 × as long as 2HT).

**Host plant.** *Salix cupularis*.

**Distribution.** China: Tibet.

**Biology.** The species colonizes the undersides of leaves of its host plant.

***Aspidophorodon salicis* Miyazaki, 1971**

*Aspidophorodon salicis* Miyazaki 1971: 183; Eastop and Hille Ris Lambers 1976: 96; Blackman and Eastop 1994: 569.

*Aspidophorodon sinisalicis* Zhang; Zhang and Zhong 1980: 58.

*Trichosiphonaphis lijiangensis* Zhang, Zhong and Zhang 1992: 389.

*Aspidophorodon (Aspidophorodon) salicis* Miyazaki; Remaudière and Remaudière 1997: 74; Stekolshchikov and Novgorodova 2010: 44; Chen et al. 2015: 567.

**Specimens examined.** Two alate viviparous females and 13 apterous viviparous females, CHINA: Yunnan (Lijiang City), 27.V.1980, No. 7165, on *Salix* sp., coll. T.S. Zhong and L.Y. Wang; two apterous viviparous females, CHINA: Gansu (Minxian County), 16.X.1985, No. 8326-1-4, on *Salix matsudana* var. *tortuosa*, coll. J.H. Li; four apterous viviparous females, CHINA: Xinjiang (Burqin County), 23.VII.2007, No. 20604, host plant unknown, coll. D. Zhang; four apterous viviparous females, CHINA: Ningxia (Jingyuan County, Mt. Liupan, altitude 1984 m), 26.VI.2008, No. 21540, on *Salix* sp., coll. J. Chen; one apterous viviparous female and one alate viviparous female, CHINA: Sichuan (Leshan City), 12.VI.2009, No. 23167, on *Salix* sp., coll. J. J. Yu and X. Y. Li; one apterous viviparous female, CHINA: Beijing (Mt. Baihua), 24.VIII.2015, No. 35920-1-1, on *Salix* sp., coll. H. Long; one apterous viviparous female, CHINA: Hebei (Mt. Wuling), 18.VII.2016, No. 37942-1-1, on *Salix* sp., coll. R.J. Zhang and S.F. Xu; two apterous viviparous females, CHINA: Shaanxi (Ankang City), 16.VII.2017, No. 41014-1-1, on Salicaceae, coll. H. Long and J.F. Ji; one apterous viviparous female, CHINA: Sichuan (Ganzi County), 18.VII.2017, No. 45762-1-1, on *Salix* sp., coll. J.F. Ji; one apterous viviparous female, CHINA: Sichuan (Mianyang City), 21.VII.2017, No. 41297-1-1, on *Salix* sp., coll. C. Gao; two apterous viviparous females (slides) and one apterous viviparous female (COI: OK668443), CHINA: Hebei (Mt. Xiaowutai), 6.V.2021, No. 49999-1-1, on *Salix* sp., coll. Y. Xu.

**Host plant.** *Polygonum* sp., *Salix pseudotangii*, *Salix udensis*, *Salix* sp.

**Distribution.** China (Beijing, Gansu, Ningxia, Sichuan, Shaanxi, Xinjiang, Yunnan), Japan, Russia (Sakhalin and the Kuril Islands).

**Biology.** This species colonizes the undersides of leaves of its host plant (Fig. 21H–J).

**Subgenus *Eoessigia* David, Rajasingh & Narayanan, 1972**

*Eoessigia* David, Rajasingh & Narayanan 1972: 35. Type species: *Eoessigia indicum* David, Rajasingh & Narayanan 1972; by original designation.

*Indotuberoaphis* Chakrabarti & Maity 1984: 198. Type species: *Indotuberoaphis sorbi* Chakrabarti & Maity 1984; by original designation.

*Margituberculatus* Zhang, Zhong & Zhang 1992: 381. Type species: *Margituberculatus longituberculatum* Zhang, Zhong & Zhang 1992; by original designation.

*Raychaudhuriella* Chakrabarti 1978: 355. Type species: *Raychaudhuriella myzaphoides* Chakrabarti 1978: 357; by original designation.  
*Aspidophorodon* (*Eoessigia*) David, Rajasingh & Narayanan: Remaudière and Remaudière 1997: 74; Stekolshchikov and Novgorodova 2010: 44; Nieto Nafría et al. 2011: 198; Chen et al. 2015.

**Comments.** Spinal processes at least present on abdominal tergite VIII; antennal tubercles each with an inconspicuous or finger-shaped process at inner apex; antenna 4–6 segmented; cauda with 4–11 setae; mainly on Rosaceae, sometimes on Salicaceae.

The subgenus contains eight species, including three new species. *Aspidophorodon* (*Eoessigia*) *indicum* (David, Rajasingh & Narayanan) is first recorded in China. *Aspidophorodon cornuatum* Qiao, 2015 is considered as a junior synonym of *Aspidophorodon longituberculatum* (Zhang, Zhong & Zhang, 1992), syn. nov., as discussed below. Species of this subgenus occur in Canada, China, India, and Russia (the Altai Republic).

#### Key to species of subgenus *Eoessigia* (based on apterous female viviparous)

- 1 SIPH shorter than cauda; PT more than 1.5 × as long as base of the segment ..... ***A. longicauda* (Richards)**
- SIPH longer than cauda; PT shorter than 1.5 × as long as base of the segment ..... **2**
- 2 Thoracic nota and abdominal tergites I–IV each with 1 pair of marginal processes ..... **3**
- Thoracic nota and abdominal tergites I–IV without marginal processes ..... **4**
- 3 Antennal tubercles each with a long finger-shaped process at inner apex; dorsum of head, thoracic nota and all abdominal tergites with paired or unpaired spinal processes; thoracic nota and abdominal tergites I–IV each with 1 pair of marginal processes ..... ***A. sorbi* (Chakrabarti & Maity)**
- Antennal tubercles each with a long horn-shaped process at inner apex; dorsum of head, thoracic nota and all abdominal tergites without spinal processes; thoracic nota and abdominal tergites I–IV each with 1 pair of long horn-shaped marginal processes ..... ***A. longituberculatum* (Zhang, Zhong & Zhang)**
- 4 Spinal processes present on abdominal tergites VII–VIII ..... ***A. vera* Stekolshchikov & Novgorodova**
- Spinal processes only present on abdominal tergite VIII ..... **5**
- 5 Median frontal tubercle strongly depressed at middle into two cylinders; abdominal tergite VIII produced caudad into triangular process ..... **6**
- Median frontal tubercle slightly depressed at middle; abdominal tergite VIII with conical spinal processes ..... **7**
- 6 Antennal tubercles each with a long finger-shaped process at inner apex, 0.077–0.095mm, higher than median frontal tubercle; rostrum reaching mid-coxae, URS 2.21–3.18 × as long as its width, 1.31–1.62 × as long as

- 2HT; triangular spinal processes on abdominal tergite VIII blunt at apex .....  
 .....*A. furcatum* Qiao & Xu, sp. nov.
- Antennal tubercles each with a short finger-shaped process at inner apex, 0.027–0.047 mm, as high as median frontal tubercle; rostrum reaching metacoxae, URS 3.28–3.42 × as long as its width, 1.56–1.92 × as long as 2HT; triangular spinal processes on abdominal tergite VIII constricted at apex .....  
 .....*A. longirostre* Qiao & Xu, sp. nov.
- 7 Antenna 5-segmented, 0.30–0.36 × as long as body length; antennal tubercles each with a weakly protuberant process at inner apex and slightly lower than median frontal tubercle; dorsum of head with distinct wrinkles between compound eyes, thoracic nota and abdominal tergites I–VII with slight wrinkles .....  
 .....*A. obtusirostre* Qiao & Xu, sp. nov.
- Antenna 6-segmented, 0.38–0.52 × as long as body length; antennal tubercles each with a short finger-shaped process at inner apex and lower than median frontal tubercle; dorsum of head with densely semicircular and wavy sculptures, thoracic nota and abdominal tergites I–VII with semicircular and wavy sculptures .....  
 .....*A. indicum* (David, Rajasingh & Narayanan)

***Aspidophorodon (Eoessigia) furcatum* Qiao & Xu, sp. nov.**

<http://zoobank.org/7BFCA822-1A5A-469E-8BD6-CE4531EA88AF>

Figs 10–12, 22A, B, Table 3

**Specimens examined. Holotype:** apterous viviparous female, CHINA: Sichuan (Ganzi City, Minya Konka, 29.55°N, 101.97°E, altitude 3617 m), 25.VII.2019, No. 45915-1-1, on *Salix* sp., coll. J.F. Ji. **Paratypes:** five apterous viviparous females (slides) and one apterous viviparous female (COI: OK668439), No. 45911-1-1, with the same collection data as holotype; two apterous viviparous females (slides) and one apterous viviparous female (COI: OK668438), CHINA: Sichuan (Luding County, Minya Konka), 20.VII.2019, No. 45884-1-1, on *Salix* sp., coll. J.F. Ji; one apterous viviparous female, CHINA: Sichuan (Luding County, Minya Konka), 22.VII.2019, No. 45896-1-1, on *Salix* sp., coll. J.F. Ji (NHMUK); one fourth instar apterous nymph, CHINA: Sichuan (Luding County, Minya Konka), 23.VII.2019, No. 45906-1-1, on *Salix* sp., coll. J.F. Ji; three fourth instar alate nymphs, CHINA: Sichuan (Luding County, Minya Konka), 27.IX.2019, No. 47741, on *Salix* sp., coll. J.F. Ji; three fourth instar alate nymphs, CHINA: Sichuan (Luding County, Minya Konka), No. 47737-1-2, on *Salix* sp., coll. J.F. Ji, two fourth instar alate nymphs CHINA: Tibet (Linshi City, 29.57°N, 94.57°E, altitude 3550 m), 30.VIII.2020, No. 49104-1-1, on *Salix* sp., coll. Y. Xu.

**Diagnosis.** Head dorsum covered with oval and wavy sculptures; median frontal tubercle well-developed, strongly imbricated, with a strong depression at middle separating it into two cylinders, hence fork-shaped; antennal tubercles each with a long finger-shaped and strongly imbricated process at inner apex, higher than median frontal tubercle; abdominal tergite VIII produced caudad into triangular spinal process

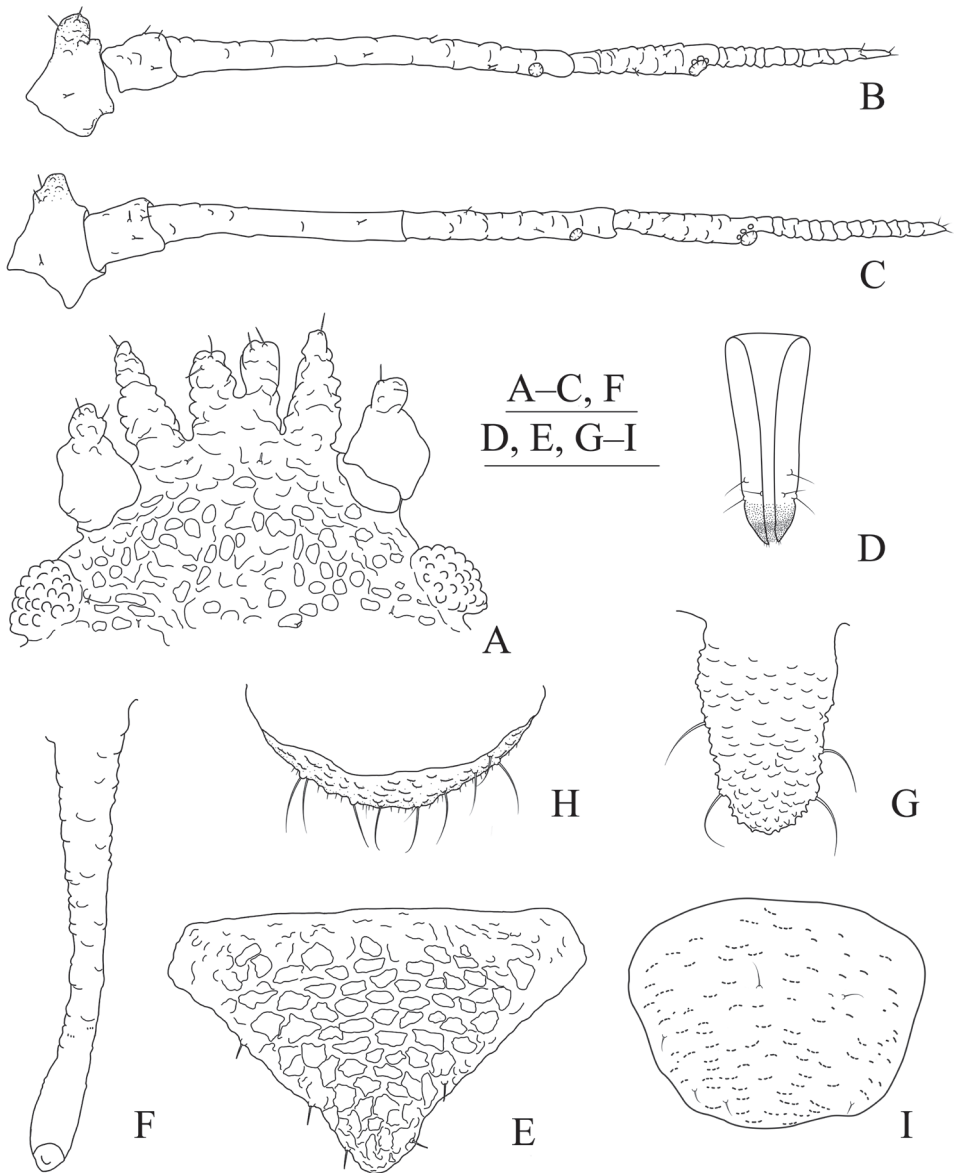


**Figure 10.** *Aspidophorodon (Eoessigia) furcatum* Qiao & Xu, sp. nov. Apterous viviparous female **A** dorsal view of head **B** antenna 4-segmented **C** antenna 5-segmented **D** ultimate rostral segment **E** spinal process of abdominal tergite VIII **F** siphunculus **G** cauda **H** anal plate **I** genital plate. Scale bars: 0.10 mm.

which reaches the end of the cauda and covered with distinctly irregular polygonal markings and marginal area with wavy sculptures.

**Description.** Apterous viviparous females: body broadly oval (Fig. 11A), yellowish in life (Fig. 22A, B).

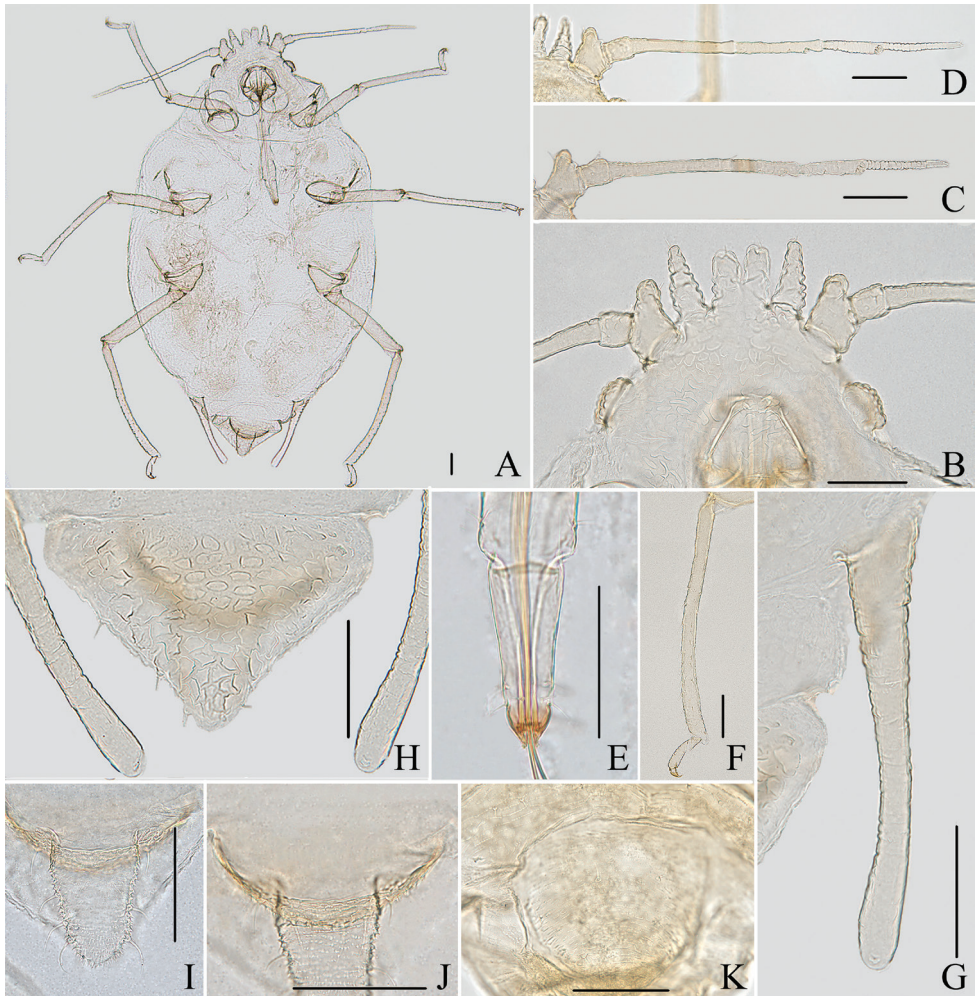


**Figure 11.** *Aspidophorodon (Eoessigia) furcatum* Qiao & Xu, sp. nov. Apterous viviparous female **A** dorsal view of body **B** dorsal view of head **C** antenna 4-segmented **D** antenna 5-segmented **E** ultimate rostral segment **F** hind tibia **G** siphunculus **H** spinal process of abdominal tergite VIII **I** cauda **J** anal plate **K** genital plate. Scale bars: 0.10 mm.

**Mounted specimens.** Body pale in color (Fig. 11A). See Table 3 for general measurements.

**Head.** Ocular tubercles small. Dorsum of head covered with oval and wavy sculptures, venter with wrinkles (Figs 10A, 11B). Median frontal tubercle well-developed, strongly imbricated, with a strong depression at the middle separating it into two cylinders, fork-shaped (Figs 10A, 11B), each cylinder with one pair of long and blunt setae at apex. Antennal tubercles undeveloped, each with a long finger-shaped, pointed, and strongly imbricated process at inner apex, higher than median frontal tubercle (Figs 10A, 11B), each process with a long and blunt seta at apex. Dorsal setae of head

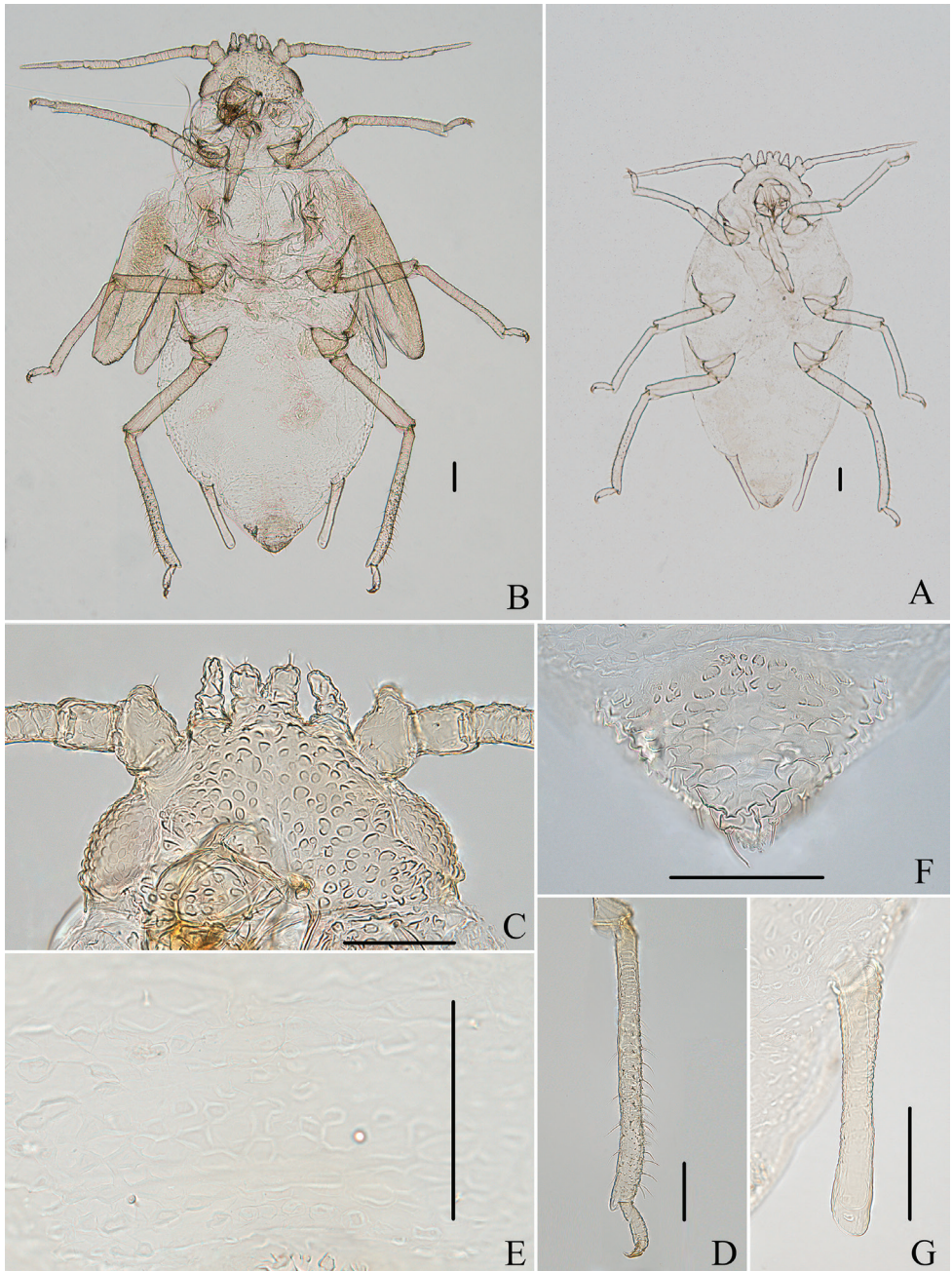


**Figure 12.** *Aspidophorodon (Eoessigia) furcatum* Qiao & Xu, sp. nov. **A** dorsal view of fourth instar apterous nymph. **B** dorsal view of body of fourth instar alate nymph. **C** dorsal view of head. **D** hind tibia and tarsi. **E** oval and wavy sculptures of abdominal tergites. **F** spinal process of abdominal tergite VIII. **G** siphunculus. Scale bars: 0.10 mm.

short and blunt, with small setal tubercles. Head with one pair of dorsal setae between antennae, and two pairs of dorsal setae between compound eyes arranged transversely. Antennae 4- or 5- segmented, Ant. I distinctly projected into short cylindrical at inner apex, 0.029–0.042mm, with two short and blunt setae at apex; Ant. I with slight wrinkles, other segments slightly imbricated (Figs 10B, C, 11C, D). Antennal setae short and blunt, Ant. I–V with 3 or 4, 3 or 4, 1 or 2, 1 or 2, 1–3 (base) +0 or 1 (PT) setae, respectively (or Ant. I–IV with 3 or 4, 3 or 4, 3 or 4, 2 or 3 (base) +1 (PT) setae, respectively), apex of PT with two or three setae. Primary rhinaria ciliated. Rostrum reaching mid-coxae, with apex pale brown; URS long wedge-shaped (Figs 10D, 11E), with three pairs of primary setae, and without accessory setae.

**Thorax.** Pronotum with oval and wavy sculptures on spino-pleural area, marginal area with wrinkles. Meso- and metanotum with wrinkles on marginal area, spino-pleural area smooth. Thoracic setae sparse, short and blunt, with small setal tubercles; pronotum with two pairs of spinal setae, arranged anteriorly and posteriorly, one pair of pleural and one pair of marginal setae; meso- and metanotum each with one pair of spinal, one pair of pleural, and two pairs of marginal setae. Legs normal, short; coxae and femora smooth, distal parts of tibiae slightly imbricated. Setae on 2/3 distal part of femora and tibiae, short and blunt; hind tibiae with a row of short and blunt setae dorsally on the middle (Fig. 11F). First tarsal chaetotaxy: 3, 3, 2. Second tarsal segments slightly imbricated.

**Abdomen.** Abdominal tergites I–VII with wrinkles on marginal area, spino-pleural area smooth; tergite VIII with irregular polygonal markings and marginal area with wavy sculptures, produced caudad into triangular spinal process reaching the end of the cauda (Figs 10E, 11H). Venter of abdominal tergites III–VIII with fine spinules arranged in rows. Dorsal setae of abdomen short and blunt, with small setal tubercles, ventral setae short and pointed. Abdominal tergites I and II each with one pair of spinal, one pair of pleural and one pair of marginal setae; tergites III–VII each with one pair of spinal and marginal setae; tergite VIII with five or six setae at margin. Spiracles reniform, open; spiracular plates slightly swollen. SIPH long spoon-shaped, incurved inward, broad at base, thin at the middle, slightly swollen distally, with imbrications, distal 1/4 smooth, obliquely truncated at tip, without flange (Figs 10F, 11G). Cauda wide tongue-shaped, slightly constricted at the middle, with spinulose imbrications and four or five setae (Figs 10G, 11I). Anal plate semicircular, spinulose (Figs 10H, 11J), with 11–14 setae. Genital plate broadly round, with sparse spinules in transverse rows (Figs 10I, 11K), with two anterior setae and four setae along the posterior margin.

**Fourth instar apterous nymph.** As in apterous viviparous females except as follows (Fig. 12A): legs normal; femora and tibia imbricated at distal part, hind tibia with numerous spinules and imbrications on 2/3 distal part. Setae on 2/3 distal part of femora and tibiae, short and blunt; hind tibiae with long pointed setae dorsally and short pointed setae ventrally, and with a row of short, thick, and blunt setae dorsally on the middle.

**Fourth instar alate nymph. Mounted specimens:** body elongated oval and body pale in color (Fig. 12B). See Table 3 for general measurements.

**Head.** As in apterous viviparous females except as follows: dorsum of head with oval sculptures, more developed than apterous viviparous females (Fig. 12C). Antennae 6-segmented, Ant. I distinctly projected into short cylindrical at inner apex, 0.026–0.031 mm. Antennae setae short and blunt, Ant. I–IV with 4, 3–4, 1–2, 2–1, 1, 2–3 (base) +0 (PT) setae, respectively. Primary rhinaria ciliated, Ant. III–V each with 20 or 21, 8, 8 immature round secondary rhinaria.

**Thorax.** As in apterous viviparous females except as follows: pronotum with oval and wavy sculptures at anterior part, pleura-marginal area with wavy sculptures; meso- and metanotum with wrinkles at spinal area, pleura-marginal area with oval and wavy sculptures. Legs normal; femora imbricated at distal part, tibia scabrous and with imbrications, hind tibia with numerous spinules and imbrications on 2/3 distal part (Fig. 12D). Setae on legs short and pointed; hind tibiae with long pointed setae dorsally and short pointed setae ventrally, and with a row of short, thick and blunt setae dorsally on middle. First tarsal chaetotaxy: 3, 3, 3.

**Abdomen.** As in apterous viviparous females except as follows: dorsal sculptures more developed than apterous viviparous females; abdominal tergites I–VII with oval and wavy sculptures (Fig. 12E), those developed on marginal area; tergites VIII produced caudad into triangular spinal process with irregular polygonal sculptures posteriorly and scaly sculptures anteriorly, marginal area with wavy sculptures (Fig. 12F).

**Etymology.** The species is named for the median frontal tubercle with a strong depression at middle creating a fork, hence the neuter adjective *furcatum* in Latin.

**Taxonomic notes.** The new species resembles *A. indicum* (David, Rajasingh & Narayanan) in head with three processes on front; dorsum of head covered with distinctly oval and wavy sculptures; abdominal tergite VIII with a spinal tubercle; but differs from it as follows: median frontal tubercle well-developed, strongly imbricated, with a strong depression at the middle separating it into two cylinders, fork-shaped; antennal tubercles each with a long finger-shaped, pointed and strongly imbricated process at inner apex, higher than median frontal tubercle (the latter: median frontal tubercle protuberant rectangular and slightly depressed at the middle; antennal tubercles each with a short cylindrical and blunt process at inner apex, lower than median frontal tubercle); abdominal tergite VIII produced caudad into triangular process (the latter: abdominal tergite VIII with conical spinal process); dorsum of head covered with distinctly oval and wavy sculptures (the latter: dorsum of head with densely semi-circular and wavy sculptures).

The new species resembles *A. longirostre* Qiao & Xu, sp. nov. in having its median frontal tubercle well-developed, strongly imbricated, with a strong depression at the middle separating it into two cylinders; abdominal tergite VIII produced caudad into triangular spinal process; SIPH long spoon-shaped, incurved inward, obliquely truncated at tip, without flange; cauda wide tongue-shaped, slightly constricted at the middle; but differs from it as follows: median frontal tubercle well-developed, 0.063–0.077 mm; a long finger-shaped process at inner apex of antennal tubercles, 0.077–0.095 mm, higher than median frontal tubercle (the latter: median frontal tubercle protuberant, 0.025–0.046 mm; a finger-shaped process at inner apex of antennal

tubercles, 0.027–0.047, as high as median frontal tubercle); rostrum reaching mid-coxae, URS long wedge-shaped, 2.21–3.18 × as long as its width, 1.31–1.62 × as long as 2HT (the latter: rostrum reaching hind coxae, URS thin and long wedge-shaped, 3.28–3.42 × as long as its width, 1.56–1.92 × as long as 2HT); abdominal tergite VIII with irregular polygonal markings and marginal area with wavy sculptures, blunt at apex (the latter: abdominal tergite VIII with oval sculptures, constricted at apex).

**Host plant.** *Salix* sp.

**Distribution.** China (Sichuan, Tibet).

**Biology.** This species colonizes the undersides of leaves of its host plant (Fig. 22A, B).

***Aspidophorodon (Eoessigia) indicum* (David, Rajasingh & Narayanan, 1972)**

Figs 13–15, 22C–F, Table 3

*Eoessigia indicum* David, Rajasingh & Narayanan 1972: 35; Eastop and Hille Ris Lambers 1976: 188; Chakrabarti and Medda 1989: 133.

*Raychaudhuriella myzaphoides* Chakrabarti 1978: 357.

*Raychaudhuriella potentillae* Chakrabarti & Maity 1984: 202.

*Aspidophorodon (Eoessigia) indicum* (David, Rajasingh & Narayanan): Rемаудиере and Rемаудиере 1997: 74; Blackman and Eastop 2006: 1098; Stekolshchikov and Novgorodova 2010: 44; Chen et al. 2015.

**Specimens examined.** One apterous viviparous female, CHINA: Tibet (Yadong County), 17.VII.2014, No. 32675-1-1, host plant unknown, coll. J. Chen and X.C. Zhu; four apterous viviparous females, CHINA: Tibet (Cuona County), 01.VI.2016, No. 37202-1-1, No. 37204-1-1, No. 37205-1-1, No. 37208-1-1, on *Cotoneaster* sp., coll. F.F. Niu; two apterous viviparous females, CHINA: Tibet (Cuona County), 03.VI.2016, No. 37225-1-1, No. 37232-1-1, on *Cotoneaster* sp., coll. F.F. Niu; one apterous viviparous female, CHINA: Tibet (Cuona County), 04.VI.2016, No. 37243-1-1, on *Cotoneaster* sp., coll. F.F. Niu; two apterous viviparous females, CHINA: Tibet (Cuona County), 07.VI.2016, No. 37278-1-1, No. 37280-1-1, on *Cotoneaster* sp., coll. F.F. Niu; one apterous viviparous female, CHINA: Tibet (Cuona County), 24.VI.2016, No. 37403-1-1, on *Cotoneaster* sp., coll. F.F. Niu; two apterous viviparous females, CHINA: Tibet (Cuona County), 03.VI.2016, No. 37229-1-1, No. 37230-1-1, host plant unknown, coll. F.F. Niu; one alate viviparous female, CHINA: Tibet (Cuona County), 03.VI.2016, No. 37223-1-1, on *Cotoneaster* sp., coll. F.F. Niu; two apterous viviparous females (slides) and one apterous viviparous female (COI: OK668434), CHINA: Tibet (Jilong County), 31.VII.2021, No. 52024-1-1, on *Cotoneaster* sp., coll. Y. Xu; two fundatrices (slides) and one fundatrix (COI: OK668447), CHINA: Tibet (Jilong County), 01.VIII.2021, No. 52044-2-1, on *Cotoneaster* sp., coll. Y. Xu.

**Comments.** The species is here first recorded in China. After several surveys in Tibet, we collected fundatrices (Figs 13A–D, 15A–L, 22F), apterous viviparous females (Figs 13E–L, 14A–J, 22C–E), and alate viviparous females (Figs 13M–Q, 14K–N)

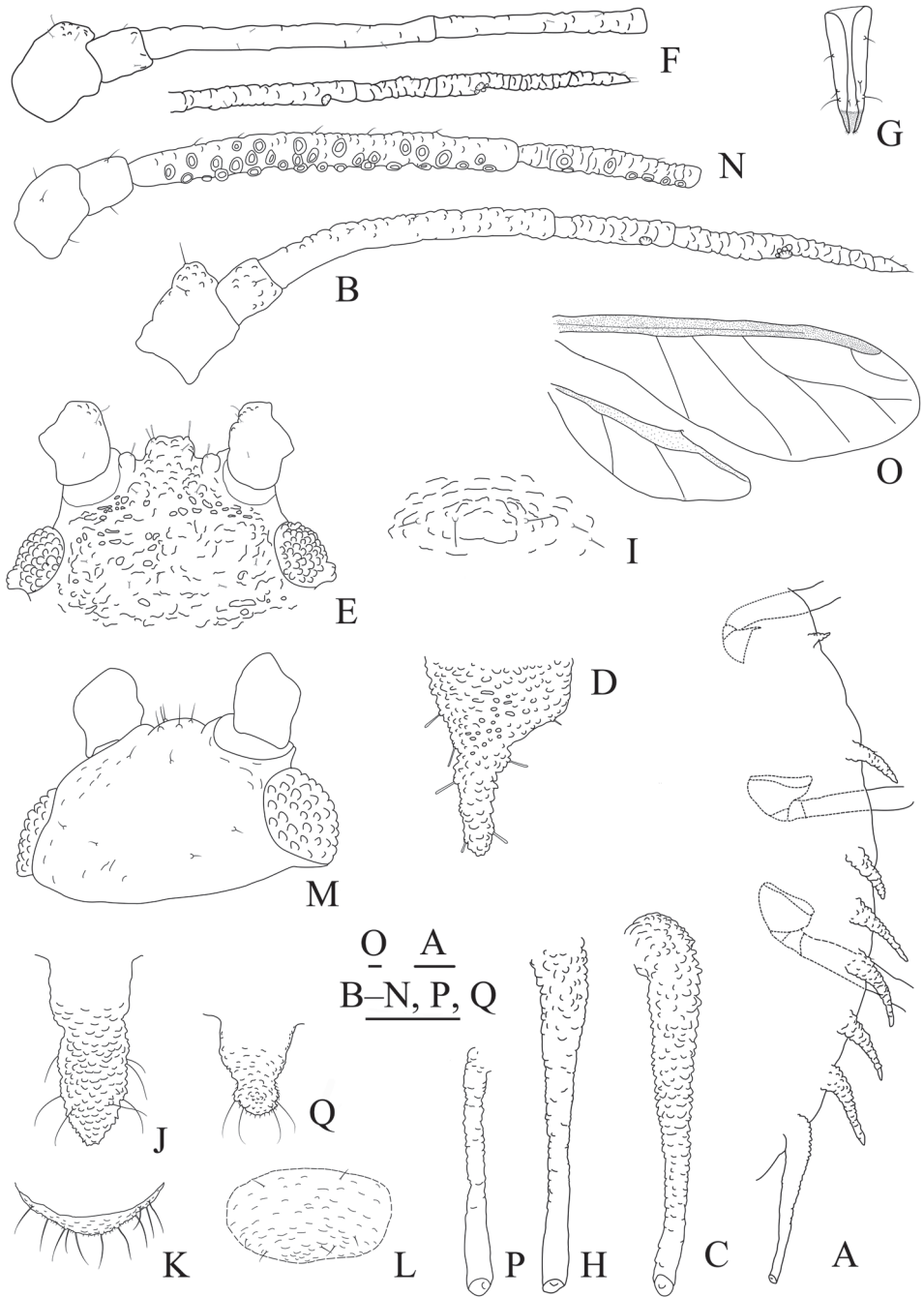


**Figure 13.** *Aspidophorodon (Eoessigia) indicum* (David, Rajasingh & Narayanan). Fundatrices **A** marginal processes of thoracic nota and abdominal tergites I–IV **B** antenna **C** siphunculus **D** spinal process of abdominal tergite VIII. Apterous viviparous female **E** dorsal view of head **F** antenna **G** ultimate rostral segment **H** siphunculus **I** spinal process of abdominal tergite VIII **J** cauda **K** anal plate **L** genital plate. Alate viviparous female **M** dorsal view of head **N** antennal segments I–IV **O** wings **P** siphunculus **Q** cauda. Scale bars: 0.10 mm.

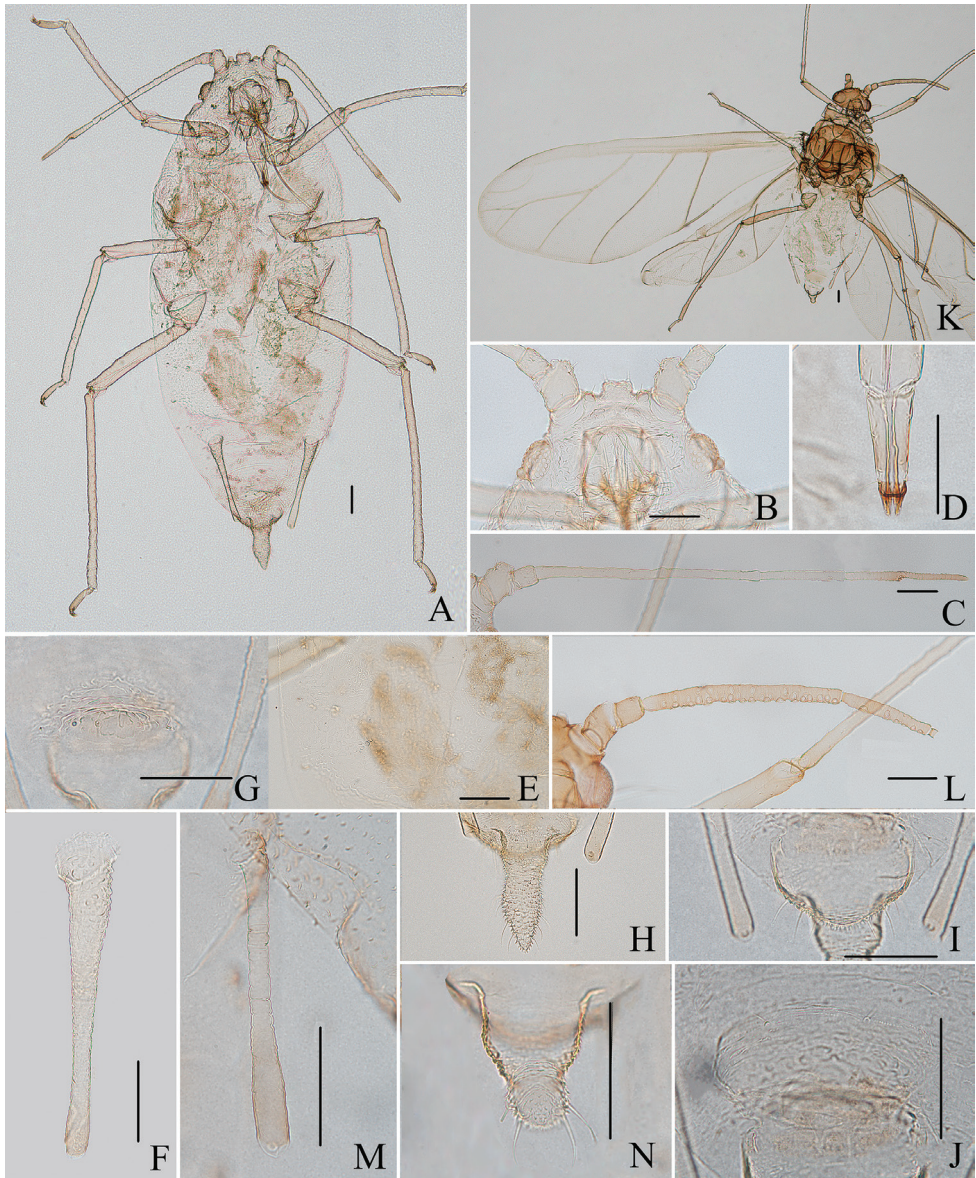


**Figure 14.** *Aspidophorodon (Eoessigia) indicum* (David, Rajasingh & Narayanan). Apterous viviparous female **A** dorsal view of body **B** dorsal view of head **C** antenna **D** ultimate rostral segment **E** sculptures of abdominal tergites **F** siphunculus **G** spinal process of abdominal tergite VIII **H** cauda **I** anal plate **J** genital plate. Alate viviparous female **K** dorsal view of body **L** antennal segments I–IV **M** siphunculus **N** cauda. Scale bars: 0.10 mm.

feeding on upper sides of *Cotoneaster* sp. along the main vein (Fig. 22C–F). The processes are variable in different morphs. Firstly, the marginal processes of thoracic nota and abdominal tergites I–IV (Figs 13A, 15E) and spinal process of abdominal tergite VIII (Figs 13D, 15I) are very developed in the fundatrix, but the apterae and alatae

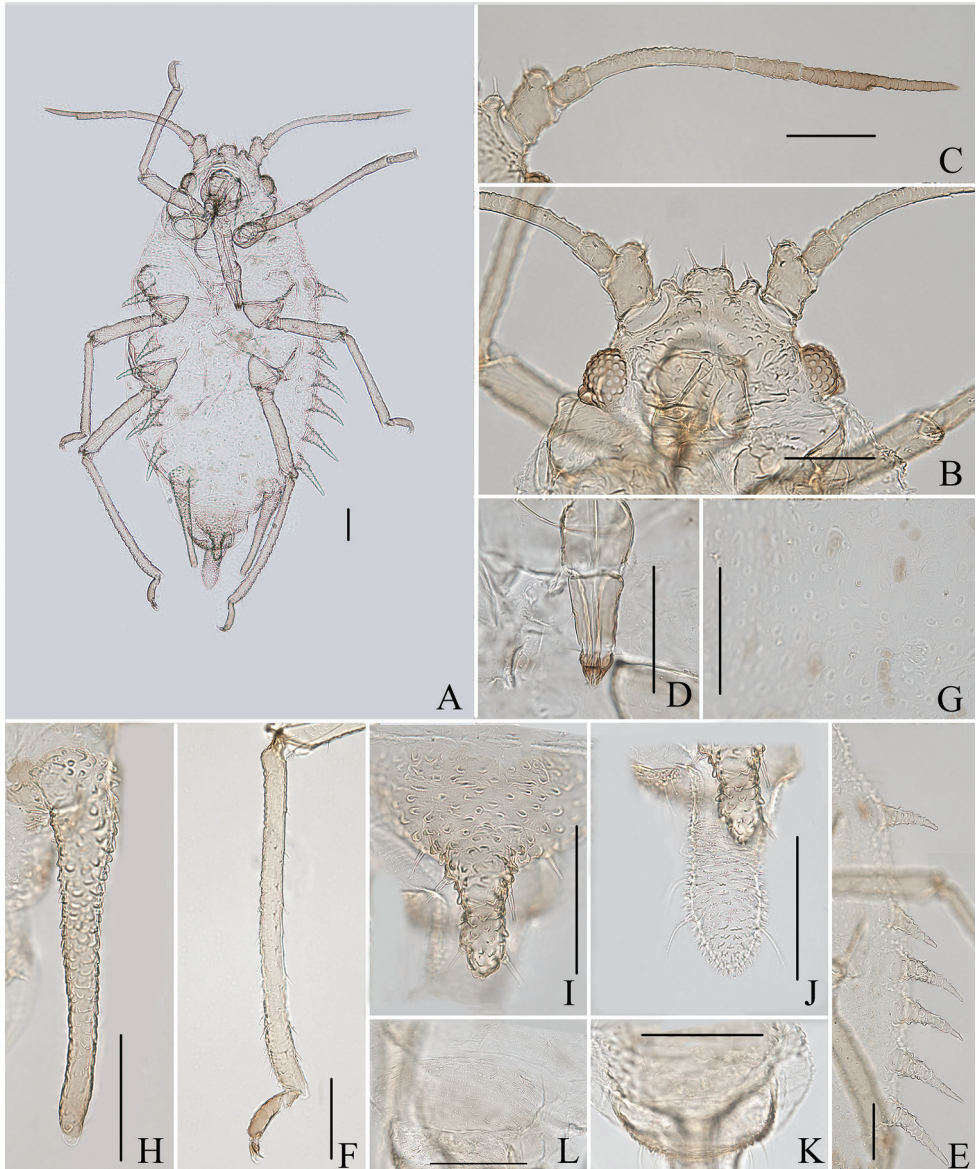


**Figure 15.** *Aspidophorodon (Eoessigia) indicum* (David, Rajasingh & Narayanan). Fundatrices **A** dorsal view of body **B** dorsal view of head **C** antenna **D** ultimate rostral segment **E** marginal processes of thoracic nota and abdominal tergites I–IV **F** hind tibia and tarsi **G** oval sculptures of abdominal tergites **H** siphunculus **I** spinal process of abdominal tergite VIII **J** cauda **K** anal plate **L** genital plate. Scale bars: 0.10 mm.

are without marginal processes, and spinal process of abdominal tergite VIII (Figs 13I, 14G) is shorter than that of the fundatrix. Secondly, about the different geographic populations of apterae, abdominal tergite VIII is with a distinctly triangular spinal process in a population from Jilong County; however, another population collected in Yadong County only has a slightly swollen spinal process.

*Aspidophoron* being neuter, the adjectival specific epithet is also neuter, so *indica* is revised as *indicum*.

**Host plant.** Primary host plants: *Cotoneaster obtusus* and *Cotoneaster* sp.; secondary host plant: *Potentilla* sp. (Chakrabarti and Medda 1989).

**Distribution.** China (Tibet), India.

**Biology.** The species colonizes on upper sides of *Cotoneaster* sp. along the main vein (Fig. 22C–F). The species is holocyclic and heteroecious, alternating between *Cotoneaster* and *Potentilla* (Chakrabarti and Medda 1989), and colonizes the undersides of *Potentilla* without ant-attendance (Chakrabarti and Maity 1984).

### *Aspidophorodon (Eoessigia) longicauda* (Richards, 1963)

*Aspidaphis longicauda* Richards 1963: 297.

*Eoessigia longicauda* Eastop & Hille Ris Lambers 1976: 95.

*Aspidophorodon (Eoessigia) longicauda* (Richards): Remaudière and Remaudière 1997: 74; Blackman and Eastop 2006: 1099; Stekolshchikov and Novgorodova 2010: 44.

**Host plant.** *Spiraea* sp.

**Distribution.** Canada.

**Biology.** The species occurs on the under surfaces of leaves of *Spiraea* sp. (Richards, 1963).

### *Aspidophorodon (Eoessigia) longirostre* Qiao & Xu, sp. nov.

<http://zoobank.org/FD1E0FEE-0054-4077-AA30-C90D6DA70956>

Figs 16–17, Table 3

**Specimens examined. Holotype:** apterous viviparous female, CHINA: Sichuan (Baoping City), 18.VIII.2003, No. 15089-1-2-1, on *Salix* sp., coll. K. Guo. **Paratypes:** two apterous viviparous females (slides) and one apterous viviparous female (COI: OK668432), No. 15089-1-1, with the same collection data as holotype (NHMUK).

**Diagnosis.** Dorsum of body covered with oval sculptures; median frontal tubercle well-developed, imbricated, with a strong depression at the middle into two cylinders; antennal tubercles each with a short finger-shaped and imbricated process at inner apex, lower than median frontal tubercle; rostrum reaching hind coxae, URS long wedge-shaped, long and thin; URS 3.28–3.42 × as long as its width, 1.56–1.92 × as long as 2HT; tergite VIII produced caudad into triangular spinal process reaching the middle of the cauda and constricted at apex and with distinctly oval sculptures.

**Description.** Apterous viviparous females: body elongated oval (Fig. 17A).

**Mounted specimens.** Body pale in color (Fig. 17A). See Table 3 for General measurements.

**Head.** Ocular tubercles small. Dorsum of head covered with oval sculptures, venter with wrinkles. Median frontal tubercle well-developed, imbricated, with a strong de-

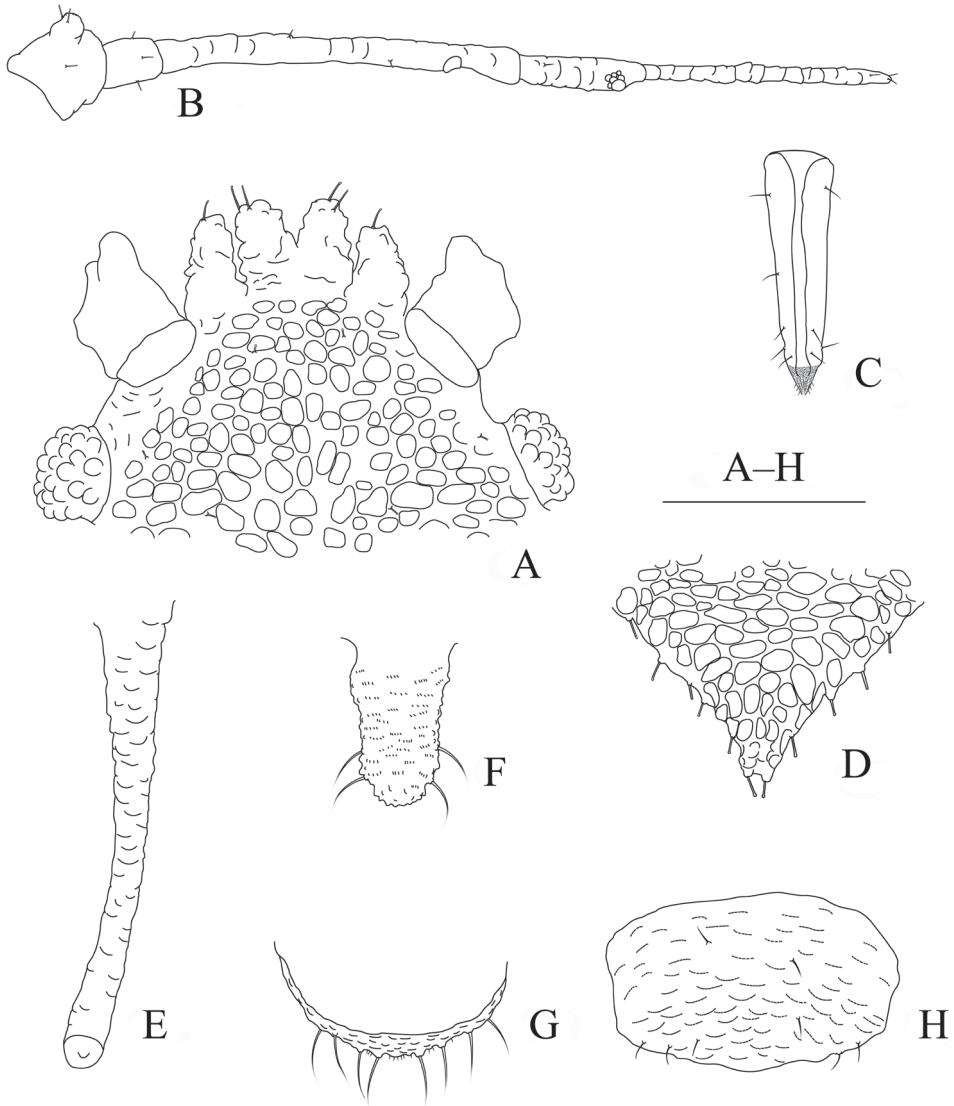


**Figure 16.** *Aspidophorodon (Eoessigia) longirostre* Qiao & Xu, sp. nov. Apterous viviparous female **A** dorsal view of head **B** antenna **C** ultimate rostral segment **D** spinal process of abdominal tergite VIII **E** siphunculus **F** cauda **G** anal plate **H** genital plate. Scale bars: 0.10 mm.

pression at middle separating it into two cylinders (Figs 16A, 17B), each cylinder with one pair of long and blunt setae at apex. Antennal tubercles undeveloped, each with a short finger-shaped and imbricated process at inner apex, the apex is blunt, as high as median frontal tubercle, each with a long and blunt seta at apex (Figs 16A, 17B). Dorsal setae of head short and capitate, with small setal tubercles. Head with one pair of dorsal setae between antennae, and two pairs of dorsal setae between compound eyes arranged transversely. Antennae 4-segmented, Ant. I distinctly projected into short cylindrical at

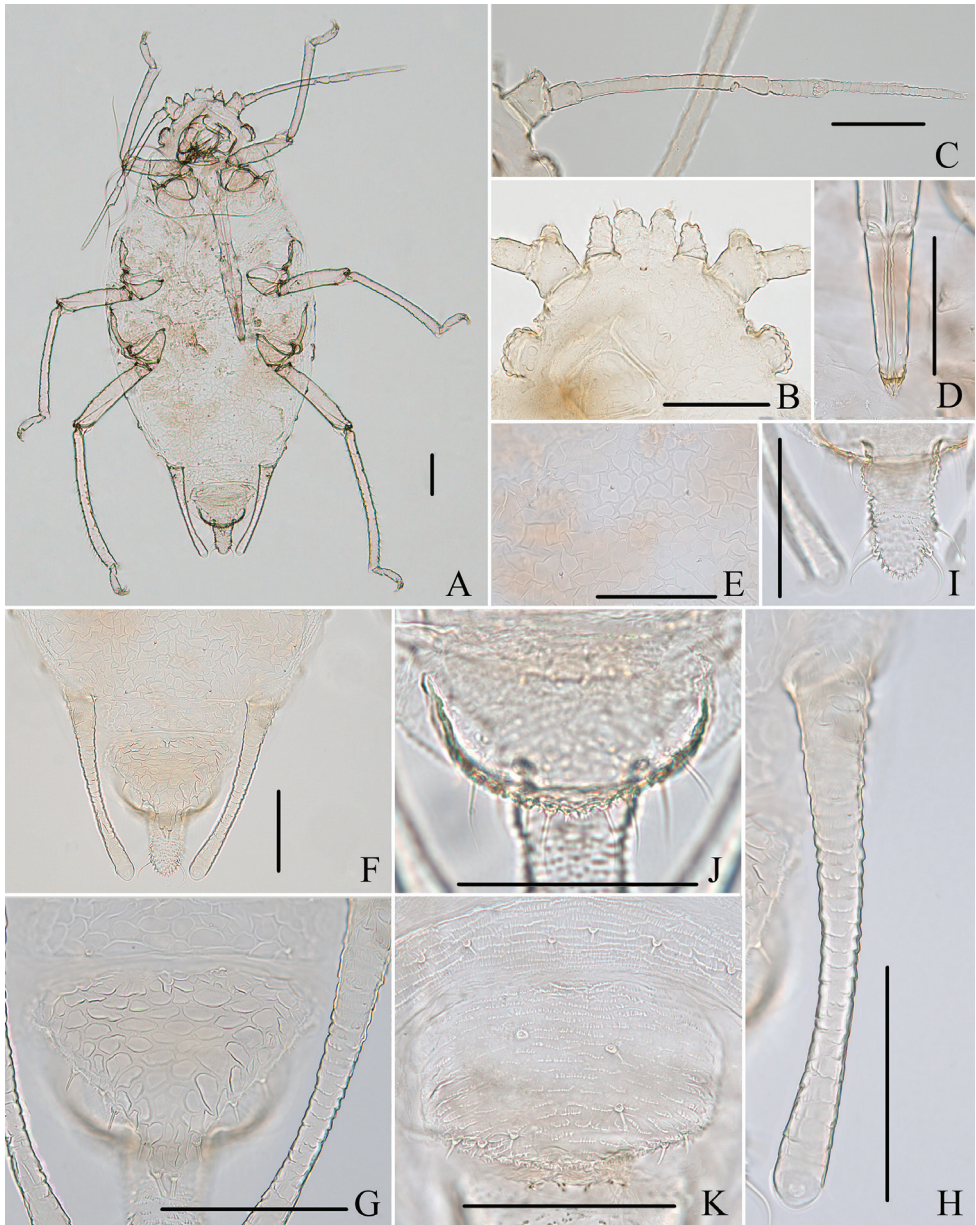


**Figure 17.** *Aspidophorodon (Eoessigia) longirostre* Qiao & Xu, sp. nov. Apterous viviparous female **A** dorsal view of body **B** dorsal view of head **C** antenna **D** ultimate rostral segment **E** oval and irregular polygonal sculptures of abdominal tergites **F** dorsal view of abdominal tergites V–VIII **G** spinal process of abdominal tergite VIII **H** siphunculus **I** cauda **J** anal plate **K** genital plate. Scale bars: 0.10 mm.

inner apex (Figs 16B, 17C), 0.014–0.023 mm, with two short and blunt setae at apex; Ant. I–II smooth, with slight wrinkles, Ant. III–IV with imbrications (Figs 16B, 17C). Antennal setae short and blunt, Ant. I–IV with 3–4, 3–4, 3–4, 1–3 (base) + 1 (PT) setae, respectively; apex of PT with two or three setae. Primary rhinaria unciliated. Rostrum

reaching hind coxae, with apex pale brown; URS long wedge-shaped, long, and thin (Figs 16C, 17D), with three pairs of primary setae and two or three accessory setae.

**Thorax.** Pronotum with oval and wavy sculptures; meso- and metanotum with oval sculptures on spinal area, pleura-marginal area with wavy and irregular polygonal sculptures. Thoracic setae sparse, short, blunt or capitate, with small setal tubercles; pronotum with two pairs of spinal setae, arranged anteriorly and posteriorly, one pair of pleural and one pair of marginal setae; meso- and metanotum each with one pair of spinal, one pair of pleural, and two pairs of marginal setae. Legs normal; coxae and femora smooth, distal parts of tibiae slightly imbricated. Setae on 2/3 distal part of femora and tibiae, short and blunt; hind tibiae with a row of short and blunt setae dorsally on middle. First tarsal chaetotaxy: 3, 3, 2. Second tarsal segments slightly imbricated.

**Abdomen.** Abdominal tergites I–VII with oval and irregular polygonal sculptures (Fig. 17F, G); tergite VIII with distinctly oval sculptures, produced caudad into triangular spinal process reaching the middle of the cauda and constricted at apex (Figs 16D, 17G). Abdominal ventral plate with fine spinules arranged in rows. Dorsal setae of abdomen short, capitate or blunt, with small bases, ventral setae short and pointed. Abdominal tergites I–II each with one pair of spinal, pleural, and marginal setae; tergites III–VII each with one pair of spino-pleural and one pair of marginal setae; tergite VIII with 9–12 setae at margin. Spiracles reniform, open; spiracular plates slightly swollen. SIPH long spoon-shaped, incurved inward, broad at base, thin at middle, slightly swollen distally, with distinct imbrications, obliquely truncated at tip, without flange (Figs 16E, 17H). Cauda wide tongue-shaped, slightly constricted at the middle, with spinulose imbrications and four setae (Figs 16F, 17I). Anal plate semicircular, spinulose (Figs 16G, 17J), with 11–14 setae. Genital plate broadly round, with sparse spinules in transverse rows (Figs 16H, 17K), with two anterior setae and 4–6 setae along the posterior margin.

**Fourth instar apterous nymph.** As in apterous viviparous females except as follows: legs normal; femora scabrous at distal part, and tibia with spinulose imbrications distributed on 2/3 distal part. Setae on legs short and blunt; hind tibiae with long pointed setae dorsally and short blunt setae ventrally, and with a row of short and blunt setae dorsally on the middle.

**Etymology.** The new species is named for its long URS, *longirostre* being the neuter form of the adjective.

**Taxonomic notes.** The new species resembles *A. indicum* (David, Rajasingh & Narayanan) in median frontal tubercle protuberant; dorsum of head covered with distinctly oval and wavy sculptures; abdominal tergite VIII with a spinal tubercle; but differs from it as follows: median frontal tubercle well-developed, imbricated, with a strong depression at the middle separating it into two cylinders, a finger-shaped and imbricated process at inner apex of antennal tubercles (the latter: median frontal tubercle protuberant rectangular and slightly depressed at the middle, a short cylindrical process at inner apex of antennal tubercles); abdominal tergite VIII produced caudad into triangular process (the latter: abdominal tergite VIII with conical spinal process); dorsum of head covered with oval sculptures (the latter: dorsum of head with densely semicircular and wavy sculptures).

**Table 3.** Morphometric data about species of the subgenus *Aspidophorodon* (*Eoessigia*) (in mm).

	<i>A. furcatum</i> Qiao & Xu, sp. nov.		<i>A. indicam</i> (David, Rajasingh & Narayanan)		<i>A. longirostre</i> Qiao & Xu, sp. nov.		<i>A. obusirostre</i> Qiao & Xu, sp. nov.		
	Apterous viviparous female (n = 8)	4 <sup>th</sup> alate nymph (n = 2)	4 <sup>th</sup> alate nymph (n = 2)	Apterous viviparous female (n = 10)	Alate viviparous female (n = 1)	Fundatrix (n = 2)	Apterous viviparous female (n = 3)	4 <sup>th</sup> alate nymph (n = 1)	Apterous viviparous female (n = 8)
Length (mm)									
Body length	1.969-2.218	1.519	1.623-1.728	1.740-2.528	1.861	1.717-1.790	1.136-1.487	1.076	1.102-1.468
Body width	0.997-1.166	0.716	0.720-0.746	0.721-1.041	0.644	0.730-0.770	0.514-0.708	0.508	0.600-0.714
Antennae									
Ant. I	0.646-0.766	0.566	0.688-0.692	0.752-1.193	/	0.645-0.660	0.451-0.568	0.296	0.389-0.484
Ant. II	0.078-0.082	0.064	0.065-0.070	0.075-0.099	0.090	0.087-0.089	0.047-0.059	0.035	0.054-0.059
Ant. III	0.042-0.055	0.045	0.057-0.059	0.046-0.060	0.063	0.046-0.047	0.033-0.037	0.034	0.034-0.040
Ant. IV	0.164-0.305	0.244	0.152-0.158	0.171-0.324	0.410	0.239	0.185-0.259	0.160	0.093-0.144
Ant. IVb	0.127-0.162	/	0.079-0.094	0.105-0.221	0.191	0.094-0.097	/	/	0.056-0.080
Ant. IVb	/	0.092	/	/	/	/	0.055-0.087	0.067	/
Ant. V	/	/	0.112-0.015	0.121-0.201	/	/	/	/	0.074-0.084
Ant. Vb	0.093-0.120	/	0.085-0.088	/	/	0.096-0.097	/	/	/
Ant. Vlb	/	/	/	0.101-0.143	/	/	/	/	/
PT	0.113-0.166	0.121	0.122-0.124	0.119-0.165	/	0.082-0.092	0.119-0.132	0.101	0.076-0.089
URS	0.115-0.129	0.107	0.104-0.112	0.096-0.132	0.118	0.094-0.100	0.123-0.128	0.122	0.054-0.066
Hind femur	0.346-0.412	0.275	0.296-0.310	0.341-0.556	0.505	0.328-0.339	0.207-0.297	0.193	0.197-0.299
Hind tibia	0.577-0.680	0.463	0.464-0.481	0.641-1.015	0.992	0.547-0.567	0.366-0.480	0.337	0.333-0.425
2HT	0.071-0.094	0.078	0.072-0.077	0.104-0.124	0.117	0.080-0.083	0.064-0.082	0.071	0.071-0.088
SIPH	0.325-0.415	0.251	0.214-0.237	0.314-0.432	0.271	0.398-0.401	0.240-0.294	0.210	0.024-0.028
BW SIPH	0.047-0.059	0.047	0.041-0.042	0.059-0.076	0.033	0.050-0.062	0.039-0.048	0.039	0.046-0.052
MW SIPH	0.024-0.032	0.023	0.025-0.040	0.020-0.026	0.018	0.033-0.041	0.016-0.018	0.018	0.017-0.021
DW SIPH	0.030-0.036	0.031	0.031-0.036	0.025-0.030	0.029	0.024-0.026	0.022-0.027	0.024	0.019-0.025
Cauda	0.093-0.128	/	/	0.179-0.246	0.106	0.167-0.170	0.084-0.095	/	0.161-0.129
BW Cauda	0.074-0.103	/	/	0.100-0.134	0.099	0.067-0.068	0.056-0.062	/	0.069-0.085
MW Cauda	0.056-0.065	/	/	0.047-0.069	0.039	0.048-0.054	0.041	/	0.052-0.066
Ant. IIIBD	0.027-0.038	0.039	0.031-0.034	0.026-0.033	0.033	0.028-0.030	0.017-0.022	0.021	0.019-0.022
Widest width of hind femur	0.062-0.069	0.064	0.056-0.058	0.057-0.072	0.059	0.062-0.068	0.044-0.051	0.050	0.053-0.151
MW hind tibia	0.033-0.040	0.044	0.037-0.041	0.029-0.037	0.027	0.034	0.024-0.027	0.031	0.023-0.029
Cephalic setae	0.012-0.017	0.012	0.015-0.016	0.020-0.028	0.026	0.029-0.030	0.010-0.017	0.015	0.031-0.038
Dorsal setae of head	0.007-0.010	0.007	0.006-0.007	0.004-0.006	0.011	/	0.005-0.007	0.006	/
Dorsal setae of head between antennae	/	/	/	0.004-0.009	0.011	0.017-0.025	/	/	0.030-0.035

Parts	<i>A. fuscitatum</i> Qiao & Xu, sp. nov.		<i>A. indicam</i> (David, Rajasingh & Narayanan)		<i>A. longirostre</i> Qiao & Xu, sp. nov.		<i>A. obusirostre</i> Qiao & Xu, sp. nov.			
	Apterous viviparous female (n = 8)	4 <sup>th</sup> apterous nymph (n = 1)	4 <sup>th</sup> alate nymph (n = 2)	Apterous viviparous female (n = 10)	Alate viviparous female (n = 1)	Fundatrix (n = 2)	Apterous viviparous female (n = 3)	4 <sup>th</sup> alate nymph (n = 1)	Apterous viviparous female (n = 8)	
Length (mm)	Dorsal setae of head between compound eyes									
	Marginal setae on Tergite I	/	/	0.004–0.008	0.009	0.010–0.012	/	/	0.009–0.011	
	Spinal setae on Tergite VIII	0.006–0.010	0.004	0.005–0.006	0.004–0.007	0.010	0.008	0.004–0.008	0.008–0.009	
	Setae on Ant. III	0.015–0.021	0.016	0.014–0.026	0.018–0.025	0.017	0.024–0.026	0.013–0.018	0.032–0.040	
	Setae on hind tibia	0.004–0.008	0.006	0.004–0.006	0.005–0.009	0.011	0.006–0.007	0.004–0.005	0.006–0.008	
	Processes on antennal tubercle	0.577–0.680	0.463	0.464–0.681	0.017–0.026	0.021	0.015–0.017	0.020–0.022	0.038	0.018–0.026
		0.077–0.095	0.061	0.068–0.073	0.020–0.029	/	/	0.027–0.047	0.028	/
		0.063–0.077	0.054	0.055–0.064	/	/	/	0.025–0.046	0.024	/
	Marginal process on pronotum	/	/	/	/	/	0.064	/	/	
	Marginal process on mesonotum	/	/	/	/	/	0.127–0.141	/	/	
	Marginal process on metanotum	/	/	/	/	/	0.133–0.165	/	/	
	Marginal process on Tergite I	/	/	/	/	/	0.192–0.206	/	/	
	Marginal process on Tergite II	/	/	/	/	/	0.195–0.196	/	/	
	Marginal process on Tergite III	/	/	/	/	/	0.175–0.208	/	/	
	Marginal process on Tergite IV	/	/	/	/	/	0.201–0.224	/	/	
Spinal process on Tergite VIII	0.161–0.175	0.847	/	/	/	0.209	0.112–0.139	0.117	0.022–0.061	
Body length / Body width	1.84–2.02	2.12	2.25–2.32	2.22–2.56	2.89	2.23–2.45	2.16–2.21	2.12	1.84–2.27	
Ratio (times)	Whole antennae / Body									
	Hind femur / Ant. III	0.31–0.36	0.37	0.40–0.42	0.38–0.52	/	0.36–0.38	0.37–0.40	0.37	0.30–0.35
	Hind tibia / Body	1.13–2.20	1.23	1.87–2.04	1.34–2.07	1.23	1.37–1.42	1.05–1.20	1.21	1.45–2.23
	Ant. I / Ant. III	0.28–0.31	0.31	0.28–0.29	0.37–0.43	0.53	0.31–0.33	0.31–0.32	0.31	0.24–0.30
	Ant. II / Ant. III	0.23–0.50	0.26	0.43–0.44	0.28–0.44	0.22	0.36–0.37	0.22–0.25	0.22	0.38–0.59
	Ant. IV / Ant. III	0.15–0.30	0.18	0.36–0.39	0.18–0.27	0.15	0.19–0.20	0.14–0.18	0.21	0.26–0.37
	Ant. V / Ant. III	0.66–0.88	/	0.50–0.62	0.47–0.70	0.47	0.39–0.41	/	/	0.40–0.67
	Ant. IVb, Vb or VIb / Ant. III	/	/	0.73–0.74	0.55–0.71	/	/	/	/	/
	PT / Ant. III	0.35–0.58	0.38	0.54–0.58	0.37–0.62	/	0.40–0.41	0.30–0.35	0.42	0.51–0.81
	PT / Ant. IVb, Vb or VIb	0.45–0.78	0.50	0.79–0.80	0.40–0.78	/	0.34–0.39	0.48–0.71	0.63	0.62–0.82
	URS / BW	1.10–1.57	1.32	1.39–1.46	0.93–1.34	/	0.85–0.95	1.37–2.38	1.51	0.98–1.25
	URS / BW	2.21–3.18	2.43	2.61–2.67	2.06–2.54	2.81	2.19–2.38	3.28–3.42	3.30	1.27–1.94

Parts	<i>A. fuscatum</i> Qiao & Xu, sp. nov.		<i>A. indicam</i> (David, Rajasingh & Narayanan)		<i>A. longirostre</i> Qiao & Xu, sp. nov.		<i>A. obusirostre</i> Qiao & Xu, sp. nov.		
	Apterous viviparous female (n = 8)	4 <sup>th</sup> apterous nymph (n = 1)	4 <sup>th</sup> alate nymph (n = 2)	Apterous viviparous female (n = 10)	Alate viviparous female (n = 1)	Fundatrix (n = 2)	Apterous viviparous female (n = 3)	4 <sup>th</sup> alate nymph (n = 1)	Apterous viviparous female (n = 8)
Ratio (times)									
URS / 2HT	1.31-1.62	1.37	1.44-1.45	0.89-1.10	1.01	1.13-1.25	1.56-1.92	1.72	0.70-0.84
SIPH / Body	0.16-0.19	0.17	0.13-0.14	0.16-0.21	0.15	0.22-0.23	0.20-0.21	0.20	0.16-0.23
SIPH / Cauda	2.62-3.88	/	/	1.70-2.05	2.56	0.34-0.40	2.86-3.09	/	1.51-1.93
SIPH / BW SIPH	5.70-7.62	5.34	5.10-5.78	5.23-6.44	8.21	6.42-8.02	6.13-6.69	5.39	4.88-5.51
SIPH / MW SIPH	10.16-15.71	10.91	5.93-8.56	13.08-20.85	15.06	9.71-12.15	14.12-17.56	11.67	11.85-14.35
SIPH / DW SIPH	9.03-12.57	8.10	5.94-7.65	11.63-14.60	9.35	15.31-16.71	10.89-12.22	8.75	10.36-12.84
Cauda / BW Cauda	1.07-1.49	/	/	1.65-2.18	1.07	2.46-2.54	1.50-1.53	/	1.67-2.04
Cephalic setae / Ant. IIIBD	0.37-0.57	0.31	0.47-0.48	0.61-0.91	0.79	0.97-1.07	0.59-0.77	0.71	1.41-2.00
Marginal setae on Tergite I / Ant. III BD	0.18-0.37	0.10	0.16-0.18	0.12-0.21	0.30	0.27	0.23-0.38	0.14	0.36-0.47
Spinal setae on Tergite VIII / Ant. III BD	0.53-0.60	0.41	0.45-0.77	0.55-0.77	0.52	0.86-0.87	0.76-0.86	0.76	1.52-2.11
Setae on Ant. III / Ant. IIIBD	0.13-0.28	0.15	0.13-0.17	0.17-0.28	0.33	0.20-0.25	0.18-0.29	0.29	0.27-0.38
Setae on hind tibia / MW hind tibia	0.51-0.68	0.91	0.93-1.16	0.53-0.70	0.78	0.44-0.50	0.74-0.88	1.23	0.62-0.90
Length of processes on antennal tubercle / its basal width	1.83-2.64	1.53	1.74-2.15	0.77-1.24	/	/	0.90-1.47	1.04	/
Length of median frontal tubercle / its basal width	0.97-1.24	0.93	0.87-1.60	/	/	/	0.56-0.90	0.45	/
Length of marginal process on pronotum / its basal width	/	/	/	/	1.94-2.00	/	/	/	/
Length of marginal process on mesonotum / its basal width	/	/	/	/	2.59-3.07	/	/	/	/
Length of marginal process on metanotum / its basal width	/	/	/	/	2.80-3.41	/	/	/	/
Length of marginal process on Tergite I / its basal width	/	/	/	/	3.03-3.43	/	/	/	/
Length of marginal process on Tergite II / its basal width	/	/	/	/	3.00-3.32	/	/	/	/
Length of marginal process on Tergite III / its basal width	/	/	/	/	3.37-3.53	/	/	/	/
Length of marginal process on Tergite IV / its basal width	/	/	//	/	3.24-3.25	/	/	/	/
Length of spinal process on Tergite VIII / its basal width	0.49-0.67	0.85	/	/	/	/	0.62-0.76	1.05	0.19-0.38

The new species resembles *A. furcatum* Qiao & Xu, sp. nov. in well-developed median frontal tubercle, with a strong depression at middle separating it into two cylinders; abdominal tergite VIII produced caudad into triangular spinal process; SIPH long spoon-shaped, curved inward; cauda wide, tongue-shaped, slightly constricted at the middle. The new species differs from *A. furcatum* as follows: median frontal tubercle protuberant, 0.025–0.046mm; a finger-shaped and blunt process at inner apex of antennal tubercles, 0.027–0.047mm, as high as median frontal tubercle (the latter: median frontal tubercle well-developed, 0.063–0.077mm; a long finger-shaped and pointed process at inner apex of antennal tubercles, 0.077–0.095mm, higher than median frontal tubercle); rostrum reaching hind coxae, URS 3.28–3.42 × as long as its width, 1.56–1.92 × as long as 2HT (the latter: rostrum reaching mid-coxae, URS 2.21–3.18 × as long as its width, 1.31–1.62 × as long as 2HT); abdominal tergite VIII with oval sculptures, constricted at apex (the latter: abdominal tergite VIII with distinctly irregular polygonal makings and marginal area with wavy sculptures, blunt at apex).

**Host plant.** *Salix* sp.

**Distribution.** China (Sichuan).

**Biology.** This species colonizes the undersides of leaves of its host plant.

***Aspidophorodon (Eoessigia) longituberculatum* (Zhang, Zhong & Zhang, 1992)**

Figs 18, 21B–E

*Margituberculatus longituberculatum* Zhang, Zhong & Zhang 1992: 382; Remaudière and Remaudière 1997: 117; Blackman and Eastop 2006: 1219.

*Aspidophorodon (Aspidophorodon) cornuatum* Qiao: Chen et al. 2015: 558. Syn. nov.

*Aspidophorodon (Eoessigia) longituberculatum* (Zhang, Zhong & Zhang): Chen et al. 2015: 570.

**Specimens examined.** One alate viviparous female (Holotype), CHINA: Yunnan (Lijiang City, Mt. Yulongxue, altitude 2900 m), 27.V.1980, No. 7165-1-1-1, on *Polygonum* sp., coll. T.S. Zhong and L.Y. Wang; Holotype and paratypes of *Aspidophorodon cornuatum* Qiao, 2015 syn. nov.: one apterous viviparous female, CHINA: Tibet (Yadong County, 27.52°N, 88.97°E, altitude 2800 m), 15.VIII.2010, No. 25908-2-3-1, on *Salix cupularis*, coll. Y. Wang; five apterous viviparous females, with the same collection data as holotype. Other materials: one alate viviparous female, CHINA: Tibet (Yadong County), 11.VII.2014, 32672-1-1, on *Salix* sp., coll. J. Chen and X.C. Zhu; two apterous viviparous females, CHINA: Tibet (Motuo County), 16.IX.2020, No. 49262-1-1, on *Salix* sp., coll. Y. Xu.; one apterous viviparous female and one alate viviparous female (slide), one apterous viviparous female (COI: OK668444), one alate viviparous female (COI: OK668445), CHINA: Tibet (Bomi County), 27.VI.2021, 51707-1-1, on *Salix* sp., coll. Y. Xu.

**Comments.** The species was erected in genus *Margituberculatus* based on only one alate viviparous female (Zhang et al. 1992). Then the species was removed to the genus *Aspidophorodon* as *Aspidophorodon longituberculatum* according to the characters

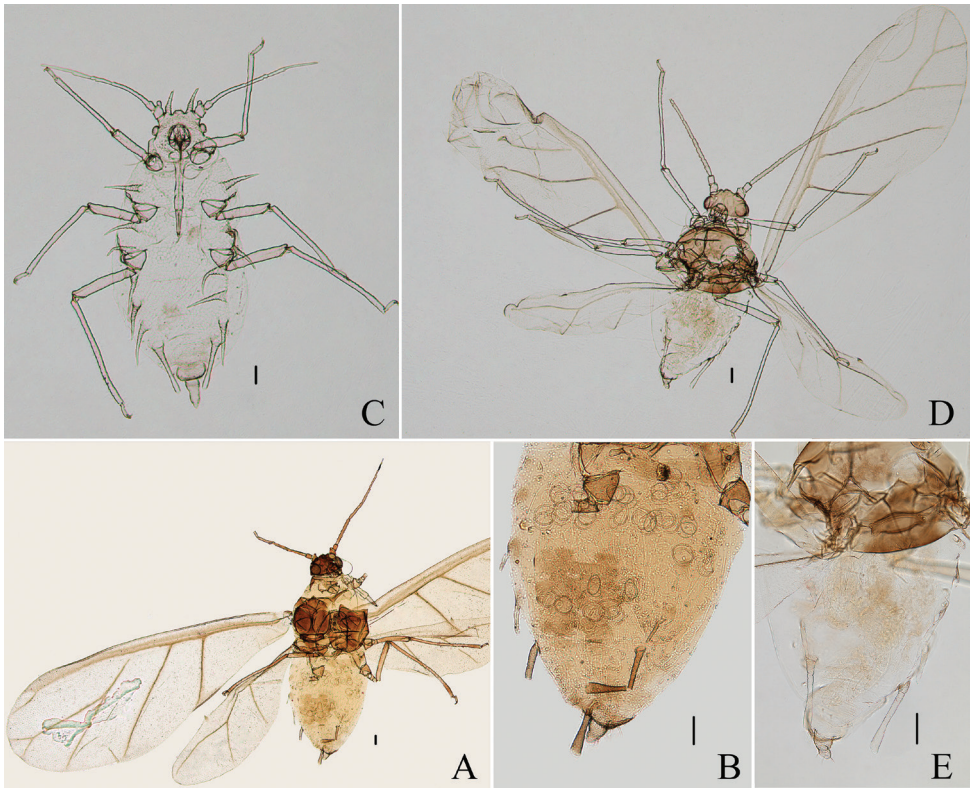


**Figure 18.** *Aspidophorodon* (*Eoessigia*) *longituberculatum* (Zhang, Zhong & Zhang, 1992). Alate viviparous female **A** dorsal view of body **B** dorsal view of abdomen. Apterous viviparous female **C** dorsal view of *Aspidophorodon cornuatum* Qiao, 2015 syn. nov. Alate viviparous female **D** dorsal view of *Aspidophorodon cornuatum* Qiao, 2015 syn. nov. **E** dorsal view of abdomen of *Aspidophorodon cornuatum* Qiao, 2015 syn. nov. Scale bars: 0.10 mm.

of processes and siphunculi; meanwhile, *Aspidophorodon cornuatum* was described as a new species (Chen et al. 2015). At that time, there were no alate viviparous females of *Aspidophorodon cornuatum*, so it was difficult to compare with the two species. After several surveys in southwest China, apterous viviparous female (Fig. 18C) and alate viviparous female (Fig. 18D) of *Aspidophorodon cornuatum* were collected. The alate viviparous female of *Aspidophorodon cornuatum* is with marginal processes on abdominal tergites I–IV (Fig. 18E) which is the same as *Aspidophorodon longituberculatum* (Fig. 18A, B). The molecular data of alate viviparous females of *Aspidophorodon longituberculatum* and apterous viviparous females of *Aspidophorodon cornuatum* support they are the same species (Fig. 23). So, *Aspidophorodon cornuatum* Qiao, 2015 should be considered as junior synonym of *Aspidophorodon longituberculatum* (Zhang, Zhong & Zhang, 1992).

*Aspidophoron* being neuter, the adjectival specific epithet is also neuter, so *longituberculatus* is revised as *longituberculatum*.

**Host plant.** *Salix cupularis*.

**Distribution.** China (Yunnan, Tibet).

**Biology.** The species occurs on the undersides of leaves along the main vein of host plants (Fig. 21B–E).

***Aspidophorodon (Eoessigia) sorbi* (Chakrabarti & Maity, 1984)**

*Indotuberoaphis sorbi* Chakrabarti & Maity 1984: 198; Blackman and Eastop 1994: 727; Remaudière and Remaudière 1997: 104.

*Aspidophorodon (Eoessigia) sorbi* (Chakrabarti & Maity): Stekolshchikov and Novgorodova 2010: 43.

**Host plant.** *Sorbus foliolosa*.

**Distribution.** India.

**Biology.** This species occurs on the undersides of young leaves of *Sorbus foliolosa*. No ant-attendance was noticed (Chakrabarti and Maity 1984).

***Aspidophorodon (Eoessigia) obtusirostre* Qiao & Xu, sp. nov.**

<http://zoobank.org/47423FD8-010A-4191-B9CA-A17C67273CB9>

Figs 19–20, Table 3

**Specimens examined.** *Holotype*: apterous viviparous female, CHINA: Beijing (Mt. Dongling, 40.03°N, 115.42°E, altitude 2063m), 24.VIII.2015, No. 35918-1-1; on *Potentilla* sp., coll. H. Long; *Paratypes*: five apterous viviparous females (slides) and one apterous viviparous female (COI: OK668433), 35918-1-2 with the same collection data as holotype; two apterous viviparous females, 35918-1-3, with the same collection data as holotype (NHMUK).

**Diagnosis.** Median frontal tubercle protuberant, rectangular, with a shallow depression at middle; antennal tubercles each with a low process at inner apex, lower than median frontal tubercle; rostrum reaching mid-coxae, URS wedge-shaped, short and blunt, 1.27–1.94 × as long as its width, 0.70–0.84 × as long as 2HT; cauda long tongue-shaped with 6–11 setae, including two pairs of very long and pointed setae and 2–7 short and pointed setae.

**Description.** Apterous viviparous females: body elongated oval (Fig. 20A), yellowish in life.

**Mounted specimens.** Body pale, PT, distal part of rostrum, tarsi, distal parts of SIPH and anal plate pale brown, other parts pale in color (Fig. 20A). See Table 3 for general measurements.

**Head.** Ocular tubercles small. Dorsum of head covered with wavy sculptures (Figs 19A, 20B), those distinctly developed between compound eyes. Median frontal tubercle protuberant, rectangular, with a shallow depression at middle

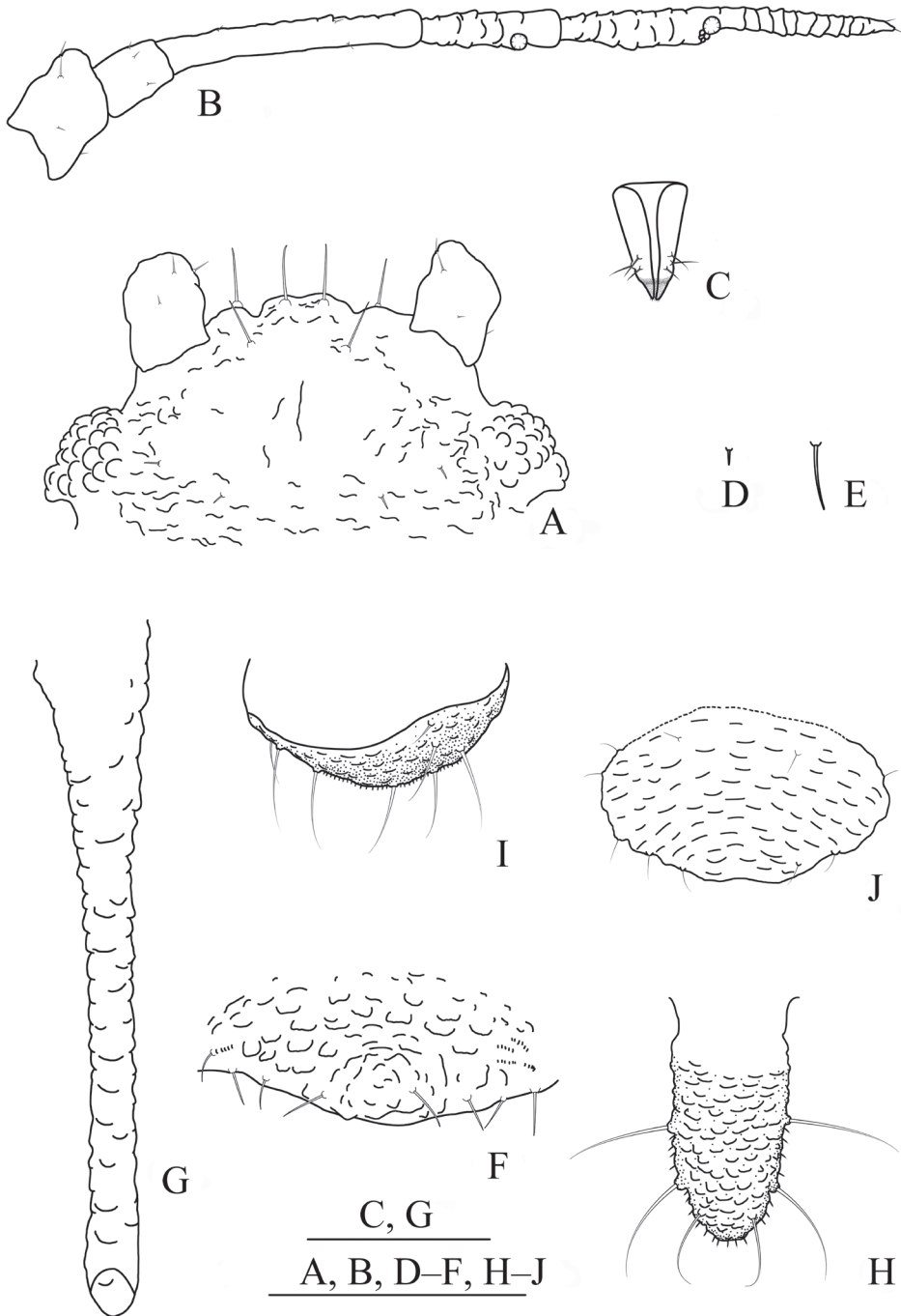


**Figure 19.** *Aspidophorodon* (*Eoessigia*) *obtusirostre* Qiao & Xu, sp. nov. Apterous viviparous female **A** dorsal view of head **B** antenna **C** ultimate rostral segment **D** marginal seta of abdominal tergite I **E** spinal seta of abdominal tergite VIII **F** spinal process of abdominal tergite VIII **G** siphunculus **H** cauda **I** anal plate **J** genital plate. Scale bars: 0.10 mm.

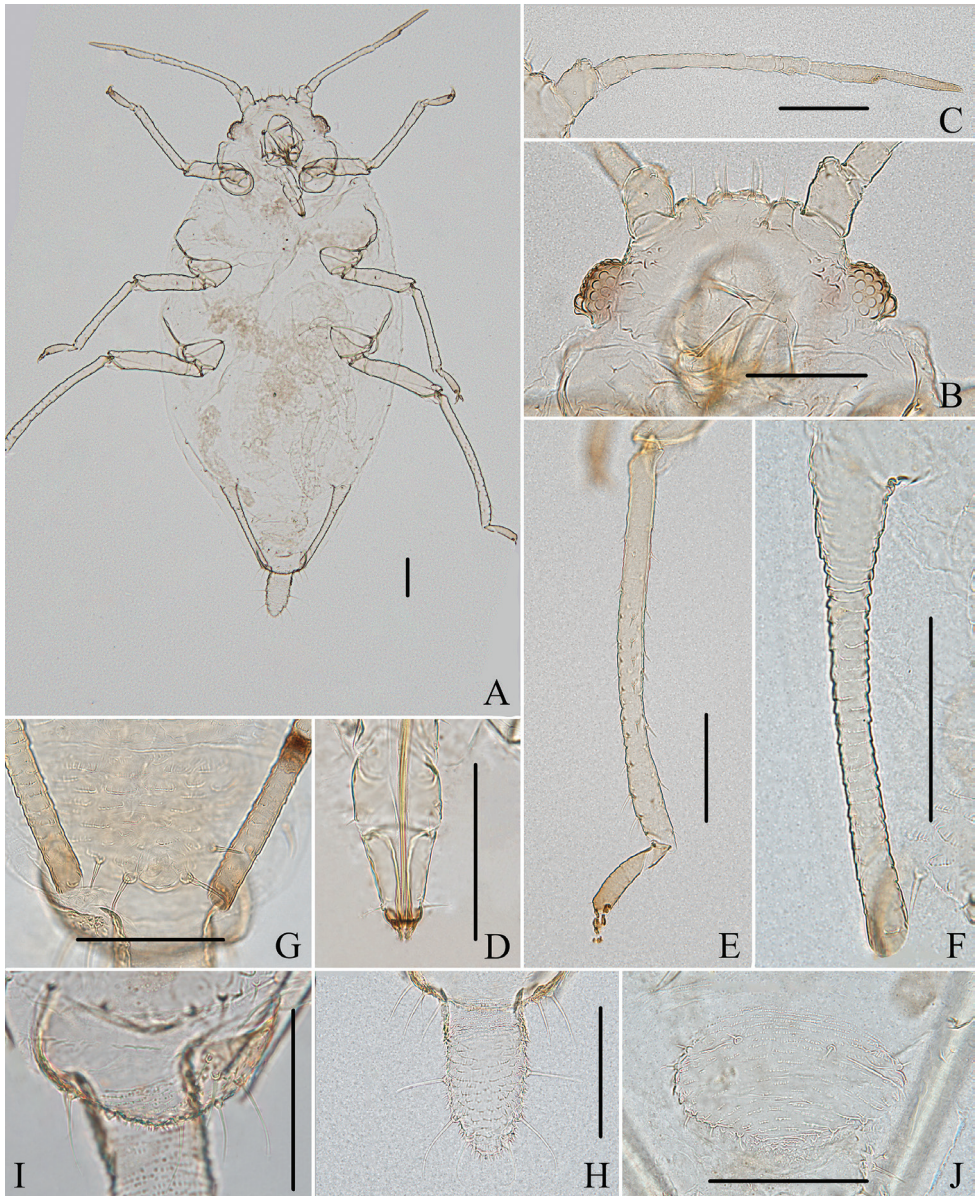


**Figure 20.** *Aspidophorodon (Eoessigia) obtusirostre* Qiao & Xu, sp. nov. Apterous viviparous female **A** dorsal view of body **B** dorsal view of head **C** antenna **D** ultimate rostral segment **E** hind tibia and tarsi **F** si-phunculus **G** spinal process of abdominal tergite VIII **H** cauda **I** anal plate **J** genital plate. Scale bars: 0.10 mm.

(Figs 19A, 20B), with one pair of thick and blunt setae on venter. Antennal tubercles undeveloped, each with a low process at inner apex, and lower than median frontal tubercle (Figs 19A, 20B), each process with a thick and blunt seta at apex, occasionally with two thick and blunt setae. Head with one pair of dorsal setae

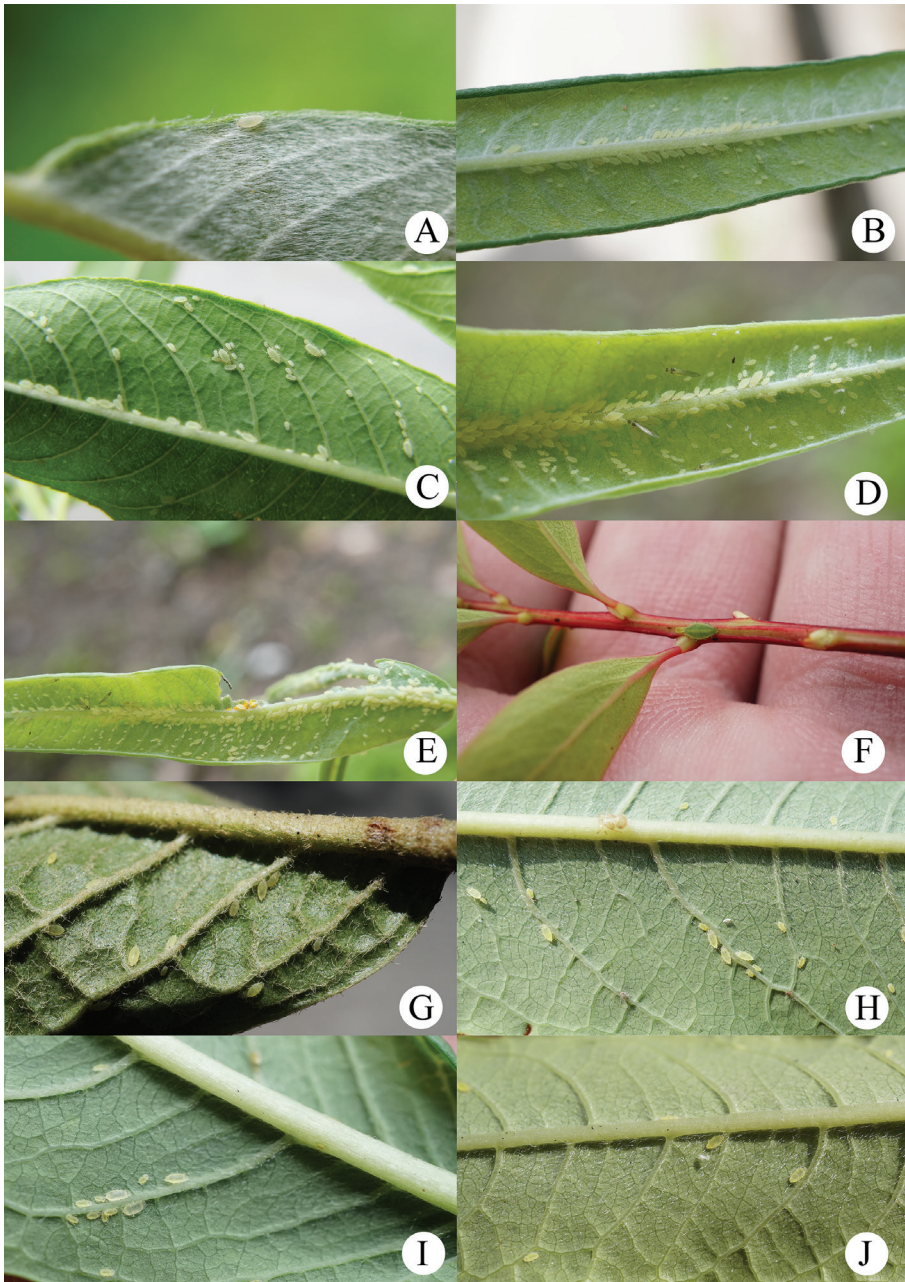


**Figure 21.** The ecological photos of *Aspidophorodon* in the field **A** an aptera of *Aspidophorodon capitatum* Qiao & Xu, sp. nov. on underside of leaf **B, C** the apterae and nymphs of *Aspidophorodon longituberculatum* (Zhang, Zhong & Zhang) on main veins and part lateral veins of underside of leaf **D, E** the apterae, alatae and nymphs of *Aspidophorodon longituberculatum* (Zhang, Zhong & Zhang) on main veins and part lateral veins of underside of leaves **F** an aptera and a nymph of *Aspidophorodon harvensis* Verma on a twig **G** the apterae of *Aspidophorodon obtusum* Qiao on underside of leaf **H–J** the apterae and nymphs of *Aspidophorodon salicis* Miyazaki on underside of leaf.

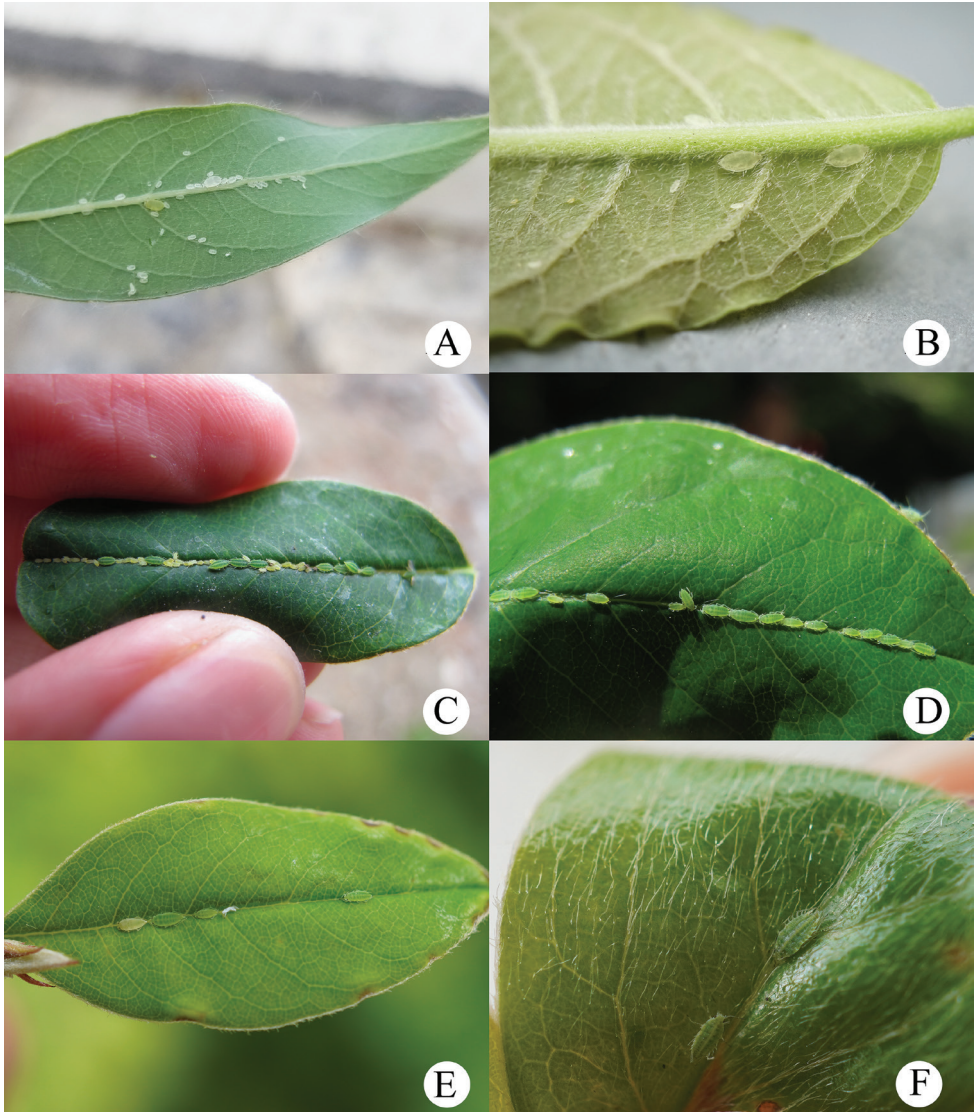


**Figure 22.** The ecological photos of *Aspidophorodon* in the field **A, B** the apterae and nymphs of *Aspidophorodon furcatum* Qiao & Xu, sp. nov. on undersides of leaves **C–E** the apterae and nymphs of *Aspidophorodon indicum* (David, Rajasingh & Narayanan) on main veins of upperside of leaves **F** the fundatrices of *Aspidophorodon indicum* (David, Rajasingh & Narayanan) on main vein of upperside of leaf.

between antennae, thick and blunt, and two pairs of dorsal setae between compound eyes arranged transversely, short and blunt. Antennae 5-segmented, Ant. I slightly projected at inner apex, Ant. I–III smooth, Ant. IV–V slightly imbricated (Figs 19B, 20C). Antennal setae short and blunt, Ant. I–V with 4–5, 3–4, 1–2, 0–2, 0–2 (base) +0–1 (PT) setae, respectively; apex of PT with two or three setae. Primary rhinaria ciliated. Rostrum reaching mid-coxae; URS wedge-shaped, short

and blunt (Figs 19C, 20D), with three pairs of primary setae, and without accessory setae.

**Thorax.** Prothorax nota with wrinkles, those developed on spino-pleural area. Meso- and metanotum with wrinkles on marginal area, spino-pleural area smooth. Thoracic setae sparse, short and blunt, with small setal tubercles; pronotum with two pairs of spinal setae, arranged in anterior and posterior pairs, one pair of pleural and one pair of marginal setae; meso- and metanotum each with one pair of spinal, one pair of pleural setae, two pairs of marginal setae, respectively. Legs normal, smooth. Setae on 2/3 distal part of femora and tibiae, short and blunt; hind tibiae with a row of short and blunt setae dorsally on the middle (Fig. 20E). First tarsal chaetotaxy: 3, 2, 2. Second tarsal segments slightly imbricated.

**Abdomen.** Abdominal tergites I–VII with wrinkles, those distinctly developed on marginal area; tergite VIII with scaly sculptures, swollen into conical spinal process, with 7–10 long, thick, and blunt setae at margin (Figs 19F, 20G). Venter of abdominal tergites III–VIII with fine spinules arranged in rows. Dorsal setae of abdominal tergites I–VI short, thick, and blunt (Fig. 19D), tergite VII long, thick, and blunt, occasionally short, thick, and blunt, tergite VIII long, thick, and blunt with distinct setal tubercles (Fig. 19E); ventral setae short and pointed. Abdominal tergites I and II each with one pair of spinal, pleural, and marginal setae; tergites III–VII each with one pair of spinal and marginal setae. Spiracles reniform, open or closed; spiracular plates slightly swollen. SIPH long spoon-shaped, broad at base, thin at the middle, swollen distally, with developed imbrications, obliquely truncated at tip, without flange (Figs 19G, 20F). Cauda long tongue-shaped, with spinulose imbrications, slightly constricted at base and weakly pointed at apex (Figs 19H, 20H); with 6–11 setae, including two pairs of very long and pointed setae, 0.055–0.061mm and 2–7 short and pointed setae, 0.027–0.041mm. Anal plate semicircular, spinulose (Figs 19I, 20I), with 8–13 setae. Genital plate transversely oval, with sparse spinules in transverse stripes (Figs 19J, 20J), with 4 or 5 anterior setae and 5–7 setae along the posterior margin.

**Etymology.** The new species is named for its short and blunt URS. The Latin word *obtus* means blunt, and *rostre* for rostrum, *obtusirostre* being the neuter form of the adjective.

**Taxonomic notes.** The new species resembles *A. indicum* (David, Rajasingh & Narayanan) in median frontal tubercle protuberant, rectangular; dorsal setae of head between antennal tubercles thick and blunt; abdominal tergite VIII with conical spinal process; SIPH long spoon-shaped; but differs from it as follows: dorsum of head covered with wavy sculptures, those distinctly developed between compound eyes, thoracic nota and abdominal tergites I–VII with wavy sculptures (the latter: dorsum of head with densely semicircular and wavy sculptures, thoracic nota, and abdominal tergites I–VII with semicircular and wavy sculptures); antennae 5-segmented, 0.30–0.36 × as long as body length (the latter: antennae 6-segmented, 0.38–0.52 × as long as body length); URS short and blunt, 1.27–1.94 × as long as the basal width, 0.70–0.84 × as long as 2HT (the latter: URS long wedge-shaped, 2.06–2.54 × as long as the basal width, 0.89–1.10 × as long as 2HT).

**Host plant.** *Potentilla* sp.

**Distribution.** China (Beijing).

**Biology.** The species colonizes the undersides of leaves of its host plant and with ant-attendance.

### *Aspidophorodon (Eoessigia) vera* Stekolshchikov & Novgorodova, 2010

*Aspidophorodon (Eoessigia) vera* Stekolshchikov & Novgorodova, 2010: 39.

**Host plant.** *Potentilla fruticosa*.

**Distribution.** Russia (the Altai Republic).

**Biology.** The species feeds along the margins on the underside of leaves of its host plant (Stekolshchikov and Novgorodova 2010).

### DNA barcoding

The final alignments of COI sequences consisted of 658 nucleotides, including 119 parsimony-informative sites. Pairwise sequence divergences of the gene among the *Aspidophorodon* species are presented in Table 4. The interspecific genetic distances of new species and known species averaged 6.98% (range: 3.93%–8.97%) for COI closely corresponding to the divergence of *Aspidophorodon* taxa base on four species (mean: 6.88%; range: 5.29%–7.68%) (Chen et al. 2015). The validity of species was well-supported on NJ tree (>95% bootstrap) (Fig. 23). At the same time, *Aspidophorodon cornuatum* and *Aspidophorodon longituberculatum* formed a clade (Fig. 23) and the genetic distance between the two species is 0.00%–0.46%, so the result proved *A. cornuatum* was a junior synonym of *A. longituberculatum*. However, the subgenera were not monophyletic groups on NJ tree, and this needs more evidence and more

**Table 4.** Kimura's two-parameter genetic distances among *Aspidophorodon* species samples based on COI.

	1	2	3	4	5	6	7	8	9	10	11	12	13
1. <i>A. capitatum</i> sp. nov.													
2. <i>A. cornuatum</i> syn. nov.	0.082												
3. <i>A. furcatum</i> sp. nov.	0.079	0.085											
4. <i>A. barvense</i>	0.069	0.058	0.072										
5. <i>A. indicum</i>	0.079	0.065	0.076	0.070									
6. <i>A. longicauda</i>	0.075	0.079	0.078	0.075	0.073								
7. <i>A. longicornutum</i> sp. nov.	0.069	0.070	0.064	0.054	0.072	0.066							
8. <i>A. longirostre</i> sp. nov.	0.077	0.075	0.056	0.062	0.070	0.070	0.056						
9. <i>A. longituberculatum</i>	0.080	0.005	0.085	0.057	0.066	0.080	0.069	0.076					
10. <i>A. musaicum</i>	0.074	0.060	0.077	0.065	0.081	0.075	0.072	0.076	0.061				
11. <i>A. obtusirostre</i> sp. nov.	0.076	0.067	0.079	0.057	0.052	0.078	0.070	0.074	0.067	0.084			
12. <i>A. obtusum</i>	0.074	0.050	0.064	0.062	0.074	0.078	0.069	0.081	0.047	0.065	0.081		
13. <i>A. reticulatum</i> sp. nov.	0.079	0.062	0.086	0.072	0.080	0.077	0.071	0.090	0.061	0.072	0.086	0.039	
14. <i>A. salicis</i>	0.079	0.074	0.088	0.073	0.072	0.071	0.063	0.064	0.073	0.068	0.086	0.075	0.085

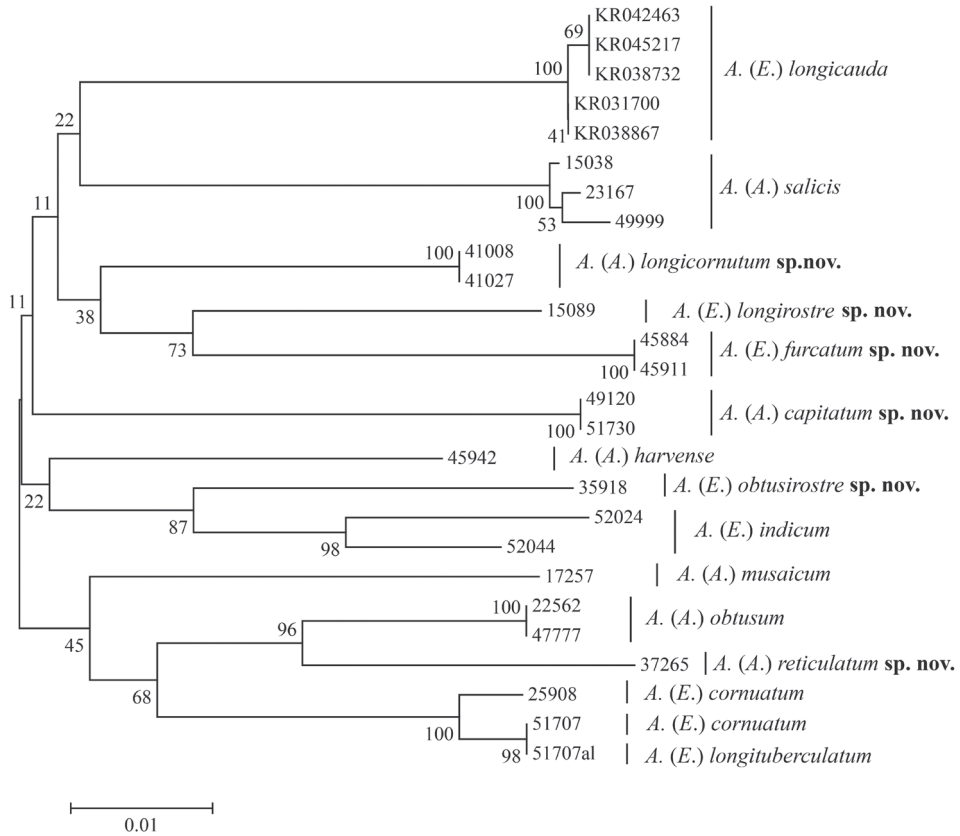


**Figure 23.** Neighbour-joining tree for *Aspidophorodon* samples based on COI sequences.

samples to prove. In this study, we also followed the traditional taxonomic system to divide two subgenera in *Aspidophorodon*. According to the distinct morphological characteristics in description and interspecific genetic distances between species, the six new species were supported.

## Discussion

The species in *Aspidophorodon* were identified by stable characters: the shape and variability of processes on the frons, the form of markings on the dorsum, the shape of the ultimate rostral segment, the sculptures on the siphunculi, and the shape of the cauda. Some species in the genus have developed spinal and marginal processes on the abdominal tergites. The presence or absence of the spinal and marginal processes on abdominal tergites are inconsistent within a species, but the shape of processes is consistent. *Aspidophorodon salicis* has short conical marginal processes on abdominal tergites I–IV in the fundatrix, whereas the apterous viviparous female and the alate viviparous

female are without such processes. The populations of *Aspidophorodon obtusum* feeding on *Salix* sp. have cylindrical marginal processes on abdominal tergites I–IV, while the ones feeding on *Cotoneaster* sp. have no marginal processes. *Aspidophorodon indicum* has long conical marginal processes on abdominal tergites I–IV and spinal processes on abdominal tergite VIII in the fundatrix, whereas the apterous viviparous female and the alate viviparous female have no marginal processes and shorter spinal processes on abdominal tergite VIII. Hence, the processes tend to reduce in size during the life of the colony. The median frontal tubercle, processes on antennal tubercles, and sculptures of the body are relatively stable to enable identification of the species.

## Acknowledgements

We express great thanks to all collectors for their assistance in aphid collection and to F.D. Yang for making slides. The work was supported by the National Natural Sciences Foundation of China (Grant Nos. 32030014, 31970451 and 31772492), the Key Collaborative Research Program of the Alliance of International Science Organizations (Grant No. ANSO-CR-KP-2020-04), the Second Tibetan Plateau Scientific Expedition and Research (STEP) program (Grant No. 2019QZKK05010601) and the Youth Innovation Promotion Association of Chinese Academy of Sciences (Grant No. 2020087).

## References

- Blackman RL, Eastop VF (1994) Aphids on the World's Trees. An Identification and Information Guide. CAB International, Wallingford, 987 pp.
- Blackman RL, Eastop VF (2006) Aphids on the World's Herbaceous Plants and Shrubs. John Wiley and Sons Ltd., Chichester, 1439 pp.
- Chakrabarti S (1978) A new genus and two new species of aphids (Homoptera: Aphididae) from north-west India. Zoological Journal of the Linnean Society 62(4): 355–363. <https://doi.org/10.1111/j.1096-3642.1978.tb01046.x>
- Chakrabarti S, Maity SP (1984) A new genus and four new species of aphids (Homoptera: Aphididae) from Northwest Himalaya, India. Oriental Insects 18(1): 195–212. <https://doi.org/10.1080/00305316.1984.10432203>
- Chakrabarti S, Medda PK (1989) Taxonomic studies on some aphids (Homoptera: Aphididae) from India. Oriental Insects 23(1): 133–141. <https://doi.org/10.1080/00305316.1989.11835502>
- Chen J, Zhang B, Zhu XC, Jiang LY, Qiao GX (2015) Review of the aphid genus *Aspidophorodon* Verma, 1967 with descriptions of three new species from China (Hemiptera: Aphididae: Aphidinae). Zootaxa 4028(4): 551–576. <https://doi.org/10.11646/zootaxa.4028.4.6>
- David SK, Rajasingh SG, Narayanan K (1972) New genus, new species and new morphs of aphids (Homoptera) from India. Oriental Insects 6(1): 35–43. <https://doi.org/10.1080/0305316.1972.10434051>

- Eastop VF, Hille Ris Lambers D (1976) Survey of the World's Aphids. Dr. W Junk BV, Publishers, The Hague, 573 pp.
- Favret C (2022) Aphid Species File. Version 5.0/5.0. <http://aphid.speciesfile.org> [accessed 9 February 2022]
- Kimura M (1980) A simple method for estimating evolutionary rate of base substitutions through comparative studies of nucleotide sequences. *Journal of Molecular Evolution* 16(2): 111–120. <https://doi.org/10.1007/BF01731581>
- Kumar S, Stecher G, Tamura K (2016) MEGA7: Molecular Evolutionary Genetics Analysis version 7.0 for bigger datasets. *Molecular Biology and Evolution* 33(7): 1870–1874. <https://doi.org/10.1093/molbev/msw054>
- Miyazaki M (1971) A revision of the tribe Macrosiphini of Japan (Homoptera: Aphididae, Aphidinae). *Insecta Matsumurana* 34(1): 1–247.
- Nieto Nafría JM, Favret C, Akimoto S, Barbagallo S, Chakrabarti S, Mier Durante MP, Miller GL, Qiao GX, Sano M, Pérez Hidalgo N, Stekolshchikov AV, Wegierek P (2011) Register of genus-group taxa of Aphidoidea. In: Nieto Nafría JM, Favret C (Eds) Registers of Family-Group and Genus-Group Taxa of Aphidoidea (Hemiptera Sternorrhyncha). Universidad der León, Área de Publicaciones, León, 81–404.
- Remaudière G, Remaudière M (1997) Catalogue of the World's Aphididae. Homoptera Aphidoidea. Institut National de la Recherche Agronomique, Paris, 473 pp.
- Richards WR (1963) A new species of *Aspidaphis* Gillette (Homoptera: Aphididae). *Canadian Entomologist* 95(3): 296–299. <https://doi.org/10.4039/Ent95296-3>
- Stekolshchikov AV, Novgorodova TA (2010) A new species of *Aspidophorodon* Verma (Hemiptera, Aphididae) from the Altai Republic. *Zootaxa* 2566(1): 39–44. <https://doi.org/10.11646/zootaxa.2566.1.3>
- Thompson JD, Higgins DG, Gibson TJ (1994) Clustal W: Improving the sensitivity of progressive multiple sequence alignment through sequence weighting, position-specific gap penalties and weight matrix choice. *Nucleic Acids Research* 22(22): 4673–4680. <https://doi.org/10.1093/nar/22.22.4673>
- Verma KD (1967) A new aphid genus from north-western India (Homoptera: Aphididae). *Indian Journal of Entomology* 28(4): 507–509.
- Zhang GX, Zhong TS (1980) New species and new subspecies of Chinese Macrosiphinae (I) (Homoptera: Aphididae). *Entomotaxonomia* 2(1): 53–63.
- Zhang GX, Zhong TS, Zhang WY (1992) Homoptera: Aphidoidea. In: Chinese Academy of Sciences (Ed.). The Comprehensive Scientific Expedition to the Qinghai-Xizang Plateau, Insects of the Hengduan Mountains Regions. Vol. 1. Science Press, Beijing, 360–403.



# The green lacewing genus *Anachrysa* Hölzel, 1973 (Neuroptera, Chrysopidae): a new species, two new combinations, and updated key to species

Yunlong Ma<sup>1</sup>

<sup>1</sup> Engineering Research Center for Forest and Grassland Disaster Prevention and Reduction, Mianyang Normal College, Mianxing West Road, 621000, Mianyang, China

Corresponding author: Yunlong Ma ([bjfuconidium@126.com](mailto:bjfuconidium@126.com))

---

Academic editor: Davide Badano | Received 7 March 2022 | Accepted 14 May 2022 | Published 16 June 2022

---

<http://zoobank.org/01CD4BC7-250B-4673-8D73-A072C037A63A>

---

**Citation:** Ma Y (2022) The green lacewing genus *Anachrysa* Hölzel, 1973 (Neuroptera, Chrysopidae): a new species, two new combinations, and updated key to species. ZooKeys 1106: 57–66. <https://doi.org/10.3897/zookeys.1106.83229>

---

## Abstract

A new species, *Anachrysa adamsi* **sp. nov.**, from Yunnan, China is described. Two new combinations are proposed, namely *Anachrysa alviolata* (Yang & Yang, 1990), **comb. nov.** and *Anachrysa triangularis* (Yang & Wang, 1994), **comb. nov.** An updated key to species is also provided.

## Keywords

Key, new combinations, new species

## Introduction

*Anachrysa* was established as a subgenus of the genus *Chrysopidia* Navás, 1910 by Hölzel (1973). A taxonomic study of the genus was conducted (Ma and Liu 2021), in which we raised *Anachrysa* to full generic status, reported two new species from China, and proposed five new combinations. Following these taxonomic changes, the genus contained seven species occurring in the Oriental Region. Breitkreuz et al.

(2022) also suggested that *Anachrysa* should be elevated to generic rank and excluded from *Chrysopidia*. For the work on the genus *Apertochrysa* Tjeder, 1966 from China, I re-examined many type specimens of species in the genus. I found that *Chrysopidia alviolata* Yang & Yang, 1990 and *Chrysopidia triangularis* Yang & Wang, 1994 should be transferred to the genus *Anachrysa* based on their external morphology and genital characters. Thus, here I propose two new combinations, *Anachrysa alviolata* (Yang & Yang, 1990), comb. nov. and *Anachrysa triangularis* (Yang & Wang, 1994), comb. nov. I also describe a new species, *Anachrysa adamsi* sp. nov., from Yunnan, China based on novel material. Finally, I update the previous key to the species of *Anachrysa* provided in our previous paper (Ma and Liu 2021). These changes increase the number of species in the genus to ten, all of which occur in the Oriental Region.

## Materials and methods

Terminology for wing venation used in this paper follows Tillyard (1916), Tauber (2003), and Tauber et al. (2017). Terminology for genitalia follows Tjeder (1970), Principi (1977), Adams and Penny (1985), Brooks and Barnard (1990), Tauber (2003), and Tauber et al. (2017). Measurements on the methodology of head width, ratio of head width to eye width, and lengths and widths of prothorax and wings were provided in one of our previous works (Ma et al. 2020). The holotype of *Anachrysa adamsi* sp. nov. is deposited in the Invertebrate Collection of Engineering Research Center for Forest and Grassland Disaster Prevention and Reduction, Mianyang Normal College, Mianyang, China (MYNC). Other collections with primary types of relevant species cited in this paper are Entomological Museum, China Agricultural University, Beijing, China (CAU).

## Taxonomy

### *Anachrysa* Hölzel, 1973

*Anachrysa* Hölzel, 1973: 356 (as a subgenus of *Chrysopidia* Navás); Brooks and Barnard 1990: 206; Ma et al. 2021: 282 (as an independent genus); Breitreuz et al. 2021: 17.

**Type species.** *Chrysopidia (Anachrysa) elegans* Hölzel, 1973.

**Diagnosis.** See Ma and Liu (2021).

### *Anachrysa alviolata* (Yang & Yang, 1990), comb. nov.

Fig. 1A–H

*Navasius alviolatus* Yang & Yang, 1990: 329 (original: *Navasius* Yang and Yang (nec Esben-Petersen); type locality: Jianfengling (Hainan); holotype in CAU); Yang 1995:

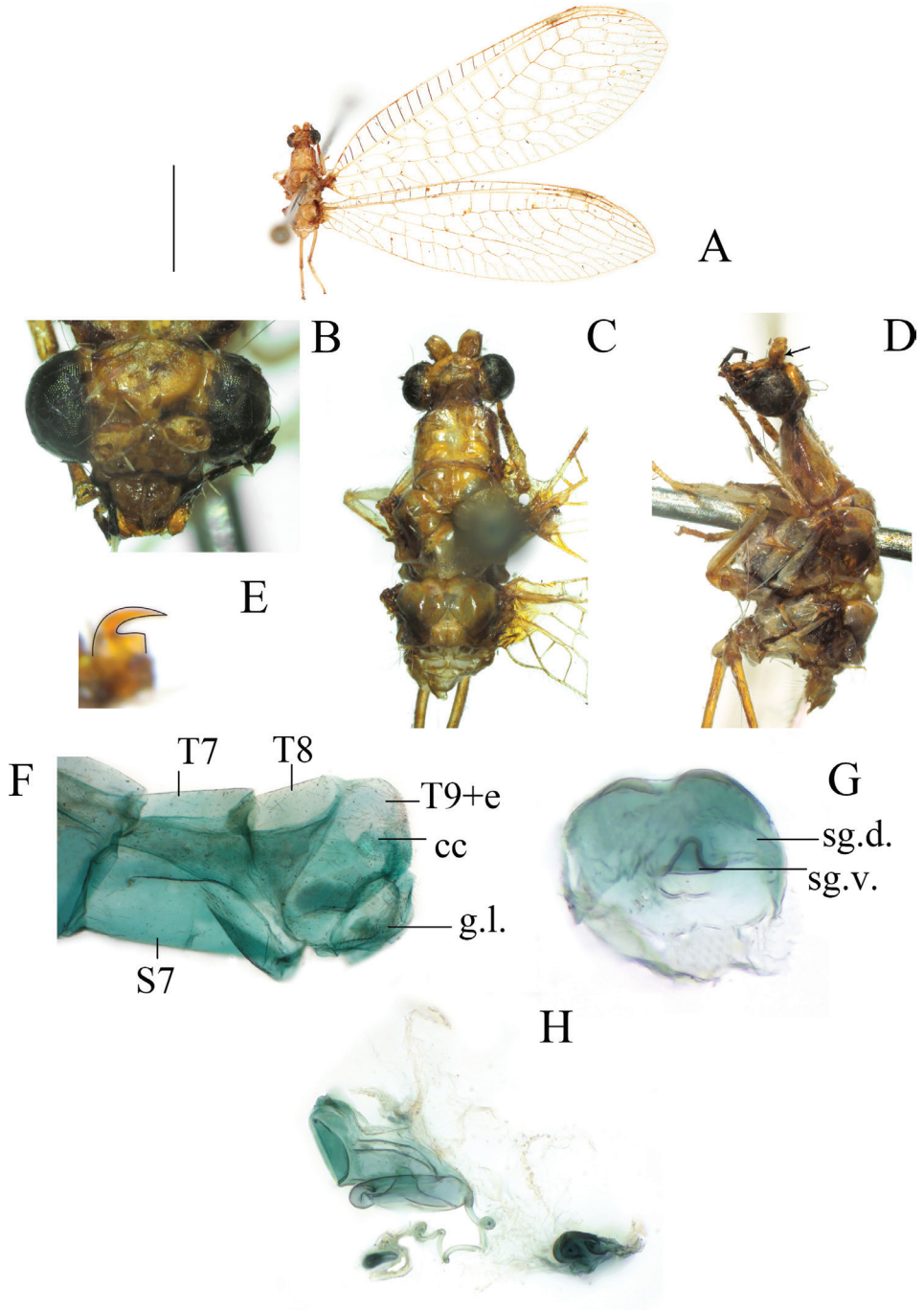


**Figure 1.** *Anachrysa alviolata* (Yang & Yang, 1990) (holotype, female, CAU) **A** habitus **B** head, frontal view **C** head and thorax, dorsal view **D** head and prothorax, lateral view. The arrow indicates the reddish-brown stripe **E** pretarsal claw (emphasized) **F** segment A7-terminus, lateral view **G** subgenitale **H** spermateca. Abbreviations: **cc** callus cerci **g.l.** gonaphophyses lateralis **S7** sternite 7 **sg.d.** dorsal lobe of subgenitale **sg.v.** ventral lobe of subgenitale **T7** tergite 7 **T8** tergite 8 **T9+e** tergite 9 + ectoproc. Scale bar: 5.0 mm (**A**).

29 (*Dichochrysa*); Yang et al. 2005: 149 (*Dichochrysa*); Breitkreuz et al. 2021: 219 (*Apertochrysa*).

**Material examined.** *Holotype* ♀ (CAU), Hainan, Jianfengling (尖峰岭), 20.IV.1982.

**Diagnosis.** Epistomal suture with reddish-brown stripe; gena with brownish stripe connected to clypeal markings; scape with reddish-brown stripe. Pronotum without small medio-lateral spots; pretarsal claw with basal dilation ca. half as long as claw hook. Forewing with clearly discernible markings; gradates brownish; distal cubital cell (dcc) without reddish-brown spots.

**Distribution.** China (Neimenggu, Hainan, Sichuan, Ningxia).

**Remarks.** After re-examination of the holotype of *Navasius alviolata*, I noticed that it has clearly discernible markings, reddish-brown prestigmatic spots, and three series of gradate crossveins on the forewing and reddish-brown prestigmatic spots on the hind wing, all of which fit well with the generic characters of *Anachrysa*. Thus, I hereby transfer this species to *Anachrysa*. Although I did not examine specimens from Neimenggu, Sichuan, and Ningxia, I suggest that these distribution reports are incorrect, because of a misidentification of the species. *Anachrysa* species are characterized by narrow distributions, thus, the old data should be used with caution, awaiting confirmation.

*Anachrysa triangularis* (Yang & Wang, 1994), **comb. nov.**

Fig. 2A–K

*Dichochrysa triangularis* Yang & Wang, 1994: 68 (original: *Dichochrysa*; type locality: Ruili (Yunnan); holotype in CAU); Yang et al. 2005: 199 (*Dichochrysa*); Breitkreuz et al. 2021: 219 (*Apertochrysa*).

**Material examined.** *Holotype* ♂ (CAU), Yunnan, Ruili, Mengxiu (勐休), 5.V.1981, Yang Chikun (杨集昆).

**Diagnosis.** Frontoclypeal sulcus with brownish stripe; gena with brownish stripe connected to clypeal markings; scape and pedicel with reddish-brown stripe. Pronotum without small medio-lateral spots; pretarsal claw with basal dilation ca. half as long as claw hook. Forewing with clearly discernible markings, with two series of brownish gradate crossveins; distal cubital cell (dcc) with reddish brown spots. Tergite 9 + ectoproct without projected peak in lateral view.

**Distribution.** China (Yunnan).

**Remarks.** The holotype of *Dichochrysa triangularis* has reddish-brown prestigmatic spots and reddish-brown markings on the forewing. The gonarc complex of this species also fits the typical shape of *Anachrysa*. Based on these characters, the species is transferred to *Anachrysa* and its diagnostic characters, e.g., two series of gradate crossveins on the forewing and hind wing, are considered to be interspecific variation within the genus.

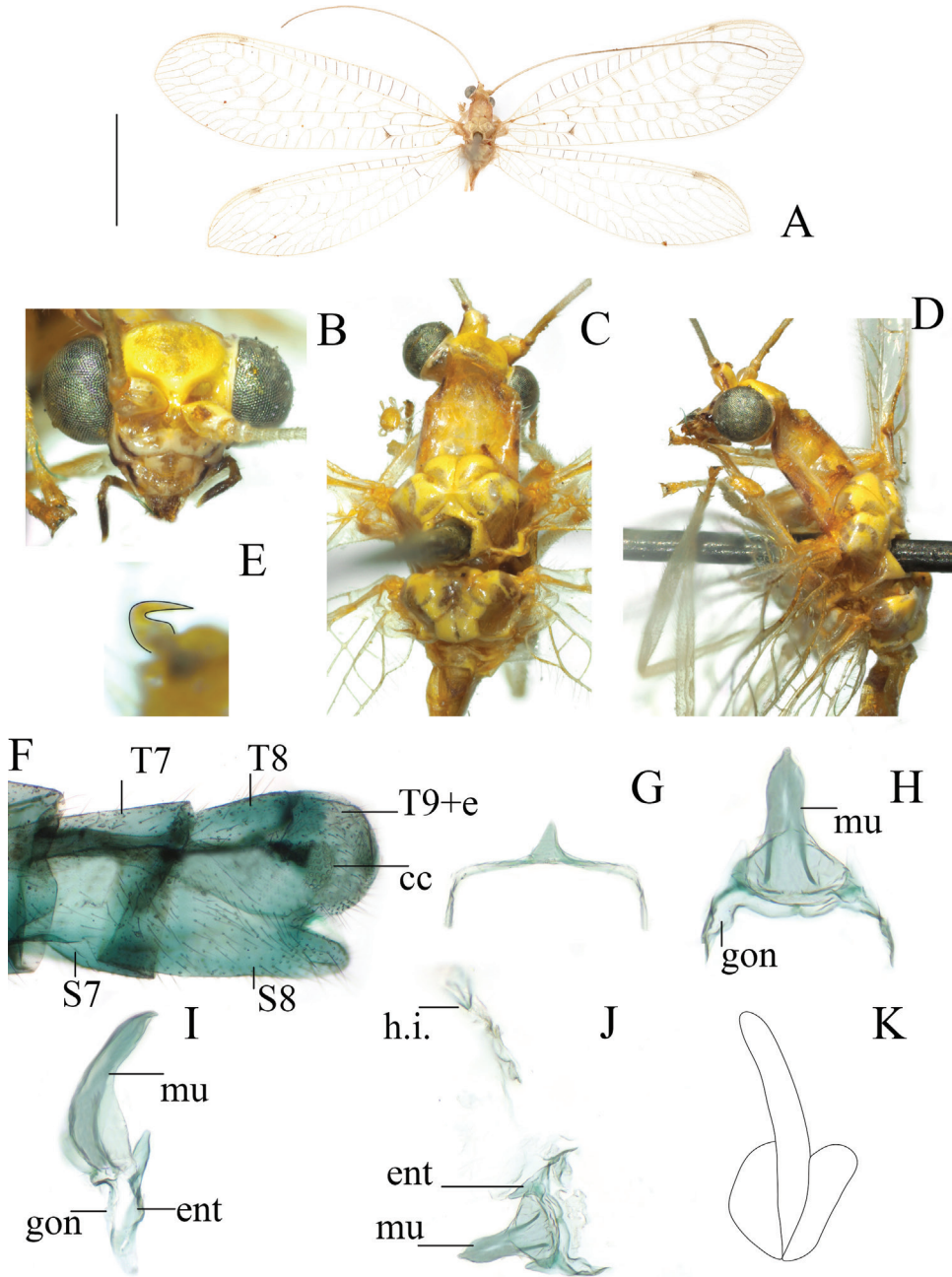


**Figure 2.** *Anachrysa triangularis* (Yang & Wang, 1994) (holotype, male, CAU) **A** habitus **B** head, frontal view **C** head and thorax, dorsal view **D** head and prothorax, lateral view **E** pretarsal claw (emphasized) **F** segment A7-terminus, lateral view **G** tignum **H** gonarcal complex, dorsal view **I** gonarcal complex, lateral view **J** gonarcal complex and hypandrium internum **K** line drawing of gonapsis. Abbreviations: cc callus cerci ent entoprocessus gon gonarcus h.i. hypandrium internum mu mediuncus S7 sternite 7 S8 sternite 8 T7 tergite 7 T8 tergite 8 T9+e tergite 9+ectoproct. Scale bar: 5.0 mm (**A**).

***Anachrysa adamsi* sp. nov.**

<http://zoobank.org/4F152274-27CF-4220-92DB-DC84DD0F0A20>

Fig. 3A–L

**Material examined.** *Holotype* ♂ (MYNC), Yunnan, Honghe, Lyuchun county (绿春县), 1800 m, V.2021, Li Shen (李申).

**Diagnosis.** Epistomal suture with light stripe; gena with brownish stripe connected to clypeal markings; scape and pedicel with reddish-brown stripe. Pronotum with medio-lateral spots; pretarsal claw with basal dilation ca. one third as long as claw hook. Forewing with indistinct markings, gradates brownish; distal cubital cell (dcc) with reddish-brown spots. Tergite 9 + ectoproct with projected peak in lateral view.

**Description. Measurements:** Head width 1.30 mm; ratio of head width to eye width 2.00; prothorax 0.70 mm long, 0.90 mm wide. Forewing 17.00 mm long, 5.50 mm wide; 14 radial cells; 3 Banksian cells (b cells), 5 lower Banksian cells (b' cells); 9 inner gradates, 5 median gradates, 8 outer gradates. Hind wing 15.50 mm long, 4.50 mm wide; 13 or 14 radial cells; 2 Banksian cells (b cell), 5 lower Banksian cell (b' cells); 8 inner gradates, 2 or 3 median gradates, 6 or 7 outer gradates.

**Head.** Not spotted; frons with epistomal suture marked with light reddish stripe; gena marked with brownish stripe connected with clypeal markings; tentorial pits unmarked; scape and pedicel with reddish stripe; clypeus with lateral area marked with light brownish markings; maxillary palp with palpomeres 3–5 brownish; labial palp with palpomere 3 brownish.

**Thorax.** Pronotum with reddish lateral stripe and medio-lateral spots. Pretarsal claw with basal dilation ca. one third as long as claw hook.

**Wings.** Forewing narrow, hyaline, without clearly discernible markings; some basal costal crossveins, crossveins between the first cubital cell and the second cubital cell ( $cu_2$ ), distal cubital cell (dcc) and first anal vein (1A) brownish; hind wing narrow, more acutely tapering apically than forewing, hyaline; almost all veins, except some costal crossveins, pale green.

**Abdomen.** Pale green. Abdominal setae white, microsetae dense, and long setae sparse.

**Male.** Tergite 9 + ectoproct triangular, ca. twice as long as tergite 8, base proximally prominent dorsally, with an angulate peak in lateral view, dorsal invagination ca. 2/3 length of tergite 9 + ectoproct; callus cerci circular. Sternite 8 + 9 fused, with line of fusion not demarcated, posterior margin rounded. Tignum, gonapsis, and hypandrium internum present; tignum narrow, with relatively weak projection; gonarcus narrow, ca. half the length of mediuncus; entoprocessus long, narrow, slightly shorter than gonarcus, without unarticulated process; mediuncus relatively straight; gonapsis with triangular lateral wings, stem long and expanded subapically; hypandrium internum small, with two short, dense arms, with mesal comes.

**Female.** Unknown.

**Distribution.** China (Yunnan).

**Etymology.** The new species is dedicated to Prof. Phillip Anthony Adams, who made great contributions to the taxonomy of Chrysopidae.

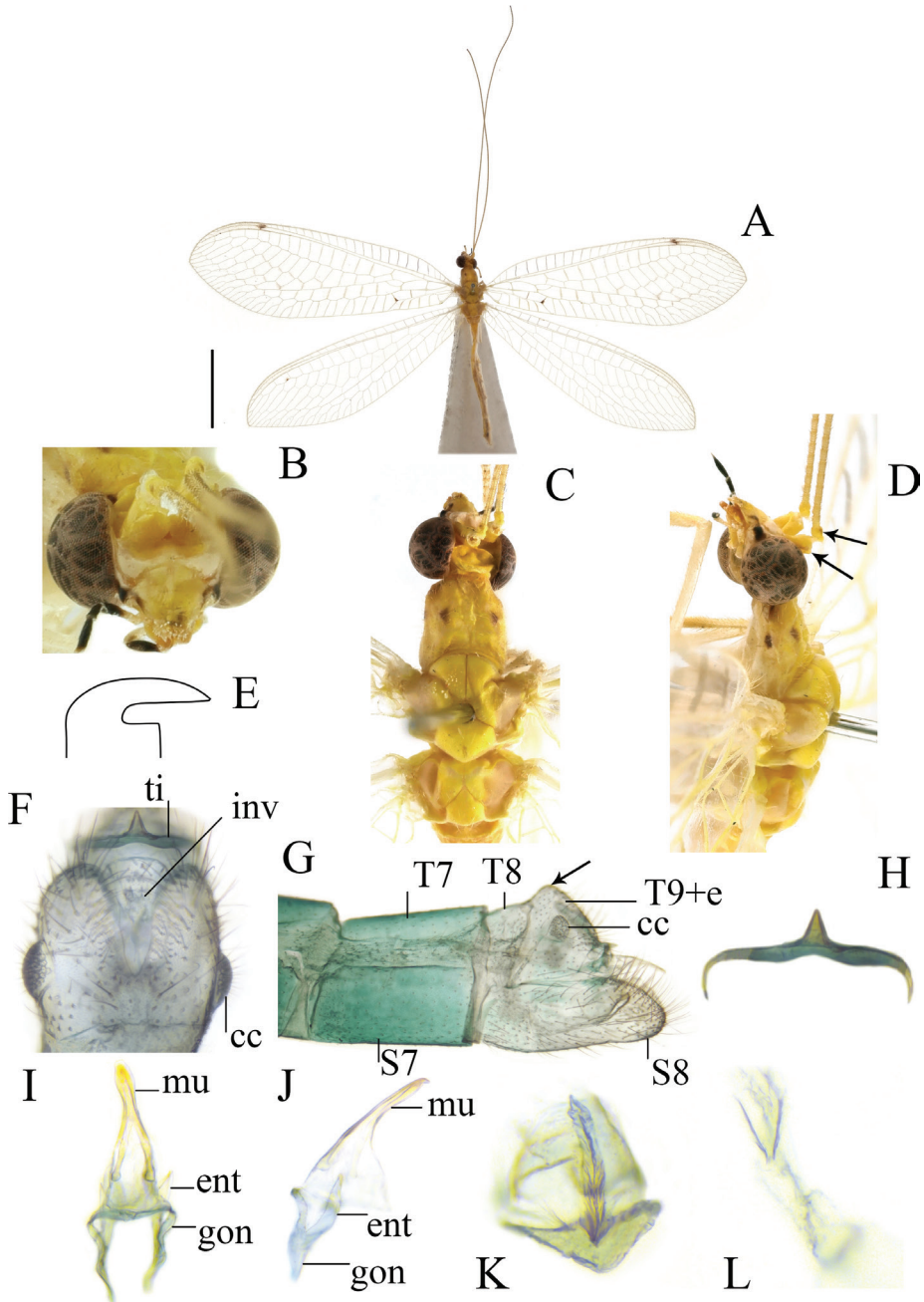


**Figure 3.** *Anachrysa adamsi* sp. nov. (holotype, male, MYNC) **A** habitus **B** head, frontal view **C** head and thorax, dorsal view **D** head and prothorax, lateral view. The arrow indicates the reddish-brown stripe **E** pretarsal claw (emphasized) **F** segment A7-terminus, dorsal view **G** segment A7-terminus, lateral view. The arrow indicates the angulate peak **H** tignum **I** gonarcal complex, dorsal view **J** gonarcal complex, lateral view **K** gonapophysis **L** hypandrium internum. Abbreviations: **cc** callus cerci **ent** entoprocessus **gon** gonarcus **inv** dorsal invagination **mu** mediuncus **S7** sternite 7 **S8** sternite 8 **T7** tergite 7 **T8** tergite 8 **T9+e** tergite 9+ectoproct. Scale bar: 5.0 mm (**A**).

**Remarks.** The new species can be distinguished from its congeners by the following characters: pronotum with medio-lateral spots (absent in *A. holzeli*, *A. triangularis*, and *A. alviolata*), scape with a reddish-brown stripe (absent in *A. lifashengi* and *A. luna*) and absence of an unarticulated process on the entoprocessus (present in *A. lifashengi* and *A. luna*), cubital cell (dcc) with reddish-brown spots (absent in *A. xiangana*) and tergite 9 + ectoproct with a dorsally projected peak in lateral view (absent in *A. trigonia*). *Anachrysa adamsi* resembles *A. erato* in having medio-lateral spots on the pronotum and a similar gonarc complex. However, *A. adamsi* differs from *A. erato* by the scape having a reddish-brown stripe (absent in *A. erato*) and gonapsis with small and narrow lateral wings (large and broad wings in *A. erato*). *Anachrysa adamsi* is also similar to *A. elegans* in having medio-lateral spots on the pronotum and a similar gonarc complex and gonapsis. The two species differ in several details, such as scape with a reddish-brown stripe (absent in *A. elegans*), the absence of discernible markings on the forewing (present in *A. elegans*) and few brownish crossveins (several in *A. elegans*), the relatively straight mediuncus (curved in *A. elegans*) and triangular lateral wings on the gonapsis (rounded in *A. elegans*).

#### Updated key to species of *Anachrysa* by Ma and Liu (2021)

- |   |   |   |
|---|---|---|
| 1 | Pronotum without distinct medio-lateral spots .....   | 2   |
| – | Pronotum with distinct medio-lateral spots (Fig. 3C) .....  | 4   |
| 2 | Scape without reddish-brown stripe .....  | <b><i>A. holzeli</i> (Wang &amp; Yang, 1992)</b>                  |
| – | Scape with reddish-brown stripe (Figs 1D, 2D, 3D) .....   | 3   |
| 3 | Distal cubital cell (dcc) with reddish-brown spots (Fig. 2A) .....  |   |
|   | .....   | <b><i>A. triangularis</i> (Yang &amp; Wang, 1994), comb. nov.</b> |
| – | Distal cubital cell (dcc) without reddish-brown spots (Fig. 1A) .....   |   |
|   | .....   | <b><i>A. alviolata</i> (Yang &amp; Yang, 1990), comb. nov.</b>    |
| 4 | Scape with reddish-brown stripe (Figs 1D, 2D, 3D) .....   | 5   |
| – | Scape without reddish-brown stripe .....  | 7   |
| 5 | Male tergite 9 + ectoproct without dorsally projected peak in lateral view .....                                |   |
|   | .....   | <b><i>A. trigonia</i> (Wang &amp; Yang, 2005)</b>                 |
| – | Male tergite 9 + ectoproct with dorsally projected peak in lateral view (Fig. 3G) .....                         | 6   |
| 6 | Distal cubital cell (dcc) without reddish-brown spots .....   |   |
|   | .....   | <b><i>A. xiangana</i> (Wang &amp; Yang, 1992)</b>                 |
| – | Distal cubital cell (dcc) with reddish-brown spots (Figs 2A, 3A) .....  |   |
|   | .....   | <b><i>A. adamsi</i> sp. nov.</b>                                  |
| 7 | Male tergite 9 + ectoproct without dorsally projected peak in lateral view; entoprocessus strongly curved ..... |   |
|   | .....   | <b><i>A. luna</i> Ma &amp; Liu, 2021</b>                          |
| – | Male tergite 9 + ectoproct with dorsally projected peak in lateral view; entoprocessus straight .....           | 8   |
| 8 | Gonapsis with large and broad lateral wings .....   | 9   |
| – | Gonapsis with small and narrow lateral wings .....  | <b><i>A. elegans</i> (Hölzel, 1973)</b>                           |

- 9 Entoprocessus with subapical unarticulated process; lateral wings on gonapsis tapered outwards..... *A. lifashengi* Ma & Liu, 2021
- Entoprocessus without subapical unarticulated process; lateral wings on gonapsis rounded..... *A. erato* (Hölzel, 1973)

**Notes.** *A. elegans* and *A. erato* do not have a reddish-brown stripe on their scapes, contrary to the statement previously provided in the key by Ma and Liu (2021).

## Acknowledgements

The study was supported by a pilot grant (QD2021A30) provided by Mianyang Normal College.

## References

- Adams PA, Penny ND (1985) Neuroptera of the Amazon Basin. Part 11a. Introduction and Chrysopini. *Acta Amazonica* 15(3–4): 413–479. <https://doi.org/10.1590/1809-43921985153479>
- Breitkreuz L, Duelli P, Oswald JD (2021) *Apertochrysa* Tjeder, 1966, a new senior synonym of *Pseudomallada* Tsukaguchi, 1995 (Neuroptera: Chrysopidae: Chrysopinae). *Zootaxa* 4966(2): 215–225. <https://doi.org/10.11646/zootaxa.4966.2.8>
- Breitkreuz LCW, Garzón-Orduña IJ, Winterton SL, Engel ME (2022) Phylogeny of Chrysopidae (Neuroptera), with emphasis on morphological trait evolution. *Zoological Journal of the Linnean Society* 194 (4): 1374–1395. <https://doi.org/10.1093/zoolinlean/zlab024>
- Brooks SJ, Barnard PC (1990) The green lacewings of the world: A generic review (Chrysopidae). *Bulletin of the British Museum of Natural History. Entomology* 59: 117–286.
- Hölzel H (1973) Neuroptera aus Nepal I. Chrysopidae. *Khumbu Himal* 4: 333–388.
- Ma YL, Liu XY (2021) The green lacewing genus *Anachrysa* Hölzel, 1973 stat. nov. (Neuroptera: Chrysopidae) from China, with description of two new species. *Zootaxa* 4941(2): 281–290. <https://doi.org/10.11646/zootaxa.4941.2.8>
- Ma YL, Yang XK, Liu XY (2020) Notes on the green lacewing subgenus *Ankylopteryx* Brauer, 1864 (s. str.) (Neuroptera, Chrysopidae) from China, with description of a new species. *ZooKeys* 906: 41–71. <https://doi.org/10.3897/zookeys.906.46438>
- Principi MM (1977) Contributi allo studio dei Neurotteri italiani. XXL. La morfologia addominale ed il suo valore per la discriminazione generica nell'ambito delle Chrysopinae. *Bollettino dell'Istituto di Entomologia della Università degli Studi di Bologna* 31: 325–360.
- Tauber CA (2003) Generic characteristics of Chrysopodes (Neuroptera: Chrysopidae), with new larval descriptions and a review of species from the United States and Canada. *Annals of the Entomological Society of America* 96(4): 472–490. [https://doi.org/10.1603/0013-8746\(2003\)096\[0472:GCOCNC\]2.0.CO;2](https://doi.org/10.1603/0013-8746(2003)096[0472:GCOCNC]2.0.CO;2)

- Tauber CA, Sosa F, Albuquerque GS, Tauber MJ (2017) Revision of the Neotropical green lacewing genus *Ungla* (Neuroptera, Chrysopidae). *ZooKeys* 674: 1–188. <https://doi.org/10.3897/zookeys.674.11435>
- Tillyard RJ (1916) The wing-venation of the Chrysopidae. *Proceedings of the Linnean Society of New South Wales* 61: 221–248[2 pls].
- Tjeder B (1970) Neuroptera. In: Tuxen SL (Ed.) *Taxonomist's Glossary of Genitalia in Insects*. 2<sup>nd</sup> edition. Munksgaard, Copenhagen, 89–99.
- Yang XK (1995) The revision on species of genus *Dichochrysa* (Neuroptera: Chrysopidae) from China. *Entomotaxonomia* 17(Suppl.): 26–34. [in Chinese, with English summary]
- Yang CK, Wang XX (1994) The golden eyes of Yunnan with descriptions of some new genus and species (Neuroptera: Chrysopidae). *Journal of Yunnan Agricultural University* 9(2): 65–74. [in Chinese, with English summary]
- Yang XK, Yang CK (1990) *Navasius*, a new genus of Chrysopinae (I) (Neuroptera: Chrysopidae). *Acta Zootaxonomica Sinica* 15: 327–338. [in Chinese, with English summary]
- Yang XK, Yang CK, Li WZ (2005) *Fauna Sinica: Insecta, Volume 39: Neuroptera: Chrysopidae*. Science Press, Beijing, 398 pp [4 pls] [in Chinese, with English summary]

# Notes on the green lacewing subgenus *Chrysopidia* (s. str.) Navás, 1910 (Neuroptera, Chrysopidae), with description of a new species from China

Yunlong Ma<sup>1</sup>

<sup>1</sup> Engineering Research Center for Forest and Grassland Disaster Prevention and Reduction, Mianyang Normal College, Mianxing West Road, 621000, Mianyang, China

Corresponding author: Yunlong Ma ([bjfuconidium@126.com](mailto:bjfuconidium@126.com))

---

Academic editor: Davide Badano | Received 7 March 2022 | Accepted 4 June 2022 | Published 16 June 2022

---

<http://zoobank.org/9D207F3D-8FA5-42A0-8B20-5BB22FF24218>

---

**Citation:** Ma Y (2022) Notes on the green lacewing subgenus *Chrysopidia* (s. str.) Navás, 1910 (Neuroptera, Chrysopidae), with description of a new species from China. ZooKeys 1106: 67–80. <https://doi.org/10.3897/zookeys.1106.83232>

---

## Abstract

A taxonomic study of the green lacewing subgenus *Chrysopidia* (s. str.) from China is presented. Based on the examination of type specimens of the genus reported by previous Chinese scholars and the line drawings of *Chrysopidia manipurensis* provided by Ghosh (1990), I proposed five new combinations: *Apertochrysa platypa* (Yang & Yang, 1990), **comb. nov.**, *Apertochrysa yangi* (Yang, 1997), **comb. nov.**, *Apertochrysa shennongana* (Yang & Wang, 1990), **comb. nov.**, *Apertochrysa zhaoi* (Yang & Wang, 1990), **comb. nov.**, and *Apertochrysa manipurensis* (Ghosh, 1990), **comb. nov.** As for *Chrysopidia sinica* Yang & Wang, 1990, I still treat it as a valid species until supplementary specimens are available because the gonarc complex of the type specimen is missing. A new species *Chrysopidia* (*Chrysopidia*) *tjederi* **sp. nov.** is also described based on new materials. A key to all known species of this subgenus is also provided.

## Keywords

Key, new species, taxonomic study

## Introduction

The green lacewing genus *Chrysopidia* was established by Navás (1910), with *Chrysopidia nigrata* Navás, 1910 as its type species by monotypy. The genus currently includes 19 species in the Palaearctic and Oriental regions. The genus is characterized by the broad costal area of the forewing, sinuate radial crossveins in the apical half,

Copyright Yunlong Ma. This is an open access article distributed under the terms of the Creative Commons Attribution License (CC BY 4.0), which permits unrestricted use, distribution, and reproduction in any medium, provided the original author and source are credited.

the slightly inclined or straight long costal setae, the presence of a dorsoapical invagination on tergite 9, as well as ectoproct in males and long vela and shallow spermathecal impression in females. Previously, this genus consisted of three subgenera, i.e., *Chrysopidia* (*s. str.*), *Chrysotropia* Navás, and *Anachrysa* Hölzel. The subgenus *Chrysotropia* was established as an independent genus by Navás (1911) and subsequently treated as a subgenus of *Chrysopidia* (*s.l.*) on account of similar external and genital characters. The subgenus *Anachrysa* was excluded from *Chrysopidia* (*s.l.*) and raised to generic level by Breitkreuz et al. (2022) and Ma and Liu. (2021). Thus, the genus *Chrysopidia* (*s.l.*) includes at present two subgenera, *Chrysopidia* (*s. str.*) and *Chrysotropia* Navás. The study of type specimens of the four species of this subgenus described from China suggests that they should be excluded from *Chrysopidia* (*s. str.*) and transferred to *Apertochrysa*, based on morphological and genital characters. I did not examine the type specimen of *Chrysopidia manipurensis* Ghosh, 1990, but morphological and genital characters showed by line drawings support the removal of this taxon from *Chrysopidia* and the transfer to *Apertochrysa*. Thus, I herein propose five new combinations: i.e., *Apertochrysa platypa* (Yang & Yang, 1990), comb. nov., *Apertochrysa yangi* (Yang, 1997), comb. nov., *Apertochrysa shennongana* (Yang & Wang, 1990), comb. nov., *Apertochrysa zhaoi* (Yang & Wang, 1990), comb. nov., and *Apertochrysa manipurensis* (Ghosh, 1990), comb. nov. Finally, *Chrysopidia sinica* Yang & Wang, 1990, it is quite similar to *Chrysopidia remanei* Hölzel, 1973, but no significant external differences between them were found. Unfortunately, the gonarc complex of *C. sinica* is missing. Here, I still treat *C. sinica* as a valid species until additional specimens are available. This study aims to present an overview of the species of *Chrysopidia* (*s. str.*) from China, describe a new species based on novel material from China, and provide a key to all known species.

## Materials and methods

Terminology of wing venations used in this paper follows Tillyard (1916), Tauber (2003), and Tauber et al. (2017). Terminology of genitalia follows Tjeder (1970), Principi (1977), Adams and Penny (1985), Brooks and Barnard (1990), Tauber (2003), and Tauber et al. (2017). Measurements on the methodology of head width, ratio of head width to eye width, and the length and width of prothorax and wings were provided in our previous work (Ma et al. 2020). The holotype of *Chrysopidia* (*Chrysopidia*) *tjederi* sp. nov. is deposited in the Invertebrate Collection of Engineering Research Center for Forest and Grassland Disaster Prevention and Reduction, Mianyang Normal College, Mianyang, China (MYNC). Other collections with primary types of species cited in this paper are Entomological Museum, China Agricultural University, Beijing, China (CAU), Institute of Zoology, China Academy of Sciences, Beijing, China (IZCAS) and National Zoological Collection, Zoological Survey of India, West Bengal, India (NZSI) and Zoologische Staatssammlung, Munich, Germany (ZSM).

## Taxonomy

### Subgenus *Chrysopidia* Navás, 1910

*Chrysopidia* Navás 1910: 54; Hölzel 1973: 359; Brooks and Barnard 1990: 207.

**Type species.** *Chrysopidia nigrata* Navás, 1910, by monotypy.

**Diagnosis (adapted from Brooks and Barnard 1990).** Forewing 13.00–16.00 mm. Head unmarked or with red stripe on scape, gena, and between scape and vertex (supra-antennal area). Head width/eye width ratio 2.00–2.50; left mandible with small tooth; antenna as long as or longer than forewing. Pronotum slightly elongate; unmarked or with brown lateral spot or red median spot; mesonotum unmarked or with red lateral spot on prescutum. Forewing with costal area broadened; costal and radial crossveins black at each end; costal setae long, slightly inclined or erect; pterostigma unmarked; radial crossveins in apical half sinuate; gradates in three rows. Hind wing often with black suffusion on apical posterior margin; gradates in three rows. Male genitalia: callus cerci ovate or rounded; apodemes usually absent; tergite 9 + ectoproct with deep dorsoapical invagination; tignum, gonapsis, and median plate absent; entoprocessus short; gonarcus long and narrow; mediuncus long, expanded subapically, strongly curved ventrally; gonosaccus large; gonosetae long, dense. Female genitalia: sternite 7 straight apically; subgenitale bilobed; spermatheca narrow, with shallow ventral impression; vela long; spermathecal duct long or short, sinuous.

**Species of the subgenus.** *Chrysopidia ignobilis* (Walker, 1860) (“Hindustan”, India), *Chrysopidia fuscata* (Navás, 1914) (Sichuan and Yunnan, China), *Chrysopidia nigrata* (Navás, 1914) (Darjeeling, India), *Chrysopidia numerosa* (Navás, 1914) (Darjeeling, China), *Chrysopidia regulata* (Navás, 1914) (Sichuan and Yunnan, China), *Chrysopidia jiriana* Hölzel, 1973 (Jiri, Nepal), *Chrysopidia jocasta* Hölzel, 1973 (Jiri, Nepal), *Chrysopidia junbesiana* Hölzel, 1973 (Junbesi, Nepal), *Chrysopidia junbesiana* Hölzel, 1973 (Junbesi, Nepal), *Chrysopidia remanei* Hölzel, 1973 (Junbesi, Nepal), *Chrysopidia sinica* Yang & Wang, 1990 (Hubei, China), *Chrysopidia flavilineata* Yang & Wang, 1994 (Yunnan, China), and *Chrysopidia tjederi* sp. nov. (Sichuan, China).

**Distribution.** Oriental region.

Species previously attributed to *Chrysopidia* (s. str.)

*Apertochrysa platypa* (Yang & Yang, 1991), comb. nov.

*Chrysopidia platypa* Yang and Yang 1991a: 215 (original: *Tjederina*; type locality: Haikou (Hainan); holotype in CAU); Yang et al. 2005: 126 *Chrysopidia* (*Chrysopidia*)

**Material examined.** *Holotype* 1♂ (CAU), Hainan, Haikou (海口), Hainan Institute of Tropical Crops [= Hainan University], 13.IX.1981.

**Distribution.** China (Hainan).

**Remarks.** The species *Chrysopidia platypa* (Yang & Yang, 1991), reported by Yang and Yang (1991) originally belongs to the genus *Tjederina*, which is a nomen nudum appearing in Yang and Wang (1990). Later, it was transferred to the genus *Dichochrysa* by Yang (1997). Yang et al. (2005) transferred it in the genus *Chrysopidia* based on sternite 8 exceeding the apex of tergite 9 + ectoproct. I re-examined the holotype and found it has the characters typical of *Apertochrysa*, a genus erected by Tjeder (1966) and re-established as a senior synonym of *Pseudomallada* Tsukaguchi, 1995 by Breitkreuz et al. (2021). *Apertochrysa* is characterized by presence of straight radial crossveins, basal inner gradate crossveins not meeting pseudomedia (Psm) in both wings, and gonapsis present. These characters suggest transferring this species to *Apertochrysa*.

***Apertochrysa yangi* (Yang, 1997), comb. nov.**

*Chrysopidia yangi* Yang and Lin 1997: 599 (original: *Chrysopidia* (*Chrysopidia*); type locality: Xingshan (Hubei); holotype in IZCAS); Yang et al. 2005: 133 (*Chrysopidia* (*Chrysopidia*)).

**Material examined. Holotype** 1♂ (IZCAS), Huibei, Xingshan, Longhe Forestry (龙河林场), 14.IX.1994 Yaojian (姚建).

**Distribution.** China (Hubei).

**Remarks.** *Chrysopidia yangi* was described from both sexes by Yang in Yang and Lin (1997), but only the holotype (male) was available to me for study. After re-examination, I found it has these characters: (1) narrow costal areas on forewing; (2) radial crossveins straight; (3) basal inner gradate crossveins not meeting pseudomedia (Psm) in both wings; (4) tignum present. All these characters fit with the diagnosis of *Apertochrysa*, so I transfer it to this genus. Moreover, I confirm that the presence of three series of gradate crossveins on both wings of this species is caused by doubled occasional crossveins.

***Apertochrysa shennongana* (Yang & Wang, 1990), comb. nov.**

*Chrysopidia shennongana* Yang and Wang 1990: 154 (original: *Chrysopidia*; shennongjia (Hubei); holotype in CAU); Yang et al. 2005: 128 (*Chrysopidia* (*Chrysopidia*)).

**Material examined. Holotype** 1♀ (CAU), Hubei, Shennongjia (神农架), 2.VI.1984, 1700 m, Chikun Yang (杨集昆).

**Distribution.** China (Hubei).

**Remarks.** *Chrysopidia shennongana* was described by Yang and Wang (1990) based on a single female. After re-examination the holotype, I discovered it has typical characters of *Apertochrysa*, e.g., narrow costal areas on the forewings, straight radial crossveins,

basal inner gradate crossveins not meeting pseudomedia (Psm) in both wings, and the spermatheca with long vela. Thus, I exclude it from *Chrysopidia* (s.l.) and allocate it to *Apertochrysa*. The presence of three series of gradate crossveins on both wings is the same case as *C. platypa* and *C. yangi*.

***Apertochrysa zhaoi* (Yang & Wang, 1990), comb. nov.**

*Chrysopidia zhaoi* Yang and Wang 1990: 156 (original: *Chrysopidia*; type locality: Shennongjia (Hubei); holotype in CAU); Yang et al. 2005: 133 (*Chrysopidia* (*Chrysopidia*)).

**Material examined. Holotype** 1♀ (CAU), Hubei, Shennongjia, Songbai Town (松柏镇), 24.VI.1984, 700–800 m, Xinli Wang (王心丽).

**Distribution.** China (Hubei).

**Remarks.** The case is same with *A. shennongana*, and therefore I exclude it from *Chrysopidia* (s.l.) and allocate it to *Apertochrysa*.

***Apertochrysa manipurensis* (Ghosh, 1990), comb. nov.**

*Chrysopidia manipurensis* Ghosh 1990: 344 (original: *Chrysopidia*; type locality: Manipur (India); holotype in NZSI).

**Distribution.** India (Manipur).

**Remarks.** As for *Chrysopidia manipurensis*, I did not examine the type material, but it is easy to recognize diagnostic characters from the original literature and line drawings. Although it has three gradates on the forewing, the shape of the gonarc complex is typical of *Apertochrysa*. Based on the narrow costal areas on forewing, straight radial crossveins, basal inner gradate crossveins not meeting pseudomedia (Psm) in both wings, and the shape of its gonarc complex, I exclude it from *Chrysopidia* (s.l.) and assign it to *Apertochrysa*.

**Chinese species**

***Chrysopidia* (C.) *flavilineata* Yang & Wang, 1994**

Fig. 1A–H

*Chrysopidia* (C.) *flavilineata* Yang and Wang 1994: 65 (original: *Chrysopidia*; type locality: Nanjingli (Yunnan, Ruili); holotype in CAU); Yang et al. 2005: 124 (*Chrysopidia* (*Chrysopidia*)).

**Material examined. Holotype** ♂, Yunnan, Ruili, Nanjingli (南京里), 5.V.1981, Li Fasheng (李法圣).

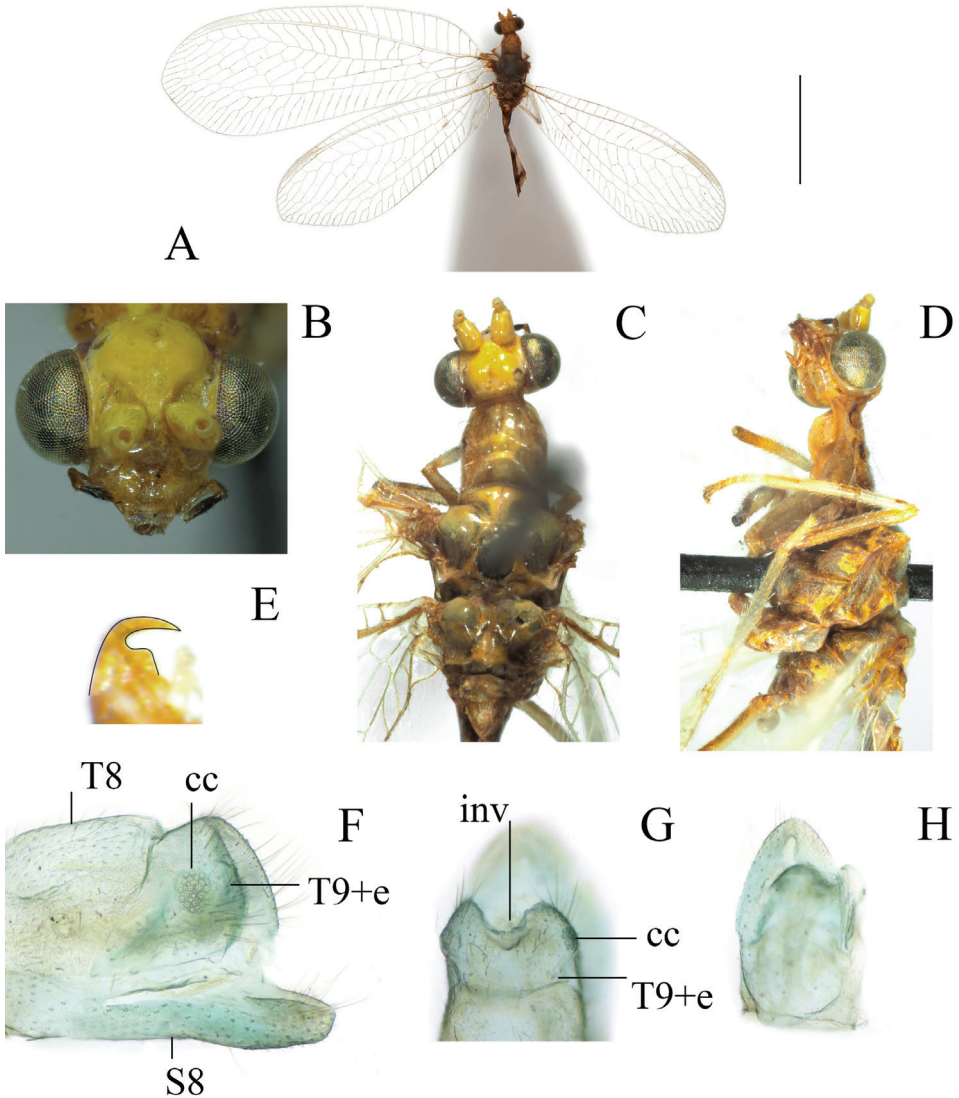


**Figure 1.** *Chrysopidia (Chrysopidia) flavilineata* (Yang & Wang, 1994) (holotype, male, CAU) **A** habitus **B** head, frontal view **C** head and thorax, dorsal view **D** head and prothorax, lateral view **E** pretarsal claw (emphasized) **F** segment A-terminus, lateral view **G** segment A8 terminus, dorsal view **H** sternite 8. Abbreviations: **cc** callus cerci **inv** dorsal invagination **S8** sternite 8 **T8** tergite 8 **T9+e** tergite 9 + ectoproct. Scale bar: 5.0 mm (**A**).

**Diagnosis.** Circumocular with reddish stripe; epistomal suture with light stripe; gena unmarked; scape and pedicel without any stripe; pretarsal claw with basal dilation circa half as long as claw hook. Gradate crossveins pale green on both wings. Tergite 9 + ectoproct with straight dorsal and posterior margin; sternite 8 moderately exceeding the apex of tergite 9 + ectoproct.

**Distribution.** China (Yunnan).

***Chrysopidia* (C.) *fuscata* Navás, 1914**

*Chrysopidia* (C.) *fuscata* Navás 1914: 12 (original: *Chrysopidia*; type locality: “Tali” [Dali] (Yunnan); holotype depository unknown); Banks 1942 [1940]: 188 (*Chrysopidia*); Banks 1947: 98 (*Chrysopidia*); Brooks and Barnard 1990: 271 (*Chrysopidia* (*Chrysopidia*)); Yang et al. 2005: 125 (*Chrysopidia* (*Chrysopidia*)).

**Distribution.** China (Sichuan, Yunnan).

**Remarks.** The depository of the type is unknown (probably missing). I also did not examine other specimens belonging to this species, so additional information cannot be provided at present.

***Chrysopidia* (C.) *regulata* Navás, 1914**

*Chrysopidia* (C.) *regulata* Navás 1914: 12 (original: *Chrysopidia*; type locality: “Tali” [Dali] (Yunnan) and Darjeeling (India); syntype depository unknown); Banks 1942 [1940]: 187 (*Chrysopidia*); Yang et al. 2005: 127 (*Chrysopidia* (*Chrysopidia*)).

**Distribution.** China (Sichuan, Yunnan).

**Remarks.** For similar reasons mentioned above for *C. fuscata*, supplementary description and photographs of characters cannot be given at this time.

***Chrysopidia* (C.) *remanei* Hölzel, 1973**

Fig. 2A–H

*Chrysopidia* (C.) *remanei* Hölzel 1973: 360 (original: *Chrysopidia*; type locality: Junbesi (Nepal); holotype in ZSM); Yang et al. 2005: 127 *Chrysopidia* (*Chrysopidia*).

**Material examined.** 1♂ (CAU), Xizang, Yatung, 2018.VII.12, light trap, Yang Qicheng (杨棋程).

**Diagnosis.** Circumocular without reddish stripe; epistomal suture with short reddish stripe; gena unmarked; scape and pedicel without any stripe; pretarsal claw with basal dilation about half as long as claw hook. Forewing with costal area expanded outwards at median part; gradate crossveins brownish. Tergite 9 + ectoproct with straight dorsal and posterior margin; sternite 8 slightly exceeding the apex of tergite 9 + ectoproct; entoprocessus of gonarcular complex with unarticulated process near apex.

**Distribution.** China (Xizang); Nepal (Junbesi).

**Remarks.** The specimen from Yatung has characters typical of *Chrysopidia* (C.) *remanei*, e.g., forewing with median costal area expanded and entoprocessus with subapical process, which confirms the identification of this species.

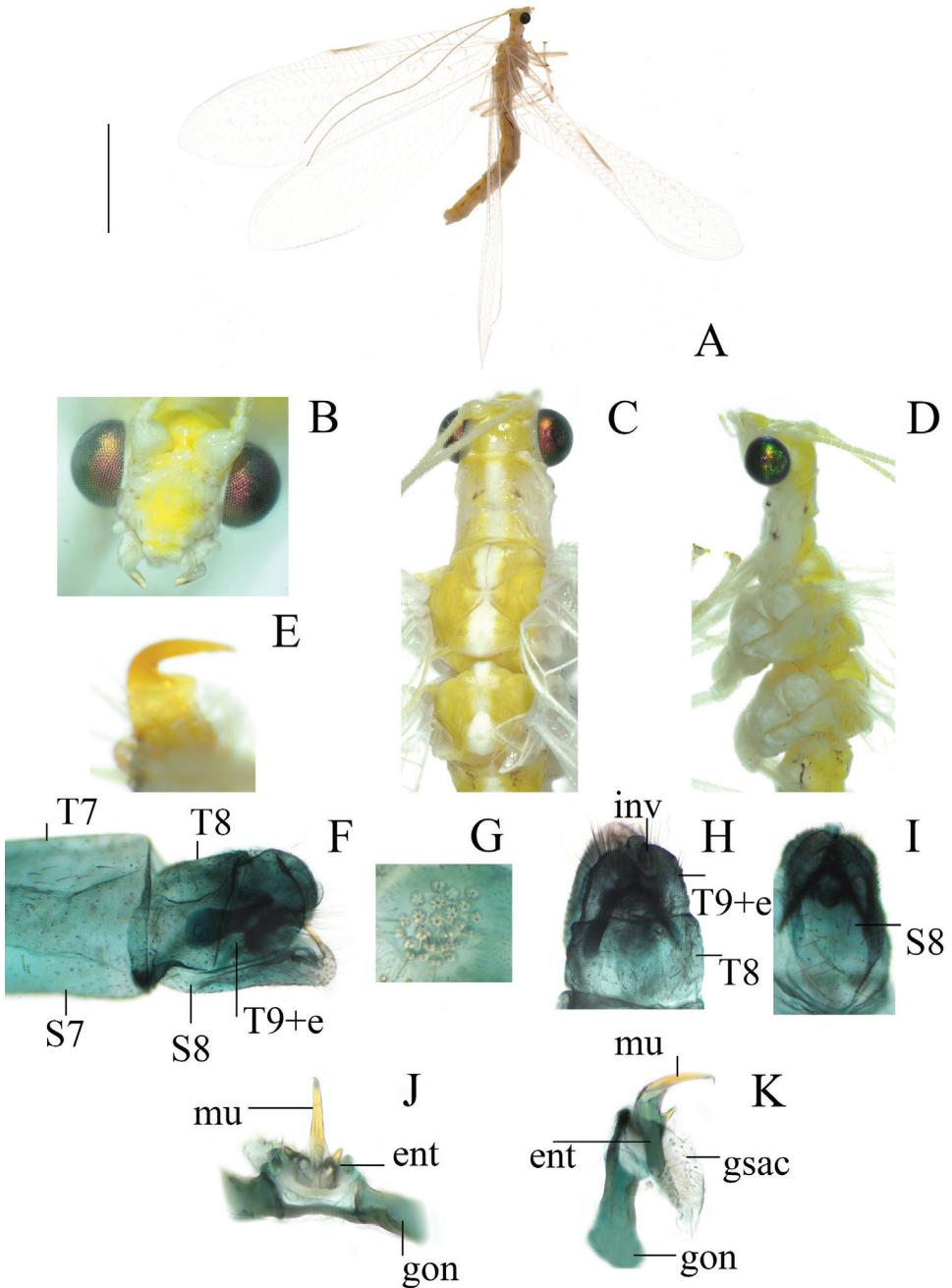


**Figure 2.** *Chrysopidia (Chrysopidia) remanei* Hölzel, 1973 (Xizang, Yatung, male, CAU) **A** habitus **B** head, frontal view **C** head and thorax, dorsal view **D** head and prothorax, lateral view **E** pretarsal claw **F** segment A7-terminus, dorsal view **G** callus cerci **H** segment A8 terminus, dorsal view **I** sternite 8 **J** gonarc complex, dorsal view **K** gonarc complex, lateral view. Abbreviations: **ent** entoprocessus **gsac** gonosaccus **gon** gonarcus **inv** dorsal invagination **mu** mediuncus **S7** sternite 7 **S8** sternite 8 **T7** tergite 7 **T8** tergite 8 **T9+e** tergite 9 + ectoproc. Scale bar: 5.0 mm (**A**).

***Chrysopidia* (C.) *sinica* Yang & Wang, 1990**

*Chrysopidia* (C.) *sinica* Yang and Wang 1990: 155 (original: *Chrysopidia*; type locality: Shennongjia (Hubei); holotype in CAU); Yang et al. 2005: 129 (*Chrysopidia* (*Chrysopidia*)).

**Material examined.** *Holotype* 1♂ (CAU), Hubei, Shennongjia (神农架), 1700 m, 2.VI.1984, Yang Chikun (杨集昆).

**Distribution.** China (Hubei).

**Remarks.** I re-examined the holotype and did not find any significant external differences between *C. remanei* and *C. sinica*. I doubt that this species may be a junior synonym of *C. remanei*. Yang and Wang (1990) stated the gonarcular complex of this species was different from that of *C. remanei* and provided line drawings of gonarcular complex. Based on my re-examination of many types described by Chikun Yang, the line drawing of the gonarcular complex is often inaccurate. Therefore, it is necessary to re-examine the gonarcular complex of the species. Unfortunately, the sclerite is missing and, thus, I could not make any determination. This species is not included in the present key, but still treated as a valid species until more specimens are available.

***Chrysopidia* (C.) *tjederi* sp. nov.**

<http://zoobank.org/AFEB3BCE-539C-4E0B-8ACB-CFF413BC1F3D>

Fig. 3A–J

**Material examined.** *Holotype* 1♂ (MYNC), Sichuan, Mianyang, Mojia town, Mianyang Normal College (磨家镇, 绵阳师范学院), 24.X.2021, Ma Yunlong (马云龙). Paratype ♂, the same data as holotype.

**Diagnosis.** Circumocular with reddish stripe extending to inner ocular margin; epistomal suture with reddish markings connected with clypeal markings; gena unmarked; scape, pedicel, and flagellum with reddish stripe; pretarsal claw with basal dilation circa half as long as claw hook. Forewing with gradate crossveins black. Tergite 9 + ectoproct with rounded dorsal and posterior margin; sternite 8 greatly exceeding the apex of tergite 9 + ectoproct; entoprocessus of gonarcular complex broad, without unarticulated process.

**Description. Measurements:** head width 1.00 mm; ratio of head width/eye width 2.20; prothorax 0.70 mm long, 0.77 mm wide. Forewing 13.00 mm long, 4.50 mm wide; 11 radial cells; 5 Banksian cells (b cells), 4 lower Banksian cells (b' cells); 6 inner gradates, 3 median gradates, 7 outer gradates. Hind wing 11.50 mm long, 3.50 mm wide; 10 radial cells; 4 Banksian cells (b cell), 4 lower Banksian cell (b' cells); 5–6 inner gradates, 0–1 median gradates, 5 outer gradates.

**Head:** vertex pale green, immaculate, with shallow groove; circumocular with reddish stripe extending to inner ocular margin; epistomal suture of frons with reddish markings; gena unmarked; tentorial pits with reddish margins; scape, pedicel, and

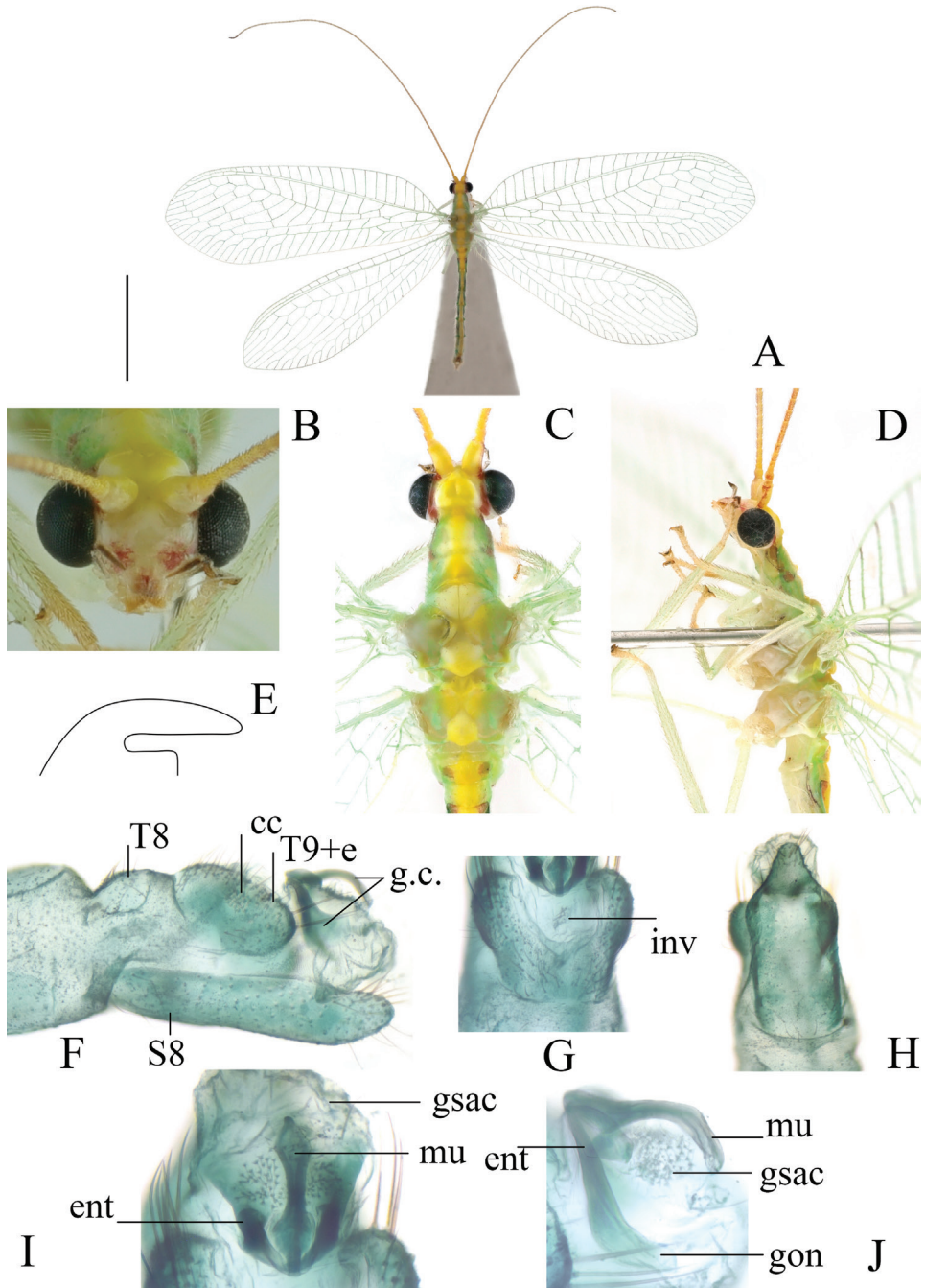


**Figure 3.** *Chrysopidia (Chrysopidia) tjederi* sp. nov. (holotype, male, MYNC) **A** habitus **B** head, frontal view **C** head and thorax, dorsal view **D** head and prothorax, lateral view **E** line drawing of pretarsal claw **F** segment A8-terminus, dorsal view **G** tergite 9 + ectoproct **H** sternite 8 **I** gonarcal complex, dorsal view **J** gonarcal complex, lateral view. Abbreviations: **ent** entoprocessus **g.c.** gonarcal complex **gsac** gonosaccus **gon** gonarcus **inv** dorsal invagination **mu** mediuncus **S8** sternite 8 **T8** tergum 8 **T9+e** tergite 9 + ectoproct. Scale bar: 5.0 mm (**A**).

flagellum with reddish stripe; clypeus with reddish markings connected with frontal markings; labrum with reddish markings; maxillary palp with palpomeres 3–5 brownish; labial palp with palpomere 3 brownish.

**Thorax:** pronotum with reddish lateral stripe and with yellowish median stripe; mesonotum and metanotum with yellowish median stripe; pretarsal claw with basal dilation circa half the length of claw hook.

**Wings:** forewing narrow, hyaline; most costal and radial crossveins at each end, basal part of radial sector, branches of radial sector at junctions with pseudomedia (Psm), gradate crossveins, crossveins between pseudomedia (Psm) and pseudocubitus (Psc) except the first one, crossvein between the first cubital cell and the second cubital cell ( $cu_2$ ) and crossvein between the second cubital cell ( $cu_2$ ) and distal cubital cell ( $cu_3$ ) black; hind wing narrow, more acutely tapered apically than forewing, hyaline; most costal crossveins black at each end or entirely black; apical posterior margin with black suffusion.

**Abdomen:** pale green, having yellowish median stripe, with reddish brown markings on terga 1–7. Abdominal setae white, microsetae dense, and long setae sparse.

**Male:** tergite 9 + ectoproct oval, circa 3× as long as tergite 8, with rounded dorsal and posterior margin, dorsal invagination about half length of tergite 9 + ectoproct; callus cerci rounded, as long as wide. Sterna 8 + 9 fused, very narrow, circa 3.5× as long as wide, with line of fusion not demarcated, lateral margin straight and abruptly tapered near apex, posterior margin rounded, greatly exceeding the apex of tergite 9 + ectoproct. Tignum, gonapsis, and hypandrium internum absent; gonarcus narrow, slightly longer than mediuncus; entoprocessus broad; mediuncus straight at basal half, abruptly curved at apical half, forming right angles with gonarcus.

**Female:** unknown.

**Distribution.** China (Sichuan).

**Etymology.** The new species is dedicated to Prof. Bo Tjeder, great Swedish neuropterist and dipterist.

**Remarks.** The new species is distinguished by the presence of a reddish brown stripe on scape (absent in *C. flavilineata*, *C. jocasta*, *C. junbesiana*, and *C. regulata*), absence of black spots on the mesonotum and metanotum (present in *C. nobilis*); forewing span (<15.00 mm in *C. tjederi* versus >15.00 mm in *C. numerosa*, *C. fuscata*, and *C. nirgrata*), costal area not expanded (median part of costal area expanded in *C. remanei* and *C. sinica*), and angles between gonarcus and entoprocessus (right angles in *C. tjederi* versus obtuse angles in *C. jiriana*).

### Key to all species of *Chrysopidia* (s. str.) Navás, 1910\*

\**C. sinica* is not included in the key. See remarks for this species.

- 1 Mesonotum or/and metanotum with black spots.....2
- Mesonotum or/and metanotum without black spots.....3
- 2 Mesonotum and metanotum with black spots ..... *C. jocasta* Hölzel, 1973
- Only mesonotum with black spots..... *C. ignobilis* (Walker, 1860)

3	Forewing >20.00 mm .....	<i>C. numerosa</i> Navás, 1914
–	Forewing <20.00 mm .....	4
4	Forewing with costal area expanded medially (Fig. 2A) .....	<i>C. remanei</i> Hölzel, 1973
–	Forewing with costal area not expanded medially.....	5
5	Scape without reddish brown stripe .....	6
–	Scape with reddish brown stripe (Fig. 3D) .....	8
6	Maxillary and labial palp pale green or yellowish....	<i>C. regulata</i> Navás, 1914
–	Maxillary and labial palp with apical segment brownish (Figs 2B, 3B) .....	7
7	Forewing with basal radial crossveins entirely black; most gradate crossveins black or brownish .....	<i>C. junbesiana</i> Hölzel, 1973
–	Forewing with radial crossveins pale green; gradate crossveins pale green (Fig. 1A) .....	<i>C. flavilineata</i> Yang & Wang, 1994
8	Forewing >15.00 mm .....	9
–	Forewing <15.00 mm .....	10
9	Mesonotum with reddish spots .....	<i>C. fuscata</i> Navás, 1914
–	Mesonotum without reddish spots.....	<i>C. nigrata</i> Navás, 1910
10	Gonarcus longer than mediuncus; mediuncus forming right angles with gonarcus (Fig. 3J).....	<i>C. tjederi</i> sp. nov.
–	Gonarcus shorter than mediuncus; mediuncus forming obtuse angles with gonarcus .....	<i>C. jiriana</i> Hölzel, 1973

## Acknowledgements

The study was supported by a pilot grant (QD2021A30) provided by Mianyang Normal College.

## References

- Adams PA, Penny ND (1985) Neuroptera of the Amazon Basin. Part 11a. Introduction and Chrysopini. *Acta Amazonica* 15(3–4): 413–479. <https://doi.org/10.1590/1809-43921985153479>
- Banks N (1942[1940]) Report on certain groups of neuropteroid insects from Szechwan, China. *Proceedings of the United States National Museum* 88(3079): 173–220. <https://doi.org/10.5479/si.00963801.88-3079.173>
- Banks N (1947) Some neuropterous insects from Szechwan, China. *Fieldiana: Zoology. Chicago Natural History Museum* 31: 97–107. <https://doi.org/10.5962/bhl.title.2821>
- Breitkreuz L, Duelli P, Oswald JD (2021) *Apertochrysa* Tjeder, 1966, a new senior synonym of *Pseudomallada* Tsukaguchi, 1995 (Neuroptera: Chrysopidae: Chrysopinae). *Zootaxa* 4966(2): 215–225. <https://doi.org/10.11646/zootaxa.4966.2.8>

- Breitkreuz LCW, Garzón Orduña IJ, Winterton SL, Engel ME (2022) Phylogeny of Chrysopidae (Neurptera), with emphasis on morphological trait evolution. *Zoological Journal of the Linnean Society* 194(4): 1374–1395. <https://doi.org/10.1093/zoolinnea/zlab024>
- Brooks SJ, Barnard PC (1990) The green lacewings of the world: A generic review (Chrysopidae). *Bulletin of the British Museum of Natural History. Entomology* 59: 117–286.
- Ghosh SK (1990) Contribution to the taxonomical studies of Neuroptera (suborder Planipennia) from eastern India. III. Family Chrysopidae. *Records of the Zoological Survey of India* 86: 329–354.
- Hölzel H (1973) Neuroptera aus Nepal I. Chrysopidae. *Khumbu Himal* 4: 333–388.
- Ma YL, Liu XY (2021) The green lacewing genus *Anachrysa* Hölzel, 1973 stat. nov. (Neuroptera: Chrysopidae) from China, with description of two new species. *Zootaxa* 4941(2): 281–290. <https://doi.org/10.11646/zootaxa.4941.2.8>
- Ma YL, Yang XK, Liu XY (2020) Notes on the green lacewing subgenus *Ankylopteryx* Brauer, 1864 (*s. str.*) (Neuroptera, Chrysopidae) from China, with description of a new species. *ZooKeys* 906: 41–71. <https://doi.org/10.3897/zookeys.906.46438>
- Navás L (1910) Crisópidos (Ins. Neur.) nuevos. *Brotéria (Zoológica)* 9: 38–59.
- Navás L (1911) Nouvelles formes de Chrysopides (Ins. Névr.) de France. *Annales de l'Association des Naturalistes de Levallois-Perret* 17: 12–14.
- Navás L (1914) Neuroptera asiatica. III series. *Russkoe Entomologicheskoe Obozrenie [= Revue Russe d'Entomologie]* 14: 6–13.
- Principi MM (1977) Contributi allo studio dei Neurotteri italiani. XXL. La morfologia addominale ed il suo valore per la discriminazione generica nell'ambito delle Chrysopinae. *Bollettino dell'Istituto di Entomologia della Università degli Studi di Bologna* 31: 325–360.
- Tauber CA (2003) Generic characteristics of Chrysopodes (Neuroptera: Chrysopidae), with new larval descriptions and a review of species from the United States and Canada. *Annals of the Entomological Society of America* 96(4): 472–490. [https://doi.org/10.1603/0013-8746\(2003\)096\[0472:GCOCNC\]2.0.CO;2](https://doi.org/10.1603/0013-8746(2003)096[0472:GCOCNC]2.0.CO;2)
- Tauber CA, Sosa F, Albuquerque GS, Tauber MJ (2017) Revision of the Neotropical green lacewing genus *Ungla* (Neuroptera, Chrysopidae). *ZooKeys* 674: 1–188. <https://doi.org/10.3897/zookeys.674.11435>
- Tillyard RJ (1916) The wing-venation of the Chrysopidae. *Proceedings of the Linnean Society of New South Wales* 61: 221–248. [2 pls]
- Tjeder B (1966) Neuroptera-Planipennia. The lace-wings of Southern Africa. 5. Family Chrysopidae. *South African Animal Life* 12: 228–534.
- Tjeder B (1970) Neuroptera. In: Tuxen SL (Ed.) *Taxonomist's Glossary of Genitalia in Insects*, 2<sup>nd</sup> edition. Munksgaard, Copenhagen, 89–99.
- Yang XK (1997) Catalogue of the Chinese Chrysopidae (Neuroptera). *Serangga* 2: 65–108.
- Yang XK, Lin ST (1997) Neuroptera: Chrysopidae. in Yang X-k (Ed.) *Chang Jiang San Xia ku qu kun chong [= Insects of the Three Gorge Reservoir area of Yangtze river]*. Vol. 1. Chongqing Publishing House, Chongqing, 593–608. [974 pp] [in Chinese, with English summary]

- Yang CK, Wang XX (1990) Eight new species of green lacewings from Hubei Province (Neuroptera: Chrysopidae). *Journal of Hubei University* 12: 154–163. [Natural Science Edition, in Chinese, with English summary]
- Yang CK, Wang XX (1994) The golden eyes of Yunnan with descriptions of some new genus and species (Neuroptera: Chrysopidae). *Journal of Yunnan Agricultural University* 9(2): 65–74. [in Chinese, with English summary]
- Yang XK, Yang CK (1991) Four new species of lacewing (Neuroptera: Chrysopidae). *Acta Entomologica Sinica* 34: 212–217. [in Chinese, with English summary]
- Yang XK, Yang CK, Li WZ (2005) *Fauna Sinica: Insecta, Volume 39: Neuroptera: Chrysopidae*. Science Press, Beijing, 398 pp. [4 pls] [in Chinese, with English summary]

# Phlebotomine sand flies (Diptera, Psychodidae) from Spain: an updated checklist and extended distributions

Daniel Bravo-Barriga<sup>1</sup>, Ignacio Ruiz-Arrondo<sup>2</sup>, Rosa Estrada Peña<sup>3</sup>,  
Javier Lucientes<sup>3</sup>, Sarah Delacour-Estrella<sup>3,4</sup>

**1** Universidad de Extremadura, Facultad de Veterinaria, Departamento de Sanidad Animal, Parasitología, Avda. Universidad s/n, 10003 Cáceres, Spain **2** Center for Rickettsiosis and Arthropod-Borne Diseases, Hospital Universitario San Pedro-CIBIR, Logroño, Spain **3** Animal Health Department, The AgriFood Institute of Aragon (IA2), School of Veterinary Medicine, University of Zaragoza, 50013 Zaragoza, Spain **4** Departamento de Investigación y Desarrollo (I+D). Quimera. B.S. Calle Olivo, 14, 50016 La Puebla de Alfindén, Spain

Corresponding author: Ignacio Ruiz-Arrondo ([irarrondo@riojasalud.es](mailto:irarrondo@riojasalud.es))

---

Academic editor: Gunnar Kvifte | Received 30 January 2022 | Accepted 19 May 2022 | Published 17 June 2022

<http://zoobank.org/974EEF81-20DE-4E68-9145-351128B6AB62>

---

**Citation:** Bravo-Barriga D, Ruiz-Arrondo I, Estrada Peña R, Lucientes J, Delacour-Estrella S (2022) Phlebotomine sand flies (Diptera, Psychodidae) from Spain: an updated checklist and extended distributions. ZooKeys 1106: 81–99. <https://doi.org/10.3897/zookeys.1106.81432>

---

## Abstract

Phlebotomine sand flies (Diptera: Psychodidae) are the natural vectors of *Leishmania* spp. (Kinetoplastida: Trypanosomatidae) and phleboviruses (Bunyavirales: Phenuiviridae). In Spain, these vectors appear to be increasing their geographical distribution and have serious repercussions on public and veterinary health, encouraging studies of sand flies and their associated pathogens. An up-to-date and easily accessible compendium of current and historical data on their presence and detailed distribution is a crucial step towards the development and implementation of appropriate preventive strategies. A checklist on the presence and distribution of sand flies in Spain is compiled from data extracted from a comprehensive review of scientific literature published between 1909 and 2021 and our new records on the presence of sand flies specimens collected under the entomological surveillance of bluetongue vectors from the Spanish Ministry of Agriculture, Fishery and Food (MAPA) during the period 2004–2021. In total, 13 Spanish species of sand flies (two of them with controversial status) belonging to two genera and six subgenera are presented in this updated checklist, including new distribution data for seven species, among which several stand out as confirmed or suspected vectors of *Leishmania infantum*: *Phlebotomus ariasi*, *Ph. langeroni*, *Ph. mascittii*, and *Ph. perniciosus*.

## Keywords

Catalogue, *Leishmania*, phlebovirus, *Phlebotomus*, sand fly–borne viruses, *Sergentomyia*, spatial distribution, taxonomy

## Introduction

Phlebotomine sand flies are a major public and veterinary health concern due to their haematophagous habits that allow these insects to be natural vectors of *Leishmania* spp. (Kinetoplastida: Trypanosomatidae), arboviruses (phlebovirus, vesiculovirus, and orbivirus) (Akhoundi et al. 2016; Ayhan and Charrel 2017) and, in South America, also the bacterium *Bartonella bacilliformis* (Sánchez Clemente et al. 2012). In Europe in recent years, the density of sand flies has increased in endemic areas or has spread into new areas (Medlock et al. 2014), causing progressively more autochthonous outbreaks of phlebotomine-borne diseases (González et al. 2017; García San Miguel et al. 2021). More than 50 species of *Phlebotomus* Loew, 1845 have been described in Europe, North Africa, the Middle East, and the Caucasus, and eleven of them are implicated in the transmission of pathogens (Alten et al. 2016). Updated studies on taxonomic, spatiotemporal, and bio-ecological aspects, as well as the epidemiological status, of sand flies are crucial to develop effective entomological surveys and control plans. Furthermore, a global review of the information available can be useful in detecting regions lacking data. For easier access, all this information must be compiled, ordered, and updated, allowing effective management for students, professors, general researchers, medical and veterinary entomologists, animal and public health authorities, and public and private institutions involved in the study and control of sand flies and their related pathogens.

The first report of sand flies in Spain dates back to 1909 (Czerny and Strobl 1909) when a female of *Phlebotomus ariasi* Tonnoir, 1921 was found in Madrid but mistakenly reported as *Phlebotomus papatasi* (Scopoli, 1786). Other females from the same sample were not identified, but dry-preserved and assumed to be identical to the first, until León Sanz et al. (1998) analyzed them, adding more details to the document by Czerny and Strobl (1909), identifying more females of *Ph. ariasi* and *Phlebotomus perniciosus* Newstead, 1911.

Most of the studies on the presence and phenology of sand flies in Spain are concentrated between the 1970s to 1990s, where authors such as Francisco Morillas-Márquez (Morillas-Márquez et al. 1982a, b, 1983a, 1991), Ezequiel Martínez-Ortega (Martínez-Ortega et al. 1982; Martínez-Ortega 1986; Martínez-Ortega and Conesa Gallego 1987a), Jean-Antoine Rioux (Rioux et al. 1974, 1975, 1984), Montserrat Gállego (Gállego et al. 1990) and Javier Lucientes (Lucientes-Curdi et al. 1991, 1995) improved the distributional knowledge, the biology, their epidemiological role, and also the description of two new species (Úbeda Ontiveros et al. 1982; Morillas-Márquez et al. 1983b).

Gil Collado et al. (1989) carried out a review of the distribution, morphology, and biology of sand flies in Spain and described eleven species. Later, Gállego Berenguer et al. (1992) updated these data on the distribution of sand flies in the northeast of the Iberian Peninsula and the Balearic Islands. Since then, one new species has been described (Depaquit et al. 1998), another was reported for the first time for Spain (Martínez-Ortega et al. 1996), and corrections were made in the identification of historical sand fly collections (León Sanz et al. 1999).

In recent years, further investigations have been initiated mainly focusing on the role of these insects as vectors of *Leishmania* spp. and phleboviruses (Sanbonmatsu-

Gámez 2005; Barón et al. 2011; Alcover et al. 2014; Ballart et al. 2014; Bravo-Barriga et al. 2016; Remoli et al. 2016), especially as a result of the largest outbreak of human leishmaniosis in Madrid in 2009 (Jiménez et al. 2013; González et al. 2017, 2021). In light of this new situation, the geographical and epidemiological status of phlebotomine knowledge in our country has been substantially improved.

The aim of this study is to update the list of sand flies present in Spain by compiling the distribution records by provinces contained in the bibliography, and to increase the information by adding our own entomological results carried out between 2004 and 2021 in all Spanish regions based on collections from the MAPA. The updated data provided will be useful for the design of new research, surveillance, and vector control programmes as well as the assessment of the risk of pathogens transmission by sand flies in Spain.

## Materials and methods

### Data collection

Knowledge of the distribution of Spanish sand fly species has been synthesised from two sources:

1. A comprehensive review of 136 scientific articles and grey literature (such as government reports, conference proceedings, graduate dissertations, and relevant MSc theses) published between 1909 and 2021. For doctoral theses written by article compendium, only their publications were taken into account. These materials were sourced through PubMed, ResearchGate, Scopus, Web of Science, Google Scholar, and digital repositories (e.g., Digital.CISC, TESEO, Dehesa, and Dialnet) using the following keywords in English, French, and Spanish: Phlebotominae, Phlebotomine, *Phlebotomus*, sandfly, sand flies, Phlébotomes, flebotomos, Spain, Espagne, España, *Leishmania*, leishmaniosis, leishmaniasis, and phlebovirus.

Some earlier materials that were difficult to obtain were provided courtesy of an exchange between experts. The retrieved papers form the basis for the checklist which was used to confirm species records and are thus dependent on the quality of the identification made by the authors at the time of publication of the record. The bibliographic references associated with each species recorded for Spain are presented in Suppl. material 1.

2. Unpublished entomological data of sand flies collected in traps for the monitoring of *Culicoides* biting midges (Diptera: Ceratopogonidae), vectors of the blue-tongue virus (BTV). Since 2000, a national surveillance, control, and eradication of BTV programme has been carried out in Spain supported by the MAPA and coordinated by the University of Zaragoza (Zaragoza, Spain).

The surveillance data presented here are based on the analysis of 1179 sample points belonging to 1040 municipalities between 2004 and 2021 from almost all Spanish provinces except the autonomous cities Ceuta and Melilla. All islands of the Balearic Archipelago (Mallorca, Menorca, Ibiza, and Formentera) are considered as a

single province; however, we do indicate the sand fly species when they are recorded for the first time in a specific island.

Each collection site was georeferenced using a Garmin GPS 12 Global Position Device with geographical coordinate system (EPSG: 23030-ED50/UTM zone 30N). CDC-UV traps (Miniature Blacklight trap 1212, John W. Hock Company, Gainesville, FL, USA) were placed overnight once a week throughout the year long in a variable number of animal holdings composed mainly of sheep, goats, and cattle. These traps collect not only *Culicoides* but also many other insects that exhibit a positive phototropism such as sand flies and mosquitoes, among others.

Captured specimens were stored in 70% ethanol and morphological identification was carried out following the characters described by Martínez-Ortega and Conesa Gallego (1987b) and Gállego Berenguer et al. (1992). Female specimens were identified by microscopic observation of the spermatheca, after dissection and slide mounting of the last three abdominal segments with Hoyer's solution. Males were identified by direct stereomicroscopic observation of the features of the external genitalia.

The species included in this list are ordered alphabetically by subfamily, genus, and subgenus. Species names include authorities and year (Table 1). Nomenclaturally, we have used the organisation and abbreviations proposed by Rispaill and Léger (1998) and Marcondes (2007) for the genera and subgenera of Phlebotominae. The subgenus *Abonnencius* proposed by Morillas-Márquez and Guevara Pozo (1994) for *Phlebotomus fortunatarum* Úbeda Ontiveros et al. (1982), an endemic species of the Canary Islands (Spain), has also been included. The status of some species in Spain is also briefly discussed in the Notes section.

## Current distribution

The distribution maps of each species have been made at province level (NUTS3) using the software QGIS Geographic Information System, version 3.22.0 (2021). The reference coordinate system established in the work was EPSG:4258-ETRS89. QGIS Association, <http://www.qgis.org>. (Figs 1–13).

Each figure shows the origin of the knowledge of the distribution of each species:

1. From data obtained from the literature review: Grey provinces for presence and white for absence of the species.
2. From the positive sampling points (black) of our entomological surveillance: If any of these sampling points is the first report for that province, that province is highlighted in green.

## Results

From the comprehensive bibliography reviewed, a total of 13 sand fly species have been reported in Spain (Table 1), although two of them have a controversial status

(*Ph. longicuspis* Nitzulescu, 1930 and *Ph. riouxi* Depaquit, Killick-Kendrick & Léger, 1998) and are discussed in the Notes section. According to the nomenclatural criteria used, these 13 species belong to two genera and six subgenera, as follows: *Phlebotomus* (*Abonnencius*) (one species), *Ph.* (*Larrousius*) (four species), *Ph.* (*Paraphlebotomus*) (four species), *Ph.* (*Phlebotomus*) (one species), *Ph.* (*Transphlebotomus*) (one species), *Sergentomyia* (*Sergentomyia*) (two species).

As a result of sand fly data collected between 2004 to 2021 as part of the entomological surveillance programme of *Culicoides* biting midges in Spain we record seven species of sand flies for the first time in some Spanish provinces, listed as follows. The

**Table 1.** Checklist of sand flies species recorded in Spain, classified by genus and subgenus.

Genus	Subgenus	Species	Author/Year
<i>Phlebotomus</i>	<i>Abonnencius</i>	<i>fortunatarum</i> *	Úbeda Ontiveros, Morillas-Márquez, Guevara Benítez, López Roman & Cutillas Barrios, 1982
	<i>Larrousius</i>	<i>ariasi</i>	Tonnoir, 1921
		<i>langeroni</i>	Nitzulescu, 1930
		<i>longicuspis</i> *	Nitzulescu, 1930
		<i>pernicius</i>	Newstead, 1911
	<i>Paraphlebotomus</i>	<i>alexandri</i>	Sinton, 1928
		<i>chabaudi</i>	Croset, Abonnenc & Rioux, 1970
		<i>riouxi</i> *	Depaquit, Killick-Kendrick & Léger, 1998
		<i>sergenti</i>	Parrot, 1917
	<i>Phlebotomus</i>	<i>papatasi</i>	(Scopoli, 1786)
	<i>Transphlebotomus</i>	<i>mascittii</i> *	Grassi, 1908
<i>Sergentomyia</i>	<i>Sergentomyia</i>	<i>fallax</i>	(Parrot, 1921)
		<i>minuta</i>	(Rondani, 1843)

\*Species with Notes. The list of references used to generate the distribution map for each species is provided in Suppl. material 1.

distribution of the main *Leishmania* vectors is widened in five provinces for *Ph. perniciosus* (Fig. 1) and in ten provinces for *Ph. ariasi*, including the island of Menorca, for the first time (Fig. 2). *Phlebotomus papatasi* is detected in eight new provinces in the centre and north of the country, as well as on the island of Menorca (Fig. 3). Regarding *Ph. sergenti* Parrot, 1917, a new province is cited but it is absent in the northwest of the Iberian Peninsula (Fig. 4). The distribution of *Phlebotomus mascittii* Grassi, 1908 is extended to two more provinces on the Cantabrian basin (Fig. 5). As for *Ph. langeroni* Nitzulescu, 1930, its presence is extended to one more province in the centre of the Iberian Peninsula (Fig. 6). Finally, the presence of the species *Se. minuta* (Rondani, 1843) is broadened to six more provinces (Fig. 7), being found in practically the whole country. It should be noted that, *Ph. alexandri* Sinton, 1928 (Fig. 8), *Ph. chabaudi* Croset, Abonnenc & Rioux, 1970 (Fig. 9), *Ph. riouxi* (Fig. 10), *Ph. longicuspis* (Fig. 11), *Se. fallax* (Parrot, 1921) (Fig. 12), as well as the endemic species of the Canary Islands, *Ph. fortunatarum* (Fig. 13), have not been detected in the course of the national entomological surveillance programme, maybe due to the use of biased sampling methods or specific trapping in ruminant farms.

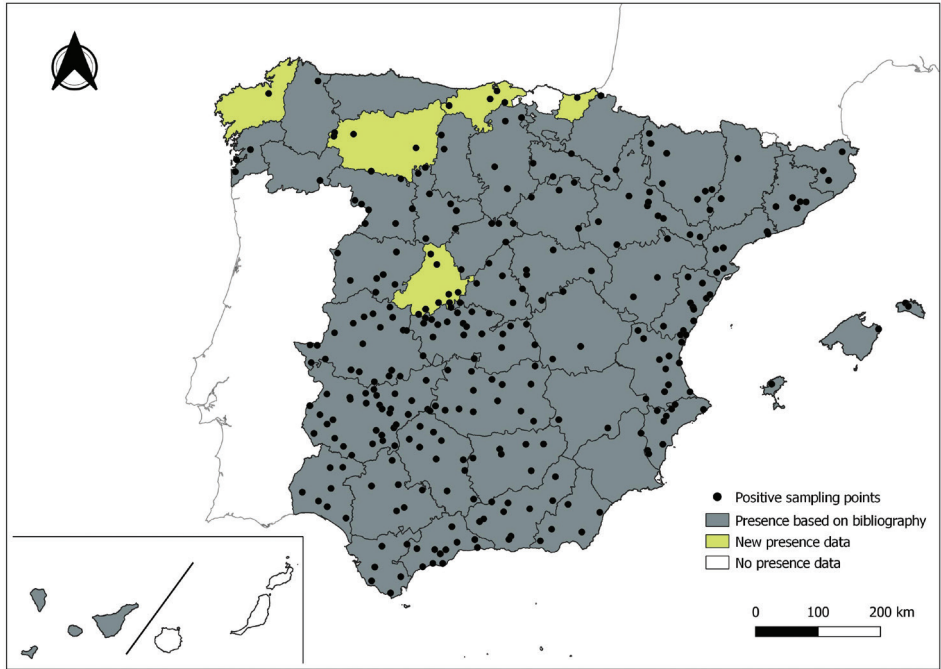


**Figure 1.** Distribution of *Phlebotomus perniciosus* in Spain.

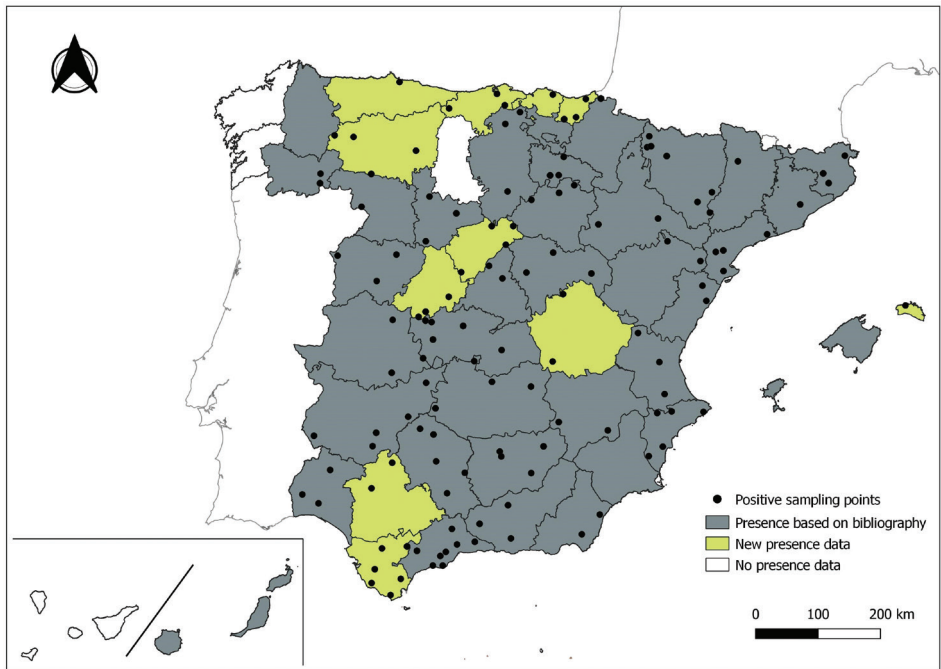


**Figure 2.** Distribution of *Phlebotomus ariasi* in Spain.

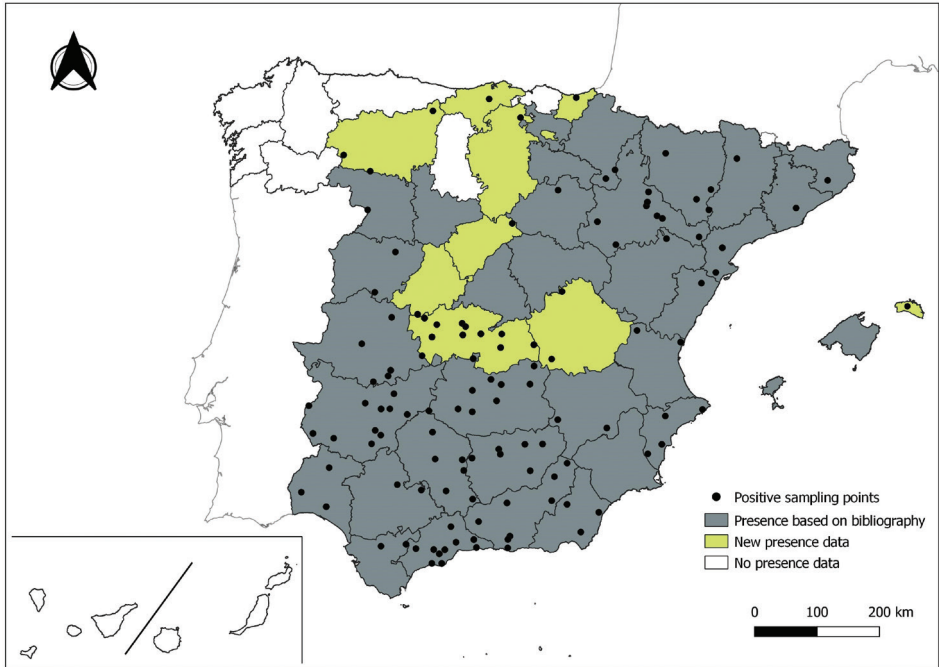


**Figure 3.** Distribution of *Phlebotomus papatasi* in Spain.

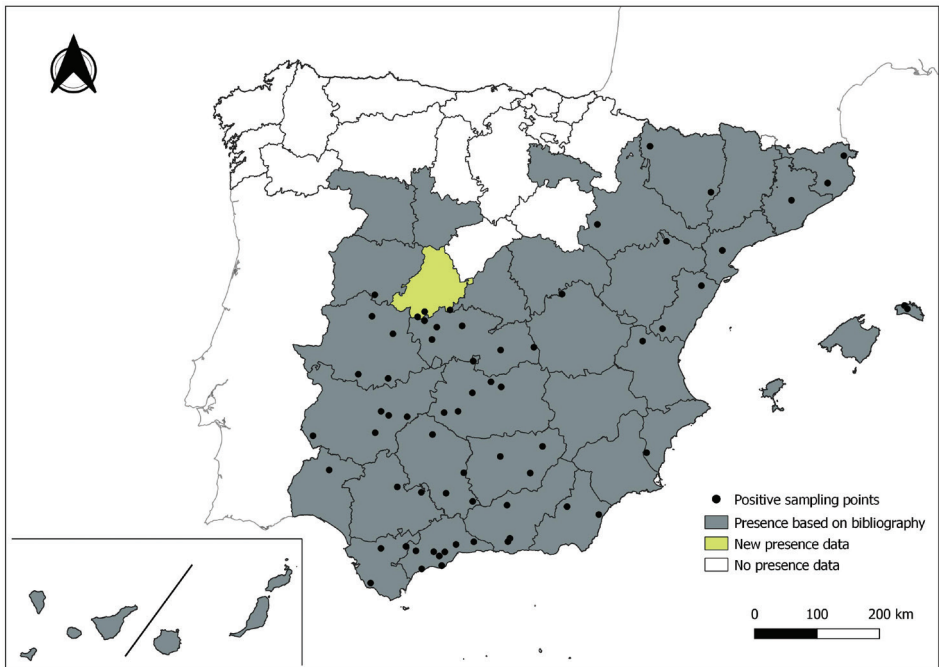


**Figure 4.** Distribution of *Phlebotomus sergenti* in Spain.

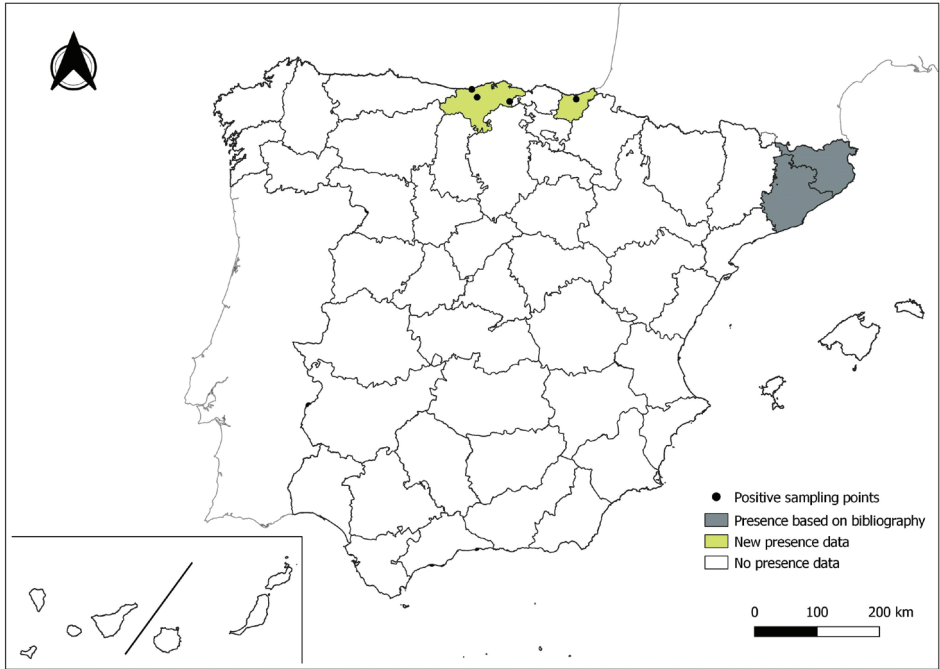


**Figure 5.** Distribution of *Phlebotomus mascittii* in Spain.

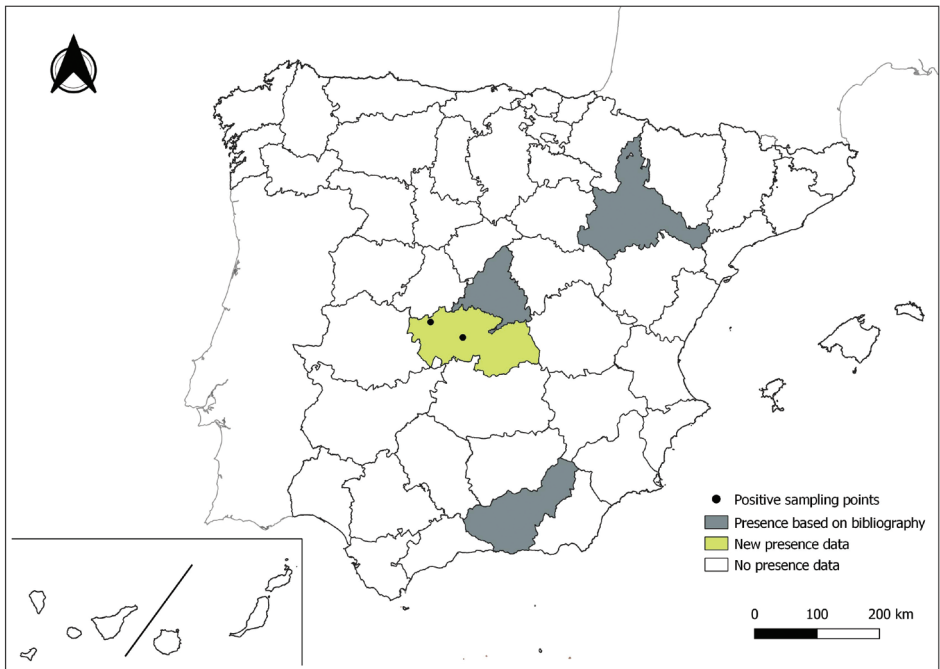


**Figure 6.** Distribution of *Phlebotomus langeroni* in Spain.

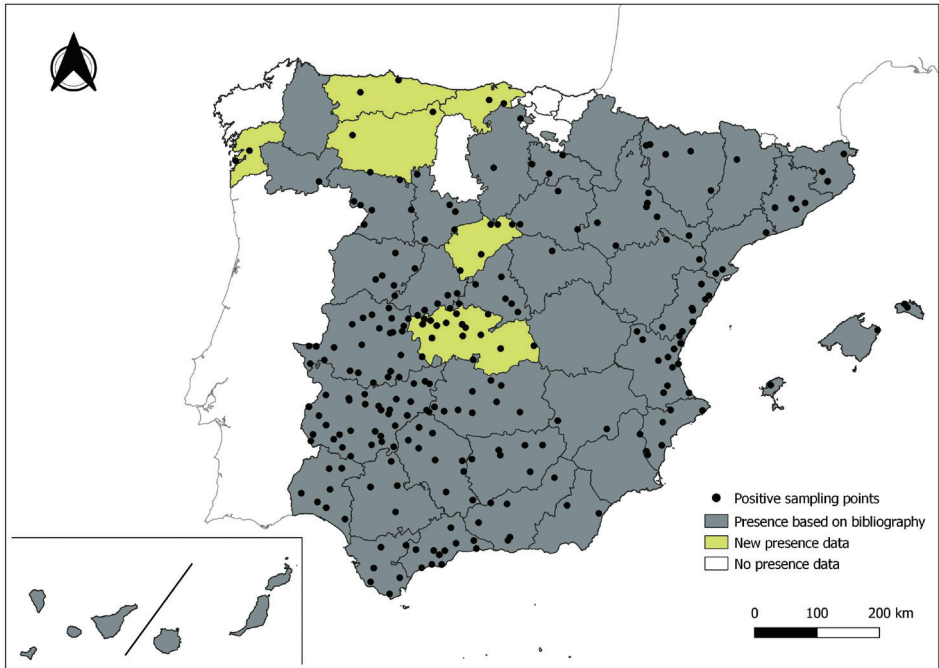


**Figure 7.** Distribution of *Sergentomyia minuta* in Spain.

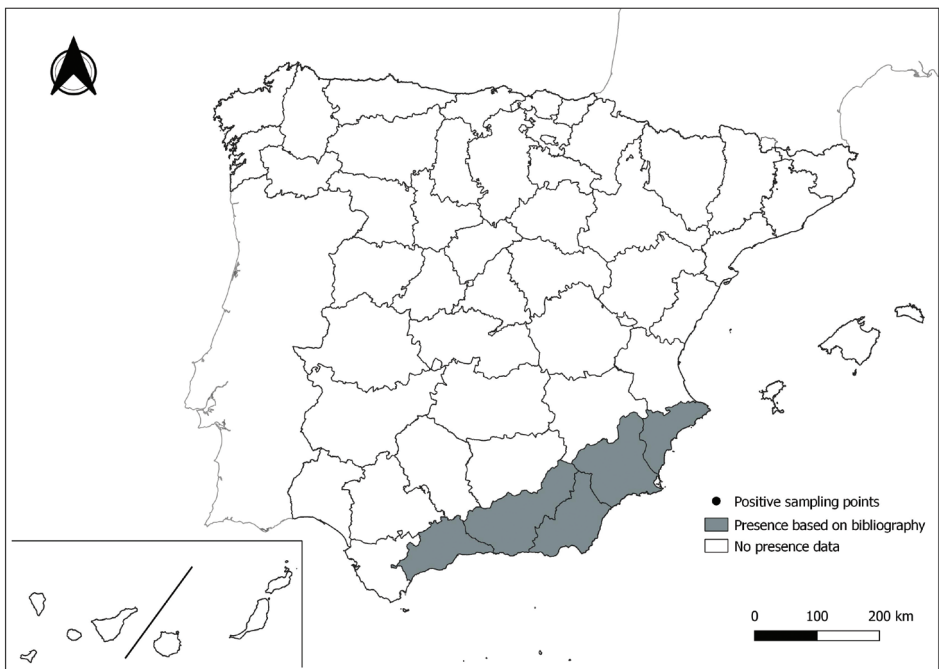


**Figure 8.** Distribution of *Phlebotomus alexandri* in Spain.



**Figure 9.** Distribution of *Phlebotomus chabaudi* in Spain.

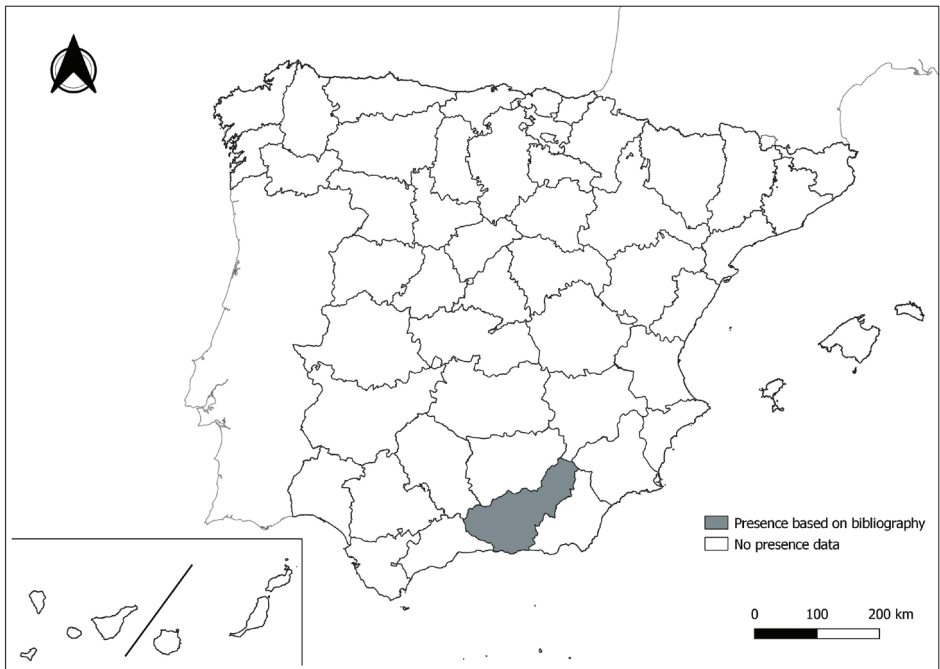


**Figure 10.** Distribution of *Phlebotomus riouxi* in Spain.

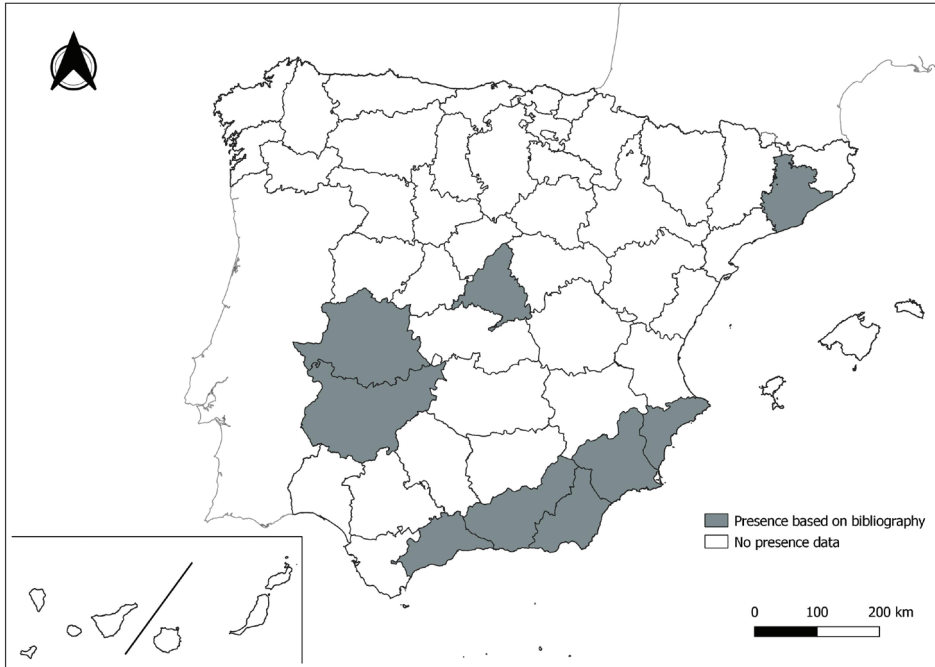


**Figure 11.** Distribution of *Phlebotomus longicuspis* in Spain.



**Figure 12.** Distribution of *Sergentomyia fallax* in Spain. Note its absence from peninsula Spain.



**Figure 13.** Distribution of *Phlebotomus fortunatarum* in Spain. Note its absence from peninsula Spain.

## Notes

I. *Phlebotomus fortunatarum* is an endemic species from the Canary Islands (Spain), which was described for the first time in Gran Canaria island in 1982 (Úbeda Ontiveros et al. 1982), and later in other islands (Morillas-Márquez et al. 1984; Lane and Alexander 1988; Martínez-Ortega et al. 1988). Due to its morphological characteristics (Úbeda Ontiveros and Morillas-Márquez 1983), it could not be included in the subgenera already available, so the subgenus *Abonnenci* was proposed by Morillas-Márquez et al. (1984). However, Lane and Alexander (1988) rejected the subgenus *Abonnenci* and included *Ph. fortunatarum* in the subgenus *Anaphlebotomus*. Some years later, Morillas-Márquez and Guevara Pozo (1994) discussed and proved the validity of the subgenus *Abonnenci*, which according to the authors, should be retained until new complete classification proposed for the entire genus *Phlebotomus*.

II. *Phlebotomus longicuspis* was first described in Tunisia as a variety of *Ph. langeroni* and was elevated to species status by Parrot (1936). This species is now considered common in North Africa (Pesson et al. 2004). Since its detection in Spain in 1982 by Morillas-Márquez et al. (1982b), numerous authors have cited the presence of this species based exclusively on male specimens in many regions, mainly in the south and east of the country (Martínez-Ortega et al. 1982; Rosado Maestre 1997; Blázquez Martín 1998; Martín-Sánchez et al. 2000). However, the morphological similarities

of the copulatory structure with *Ph. perniciosus* have generated controversy about the validity of *Ph. longicuspis*. The difficulty of correctly determining the males of each species, together with numerous intermediate stages, have led authors such as Morillas-Márquez et al. (1991) and Collantes and Martínez-Ortega (1997) to conclude that this taxonomic criterion is not discriminatory. Nevertheless, Di Muccio et al. (2000) carried out a phylogenetic analysis on specimens of *Phlebotomus* species belonging to the subgenus *Larrousius* from Morocco using ITS2 rDNA sequences and suggested that they are a distinct species, despite slight morphological differences. In addition, isoenzyme studies and comparative DNA sequencing of a mitochondrial cytochrome b fragment (mtDNA) showed that some sympatric populations of *Ph. perniciosus* and *Ph. longicuspis* have the characteristics of a biological species (Pesson et al. 2004). Interspecific gene introgression and a new sibling species have been detected, making identification even more difficult. The proximity of Spain to North Africa increases the possibility of detecting specimens with intermediate characters (Collantes and Martínez-Ortega 1997). Old records based on morphology may not necessarily reflect the true geographical distribution or occurrence of *Ph. longicuspis* presented here for Spain. All records of *Ph. longicuspis* in Spain are from the 1980s and 1990s, when molecular tools were not used and the taxonomic identification of sand flies was based solely on morphological criteria. Currently, the Spanish sand fly specialist community assumes that records of *Ph. longicuspis* in Spain are all probably *Ph. perniciosus*. Therefore, we consider the presence of *Ph. longicuspis* in Spain uncertain, although we show its recorded distribution from the literature in Fig. 11. Actual genetic characterisation of more populations would be necessary to improve our knowledge and verify the current status of this species in Spain.

III. *Phlebotomus riouxi* was first described by Depaquit et al. (1998) based on specimens from Morocco, Tunisia, and Spain. *Phlebotomus riouxi* is a species closely related to *Ph. chabaudi*, with subtle morphological differences in some structures (Depaquit et al. 1998; Lehrter et al. 2017). Molecular studies on several populations from Algeria and Tunisia supported the validity of both *Ph. riouxi* and *Ph. chabaudi* as typological species (Bounamous et al. 2008; Boudabous et al. 2009; Lehrter et al. 2017). However, Tabbabi et al. (2014) proposed considering both species as synonyms after molecular analysis of specimens from a single locality in Tunisia. Thus, even if both species have been reported in Spain (Figs 9, 10), reservations remain because, despite regular works on sand flies in the province of Granada, *Ph. riouxi* has not been detected again. We consider the records of *Ph. riouxi* in Spain as *Ph. chabaudi* and therefore the presence of the former species is uncertain in Spain.

IV. *Phlebotomus mascittii* was first detected in the early 1980s in Barcelona and Girona (north-eastern Spain) (Rioux et al. 1984). However, since then it has not been found until our detection through the entomological surveillance of blue-tongue vectors (Fig. 5). Furthermore, during a two-year (2019–2020) local research project aimed at revealing the diversity of bloodsucking dipteran pests in urban and rural areas of the Basque Country (northern Spain), specimens were detected in an urban cemetery. All of these new reports along the Cantabrian cor-

nice (northern Spain) motivated the realisation of a study recently focused on this species, which delved into the distribution of its different haplotypes (Alarcón-Elbal et al. 2021).

## Acknowledgements

We thank the Spanish Ministry of Agriculture, Fishery and Food (MAPA) for allowing access to data from the Spanish National Surveillance control and eradication of Bluetongue programme.

## References

- Akhoundi M, Kuhls K, Cannet A, Votýpka J, Marty P, Delaunay P, Sereno D (2016) A historical overview of the classification, evolution, and dispersion of *Leishmania* parasites and sandflies. *PLoS Neglected Tropical Diseases* 10(3): e0004349. <https://doi.org/10.1371/journal.pntd.0004349>
- Alarcón-Elbal PM, González MA, Delacour-Estrella S, Bravo-Barriga D, Estrada Peña R, Goiri F, García-Pérez AL, Lucientes J (2021) First findings and molecular data of *Phlebotomus mascittii* (Diptera: Psychodidae) in the Cantabrian Cornice (Northern Spain). *Journal of Medical Entomology* 58(6): 2499–2503. <https://doi.org/10.1093/jme/tjab091>
- Alcover MM, Ballart C, Martín-Sánchez J, Serra T, Castillejo S, Portús M, Gállego M (2014) Factors influencing the presence of sand flies in Majorca (Balearic Islands, Spain) with special reference to *Phlebotomus perniciosus*, vector of *Leishmania infantum*. *Parasites & Vectors* 7(1): 1–12. <https://doi.org/10.1186/1756-3305-7-421>
- Alten B, Maia C, Afonso MO, Campino L, Jiménez M, González E, Molina R, Bañuls AL, Prudhomme J, Vergnes B, Toty C, Cassan C, Rahola N, Thierry M, Sereno D, Bongiorno G, Bianchi R, Khoury C, Tsigotakis N, Dokianakis E, Antoniou M, Christodoulou V, Mazeris A, Karakus M, Ozbel Y, Arserim SK, Erisoz Kasap O, Gunay F, Oguz G, Kaynas S, Tsertsvadze N, Tskhvaradze L, Giorgobiani E, Gramiccia M, Volf P, Gradoni L (2016) Seasonal dynamics of phlebotomine sand fly species proven vectors of Mediterranean leishmaniasis caused by *Leishmania infantum*. *PLoS Neglected Tropical Diseases* 10(2): e0004458. <https://doi.org/10.1371/journal.pntd.0004458>
- Ayhan N, Charrel RN (2017) Of phlebotomines (sand flies) and viruses: A comprehensive perspective on a complex situation. *Current Opinion in Insect Science* 22: 117–124. <https://doi.org/10.1016/j.cois.2017.05.019>
- Ballart C, Guerrero I, Castells X, Barón S, Castillejo S, Alcover MM, Portús M, Gállego M (2014) Importance of individual analysis of environmental and climatic factors affecting the density of *Leishmania* vectors living in the same geographical area: The example of *Phlebotomus ariasi* and *P. perniciosus* in northeast Spain. *Geospatial Health* 8(2): 389–403. <https://doi.org/10.4081/gh.2014.28>

- Barón SD, Morillas-Márquez F, Morales-Yuste M, Díaz-Sáez V, Irigaray C, Martín-Sánchez J (2011) Risk maps for the presence and absence of *Phlebotomus perniciosus* in an endemic area of leishmaniasis in southern Spain: Implications for the control of the disease. *Parasitology* 138(10): 1234–1244. <https://doi.org/10.1017/S0031182011000953>
- Blázquez Martín A (1998) Análisis de *Phlebotomus* (Diptera, Psychodidae) en la alta Extremadura: Taxonomía, distribución y fenología. PhD Thesis, University of Extremadura, Spain.
- Boudabous R, Bounamous A, Jouet D, Depaquit J, Augot D, Ferté H, Berchi S, Couloux A, Veuille M, Babba H (2009) Mitochondrial DNA differentiation between two closely related species, *Phlebotomus (Paraphlebotomus) chabaudi* and *Phlebotomus (Paraphlebotomus) riouxi* (Diptera: Psychodidae), based on direct sequencing and Polymerase Chain Reaction-Restriction fragment length polymorphism. *Annals of the Entomological Society of America* 102(3): 347–353. <https://doi.org/10.1603/008.102.0301>
- Bounamous A, Boudabous R, Jouet D, Augot D, Ferté H, Babba H, Berchi S, Depaquit J (2008) Caractérisation moléculaire et morphologique de deux espèces affines de *Paraphlebotomus*: *Phlebotomus chabaudi* Croset, Abonnenc & Rioux, 1970 et *Ph. riouxi* Depaquit, Killick-Kendrick & Léger, 1998 (Diptera: Psychodidae). *Parasite (Paris, France)* 15(4): 565–571. <https://doi.org/10.1051/parasite/2008154565>
- Bravo-Barriga D, Parreira R, Maia C, Afonso MO, Blanco-Ciudad J, Serrano FJ, Pérez-Martín JE, Frontera E (2016) Detection of *Leishmania* DNA and blood meal sources in phlebotomine sand flies (Diptera: Psychodidae) in western of Spain: update on distribution and risk factors associated. *Acta Tropica* 164: 414–424. <https://doi.org/10.1016/j.actatropica.2016.10.003>
- Collantes F, Martínez-Ortega E (1997) Sobre la validez taxonómica de *Phlebotomus longicuspis* (Nitzulescu, 1931) (Diptera: Psychodidae). *Boletín de la Asociación Española de Entomología*. 21: 141–146.
- Czerny L, Strobl G (1909) Spanische Dipteren III. Beitrag. *Verhandlungen der kaiserlich-königlichen zoologisch-botanischen Gesellschaft in Wien* 59: 121–301.
- Depaquit J, Léger N, Killick-Kendrick R (1998) Description de *Phlebotomus (Paraphlebotomus) riouxi* n. sp. (Diptera-Psychodidae) d'Afrique du Nord. *Parasite (Paris, France)* 5(2): 151–158. <https://doi.org/10.1051/parasite/1998052151>
- Di Muccio T, Marinucci M, Frusteri L, Maroli M, Pesson B, Gramiccia M (2000) Phylogenetic analysis of *Phlebotomus* species belonging to the subgenus *Larrousius* (Diptera, Psychodidae) by ITS2 rDNA sequences. *Insect Biochemistry and Molecular Biology* 30(5): 387–393. [https://doi.org/10.1016/S0965-1748\(00\)00012-6](https://doi.org/10.1016/S0965-1748(00)00012-6)
- Gállego M, Rioux JA, Rispaïl P, Guilvard E, Gállego J, Portús M, Delalbre A, Bastien P, Martínez-Ortega E, Fisa R (1990) Primera denuncia de flebotomos (Diptera, Psychodidae, Phlebotominae) en la provincia de Lérida (España, Cataluña). *Revista Ibérica de Parasitología* 50(1–2): 123–127.
- Gállego Berenguer J, Botet J, Vynieta MP, Gállego M (1992) Los flebotomos de la España peninsular e Islas Baleares: identificación y corología: comentarios sobre los métodos de captura. In memoriam al profesor doctor D. Francisco de Paula Martínez Gómez, 579–600. <https://dialnet.unirioja.es/servlet/articulo?codigo=1166628>
- García San Miguel L, Sierra MJ, Vazquez A, Fernandez-Martínez B, Molina R, Sanchez-Seco MP, Lucientes J, Figuerola J, de Ory F, Monge S, Suarez B, Simón F (2021) Phlebovi-

- rus-associated diseases transmitted by phlebotominae in Spain: Are we at risk? *Enfermedades Infecciosas Microbiología Clínica*. Elsevier Doyma. <https://doi.org/10.1016/j.eimc.2020.02.026>
- Gil Collado J, Márquez FM, Marín MS (1989) Los flebotomos en España. *Revista de Sanidad e Higiene Pública* 63: 15–34.
- González E, Jiménez M, Hernández S, Martín-Martín I, Molina R (2017) Phlebotomine sand fly survey in the focus of leishmaniasis in Madrid, Spain (2012–2014): Seasonal dynamics, *Leishmania infantum* infection rates and blood meal preferences. *Parasites & Vectors* 10(1): e368. <https://doi.org/10.1186/s13071-017-2309-z>
- González E, Molina R, Iriso A, Ruiz S, Aldea I, Tello A, Fernández D, Jiménez M (2021) Opportunistic feeding behaviour and *Leishmania infantum* detection in *Phlebotomus perniciosus* females collected in the human leishmaniasis focus of Madrid, Spain (2012–2018). *PLoS Neglected Tropical Diseases* 15(3): e0009240. <https://doi.org/10.1371/journal.pntd.0009240>
- Jiménez M, González E, Iriso A, Marco E, Alegret A, Fúster F, Molina R (2013) Detection of *Leishmania infantum* and identification of blood meals in *Phlebotomus perniciosus* from a focus of human leishmaniasis in Madrid, Spain. *Parasitology Research* 112(7): 2453–2459. <https://doi.org/10.1007/s00436-013-3406-3>
- Lane RP, Alexander B (1988) Sandflies (Diptera: Phlebotominae) of the Canary Islands. *Journal of Natural History* 22(2): 313–319. <https://doi.org/10.1080/00222938800770241>
- Lehrter V, Bañuls AL, Léger N, Rioux JA, Depaquit J (2017) *Phlebotomus (Paraphlebotomus) chabaudi* and *Phlebotomus riouxi*: Closely related species or synonyms? *Parasite (Paris, France)* 24: e47. <https://doi.org/10.1051/parasite/2017050>
- León Sanz CM, Collantes F, Martínez-Ortega E (1998) Rectificación a la primera cita de Flebotomos (Diptera, Psychodidae) en la Península Ibérica. *Graellsia* 54(0): e114. <https://doi.org/10.3989/graellsia.1998.v54.i0.349>
- León Sanz CM, Collantes F, Martínez-Ortega E (1999) Revisión de la colección Nájera de Flebotomos (Diptera, Psychodidae) depositada en el Museo Nacional de Ciencias Naturales de Madrid. *Graellsia* 55(0): 217–221. <https://doi.org/10.3989/graellsia.1999.v55.i0.330>
- Lucientes-Curdi J, Benito-de-Martín MI, Castillo-Hernandez JA, Orcajo-Teresa J (1991) Seasonal dynamics of *Larrousius* species in Aragón (NE Spain). *Parassitologia* 33: 381–386. <https://europepmc.org/article/med/1841232>
- Lucientes-Curdi J, Castillo JA, Tang Y, Benito MI, Ferrer-Dufol M, Garcia-Salinas MJ, Peribañez MA, Guarga-Penella JL (1995) Sobre el hallazgo de *Phlebotomus perniciosus* Newstead, 1911 (Diptera Psychodidae) parasitado por *Mastophorus muris* (Gmelin, 1790) (Nematoda: Spirurina). *Zapateri* 5: 179–182.
- Marcondes CB (2007) A proposal of generic and subgeneric abbreviations for phlebotomine sandflies (Diptera: Psychodidae: Phlebotominae) of the world. *Entomological News* 118(4): 351–356. [https://doi.org/10.3157/0013-872X\(2007\)118\[351:APOGAS\]2.0.CO;2](https://doi.org/10.3157/0013-872X(2007)118[351:APOGAS]2.0.CO;2)
- Martín-Sánchez J, Gramiccia M, Pesson B, Morillas-Márquez F (2000) Genetic polymorphism in sympatric species of the genus *Phlebotomus*, with special reference to *Phlebotomus perniciosus* and *Phlebotomus longicuspis* (Diptera, Phlebotomidae). *Parasite (Paris, France)* 7(4): 247–254. <https://doi.org/10.1051/parasite/2000074247>

- Martínez-Ortega E (1986) Biology of Iberian sandflies (Diptera, Psychodidae) under natural conditions. *Annali dell'Istituto Superiore di Sanita* 22(1): 73–78. <https://pubmed.ncbi.nlm.nih.gov/3752827/>
- Martínez-Ortega E, Conesa Gallego E (1987a) Los flebotomos (Diptera, Psychodidae) del sureste de la Península Ibérica, presentación del hábitat y metodología del muestreo. *Mediterránea. Serie de Estudios Biológicos* 9: 63–86. <https://doi.org/10.14198/mdtrra1987.9.06>
- Martínez-Ortega E, Conesa Gallego E (1987b) Caracteres morfológicos de interés taxonómico de los flebotomos (Diptera, Psychodidae) de la Península Ibérica. *Anales de Biología* 11(3): 43–53. <https://revistas.um.es/analesbio/article/view/35751>
- Martínez-Ortega E, Ward RD, Martín Luengo F, Conesa Gallego E (1982) Nueva distribución de *Phlebotomus (Larrousius) longicuspis* Nitzulescu 1930 (Diptera, Phlebotomidae) en España. *Revista Ibérica de Parasitología* 42: 283–288.
- Martínez-Ortega E, Conesa Gallego E, Diaz Sánchez F (1988) Aportación al conocimiento de los flebotomos (Diptera, Psychodidae) de las Islas Canarias. *Revista Ibérica de Parasitología* 48(1): 89–893. <https://agris.fao.org/agris-search/search.do?recordID=ES8900049>
- Martínez-Ortega E, Gallego EC, Lozano HR (1996) A new sandfly from Spain: *Phlebotomus (Larrousius) langeroni* Nitzulescu, 1930 (Diptera, Psychodidae). *Parasite (Paris, France)* 3(1): 77–80. <https://doi.org/10.1051/parasite/1996031077>
- Medlock JM, Hansford KM, Van Bortel W, Zeller H, Alten B (2014) A summary of the evidence for the change in European distribution of phlebotomine sand flies (Diptera: Psychodidae) of public health importance. *Journal of Vector Ecology* 39(1): 72–77. <https://doi.org/10.1111/j.1948-7134.2014.12072.x>
- Morillas-Márquez F, Guevara Pozo D (1994) On the validity of the subgenus *Phlebotomus (Abonnencius)* (Diptera: Psychodidae: Phlebotominae). *Research and Reviews in Parasitology* 5(1): 55–56.
- Morillas-Márquez F, Úbeda Ontiveros JM, Guevara Benítez DC, González Castro J (1982a) Confirmación de la presencia en España de *Phlebotomus (Paraphlebotomus) chabaudi* Crosset, Abonnenc y Rioux, 1970 (Diptera, Phlebotomidae). *Revista Ibérica de Parasitología* 42(3): 345–346.
- Morillas-Márquez F, Guevara Benítez, D. C, Gil Collado, J, Ubeda Ontiveros JM (1982b) Presencia en España de *Phlebotomus (Larrousius) longicuspis* (Nitzulescu, 1930). *Revista Ibérica de Parasitología*, 191–196.
- Morillas-Márquez F, Guevara Benítez DC, Úbeda Ontiveros JM, González Castro J (1983a) Teratismos observados en *Sergentomyia minuta* (Rondani, 1843) (Diptera, Phlebotomidae) capturados en España. *Revista Ibérica de Parasitología* 43(2): 135–143.
- Morillas-Márquez F, Castillo Remiro A, Ubeda Ontiveros JM (1983b) Existencia de *Sergentomyia fallax* (Parrot, 1921) (Diptera, Phlebotomidae) en las Islas Canarias. In: III National congress of Parasitology, Barcelona.
- Morillas-Márquez F, Úbeda Ontiveros JM, Castillo Remiro A (1984) Nuevos datos sobre *Phlebotomus fortunatarum* Úbeda Ontiveros y cols, 1982 y presencia de *Sergentomyia fallax* (Parrot, 1921) (Diptera, Phlebotomidae) en el archipiélago Canario. *Revista Ibérica de Parasitología* 44(1): 29–38.

- Morillas-Márquez F, Sanchís Marín MC, Martín Sánchez J, Acedo Sánchez C (1991) On *Phlebotomus perniciosus* Newstead, 1911 (Diptera, Phlebotomidae) in the province of Almería in southeastern Spain. *Parassitologia* 33: 437–444.
- Parrot L (1936) Notes sur Les Phlébotomes XX. – Sur *Phlebotomus langeroni* var. *longicuspis* Nitzulescu, 1930. *Archives. Institut Pasteur d'Algerie* 14: 137–143.
- Pesson B, Ready JS, Benabdennbi I, Martín-Sánchez J, Essegir S, Cadi-Soussi M, Morillas-Marquez F, Ready D (2004) Sandflies of the *Phlebotomus perniciosus* complex: Mitochondrial introgression and a new sibling species of *P. longicuspis* in the Moroccan Rif. *Medical and Veterinary Entomology* 18(1): 25–37. <https://doi.org/10.1111/j.0269-283x.2004.0471.x>
- Remoli ME, Jiménez M, Fortuna C, Benedetti E, Marchi A, Genovese D, Gramiccia M, Molina R, Ciufolini MG (2016) Phleboviruses detection in *Phlebotomus perniciosus* from a human leishmaniasis focus in South-West Madrid region, Spain. *Parasites & Vectors* 9(1): 1–11. <https://doi.org/10.1186/s13071-016-1488-3>
- Rioux JA, Croset H, Leger N (1974) Presence in Spain of *Phlebotomus chabaudi* Croset, Abbonenc and Rioux, 1970 (Diptera - Psychodidae). *Annales de Parasitologie Humaine et Comparee* 49(4): 505–507. <https://doi.org/10.1051/parasite/1974494505>
- Rioux JA, Croset H, Leger N, Maistre M (1975) Comments on the infraspecific taxonomy of *Sergentomyia minuta* (Rondani, 1843), *S. africana*. *Annales de Parasitologie Humaine et Comparee* 50(5): 635–641. <https://doi.org/10.1051/parasite/1975505635>
- Rioux JA, Gallego J, Jarry DM, Guilvard E, Maazoun R, Périères J, Becqueriaux A, Belmonte A (1984) A new *Phlebotomus* for Spain. *Phlebotomus (Adlerius) mascittii* Grassi, 1908. *Annales de Parasitologie Humaine et Comparee* 59(4): 421–425. <https://doi.org/10.1051/parasite/1984594421>
- Rispail P, Léger N (1998) Numerical taxonomy of Old World Phlebotominae (Diptera: Psychodidae): 2. Restatement of classification upon subgeneric morphological characters. *Memorias do Instituto Oswaldo Cruz* 93(6): 787–793. <https://doi.org/10.1590/S0074-02761998000600016>
- Rosado Maestre D (1997) Estudio de flebotomos en Cáceres: taxonomía, distribución y fenología. PhD Thesis, University of Extremadura, Spain. <https://dialnet.unirioja.es/servlet/tesis?codigo=202294&info=resumen&idioma=SPA>
- Sanbonmatsu-Gámez S (2005) Infección neurológica por virus Toscana en la provincia de Granada: Estudio Clínico-Epidemiológico. PhD Thesis, University of Granada, Spain.
- Sanchez Clemente N, Ugarte-Gil CA, Solórzano N, Maguiña C, Pachas P, Blazes D, Bailey R, Mabey D, Moore D (2012) *Bartonella bacilliformis*: A systematic review of the literature to guide the research agenda for elimination. *PLoS Neglected Tropical Diseases* 6(10): e1819. <https://doi.org/10.1371/journal.pntd.0001819>
- Tabbabi A, Rhim A, Ghrab J, Martín O, Aoun K, Bouratbine A, Ready P (2014) *Phlebotomus (Paraphlebotomus) riouxi*: A synonym of *Phlebotomus chabaudi* without any proven vectorial role in Tunisia and Algeria. *Medical and Veterinary Entomology* 2(1): 51–59. <https://doi.org/10.1111/mve.12067>
- Úbeda Ontiveros JM, Morillas-Márquez F (1983) Designation of the holotype of *Phlebotomus fortunatarum* Úbeda Ontiveros et al. 1982 (Diptera, Phlebotomidae). *Revista Ibérica*

de Parasitología 43(3): 307–308. <http://bibliotecavirtual.ranf.com/i18n/consulta/registro.cmd?id=11946>

Úbeda Ontiveros JM, Morillas-Márquez F, Guevara Benítez DC, López Román R, Cutillas Barrios C (1982) Flebotomos de las Islas Canarias (España). *Revista Ibérica de Parasitología, Extra.*: 197–206.

## Supplementary material I

### List of bibliographic references associated with the distribution of sand flies by province in Spain

Authors: Daniel Bravo-Barriga, Ignacio Ruiz-Arrondo, Rosa Estrada Peña, Javier Lucientes, Sarah Delacour-Estrella

Data type: excel file.

Explanation note: The supplementary file includes the 136 references of scientific papers and grey literature listed in the checklist (ordered by ID, year and author). We also include the references of each species of sand fly by Spanish province.

Copyright notice: This dataset is made available under the Open Database License (<http://opendatacommons.org/licenses/odbl/1.0/>). The Open Database License (ODbL) is a license agreement intended to allow users to freely share, modify, and use this Dataset while maintaining this same freedom for others, provided that the original source and author(s) are credited.

Link: <https://doi.org/10.3897/zookeys.1106.81432.suppl1>



# Redescription of *Apocorophium acutum* (Crustacea, Amphipoda, Corophiidae) with material from type locality and key of world *Apocorophium* species

Benoit Guillieux<sup>1</sup>, Hugues Blanchet<sup>1</sup>, Patrice Gonzalez<sup>1</sup>

<sup>1</sup> Université de Bordeaux, CNRS, EPOC, EPHE, UMR 5805, F-33600 Pessac, France

Corresponding author: Benoit Guillieux ([benoit.guillieux@u-bordeaux.fr](mailto:benoit.guillieux@u-bordeaux.fr))

---

Academic editor: Charles Oliver Coleman | Received 9 March 2022 | Accepted 23 May 2022 | Published 17 June 2022

---

<http://zoobank.org/1F1AE2A7-EA38-48DD-9EDE-021B6CB4C57F>

---

**Citation:** Guillieux B, Blanchet H, Gonzalez P (2022) Redescription of *Apocorophium acutum* (Crustacea, Amphipoda, Corophiidae) with material from type locality and key of world *Apocorophium* species. ZooKeys 1106: 101–119. <https://doi.org/10.3897/zookeys.1106.83340>

---

## Abstract

*Apocorophium acutum* (Chevreux, 1908), the type species of the genus, was originally but only partially described by Chevreux with female specimens from Bônes (Algeria); male specimens were later described from Brittany (France). Since then, the species has been recorded in different places of the world, some of them questionable. Herein, the species is entirely redescribed with material from the type locality and Brittany, and additional material from Arcachon Bay is studied to provide biological data. The known geographical distribution of this species is summarized, and a world identification key of *Apocorophium* species is also given.

## Keywords

Corophiini, ecology, redescription, world key

## Introduction

Corophiini Leach, 1814 are generally tube-dwelling amphipods present in various marine, estuarine, and freshwater habitats, including in sandy to muddy bottoms, with hydrozoa, on algae, and among oysters, and some species can be commensal (Crawford 1937; Lincoln 1979; Bousfield and Hoover 1997). Some genera and species have a

worldwide distribution. Bousfield and Hoover (1997) reviewed in depth the superfamily Corophioidea Leach, 1814 and described the subfamily Corophiinae, 12 new genera, and a new species. Later, Myers and Lowry (2003) provided a new classification, dividing the suborder Corophiidea Leach, 1814 into two infraorders (Corophiida and Caprellida Leach, 1814) and reassigned the authority of Corophiini, Corophiinae, Corophiidae, and Corophiida to Leach (1814). Lowry and Myers (2013) replaced Corophiidea by Senticaudata Lowry & Myers, 2013.

The identification key by Bousfield and Hoover (1997) is widely used around the world, but unfortunately, the study of some original descriptions of selected Corophiini species show that their key contains mistakes; this was rectified by Gouillieux and Sauriau (2019) in their key to the species characterized by urosome segments fused with uropod 1 arising mainly ventrally.

According to Horton et al. (2021), five species belong to the genus *Apocorophium*: *A. acutum* (Chevreux, 1908), *A. curumim* Valério-Berardo & Thiago de Souza, 2009, *A. lacustre* (Vanhöffen, 1911), *A. louisianum* (Shoemaker, 1934), and *A. simile* (Shoemaker, 1934). *Apocorophium acutum*, the type species of the genus, was partially described by Chevreux (1908) and Chevreux and Fage (1925) from the Algerian Mediterranean and French Atlantic coasts. It is a well-known Mediterranean and Atlantic species (Crawford 1937; Myers 1982; Bachelet et al. 2003) and was subsequently recorded in different areas around the world with more or less detailed descriptions; however, some of these are doubtful. This paper provides a complete redescription of *A. acutum* based on females specimens from Bône (the type locality) and male specimens from Brittany (the geographical area of the first description of a male specimen), additional ecological and biological information, and an identification key to the world *Apocorophium* species.

## Materials and methods

Specimens of *Apocorophium acutum* examined come from three different localities (Fig. 1): (1) Bône, Algeria, type locality of female specimens; (2) Trébeurden, Brittany, France, 5 km from Lanion River, which is the geographical area of the first description of male specimens, and (3) Arcachon Bay, France. The specimens were examined with a stereomicroscope and a compound microscope. Body length (BL) from the anterior margin of head to the posterior end of telson and eggs' size were measured with NIS-Elements Analysis software. Females from Arcachon Bay (stations "bouée 13" and "Arcachon harbor") with intact brood pouches were separated in order to measure their fecundity: the eggs were removed from the brood pouch of each female, counted, and their diameter measured. Specimens from a third location in Arcachon Bay (station "blockhaus") were used to evaluate the relationship between body length and gender features (male characteristics features, oostegite shape and presence of eggs). Relationships between quantitative variables such as body length in females and number of eggs in the marsupium were assessed by Spearman's rank correlation in order to potentially



**Figure 1.** Sampling stations of *Apocorophium acutum* (Chevreux, 1908) used in this study. Bône (Algeria): female locality type; Trébeurden (France): 5 km from the location of the first description of a male; Arcachon Bay (France): additional material examined.

show a possible non-linear but monotone relationship between variables (Hollander and Wolfe 1973). Differences in body length among morphologically different specimens (e.g., males, egg-bearing female, female with smooth oostegite) were tested using non-parametric Kruskal-Wallis test followed by post-hoc pairwise Dunn test where significant differences were assessed by Kruskal-Wallis test (Hollander and Wolfe 1973).

For scanning electron microscope (SEM) studies, specimens were dehydrated in a graded ethanol series, critical-point dried, sputter coated with gold, and examined with a scanning electron microscope. Drawings were carried out from pictures using INKSCAPE software (v. 0.92). Specimens from Bône were loaned from the Muséum national d’Histoire naturelle (MNHN, Paris), and some specimens studied from Trébeurden were deposited in the MNHN, Paris. Molecular analyses on specimens from Trébeurden and Arcachon were carried out and sequences are available in GenBank (GenBank accession numbers: ON455206 to ON455209). Unfortunately, it was not possible to do molecular analyses with material from the type locality to compare with French specimens.

## Results

### Systematics

#### Order Amphipoda Latreille, 1816

#### Suborder Senticaudata Lowry & Myers, 2013

#### Family Corophiidae Leach, 1814

#### Subfamily Corophiinae Leach, 1814

#### Tribe Corophiini Leach, 1814

#### Genus *Apocorophium* Bousfield & Hoover, 1997

#### *Apocorophium acutum* (Chevreux, 1908)

*Corophium acutum* Chevreux 1908: 75 (original description), fig. 6.—1910: 271, h.—Chevreux and Fage 1925: 366–367, figs 359, 374.—Poisson and Legueux 1926: 320–325, figs 5,6 (Banyuls form).—Schellenberg 1928: 672–673.—Shoemaker 1934: 26–27.—Crawford 1937: 624–625.—Ruffo 1938: 147–148.—Salfi 1939: 31–62, figs 1–7.—Shoemaker 1947: 59, fig. 9.—Hurley 1954: 439–442, figs 2, 3 (in part).—Barnard 1969: 42.—Bousfield 1973: 205, fig. LXIV.—Lincoln 1979: 534, fig. 256 (in part).—Dickinson et al. 1980: 12.—Myers 1982 (in Ruffo ed.): male 188–190, fig. 126.—Barnard and Karaman 1991: 185.

*Apocorophium acutum* Bousfield and Hoover 1997: 123–125, fig. 35.—Lowry and Stoddart 2003: 88.—Ren 2006: 296–297, fig. 117.—Bano and Kazmi 2012: 113.—Hossain and Hughes 2016: 376–381, figs 2–5.

Not *Corophium acutum* Poisson and Legueux 1926: 320–325, figs 5, 6 (Caen form).—Myers 1982 (in Ruffo ed.): female 188–190, fig. 126.

Doubtful *Apocorophium acutum* Jung and Kim 2007: 247–250, fig. 1.—Demicheli and Verdi: 2018, 1169–1173, figs 1–3.

**Material examined.** ALGERIA • 6 brooding females and 1 juvenile; Bône (type locality); 4 May 1900; MNHN-IU-2013-19982; campaign MELITA, St. 677 “Melita II”, on concrete blocks removed from the harbor • 1 female, same data as for preceding; MNHN-IU-2016-3401; dissected brooding specimen.

FRANCE • many males and females; Arcachon Bay / station “bouée 13”; 44°38'07.20"N, 001°14'06.60"W; 2 m depth; 20 September 2014; Benoit Gouillieux leg.; mussels, hand-collected on submerged part of a navigation buoy; MNHN-IU-2016-3426 and MNHN-IU-2016-3427 • many males and females; Arcachon Bay / station “Arcachon harbor”; 44°39'36.53"N, 001°09'06.59"W; 0.5 m depth; 20 February 2020; Benoit Gouillieux leg.; on floating pontoons in harbor • 414 specimens; Arcachon Bay / station “blockhaus”; 44°34'00.40"N, 001°14'15.14"W; 5 m depth; between May 2018 and April 2019; Benoit Gouillieux leg.; with Hydrozoa *Amphisbetia operculata* (Linnaeus, 1758) • many males and females; Trébeurden / harbor; 48°46'12.21"N, 003°35'09.71"W; 0.5 m depth; 1 February 2020; Gabin Droual leg.; on floating pontoons (Port); MNHN-IU-2016-3392.

**Description (Figs 2–5).** Based on adults females, Chevreux collection, MNHN-IU-2016-3401 and MNHN-IU-2013-19982, Bône, Algeria, 4 May 1900, campaign MELITA, St. 677 “Melita II”, type locality.

**Head.** *Head* with rostrum pointed distally, triangular in dorsal view, reaching lateral ridge of head. *Eyes* visible in alcohol. *Antenna 1* weakly setose; peduncular article 1 rectangular, ventral margin with three robust setae, dorsomedial margin with two robust setae; length ratio of peduncular articles 1–3 = 1.00 : 0.72 : 0.31; flagellum 5-articulate, shorter than peduncle, articles 2–4 with a small aesthetascs ventrodistally. *Antenna 2* peduncular article 3 wider than long, with a pair of mediobasal robust setae; peduncular article 4 with three solitary robust setae; peduncular article 5 with a robust seta medially and a small process mediobasally; flagellum 3-articulate, distal article tiny with two robust setae. *Lower lip* inner lobe subovate, coalescent proximally, rounded apically; mandibular process small and blunt; both lobes covered with patch of pubescence medially. *Right mandible* well developed, incisor process and lacinia mobilis produced inward, bluntly tridentate; accessory setal row with three curved, finely pectinate blades, followed by tuft of pappose setae and a brush-like seta; molar well developed, massive, truncate; palp biarticulate, proximal segment shorter than distal, with 1 finely plumose seta apically, distal segment slender, with pubescence medially and long plumose seta apically. *Left mandible* similar, except for molar process which presents 2 additional blades. *Maxilla 1* outer plate armed with seven setal-teeth apically; palp biarticulate, proximal segment short, distal one extending beyond end of outer lobe, with row of seven distal setae. *Maxilla 2* inner plate with longitudinal row of pinnate setae on inner and distal margins; outer plate extending beyond end of inner one, with row of pinnate setae on distal margin. *Maxilliped* inner plate slender and elongate, basal portion with row of about nine plumose setae, inner margin with four and two pinnate setae; outer plate not reaching distal end of palp article 2, basal portion with row of about ten plumose setae, inner margin densely setose; palp 4-articulate, article 2 elongate, about three times as long as wide, inner margin densely setose, outer margin with one plumose seta distally, article 3 with rounded distal corner, distal article small, 0.24× article 3, with apical setae.

*Pereon. Gnathopod 1* subchelate; coxa ventral margin with three long plumose setae, anterior margin with two simple setae; basis anterior margin unarmed, posterodistal corner with unequal setae; ischium quadrate, with long pinnate setae posterodistally; merus short, with long pinnate setae posterodistally; carpus slightly narrowing distally, anterior margin with one median and two distal simple setae, posterior margin with two rows of pinnate setae; propodus 0.9× carpus, posterior margin slightly convex, medial portion with pectinate setae, palm transverse, slightly convex, edge laminar and transversally striated, limited posteriorly by two robust setae; dactylus falcate. *Gnathopod 2* simple; coxa small, with one long simple seta anteriorly; basis subrectangular, anterodistal and posterodistal corners with a simple seta; ischium flat, depressed, posterodistal corner with a simple seta; merus convexly curved posteriorly, with two rows of long pinnate setae along posterior margin and medial portion; carpus isosceles triangle in shape, strongly widening distally, with two small simple and few long pinnate setae posterodistally; propodus weakly narrowing distally, 1.6× carpus,

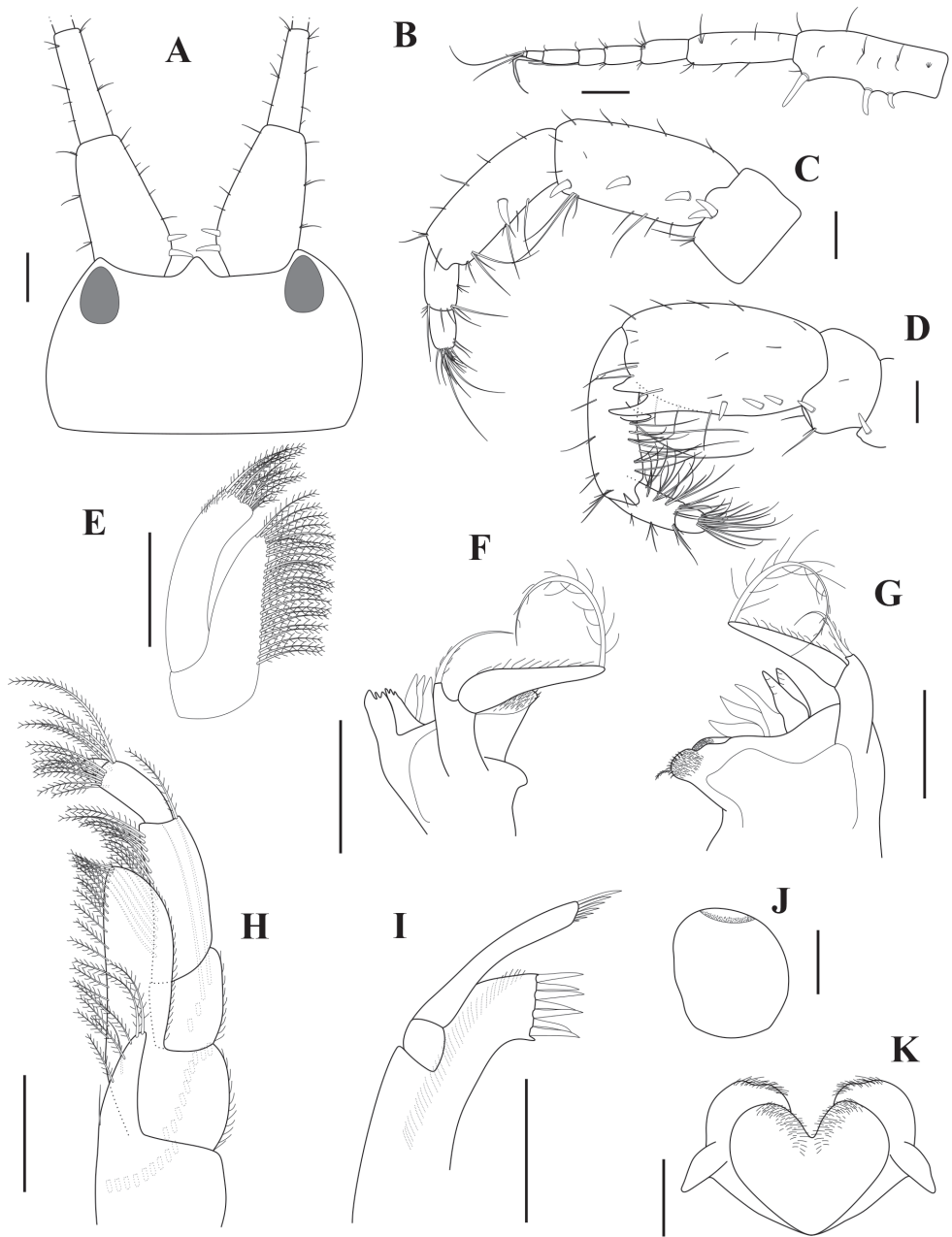


**Figure 2.** *Apocorophium acutum* (Chevreux, 1908). (A–C) brooding female, BL = 3.19 mm, MNHN-IU-2013-19982, Bône (D) male, BL = 2.32 mm, MNHN-IU-2016-3392, Trébeurden (E–K) female, BL = 3.55 mm, MNHN-IU-2016-3401, Bône. **A** head and antenna 1, dorsal view **B** left antenna 1, outer view **C** right female antenna 2, inner view **D** right male antenna 2, inner view **E** maxilla 2 **F** left mandible **G** right mandible **H** maxilla 1 **I** maxilla 1 **J** upper lip **K** lower lip. Scale bars: 0.1 mm.

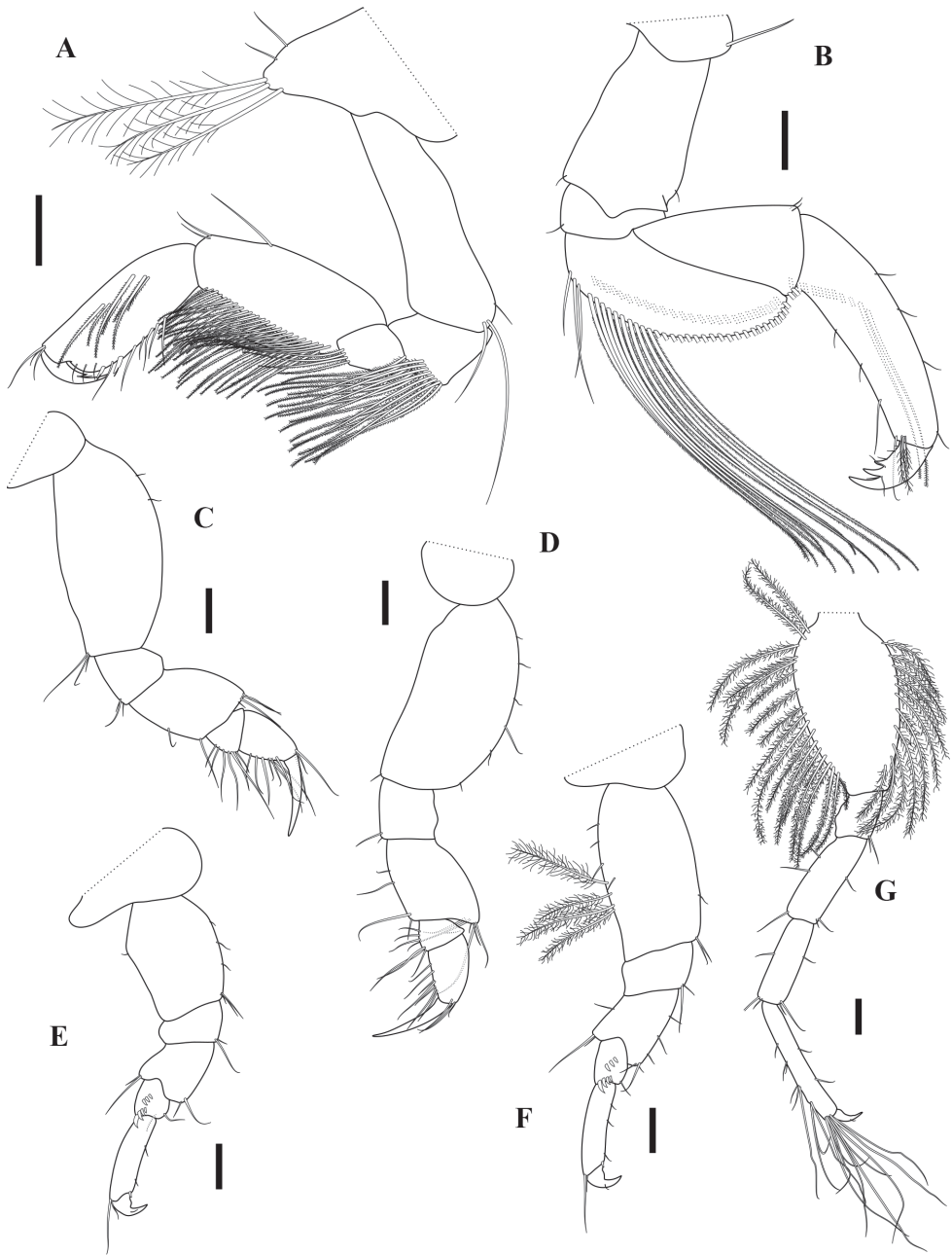


**Figure 3.** *Apocorophium acutum* (Chevreux, 1908), female BL = 3.55 mm, MNHN-IU-2016-3401. **A** right gnathopod 1, inner view **B** right gnathopod 2, outer view **C–G** right pereopods 3–7, outer view. Scale bars: 0.1 mm.

proximal third of medial portion with oblique row of pinnate setae, anterior and posterior margins sparsely setose, posterodistal corner with simple and plumose setae; dactylus short, flexor margin with two teeth and simple setae.

**Pereopod 3** coxa small; basis weakly expanded medially, anterior margin with two setules, posterior margin bare, posterodistal corner with cluster of simple setae; merus anterodistal corner with cluster of simple setae, posterior margin with one medial and one distal simple seta; carpus small, subtriangular, with setae on anterior margin; propodus about twice as long as carpus, posterior margin and anterodistal corner with simple setae; dactylus simple, subequal in length to carpus and propodus length together. **Pereopod 4** similar to pereopod 3, except basis anterior margin slightly more setose. **Pereopod 5** coxa depressed, much wider than long, narrowing distally; basis slightly widened medially, anterior margin weakly setose, posterior margin with one setule; merus widening distally, antero and posterodistal corners with simple setae; carpus short, with two oblique rows of three proximal and four distal robust setae respectively; propodus about four times as long as wide, weakly setose; dactylus short. **Pereopod 6** similar to pereopod 5, but about 1.3× longer; basis more subrectangular, with a row of setules and four plumose setae. **Pereopod 7** elongate, much longer than either pereopod 5 or 6; basis elongate-ovate, moderately expanded anteriorly, densely setose along both margins with long plumose setae; ischium to propodus linear and rectangular; length ratio of articles 2–7 = 1.00 : 0.26 : 0.52 : 0.5 : 0.56 : 0.16.

**Pleon. Epimera 1–2** subovate, ventral margins rounded, with long plumose setae; **epimeron 3** subrectangular, distinctly longer than epimera 1–2, ventral margin bare, hind margin with many long simple setae. **Urosomites 1–3** fused, without notch laterally; uropod 1 arising mainly ventrally. **Uropod 1** peduncle rectangular, about 2.2× outer ramus, ventrodiscal process present, triangular, blunt, lateral margin with row of robust setae, proximal ones short and setae like, medial margin bare except a small distal robust seta; outer ramus slightly shorter than inner, lateral margin with six robust setae, medial margin bare, three subdistal robust setae, the middle one the longest; inner ramus slightly curved medially, lateral margin with four robust setae, medial margin bare, three subdistal robust setae, the middle one the longest. **Uropod 2** peduncle longer than rami, without ventrodiscal process, outer margin with setae on distal half; rami with one distal robust seta; outer ramus slightly shorter than inner with simple setae marginally. **Uropod 3** uniramous, peduncle short, broad, with three simple setae on outer margin; ramus subelliptical, narrowing distally, margins with unequal simple setae. **Telson** fleshy, thickened, grooved centrally, subtriangular, broadest in middle.

**Male** (sexually dimorphic characters, based on specimens from Trébeurden, France, 1 February 2020, MNHN-IU-2016-3392).

**Antenna 1 and 2** (Figs 2D, 5A, D) with longer and more numerous setae; antenna 2 peduncular article 3 with a single or a pair of smaller robust setae; peduncular article 4 with 1–3 ventromedial small robust setae, with two ventrodiscal processes; peduncular article 5 without robust seta, with ventroproximal and ventrodiscal process, size of process function to maturity of the specimen.

**Variability** (based on specimens from Bône, Arcachon Bay, and Trébeurden; same data as material examined).

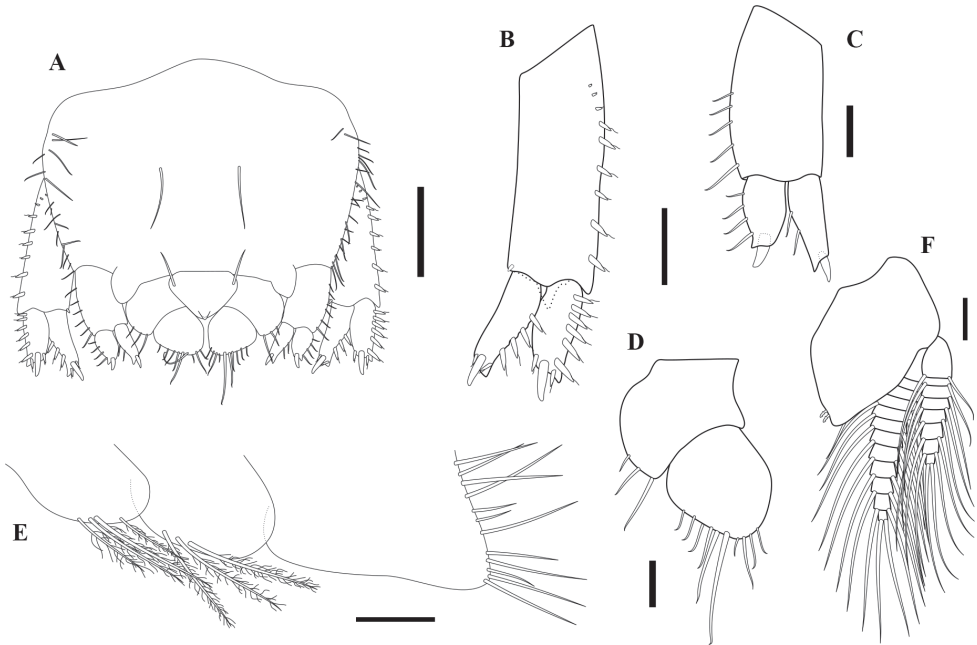


**Figure 4.** *Apocorophium acutum* (Chevreux, 1908), female BL = 3.55 mm, MNHN-IU-2016-3401 **A** pleotelson, dorsal view **B** uropod 1, dorsal view **C** uropod 2, ventral view **D** uropod 3, dorsal view **E** right epimeral plates 1–3, outer view **F** pleopod 1, dorsal view. Scale bars: 0.2 mm (**A**); 0.1 mm (**B**, **D–F**); 0.05 mm (**C**).

**Head** with rostrum reaching or not lateral ridge of head; **antenna 1** peduncular article 1 with one or two dorsomedial and two to four ventral robust setae, sometimes no left right symmetry; antenna 1 flagellum with five or six articles; **female antenna 2** peduncular article 4 with two to four robust setae, and few times in larger specimens a distal pair; **male antenna 2** peduncular article 4 with one to three medioventral robust setae, ventrodistal process subequal or the upper one slightly shorter; **maxilliped** article 2 outer margin with one to three plumose setae distally; **gnathopod 1** coxa ventral margin with one to three long plumose setae; **gnathopod 2** dactylus with generally two teeth on flexor margin for adult specimens (specimen with BL < 2.2 mm mainly juveniles with only one tooth, 1.7% of adults specimens examined with three teeth), sometimes no left right symmetry, an adult male specimen (BL = 2.46 mm) with two teeth on the left and a single tooth on the right gnathopod 2; **pereopod 3 and 4** dactylus reaching between proximal to distal end of carpus; **pereopod 5 and 6** carpus with clusters of three or four proximal and three to five distal robust setae; urosome with or without small lateral depression which looks like a vestigial notch; **uropod 1** peduncle with five to nine robust setae along outer margin, sometimes with one to three proximal simple setae, rami with three to five robust setae on outer margin; **uropod 3** peduncle shorter to subequal in length to ramus, variously expanded, with or without setae dorsally; **telson** more or less acute, dorsodistal robust setae tooth-like, mostly not observed.

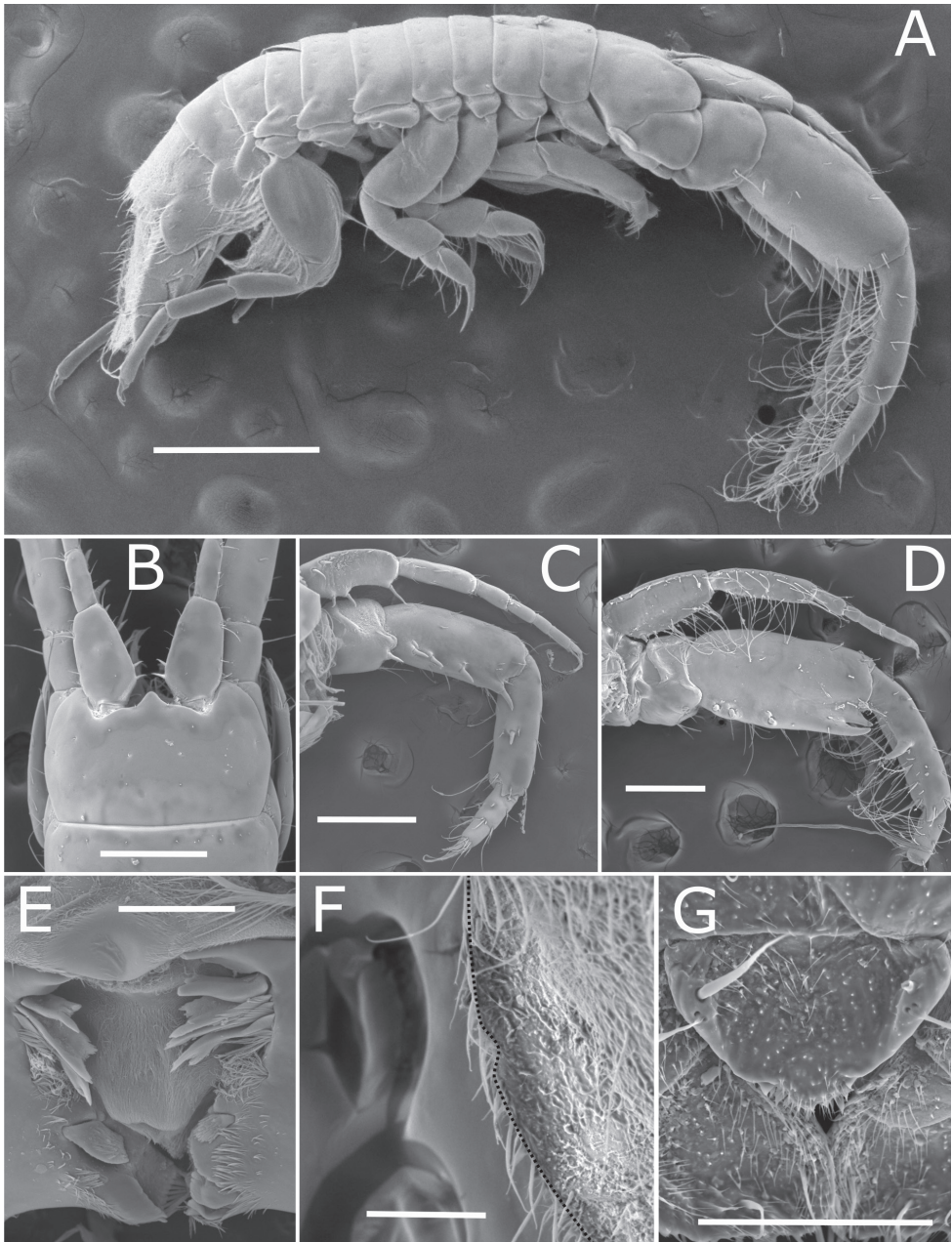


**Figure 5.** *Apocorophium acutum* (Chevreux, 1908), specimens from Arcachon Bay, station “bouée 13”, France, 20/09/2014 **A** male specimen, lateral view **B** female head, dorsal view **C** female antenna 1 and 2, inner view **D** male antenna 1 and 2, inner view **E** mandibles **F** female pleotelson, dorsolateral view showing vestigial notch (dotted edge) **G** female, telson, dorsal view. Scale bars: 0.5 mm (**A**); 0.250 mm (**B–D**); 0.05 mm (**E**); 0.1 mm (**F, G**).

**Ecological data.** Thirty-eight brooding females were examined; BL ranged from 2.49 to 4.53 mm; fecundity ranged between 4 and 37 eggs/marsupium; mean fecundity of 9 eggs/marsupium. Eggs were ovoid, with mean major and minor diameters of  $0.323 \pm 0.055$  mm and  $0.266 \pm 0.037$  mm, respectively ( $\bar{x} \pm s$ ;  $n = 351$ ). These females were collected from two locations in Arcachon bay. In both locations, there were moderate but significant positive correlation between body length and number of eggs per marsupium (Spearman's  $\rho = 0.69$  and  $0.55$ , for locations “bouée 13” and “Arcachon harbor”, respectively). There was no significant correlation between the size of eggs and the number of eggs in the marsupium of females (Spearman correlation tests,  $p$ -values  $> 0.05$ ).

Field data collected in Arcachon Bay showed that gender features could be distinguished from a body length of c. 1.7 mm. Smaller female displayed smooth oostegites, while larger female displayed ramified oostegites with or without eggs (Fig. 6; Kruskal-Wallis test followed by post-hoc Dunn tests,  $p$ -values  $< 0.05$ ). Mature female with ramified oostegites or bearing eggs reached higher size than male (Fig. 6; Kruskal-Wallis test followed by post-hoc Dunn tests,  $p$ -values  $< 0.05$ ).

## Discussion

The genus *Apocorophium* was described by Bousfield and Hoover in 1997 during their revision of the family Corophiidae, with *Corophium acutum* as the type species. Chevreux originally described *Apocorophium acutum* in 1908 with only female specimens from Bône, Algeria. Later, in 1925, Chevreux and Fage provided the first description of a male with specimens from the Lannion river mouth, Brittany, France. The species has been recorded in European waters (Mediterranean Sea and Atlantic coast), and also in the Suez Canal, Pakistan, New Zealand, South China Sea, and the Atlantic and Pacific coasts of America (Schelleberg 1928; Shoemaker 1934, 1947; Hurley 1954; Barnard 1969; Bousfield 1973; Dickinson et al. 1980; Bano and Kazmi 2012; Hossain and Hughes 2016). Even if most records and redescrptions are this species, some can be considered as doubtful due to inconsistencies (Table 1). This is the case for Korean specimens (Joung and Kim 2007) where some morphological characters differs from *A. acutum* (in parentheses): antenna 1 peduncular article 1 ventral margin bare in females and with only one distal robust seta in males (vs two to four in both sexes), female antenna 2 peduncular article 5 without robust setae (vs with one robust seta), and male antenna 2 peduncular article 4 without robust setae (vs with one to three robust setae). Specimens recently recorded from Uruguay (Demicheli and Verdi 2018) are also doubtful: urosome illustration represents lateral insertion of uropods, which infers *Monocorophium* and not *Apocorophium*. A reexamination of the specimens from Korea and Uruguay is, therefore, needed to confirm their identification, and molecular studies could be helpful for confirming identifications of species. Specimens from Bône, Brittany, and Arcachon Bay agree with the original and subsequent descriptions, apart from Korea and Uruguay specimens (see above). The only difference is related to the male antenna 2: Chevreux and Fage (1925) described and

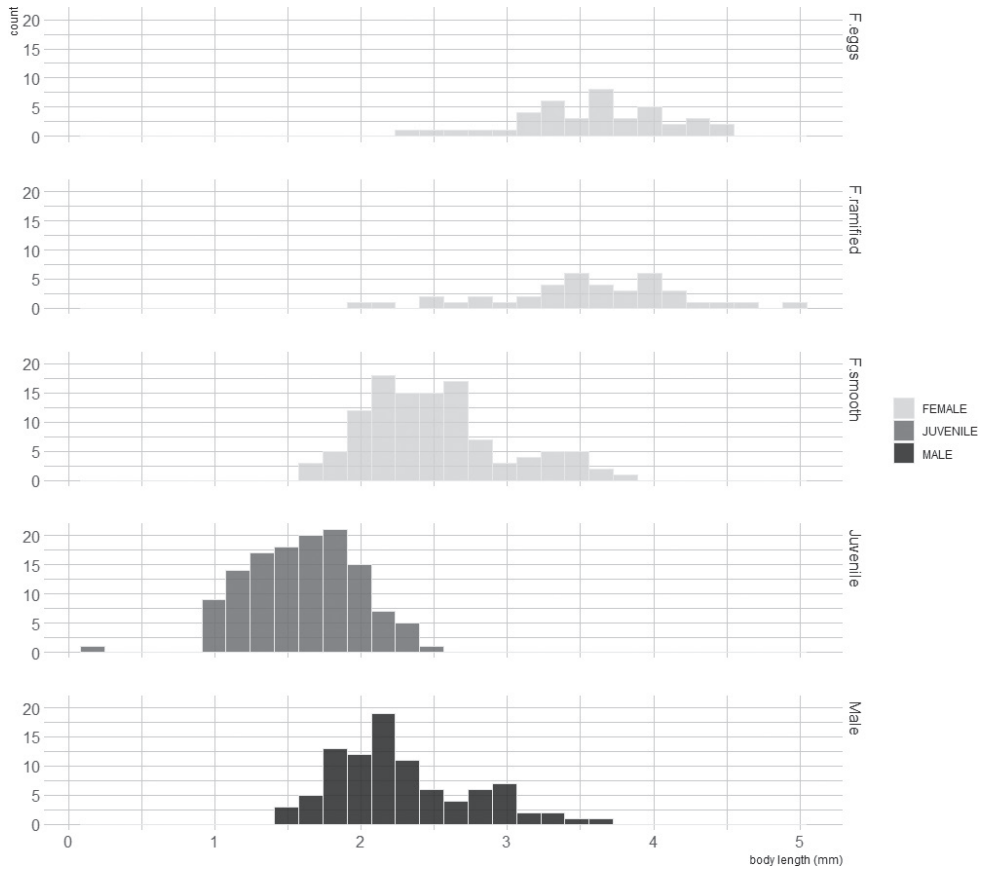


**Figure 6.** Frequency distribution of body size (in mm) for juvenile, male, female with smooth oostegites (F.smooth), female with ramified oostegites but no eggs (F.ramified), and female with eggs (F.eggs) of *Apocorophium acutum* (Chevreux, 1908) in Arcachon bay, station “blockhaus”.

illustrated male specimens without any reference to robust setae on antenna 2 peduncular articles. Examination of specimens from Brittany, as well as information from other descriptions, reveals the presence of robust setae on peduncular articles 3 and 4. This was probably an oversight during the original description. Two characters that support the close similarity of *A. acutum* to species of *Hirayamaia* are the variously expanded uropod 3 peduncle and the presence of a lateral depression on the fused urosomite in some specimens (Fig. 5F), closed to a notch morphology. However, these two genera can be distinguished by the number of teeth on gnathopod 2 dactylus: two or three in *Apocorophium* and only one in *Hirayamaia* (Gouillieux and Sauriau 2019).

Bousfield and Hoover (1997) provided a revision on the family Corophiidae for species belonging to the tribe Corophiini. They described many new genera and proposed a key, based on type species, to world genera, which has been largely used by all taxonomists. However, some mistakes have been noted by Gouillieux

**Table 1.** Main morphological characters for *Apocorophium acutum* (Chevreux, 1908) in original and subsequent descriptions.

References	Chevreux, 1908 – Original female description	Chevreux & Fage, 1925 – Original male description	Poisson & Legueux, 1926	France	Shoemaker, 1947	Hurlley, 1954	Bousfield, 1973	Lincoln, 1979	Ruffo ed., 1989	Bousfield & Hoover, 1997 (after Bousfield, 1973)	Ren, 2006	Joung & Kim, 2007	Hossain & Hughes, 2016	Demicheli & Verdi, 2018	Present study
Area	Algeria	France, Monaco	France	East coast of America	New Zealand	New England	British Isles	Italia	East China Sea	South China Sea	Korea	Uruguay	Algeria, France		
Head rostrum	No data	Short, triangular, not reaching lateral ridge of head	NO DATA	Short, triangular	Short, , not reaching lateral ridge of head	Short, triangular, not reaching lateral ridge of head	Short, triangular, not reaching lateral ridge of head	Short, triangular, not reaching lateral ridge of head	Short, triangular, not reaching lateral ridge of head	Short, triangular, not reaching lateral ridge of head	Short, triangular, not reaching lateral ridge of head	Short, triangular, reaching lateral ridge of head			
Male antenna 1 article 1 robust setae ventral margin	No data	3	3	3	4	4	3	3	3	4	3	1	No data	No data	2–4
Male antenna 1 article 1 robust setae dorsomedial margin	No data	2	0	2	0	1	2	2	2	1	2	2	No data	No data	1–2
Male antenna 2 article 4 robust setae	No data	0	0	2–4	2	2–3	1–3	1–3	2	2–3	2	0	2	No data	1–3
Male antenna 2 article 5 process	No data	Medioventral and distoventral	Medioventral and no distal	Medioventral and distoventral	Medioventral and distoventral	Medioventral and distoventral	Medioventral and no distal	Medioventral and distoventral	Medioventral and no distal	Medioventral and distoventral	Medioventral and no distal	Medioventral and distoventral	Medioventral and distoventral	No data	Medioventral and distoventral
Female antenna 1 article 1 robust setae ventral margin	3	0?	3	3	3–4	2–3	3–4	4–6	3–4	2	3–4	0	3	5	2–4
Female antenna 1 article 1 robust setae dorsomedial margin	0?	0?	0?	2	2–3	2	2–3	2	2	2	2	2	3	2	1–2
Female antenna 2 article 4 robust setae	3	3	3	3	3	3	4	6, some in pairs	3	3	3–5	3	3	3	2–4, rarely distal paired in larger specimens
Female antenna 2 article 5 distal process	Without	Without	Small	Small	Small	Small	Small	Without	Without	Small	Without	Small	Small	Small	Small

References	Chevreaux, 1908 – Original female description	Chevreaux & Fage, 1925 – Original male description	Poisson & Legueux, 1926	Shoemaker, 1947	Hurley, 1954	Bousfield, 1973	Lincoln, 1979	Ruffo ed., 1989	Bousfield & Hoover, 1997 (after Bousfield, 1973)	Ren, 2006	Joung & Kim, 2007	Hossain & Hughes, 2016	Demicheli & Verdi, 2018	Present study
Female antenna	1	1	0?	1	1	1	1	1–2	1	0–1	0	1	0?	1
2 article 5 ventral robust setae														
Gn2 dactylus number of ventral teeth	No data	2	No data	2	3	2	No data	2	2	2	2	2	2	2–3
Uropod 1 inscription	Ventral	Ventral	Ventral	Ventral	Ventral	Ventral	Ventral	Ventral	Ventral	Ventral	Ventral	Ventral	Lateral	Ventral

and Sauriau (2019) for species characterized by having urosome segments fused with uropod 1 arising mainly ventrally; they suggested that *Hirayamaia tridentia* (Hirayama, 1986) should be changed to *Apocorophium tridentia* and a partially revised key was proposed.

**Apocorophium identification key**

Based on the original descriptions of *Apocorophium* species, the authors proposed a world key to adults of *Apocorophium* species (*Hirayamaia tridentia* is herein mentioned as *Apocorophium tridentia*; female of *A. louisianum* was not included in the present key due to lack of description).

- 1 Female specimen.....2
- Male specimen.....6
- 2 Female antenna 2 peduncular article 4 with distal process.....3
- Female antenna 2 peduncular article 4 without distal process .....4
- 3 Female antenna 1 peduncular article 1 with 1 ventral and without dorsomedial robust setae; antenna 2 peduncular article 4 without robust setae; pereopods 3 and 4 dactylus shorter than propodus and carpus combined.....  
.....*A. lacustre* (Vanhöffen, 1911)\*
- Female antenna 1 peduncular article 1 with 2 ventral and without dorsomedial robust setae; antenna 2 peduncular article 4 with 1 robust seta; pereopods 3 and 4 dactylus longer than propodus and carpus combined .....  
.....*A. simile* (Shoemaker, 1934)
- 4 Female antenna 2 peduncular article 4 with pairs of robust setae .....  
.....*A. tridentia* (Hirayama, 1986)
- Female antenna 2 peduncular article 4 with row of single robust setae (can be a distal pair for larger specimens) .....5
- 5 Female antenna 2 peduncular article 4 with 4 robust setae on ventral margin and 6 robust setae on dorsomedial margin .....  
.....*A. curumim* Valério-Berardo & Thiago de Souza, 2009
- Female antenna 2 peduncular article 4 with 2 to 4 robust setae on ventral margin, without robust setae on dorsomedial margin.....  
.....*A. acutum* (Chevreux, 1908)
- 6 Male antenna 1 peduncular article 1 with proximomedial tubercule; antenna 2 peduncular article 5 without median process .....  
.....*A. louisianum* (Shoemaker, 1934)
- Male antenna 1 peduncular article 1 without proximomedial tubercule; antenna 2 peduncular article 5 with median process .....7
- 7 Male antenna 2 peduncular article 4 with robust setae on inner face.....8
- Male antenna 2 peduncular article 4 without robust setae on inner face.....9

---

\* based on original description and redescription from Bousfield 1973.

- 8 Male antenna 1 peduncular segment 1 with 2 ventral and no dorsomedial robust setae; antenna 2 peduncular segment 5 without distal process.....  
.....*A. simile* (Shoemaker, 1934)
- Male antenna 1 peduncular segment 1 with 2 to 4 ventral and 1 or 2 dorso-medial robust setae; antenna 2 peduncular segment 5 with distal process.....  
.....*A. acutum* (Chevreux, 1908)
- 9 Male antenna 1 peduncular article 1 with 2 robust setae on dorsomedial margin; rostrum papillate.....*A. tridentia* (Hirayama, 1986)
- Male antenna 1 peduncular article 1 with 0 or 1 robust seta on dorsomedial margin; rostrum triangular..... **10**
- 10 Male antenna 1 peduncular article 1 without robust setae on dorsomedial margin; uropod 3 rami shorter than peduncle..... *A. lacustre* (Vanhöffen, 1911)
- Male antenna 1 peduncular article 1 with 1 robust seta on dorsomedial margin; uropod 3 rami subequal to peduncle.....  
..... *A. curumim* Valério-Berardo & Thiago de Souza, 2009

## Ecological notes

*Apocorophium acutum* is a tube-dwelling amphipod living subtidally to 360 m, but usually between 0 and 5 m, in brackish water, in channels, on open coasts, in estuaries, and in harbors. It occurs on sponges, algae, roots of *Laminaria* J.V. Lamouroux, 1813, ascidians, hydrozoa, with coralline, oysters and *Sabellaria* Lamarck, 1818 reef, in the fouling of man-made installations (buoys, pilings, floating pontoons) (Chevreux 1908; Chevreux and Fage 1925; Poisson and Legueux 1926; Salfi 1939; Bousfield 1973; Myers 1982; Barnard and Karaman 1991; Bousfield and Hoover 1997; present paper).

Ovigerous females have been recorded in December in Suez Canal (Schellenberg 1928), between June and September in New England (USA) (Bousfield 1973); in February, March, May, July to November in British waters (Crawford 1937), and in February in Trébeurden. In Arcachon Bay (present study), examination of specimens showed presence of ovigerous females in April, May, August, October to February, and sexual maturity is reached over 1.7 mm in males and over 2.2 mm in females.

## Conclusion

The concept of cosmopolitan species is increasingly questioned. Such species are often found to be species with incomplete, early descriptions. Their redescription highlights the presence of new species, often supported by genetic analyses. The redescription of *Apocorophium acutum* was necessary in order to avoid misidentification. The molecular description of specimens from the French coast is considered to be identical to that of the type locality due to morphological similarities, but a species complex cannot be excluded until specimens from Bônes have been sequenced.

## Acknowledgements

The authors want to thank L. Corbari and P. Martin-Lefevre (MNHN, Direction des collections, Paris, France) for the loan of the Chevreaux collection specimens and for their help with depositing our specimens in the MNHN, and G. Droual (IFREMER, Plouzané, France) for the specimens collected in Brittany. Finally, the authors want to thank the crew of the Arcachon marine station boat *Planula IV*. This paper was improved by constructive comments from Robert Forsyth (ZooKeys, Copy editor), Anne Helene S. Tandberg (University of Bergen, Norway) and Rachael Peart (National Institute of Water and Atmospheric Research, New Zealand).

## References

- Bachelet G, Dauvin JC, Sorbe JC (2003) An updated checklist of marine and brackish water Amphipoda (Crustacea: Peracarida) of the southern Bay of Biscay (NE Atlantic). *Cahiers de Biologie Marine* 44: 121–151.
- Bano H, Kazmi QG (2012) A checklist of marine amphipods of Pakistan. *Fuuast Journal of Biology* 2: 113–116.
- Barnard JL (1969) Gammaridean Amphipoda of the rocky intertidal of California: Monterey Bay to La Jolla. *United States National Museum Bulletin* 258: 1–230. <https://doi.org/10.5479/si.03629236.258.1>
- Barnard JL, Karaman GS (1991) The families and genera of marine gammaridean Amphipoda (except marine gammaroids). Part 1. *Records of the Australian Museum, Supplement* 13(1): 1–417. <https://doi.org/10.3853/j.0812-7387.13.1991.91>
- Bousfield EL (1973) *Shallow-water Gammaridean Amphipoda of New England*. Cornell University Press, Ithaca.
- Bousfield EL, Hoover PM (1997) The amphipod superfamily Corophioidea on the Pacific coast of North America. Part V. Family Corophiidae: Corophiinae, new subfamily. *Systematics and distributional ecology. Amphipacifica* 2: 67–139.
- Chevreaux E (1908) Sur trois nouveaux amphipodes méditerranéens appartenant au genre *Corophium* Latreille. *Bulletin de la Société Zoologique de France* 33: 69–75. <https://doi.org/10.5962/bhl.part.19156>
- Chevreaux E (1910) Note sur les crustacés amphipodes d'Algérie et de Tunisie. *Bulletin de la Société d'Histoire Naturelle de l'Afrique du Nord* 1(9): 135–137.
- Chevreaux E, Fage L (1925) Amphipodes. *Faune de France* 9. Lechevalier, Paris.
- Crawford GI (1937) A review of the amphipod genus *Corophium* with notes on the British species. *Journal of the Marine Biological Association of the United Kingdom* 21: 589–630. <https://doi.org/10.1017/S0025315400053753>
- Dickinson JJ, Wigley RL, Brodeur RD, Brown-leger S (1980) Distribution of gammaridean Amphipoda (Crustacea) in the Middle Atlantic Bight region. NOAA Technical Report. N.M.F.S. S.S.R.F., 741, 46 pp.

- Demicheli A, Verdi A (2018) First record of *Apocorophium acutum* (Chevreux, 1908) (Amphipoda, Corophiidae, Corophiinae) from Uruguay, with notes on the biology and distribution. Check List 14(6): 1169–1173. <https://doi.org/10.15560/14.6.1169>
- Gouillieux B, Sauriau PG (2019) *Laticorophium baconi* (Shoemaker, 1934) (Crustacea: Amphipoda: Corophiidae: Corophiini): first record in European marine waters. BioInvasions Records 8(4): 848–861. <https://doi.org/10.3391/bir.2019.8.4.13>
- Hirayama A (1986) Marine gammaridean amphipoda (Crustacea from Hong Kong: the family Corophiidae, genus *Corophium*. In: Morton B (Ed.) Proceedings of the Second International Marine Biological Workshop: the marine fauna and flora of Hong Kong and southern China. Hong Kong University Press, Hong Kong, 449–484.
- Horton T, Lowry J, De Broyer C, Bellan-Santini D, Coleman CO, Corbari L, Costello MJ, Daneliya M, Dauvin JC, Fišer C, Gasca R, Grabowski M, Guerra-García JM, Hendrycks E, Hughes L, Jaume D, Jazdzewski K, Kim YH, King R, Krapp-Schickel T, LeCroy S, Lörz AN, Mamos T, Senna AR, Serejo C, Sket B, Souza-Filho JF, Tandberg AH, Thomas J, Thurston M, Vader W, Väinölä R, Vonk R, White K, Zeidler W (2021) World Amphipoda Database. *Apocorophium* Bousfield & Hoover, 1997. World Register of Marine Species. <http://www.marinespecies.org/aphia.php?p=taxdetails&id=148593> [Accessed on 2019-02-22]
- Hollander M, Wolfe DA (1973) Nonparametric Statistical Methods. John Wiley & Sons, New York.
- Hossain MB, Hughes L (2016) New species *Victoriopisa bruneiensis* and *Apocorophium acutum* (Chevreux, 1908) from Brunei (Crustacea: Peracarida: Amphipoda). Zootaxa 4117(3): 375–386. <https://doi.org/10.11646/zootaxa.4117.3.5>
- Hurley DE (1954) Studies on the New Zealand Amphipodan fauna. 7. The family Corophiidae, including a new species of *Paracorophium*. Transactions of the Royal Society of New Zealand 82: 431–460.
- Jung JW, Kim W (2007) *Apocorophium acutum* (Crustacea: Amphipoda: Corophiidae), newly recorded corophiid species in Korea. Animal Systematics, Evolution and Diversity 23(2): 247–250. <https://doi.org/10.5635/KJSZ.2007.23.2.247>
- Lamarck JB (1818) Histoire Naturelle des Animaux sans Vertèbres, présentant les caractères généraux et particuliers de ces animaux, leur distribution, leurs classes, leurs familles, leurs genres, et la citation des principales espèces qui s’y rapportent; précédées d’une Introduction offrant la détermination des caractères essentiels de l’Animal, sa distinction du végétal et des autres corps naturels, enfin, l’exposition des principes fondamentaux de la zoologie. Paris, Deterville, 5, 612 pp.
- Lamouroux JVF (1813) Essai sur les genres de la famille des thalassiphytes non articulées. Annales du Muséum d’Histoire Naturelle [Paris], 20, 21–47, 115–139, 267–293.
- Latreille PA (1816) Amphipoda. In: Nouveau dictionnaire d’Histoire naturelle, appliquée aux Arts, à l’Agriculture, à l’Économie rurale et domestique, à la Médecine, etc. Par une société de Naturalistes et d’Agriculteurs. Vol. 1. 2<sup>nd</sup> Edn. Deterville, Paris, 467–469.
- Leach WE (1814) Crustaceology. The Edinburgh Encyclopaedia 7: 383–437.
- Lincoln RJ (1979) British Marine Amphipoda: Gammaridea. British Museum (Natural History), London, 658 pp.

- Linnaeus C (1758) *Systema Naturae per regna tria naturae, secundum classes, ordines, genera, species, cum characteribus, differentiis, synonymis, locis*. Editio decima, reformata, 1. Laurentius Salvius: Holmiae, 824 pp. <https://doi.org/10.5962/bhl.title.542>
- Lowry JK, Myers AA (2013) A phylogeny and classification of the Senticaudata subord. nov. (Crustacea: Amphipoda). *Zootaxa* 3610(1): 1–80. <https://doi.org/10.11646/zootaxa.3610.1.1>
- Lowry JK, Stoddart HE (2003) Crustacea: Malacostraca: Peracarida: Amphipoda, Cumacea, Mysidacea (Vol. 19.2B). CSIRO Publishing, Melbourne, Australia.
- Myers AA (1982) Family Corophiidae. In: Ruffo S (Ed.) *The Amphipoda of the Mediterranean*. Part 1. Gammaridea (Acanthonotozomatidae to Gammaridea). *Mémoires de l'Institut Océanographique* 13: 185–208.
- Myers AA, Lowry JK (2003) A phylogeny and a new classification of the Corophiidea Leach, 1814 (Amphipoda). *Journal of Crustacean Biology* 23: 443–485. <https://doi.org/10.1163/20021975-99990353>
- Poisson R, Legueux ML (1926) Notes sur les crustacés amphipodes I Crustacés amphipodes marins littoraux de la zone dite du «trottoir» des environs de Banyuls-sur-mer. II. Etude comparée du *Corophium acutum* Chevreux et d'un *Corophium* d'eau saumâtre du canal de Caen. *Bulletin de la Société Zoologique de France* 51: 314–325.
- Ren X (2006) Crustacea, Amphipoda, Gammaridea. *Fauna Sinica Invertebrata* 41: 558.
- Ruffo S (1938) Studi sui crostacei anfipodi, VIII: gli anfipodi marini del Museo Civico di Storia Naturale di Genova, (a) gli anfipodi del Mediterraneo. *Annali del Museo Civico di Storia Naturale di Genova* 60: 127–151.
- Salfi M (1939) Ricerche etologiche ed ecologiche sugli Anfipodi tubicoli del canale delle Saline di Cagliari. *Archivio Zoologico Italiano* 27: 31–62.
- Schellenberg A (1928) Report on Amphipoda. Zoological results of the Cambridge Expedition to the Suez Canal. *Transactions of the Zoological Society of London* 22: 633–692. <https://doi.org/10.1111/j.1096-3642.1928.tb00209.x>
- Shoemaker CR (1934) The amphipod genus *Corophium* on the east coast of America. *Proceedings of the Biological Society of Washington* 47: 23–32.
- Shoemaker CR (1947) Further notes on the amphipod genus *Corophium* from the east coast of America. *Journal of the Washington Academy of Sciences* 37(2): 47–63.
- Valério-Berardo MT, Thiago de Souza AMT (2009) Description of two new species of the Corophiidae (Amphipoda, Crustacea) and register of *Laticorophium baconi* (Shoemaker, 1934) from Brazilian waters. *Zootaxa* 2215: 55–68. <https://doi.org/10.5281/zenodo.189937>
- Vanhoffen E (1911) Beiträge zur Kenntnis der Brackwasserfauna im Frischen Haff. *Sitzungsberichte Gesellschaft Naturforschung Freunde, Berlin* 9: 399–405.



# A new octocoral species of *Swiftia* (Holaxonia, Plexauridae) from the upper bathyal off Mauritania (NE Atlantic)

Íris Sampaio<sup>1,2</sup>, Lydia Beuck<sup>1</sup>, André Freiwald<sup>1</sup>

**1** Senckenberg am Meer, Marine Research Department, Südstrand 40, 26382 Wilhelmshaven, Germany

**2** University of the Azores, Rua Prof. Dr. Frederico Machado, 9901-862 Horta, Açores, Portugal

Corresponding author: Íris Sampaio ([irisfs@gmail.com](mailto:irisfs@gmail.com))

---

Academic editor: Bert W. Hoeksema | Received 29 January 2022 | Accepted 11 May 2022 | Published 17 June 2022

---

<http://zoobank.org/C96CE3F3-9927-402B-B81C-B03DD71AD379>

---

**Citation:** Sampaio I, Beuck L, Freiwald A (2022) A new octocoral species of *Swiftia* (Holaxonia, Plexauridae) from the upper bathyal off Mauritania (NE Atlantic). ZooKeys 1106: 121–140. <https://doi.org/10.3897/zookeys.1106.81364>

---

## Abstract

Three species of the genus *Swiftia* are known for the NE Atlantic Ocean and Mediterranean Sea. Remotely-operated vehicle (ROV) surveys and sampling on board RV Maria S. Merian during cruise MSM 16/3 ‘PHAETON’ in 2010 provided footage and specimens of octocorals off Mauritania. Micro-computed tomography (micro-CT) reveals, for the first time in taxonomy of octocorals, the three-dimensional arrangement of the sclerites in a polyp. *Swiftia phaeton* **sp. nov.** is described for the continental slope off Mauritania. This azooxanthellate octocoral is distinctive from NE Atlantic and Mediterranean congeners by the dark red colour of the colonies (including the polyps), the presence of a layer of rod sclerites on top of the polyp mounds, and different sizes of polyps and sclerites. Using micro-CT has allowed the observation and imaging of a layer of sclerites that is distinct from other species of the same genus. ROV images revealed live records of *S. phaeton* **sp. nov.** in submarine canyons and on cold-water coral mounds in the upper-bathyal off Mauritania (396–639 m depth), mainly attached to dead coral, coral rubble, or rocks. The new species represents an extension of the genus distribution to the tropical latitudes (17°07’N and 20°14’N) of the NE Atlantic Ocean.

## Keywords

Deep sea, gorgonian, micro-CT, NW Africa, Octocorallia, taxonomy

## Introduction

Only few deep-sea cruises have explored northwest Africa. During the 19<sup>th</sup> and the beginning of the 20<sup>th</sup> centuries, the Talisman, Michael Sars North Atlantic Deep-Sea expedition, and the Prince Albert I of Monaco, as well as expeditions of the vessels *Thalassa* and *Discovery*, made sporadic sampling (Bigelow 1911; Oñate 2017). Systematic exploration began later in the late 20<sup>th</sup> century with the Dutch CANCAP (CANarian – CAPE Verdean Deep-Sea Basin) and Mauritania II expeditions and the Cooperative Investigation of the northern part of the Eastern Central Atlantic (CINECA) program (Den Hartog 1984; Van der Land 1988; Ramos et al. 2017a).

Knowledge of benthic deep-sea faunas of Mauritania is rare despite some scientific efforts passing by its coastline (Oñate 2017; Ramos et al. 2017b). Tydeman Madeira – Mauritania – CANCAP III in 1978 and Tyro Mauritania II in 1988 were the first expeditions to focus exclusively on Mauritania (Den Hartog 1984; Van der Land 1988) and, more recently, the Spanish MAURIT surveys during 2007–2010 (Ramos et al. 2017a). These exploration efforts revealed that the Mauritanian deep sea is home of the world's largest coral mound barrier, with more than 580 km running parallel to the Mauritanian coastline (Ramos et al. 2017c; Wienberg et al. 2018). Live scleractinians were found scarcely distributed on mounds but forming vast frameworks in the submarine canyons off Mauritania (Colman et al. 2005; Westphal et al. 2012). Limited at the north by the Cap Timiris Canyon System and at the south by the Mauritanian Slide complex, the mounds are located on the upper bathyal between 450 and 550 m depth (Wien et al. 2007; Sanz et al. 2017). Mauritania has a large upwelling system increasing the productivity of its surface waters and creating a pronounced oxygen-minimum zone in deeper waters (Hagen 2001; Marañón and Holligan 1999).

Octocorals from Mauritania were mostly known from shallower depths, dominated by species of the genus *Leptogorgia* Milne Edwards, 1857 (Grasshoff 1986, 1988). The few octocorals recorded at deeper (> 200 m) Mauritanian waters were sea pens, acanthogorgiids, and plexaurids (Grasshoff 1981; Buschewski 2016; Ramos et al. 2017c; Sampaio et al. 2019). Worldwide bathymetrical records of the family Plexauridae Gray, 1859 are from 20 to 3000 m depth in tropical, temperate, and polar waters (Bayer and Weinheimer 1974; Grasshoff 1977, 1985, 1992; López-González 2006; Breedy et al. 2019; Sampaio et al. 2019). This speciose, widespread, and abundant family includes the genus *Swiftia* Duchassaing & Michelotti, 1864, whose position has been previously placed within the Gorgoniidae and Paramuriceidae and is still under discussion (Bayer 1961; Grasshoff 1977; Wirshing et al. 2005). At present, it forms part of the Plexauridae with the simplest sclerite forms: simple spindles, highly tuberculated sclerites, and bar-like rods but without thornstars in the coenenchyme (Grasshoff 1977; Bayer 1981). Three of 23 valid plexaurid species of the NE Atlantic Ocean and Mediterranean Sea belong to this genus: *Swiftia dubia* (Thomson, 1929), *S. borealis* (Kramp, 1930), and *S. rosea* (Grieg, 1887) (Grasshoff 1977). The genus is widespread throughout these ocean basins from 20 to 2400 m depth (Madsen 1970; Grasshoff 1977, 1981; Manuel 1981; Brito and Ocaña 2004; Sampaio et al. 2019). *Swiftia borealis* and *S. rosea* are distributed

in northern latitudes (Greenland, Faroe Islands, Scandinavia, Ireland, Scotland) while *S. dubia* is widespread through the central and southern NE Atlantic and Mediterranean Sea: Gulf of Biscay, Galicia, mainland of Portugal, Mid-Atlantic Ridge, Josephine Bank, Macaronesia (Azores, Madeira and Canary Islands), Cape Verde Archipelago, the Mediterranean Sea, and NW Africa (Morocco, Western Sahara, Mauritania) (Madsen 1970; Grasshoff 1977, 1981; Manuel 1981; Brito and Ocaña 2004; Sampaio et al. 2019).

In 2010, RV Maria S. Merian cruise MSM 16/3 'PHAETON - Paleoceanographic and paleoclimatic record on the Mauritanian shelf off Mauritania' visited the submarine canyons and coral-mound barrier off Mauritania with an ROV and an exploratory approach (Westphal et al. 2012). Herein we describe a new species of *Swiftia* collected during this cruise and highlight the potential of the micro-computed tomography (micro-CT) for octocoral taxonomy. The new species is the fourth of the genus reported for the NE Atlantic Ocean and Mediterranean Sea. Therefore, we increased alpha-taxonomic knowledge of a poorly explored area and have contributed to research on octocorals diversity, distribution, and conservation.

## Materials and methods

### Sampling

Octocoral colonies were collected, and corresponding video footage recorded, along the Mauritanian margin during RV Maria S. Merian cruise MSM 16/3 'PHAETON' at upper canyon flanks and coral mounds (Fig. 1) (Westphal et al. 2012). Benthic faunal sampling was performed by a grab sampler at 82 stations and by a box corer (50 × 50 cm diameter × 55 cm height) at 53 station deployments (Westphal et al. 2012). Moreover, the sampling and imaging were also performed by the remotely operated vehicle (ROV) system Sperre SubFighter 7500 DC (Tjärnö Centre for Underwater Documentation, Sven Lovén Centre for Marine Sciences Tjärnö, University of Gothenburg, Strömstad, Sweden). The equipment of the ROV encompassed a Sperre HD video camera (1080 I and 720 p), two standard video cameras, a still camera (Canon Powershot G9, 12 Mpixel), two Deep Sea Systems red lasers, and a HYDRI-LEK-5-function hydraulic manipulator type EH5 which enabled the acquisition of data and samples (Westphal et al. 2012). Twelve ROV dives were made between latitudes 17°07'N and 20°14'N and longitudes 16°39'W to 17°40'W and at depths between 417 m and 642 m on the continental slope off Mauritania (Fig. 1, Table 1).

### Taxonomy

A total of 17 colonies of *Swiftia* was collected and preserved in ethanol, denatured ≥ 96%, with ca. 1% MEK for morphological analysis (Table 1). The specimens were documented with a Nikon D700 camera and a digital light microscope (Keyence VHX-1000D) for detailed observation and further description. Taxonomic identification

**Table 1.** Sampling location of specimens of *Swiftia phaeton* sp. nov. from MSM 16/3 ‘PHAETON’ in 2010. Details: Station, date, latitude, longitude, depth, location description, sampling gear, number of sampling gear, and depository number at Senckenberg Museum or Senckenberg am Meer biological collection and number of specimens collected.

Station GeoB	Date	Coordinates	Depth (m)	Location	Gear	N	SMF/ SaM-ID	N
14873-1	10.11.10	18°57'41"N, 16°52'17"W	602	deep Timiris mound complex	ROV	5	1352	3
14874-6	10.11.10	18°57.51"N, 16°51.90"W	446	shallow Timiris mound complex	ROV	6	13113	1
14873-4	10.11.10	18°57.45"N, 16°52.11"W	498	deep Timiris mound complex	ROV	5	1469	1
14802-1	03.11.10	20°14'47"N, 17°40'11"W	595	Tanoûdért Canyon	Grab sampler	45	13112	1
14878-1	11.11.10	18°57'54"N, 16°51'11"W	493	deep Timiris Mound Complex	Box corer	50	1566	4
14886-4	12.11.10	18°39.00"N, 16°43.35"W	618	Tioulit Canyon (S)	ROV	7	1596	3
14911-1	16.11.11	17°28'55"N, 16°41'31"W	450	southern Tamxat Mound Complex	Box corer	61	1629	1
14905-1	15.11.10	17°32'27"N, 16°39'60"W	486	Central Tamxat Mound Complex	Box corer	58	1638	1

and morphological descriptions were based on external morphology (shape, size, colour, colony, and polyp form) and internal morphology (diversity, arrangements, shapes, and dimensions of the sclerites) following the terminology, identification keys, and descriptions by Grieg (1887), Madsen (1970), Grasshoff (1977), and Bayer et al. (1983). Measurements of colonies, branches, polyps, and sclerites were made with ImageJ 1.49 software. A dataset with the measurements of colonies, polyps, and sclerites of type specimens was deposited at the World Data Center Pangaea (<https://doi.pangaea.de/10.1594/PANGAEA.910893>).

To observe the outer and inner layers of sclerites, a cross-section of the coenenchyme was made. For observation of the arrangement of sclerites in a polyp, potassium hydroxide (KOH) was added to the polyp to decolour its tissue, thus allowing the observation of translucent sclerite forms (Phil Alderslade 2017, pers. comm.). In order to show the diversity of sclerites, larger colonies in better state of preservation were selected for subsampling. Fragments of these colonies were dissolved with sodium hypochlorite (household bleach) to separate sclerites. Subsequently, neutralized hydrogen peroxide was added in order to dissolve any remaining organic tissue. Sclerites were then washed three times with distilled water and two times with 96% ethanol. Finally, the sclerites were dried and mounted on scanning electron microscopy (SEM) stubs, sputter-coated with gold, and documented on Tescan VEGA3 XMU SEM at Senckenberg am Meer, Wilhelmshaven, Germany.

Two specimens (SaM-ID 1352 and 1566) were selected to perform a micro-CT scan (Skyscan, now Bruker micro-CT accessory for the SEM stated above), in order to show the arrangement of the sclerites with 3D models of the polyp of the octocoral. Before scanning, samples were dried using a Critical Point Dryer Leica EM CPD 300. This technique replaces the water in the sample by carbon dioxide, which is transformed into gas to avoid drastic damage of the sample structures, as commonly occurs

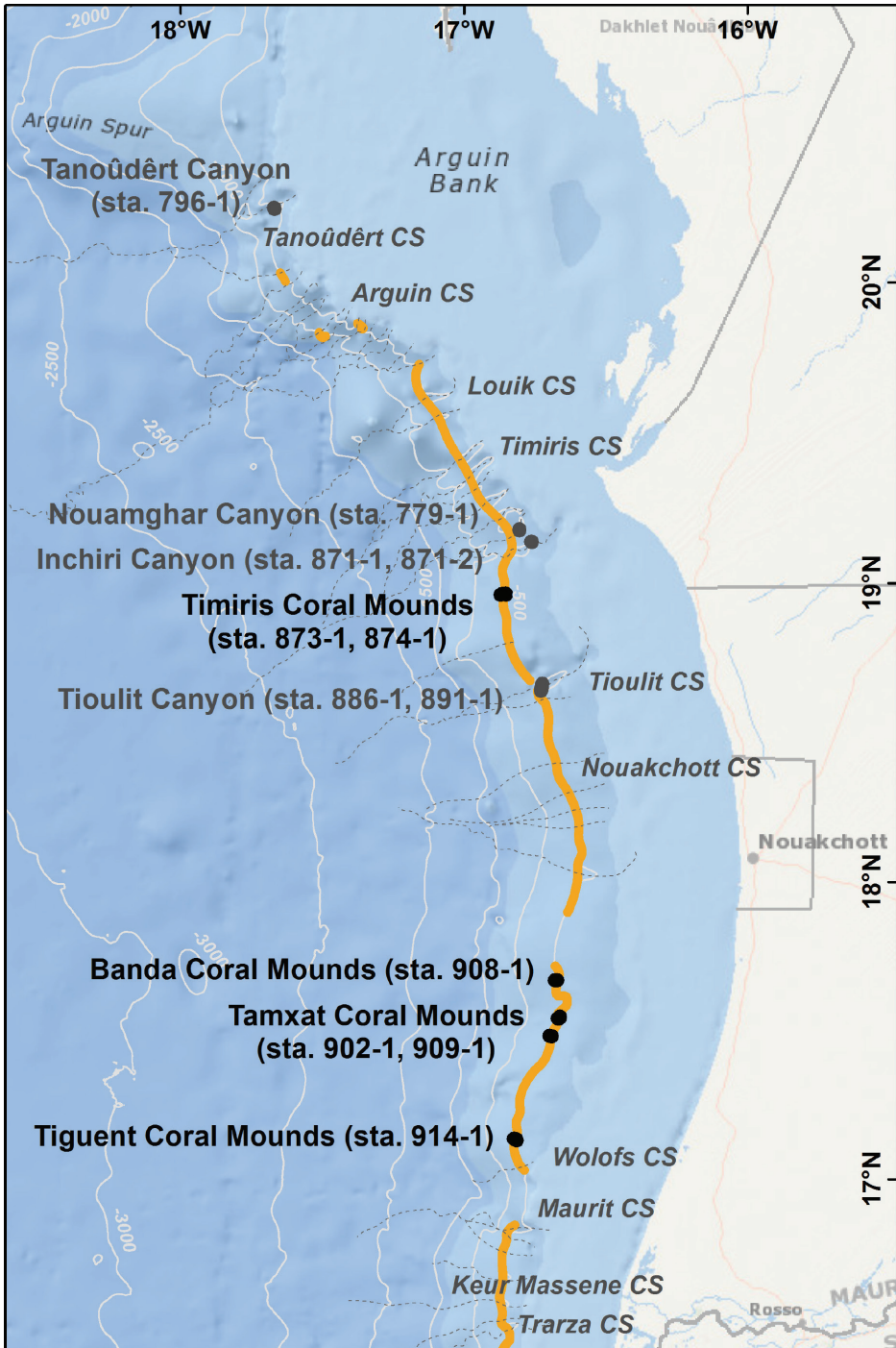


**Figure 1.** Map showing MSM 16/3 'PHAETON' ROV dive locations along the Mauritanian slope. Location names and GeoB 14 stations (sta.): grey = canyons; black = coral mounds; orange = scleractinian distributions. Basemap from ESRI (2019) ([www.esri.com](http://www.esri.com)) and contours from GEBCO (2019) ([www.gebco.net](http://www.gebco.net)), scleractinian framework distribution, canyon positions, and names from Sanz et al. (2017).

if the samples dry in air. During a micro-CT scan, the different densities of the components of a sample are captured by a high-resolution camera, detecting X-rays going through it. The following scanning parameters were used: source voltage 30 kV, source current 2 mA, pre-scan rotation step 0.45°, rotation step 0.9°, and rotation of 360° resulting in final images with a resolution of 4.6 µm and field of view of 2.4 mm. After reconstruction with NRecon ver. 1.6.3.3 (Skyscan) software, a total of 501 horizontal slices was obtained as dataset, each an image with 512 × 512 pixels. Fiji software v. 1.0 improved the contrast of the images and was used to crop excess slides and to decrease file size from 16-bit to 8-bit. This dataset was then processed with the Amira software v. 6.4 for segmentation of sclerites of the polyp with Segmentation Editor.

The holotype and one paratype are deposited in the Senckenberg Naturmuseum, Frankfurt am Main (**SMF**); two paratypes are deposited at Naturalis Biodiversity Center, Leiden (**RMNH. COEL**), and other paratypes are retained in the reference collection at the Senckenberg am Meer, Wilhelmshaven (**SaM**) Institute.

## Taxonomy

**Class Anthozoa Ehrenberg, 1834**

**Subclass Octocorallia Haeckel, 1866**

**Order Alcyonacea Lamouroux, 1812**

**Suborder Holaxonia Studer, 1887**

**Family Plexauridae Gray, 1859**

**Genus *Swiftia* Duchassaing & Michelotti, 1864**

*Swiftia* Duchassaing & Michelotti, 1864: 13; Kükenthal 1924: 236; Deichmann 1936: 185–186; Bayer 1956: F206; Grasshoff 1977: 61–62; Grasshoff 1981: 220; Bayer 1981: 932, 945; Grasshoff 1982: 946; Breedy et al. 2015: 329; Williams and Breedy 2016: 3; Breedy et al. 2019: 409.

*Stenogorgia* Verrill, 1883: 29; Deichmann 1936: 185; Bayer 1956: F206; Bayer 1981: 945; Breedy et al. 2015: 329; Williams and Breedy 2016: 3; Breedy et al. 2019: 409.

*Platycaulos* Wright & Studer, 1889: 61; Bayer 1956: F206; Bayer 1981: 945; Breedy et al. 2015: 329; Williams and Breedy 2016: 3; Breedy et al. 2019: 409.

*Callistephanus* Wright & Studer, 1889: 148–149; Bayer 1981: 945; Breedy et al. 2015: 329; Williams and Breedy 2016: 3; Breedy et al. 2019: 409.

*Allogorgia* Verrill, 1928: 7–8; Bayer 1956: F206; Bayer 1981: 945; Breedy et al. 2015: 329; Williams and Breedy 2016: 3; Breedy et al. 2019: 409.

**Type species.** *Gorgonia exserta* Ellis & Solander, 1786, by monotypy.

**Diagnosis.** Colonies dichotomous, fan-like, irregularly pinnate, unbranched or mostly branching in one plane or several planes. Colour variable among red, white, beige, pink, and orange. Axis flexible. Branches free, rarely with anastomoses. Polyps are conical, mound-like, and prominent, spread or crowded, in biserial zigzagging

distribution or all over the branch. Two to three polyp mounds appear on top of each branch. Coenenchyme has two layers of sclerites. Sclerites in coenenchyme are capstans, radiates, and spindles. Thornstars absent in coenenchyme. Polyp-mound sclerites similar to the coenenchyme sclerites, thin, sharp, small, very tuberculate spindles and, sometimes, poorly defined thornscales. Anthocodiae have or do not have long, straight, or curved rods. Collaret absent or with few rods. Tentacles have stout rods or scales.

**Key to the valid species of the genus *Swiftia* Duchassaing & Michelotti, 1864 reported from the northeast Atlantic Ocean and Mediterranean Sea**

- 1 Polyp mounds with spindles and slender thornscales..... *S. borealis*  
 – Polyp mounds with spindles and with small, highly tuberculated sclerites...2  
 2 Polyps densely crowded around the branches. Colonies red-rose. Boreal .....  
 .....*S. rosea*  
 – Polyps densely crowded around the branches or scattered, often biserial. Colonies red or white .....3  
 3 Colonies red or white. Absence of bar-like rods on top of the polyp mound. Lusitanic Atlantic and Mediterranean Sea ..... *S. dubia*  
 – Colonies dark red. Presence of bar-like rods on top of the polyp mound. Southern NE Atlantic Ocean ..... *S. phaeton* sp. nov.

***Swiftia phaeton* sp. nov.**

<http://zoobank.org/8589E3C1-D6D4-499A-BB93-C619C7E21293>

Figs 2–5

*Swiftia* sp. Sampaio et al., 2019: 7, 14, 17, 20, 21, figs 2c, 3.

**Material examined.** *Holotype:* Mauritania • Tanoûdêrt Canyon; 20°14'47"N, 17°40'11"W; depth 595 m; 3 Nov. 2010; RV Maria S. Merian exped.; stat. GeoB 14802-1; 1 colony; SMF 13112. *Paratypes:* off Mauritania • 18°51'N, 16°53'W; depth 500 m; 10 Jun. 1988; RV Tyro exped.; stat. MAU 040; 1 colony; RMNH.COEL. 42327. off Mauritania • 18°51'N, 16°53'W; depth 500 m; 10 Jun. 1988; RV Tyro exped.; stat. MAU 040; 1 colony; RMNH.COEL. 42328. Mauritania • shallow Timiris Mound Complex; 18°57'51"N, 16°51'90"W; depth 446 m; 10 Nov. 2010; RV Maria S. Merian exped.; stat. GeoB 14874-6; 1 colony; SMF 13113. Mauritania • deep Timiris Mound Complex; 18°57'41"N, 16°52'17"W; depth 602 m; 10 Nov. 2010; RV Maria S. Merian exped.; stat. GeoB 14873-1; 3 colonies; SaM-ID 1352. Mauritania • deep Timiris Mound Complex; 18°57'45"N, 16°52'11"W; depth 498 m; 10 Nov. 2010; RV Maria S. Merian exped.; stat. GeoB 14873-4; 1 colony; SaM-ID 1469. Mauritania • deep Timiris Mound Complex; 18°57'54"N, 16°51'11"W; depth 493 m; 11 Nov. 2010; RV Maria S. Merian exped.; stat. GeoB 14878-1; 4 colonies; SaM-ID 1566. Mauritania • Tioulit Canyon (S); 18°39'00"N, 16°43'35"W; depth 618 m; 12 Nov. 2010; RV Maria S. Merian exped.;

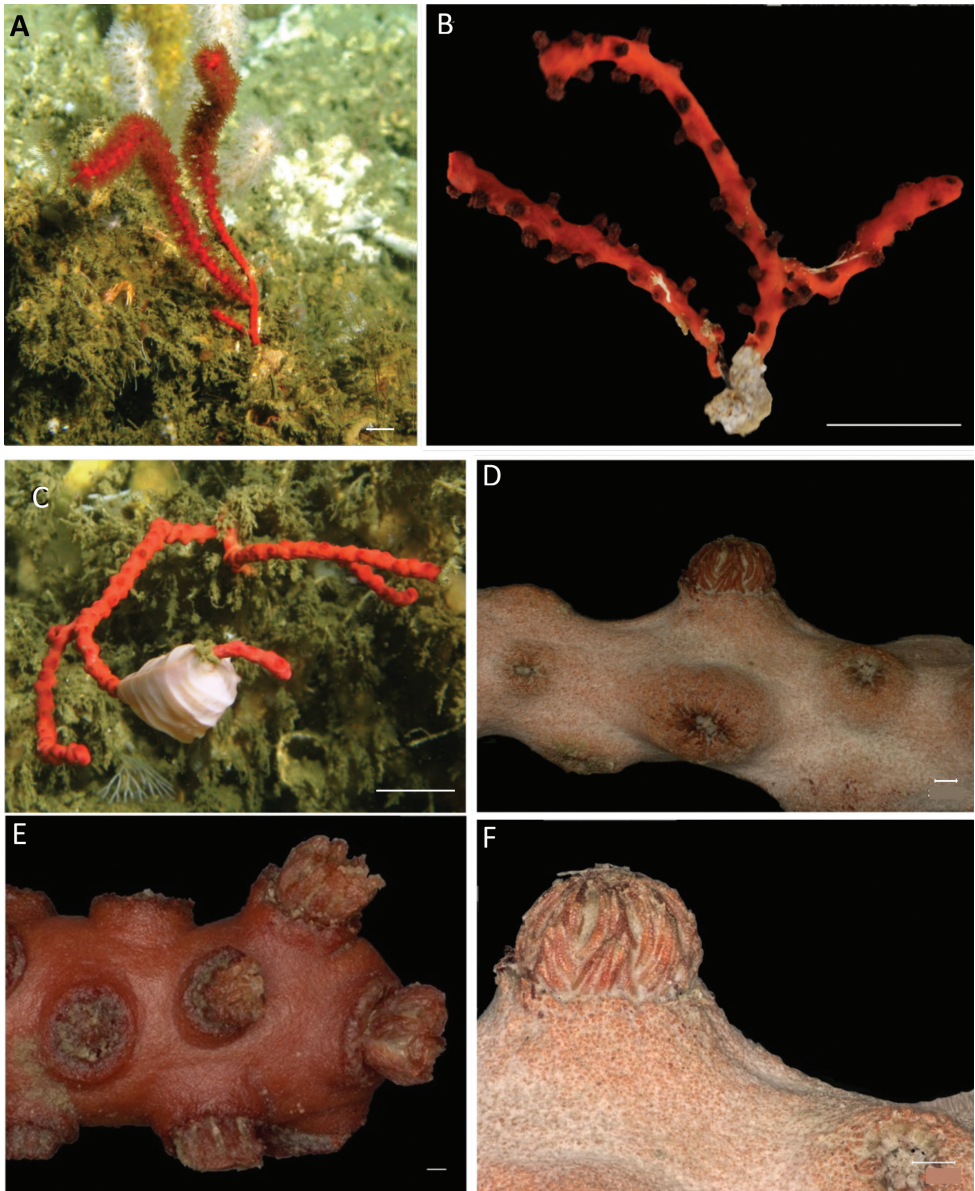


**Figure 2.** *Swiftia phaeton* sp. nov. from Mauritania **A** in situ colony with expanded polyps on coral framework (copyright Tomas Lundälv, Sven Lovén Center for Marine Infrastructure at Tjärnö, Sweden) **B** colony after ethanol preservation with expanded polyps (holotype SMF 13112) **C** in situ colony with retracted polyps on coral framework (copyright Tomas Lundälv, Sven Lovén Center for Marine Infrastructure at Tjärnö, Sweden) **D** part of a branch (paratype SMF 13113), **E** fragment of specimen with anthocodiae slightly expanded (paratype SaM-ID 1566) **F** polyp and coenenchyme details (paratype SaM-ID 1352). Scale bars: 1 cm (**A–C**); 300  $\mu$ m (**D–F**).

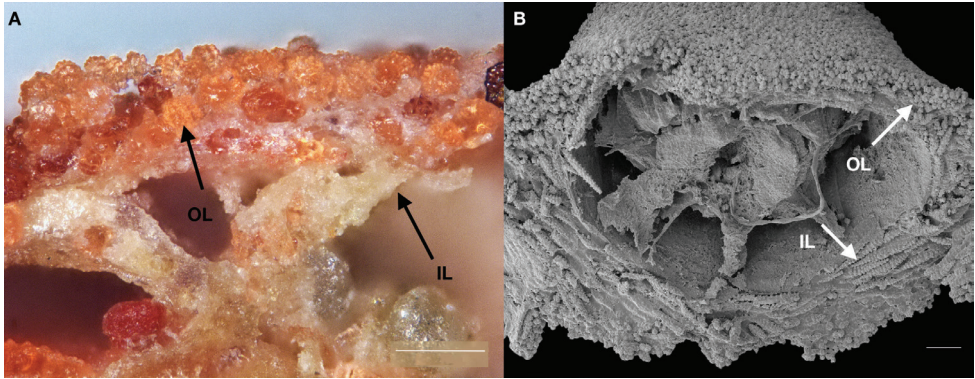


**Figure 3.** Layers of sclerites of *Swiffia phaeton* sp. nov. **A** coenenchyme under light microscope **B** polyp mound under electron microscope (paratype SaM-ID 1566). Outer layer (OL) with capstans and inner layer (IL) with spindles. Scale bars: 100  $\mu$ m.

stat. GeoB 14886-4; 3 colonies and 1 fragment; SaM-ID 1596. Mauritania • Southern Tamxat Mound Complex; 17°28'55"N, 16°41'31"W; depth 450 m; 16 Nov. 2010; RV Maria S. Merian exped.; stat. GeoB 14911-1; 1 colony; SaM-ID 1629. Mauritania • Central Tamxat Mound Complex; 17°32'27"N, 16°39'60"W; depth 486 m; 15 Nov. 2010; RV Maria S. Merian exped.; stat. GeoB 14905-1; 1 colony; SaM-ID 1638.

**Type locality.** Tanoûdêrt Canyon and Timiris Mound Complex, Mauritania upper continental slope.

**Etymology.** Species named after the German cruise MSM 16/3 'PHAETON' and treated as a name in apposition. This cruise was the first to film this species alive underwater and forming coral gardens. These ecosystems are a contradiction to the African desert into which Phaeton, son of a Greek god, transformed the continent, burning it down while falling with his chariot from the sky.

**Diagnosis.** Colonies unbranched or monopodial subdividing up to two times (Fig. 2A–C). Dark red robust colonies. Dark brown axis. Branches sparsely distributed, rarely with anastomoses. Polyp colour red, darker than coenenchyme. Polyps form a conical prominent mound, numerous and densely crowded around the branches (Fig. 2D–F). Anthocodiae red with yellowish white tentacles. Collaret absent. Coenenchyme formed by compact external layer with smaller capstans and an internal layer with long straight spindles, mostly not within a closed layer (Fig. 3). Polyp mounds with the same sclerite types, capstans and spindles, and a layer of compact dark red rods on top. Anthocodial sclerites thin warty spindles. Sclerite colours vary between dark red and transparent.

**Description.** Holotype small dark red colony scantily ramified in one plane (Fig. 2B). Colony extending up to 42.8 mm in length and up to 41.4 mm in width, attached to the substrate by an encrusting holdfast of ~ 6 mm wide in a main stem of 2 mm diameter (Fig. 2B). Colony branches up to three, thick and robust, with numerous polyps that reach 1.8–2 mm in diameter and 1.5–40.8 mm long. Polyps red,

darker than coenenchyme; abundant, well-spaced, either in biserial distribution or all over branches and mostly present on one side of colony. Approximately 5–8 polyps/cm, spaced between 1.8 and 3.4 mm, occurring on main stem and branches. Polyp mounds up to 2.5 mm high, 1.0–1.5 mm long, and 10.1–16.8 mm wide. Anthocodiae retractile within prominent polyp mounds and with yellowish white tentacles. Coenenchyme thin. Coenenchymal and polyp mound sclerites with outer layer of red or transparent small but packed capstans, 39–64  $\mu\text{m}$  long and 22–51  $\mu\text{m}$  wide (Fig. 4C); and an inner layer of long, slender, pointed, warty, mostly straight spindles of several sizes (Fig. 4A). Larger spindles 232–436  $\mu\text{m}$  long and 29–73  $\mu\text{m}$  wide, sometimes waisted (Figs 3, 4A). Smaller spindles 103–219  $\mu\text{m}$  long and 25–45  $\mu\text{m}$  wide (Figs 3, 4A). Irregularly branched spindles with expanded, warty tubercles or small immature sclerites (Fig. 4A, B), occurring in lower numbers. Polyp mound top with armature formed by layer of flat rods showed by micro-CT, 108–321  $\mu\text{m}$  long and 27–72  $\mu\text{m}$  wide (Figs 4, 5) on the distal end. Anthocodiae with spindles arranged in points, tiny capstans, and irregular flattened scales around peristome and tentacles (Fig. 5). No collar.

**Variation.** The variation of body measurements of the paratypes is presented in Table 2 and a published dataset (<https://doi.pangaea.de/10.1594/PANGAEA.910893>).

**Table 2.** Measurements of the type series of *Swiftia phaeton* sp. nov. (see Material examined) in distinct body parts. Details: body parts of the colonies, measurements per body part of the type colonies, average, standard deviation, minimum and maximum of each measurement, and number of colonies and sclerites measured.

	Body part	Measurements	Average	SD	Min	Max	N colonies/ N sclerites		
Sclerome ( $\mu\text{m}$ )	Colony (cm)	Length	5.50	2.03	3.17	9.23	9		
		Width	2.01	1.44	.25	4.14	9		
		Stem diameter	.37	.20	.13	.69	7		
	Branches (cm)	Length of branches	3.68	2.64	.15	7.65	9		
		Branch diameter	.25	.11	.10	.46	9		
	Polyps (mm)	Distance between polyps	1.55	0.79	.37	3.38	9		
		Number of polyps/cm	11	5.70	7	21	9		
		Polyp height	43	18.92	26	72	9		
		Calyx height	1.36	.41	1.09	1.83	9		
		Calyx width	2.07	.19	1.91	2.28	9		
	Coenenchyme	Large spindles	Length	281	62	193	281	9/55	
			Width	41	10	38	41	9/55	
		Small spindles	Length	170	33	90	243	9/54	
			Width	37	9	18	56	9/54	
		Capstans	Length	57	14	32	93	9/53	
			Width	36	8	23	58	9/53	
		Large spindles	Length	315	62	198	436	9/53	
			Width	41	12	17	73	9/53	
			Small spindles	Length	157	35	91	231	9/54
				Width	33	8	16	59	9/54
	Capstans	Length	52	16	22	97	9/54		
Width		32	9	13	52	9/54			
Polyps	Rods	Length	195	70	108	455	9/45		
		Width	45	14	25	77	9/45		

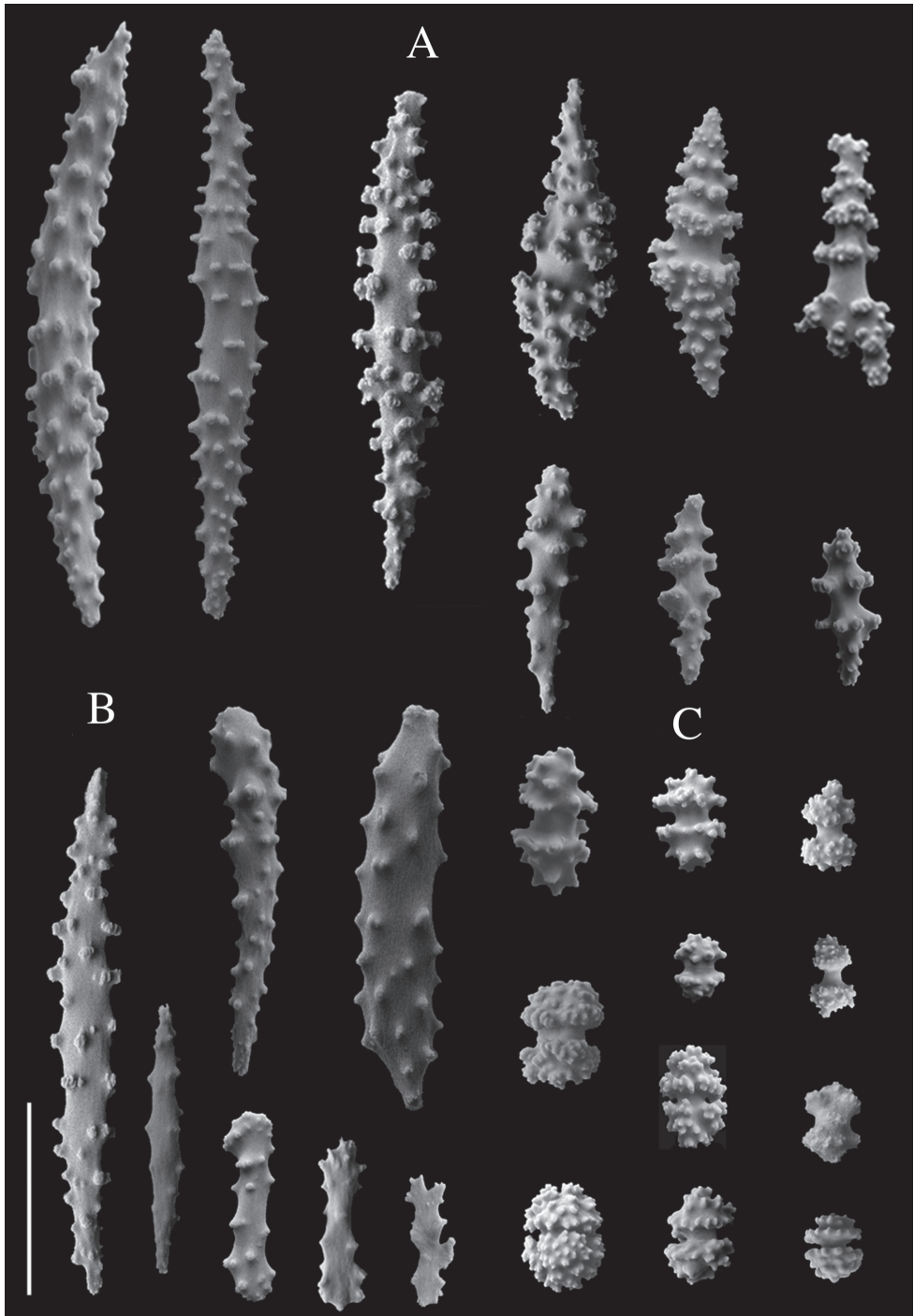


**Figure 4.** Sclerites from type specimens of *Swifitia phaeton* sp. nov. **A** overview of sclerites of the inner layer of the coenenchyme: spindles **B** polyp sclerites: spindles, rods, and scales from the tentacles **C** overview of sclerites of the outer layer of the coenenchyme: capstans (also occurring in polyp mounds). Scale bar: 100  $\mu$ m.

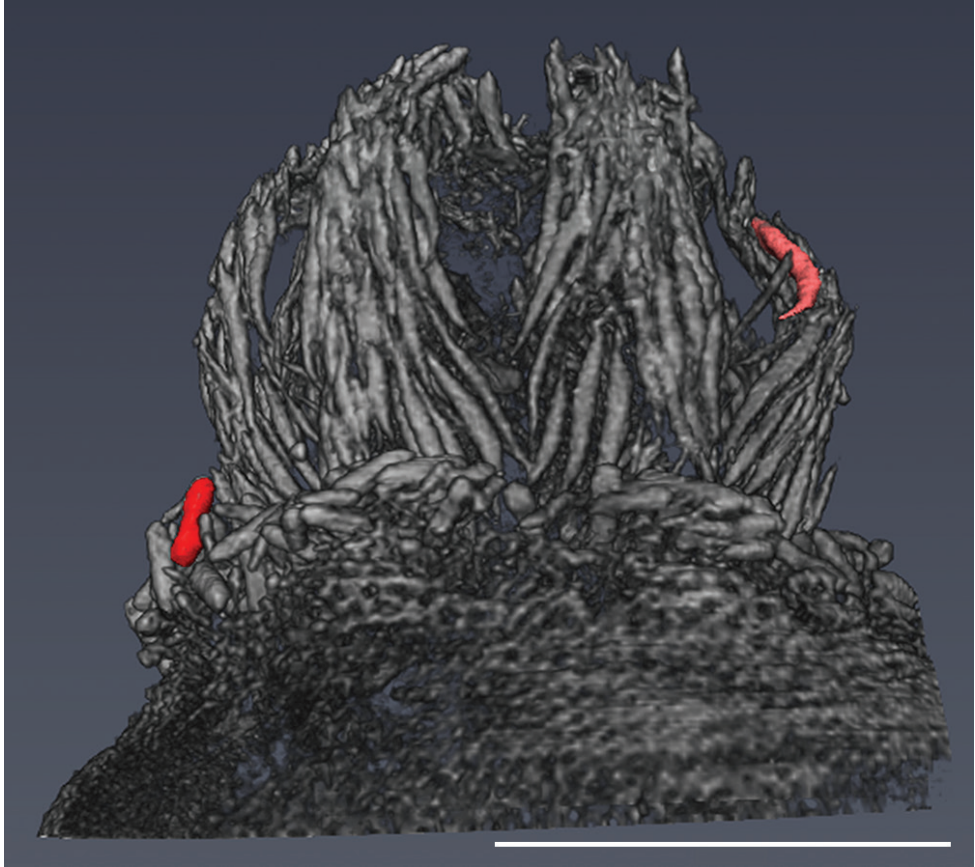


**Figure 5.** 3D reconstruction of polyp of *Swiftia phaeton* sp. nov. (paratype SaM-ID 1352). Coloured sclerites: in red, rod-forming layer on top of the polyp mound and in rose, spindle of the anthocodium. Scale bar: 1 mm.

All colonies examined were homogeneous in colouration, in agreement with the holotype. Colonies extending up to 93 mm in length but smaller in width than holotype. Colonies unbranched or branching up to two times. Branches as in holotype with 1–5 mm diameter but longer than holotype, reaching up to 77 mm length. Anastomosis present uniquely in paratype SaM-ID 1469. Polyps similar to those described for holotype, yet in most cases more densely distributed on branches of paratypes (6–21/cm) and less spaced than on holotype, 0.3–2.26 mm. Polyp mounds as those of holotype, height < 1.8 mm and 0.67–2.28 mm wide, with anthocodiae mostly retracted after preservation. Tentacles, coenenchyme, and sclerite colours and arrangements as in holotype. Sclerite sizes vary. Capstans of outer layer uniform in size along both coenenchyme and polyp mounds (22–97  $\mu\text{m}$  length; 13–58  $\mu\text{m}$  width), and with broader range of sizes than holotype. Larger spindles of inner layer of coenenchyme smaller (167–413  $\mu\text{m}$  length; 23–63  $\mu\text{m}$  width) than larger spindles of polyp mounds (198–436  $\mu\text{m}$  length; 17–73  $\mu\text{m}$  width), and with minimum sizes smaller than larger spindles of holotype. Smaller

spindles of inner layer of coenenchyme slightly bigger (90–243  $\mu\text{m}$  length; 18–56  $\mu\text{m}$  width) than smaller spindles of polyp mounds (91–231  $\mu\text{m}$  length; 16–59  $\mu\text{m}$  width), and with minimum sizes smaller than small spindles of holotype. Rods form layer on top of polyp mounds as in holotype, 108–455  $\mu\text{m}$  long, 25–77  $\mu\text{m}$  wide.

**Distribution.** This species is known to occur uniquely in the upper bathyal off Mauritania in deep-sea canyons and on deep-water coral mounds, where it lives in association with framework-forming species like *Desmophyllum pertusum* (Linnaeus, 1758) at the world largest known deep-water coral mound barrier (Ramos et al. 2017c; Wienberg et al. 2018). With the exception of the first ROV dive, *Swiftia phaeton* sp. nov. was observed in all dives of the ‘PHAETON’ expedition from north to south of Mauritania (Fig. 1, Table 3). It inhabits the canyons Tanoûdêrt, Nouamghar, Inchiri, and Tioulit and the coral mound complexes, both shallow and deep Timiris, Banda, Tamxat, and Tiguent between 20°N and 17°N at 396–639 m depth (Fig. 1, Table 3). It is widespread at Nouamghar Canyon and at the deep Timiris Mound Complex, while its occurrence varies from isolated to highly dense populations, forming monospecific or multispecific coral gardens containing other Plexauridae species (Sampaio et al. in press). Moreover, it was found attached to dead coral framework portions, coral rubble, and rocks.

**Table 3.** ROV dives performed during MSM 16/3 ‘PHAETON’ on the shelf and continental slope off Mauritania providing details of dive number, area where the dive took place, number of station, latitude, longitude, and depth at Start of dive–End of dive (SoD–EoD) in meters.

Dive No.	Area	GeoB Station	Coordinates	SoD–EoD (m)
1	Arguin south canyon	14759-1	19°44'03"N, 17°08'44"W–19°44'16"N, 17°08'50"W	546–488
2	Nouamghar canyon	14779-1	19°10'47"N, 16°48'21"W–19°10'36"N, 16°48'17"W	449–619
3	Tanoûdêrt canyon	14796-1	20°14'50"N, 17°40'12"W–20°14'35"N, 17°40'04"W	487–642
4A	Inchiri canyon	14871-1	19°08'21"N, 16°45'53"W–19°08'22"N, 16°45'49"W	519–589
4B	Inchiri canyon	14871-2	19°08'21"N, 16°45'51"W–19°08'14"N, 16°45'40"W	427–564
5	deep Timiris mound complex	14873-1	18°57'41"N, 16°52'17"W–18°57'53"N, 16°52'01"W	480–603
6	shallow Timiris mound complex	14874-1	18°58'00"N, 16°51'15"W–18°57'36"N, 16°51'04"W	429–525
7	Tioulit canyon (S)	14886-1	18°39'01"N, 16°43'35"W–18°38'29"N, 16°43'45"W	475–641
8	Tioulit canyon (N)	14891-1	18°39'51"N, 16°43'26"W–18°39'57"N, 16°43'29"W	502–592
9	Tamxat mound complex (c)	14902-1	17°32'28"N, 16°40'06"W–17°32'51"N, 16°39'41"W	396–588
10	Banda mound complex	14908	17°40'13"N, 16°40'50"W–17°40'12"N, 16°40'17"W	455–574
11	Tamxat mound complex (S)	14909-1	17°28'57"N, 16°41'57"W–17°28'57"N, 16°41'28"W	423–560
12	Tiguent mound complex	14914	17°08'12"N, 16°49'29"W–17°07'54"N, 16°48'53"W	409–515

## Discussion

This is a pioneering taxonomic study on octocorals of the deep sea off Mauritania. *Swiftia phaeton* sp. nov. is the first octocoral species discovered at the upper bathyal off Mauritania, representing the southernmost record of the genus in the NE Atlantic Ocean. Modern image technology, micro-CT, was used for the first time in the taxonomy of octocorals, revealing potential for showing diagnostic characters not imaged so far.

Through the NE Atlantic, the genus *Swiftia* (including the species *Swiftia dubia*, *S. borealis*, and *S. rosea*), is distributed from Greenland to Morocco including the Mediterranean Sea (Studer 1901; Tixier-Durivault and d'Hondt 1974; Grasshoff 1977, 1992; Manuel 1981). While *S. borealis* and *S. rosea* are inhabitants of the boreal Atlantic Ocean, *S. dubia* is widespread until the southern Macaronesian archipelagos and the Mediterranean Sea. Our record extends the known occurrence of the genus to the tropical latitudes of the NE Atlantic Ocean. Moreover, the recent observation of images of a living specimen of *S. phaeton* sp. nov. from the Fridtjof Nansen cruise to the Grand Tortue Ahmeyim oil and gas exploration area at the Senegalese-Mauritanian border is a potential distribution extension of this species (Andre Freiwald 2021, pers. comm.). Biogeographically, the species occurs in the Sahelian Upwelling ecoregion (Spalding et al. 2007), hinting at a geographical expansion for this species towards the south.

From a bathymetrical point of view, *S. dubia* is a eurybathic species, inhabiting sublittoral to abyssal depths (10–2400 m) (Grasshoff 1989; Sampaio et al. 2019). Nevertheless, the other species of this genus are more restricted in their depth ranges: *S. rosea* at the upper mesophotic and upper bathyal (20–400 m), *S. borealis* at the lower sublittoral down to the bathyal (83–1629 m), and *S. phaeton* sp. nov. at the upper bathyal (396–639 m) (Madsen 1970; Grasshoff 1977) (Table 1). However, the present geographical and bathymetrical range of *S. phaeton* sp. nov. is only based on data collected during the cruises Tyro Mauritania II, MSM 16/3 'PHAETON', and one image from the Fridtjof Nansen cruise. Further exploration and research might uncover a more complete spatial and bathymetric distributions.

Seven species of *Swiftia* are known for the North Atlantic Ocean and the Mediterranean Sea (Deichmann 1936; Grasshoff 1977). Four species, *Swiftia exserta* (Ellis & Solander, 1786), *Swiftia koreni* (Wright & Studer, 1889), *Swiftia casta* (Verrill, 1883), and *Swiftia pourtalesii* Deichmann, 1936 are exclusive to the NW Atlantic Ocean and differ from the new species (see Deichmann 1936; Goldberg 2001). *Swiftia exserta* and *S. koreni* have fewer sparsely distributed polyps in thin branches, while in *S. phaeton* sp. nov. they are numerous and crowded. Moreover, *S. exserta* and *S. casta* differ in colony colour, exclusively white in both species. Another distinct characteristic of *S. casta* and *S. pourtalesii* is the absence of capstans in their sclerome.

In the NE Atlantic Ocean and Mediterranean Sea there are three species of *Swiftia*, *S. dubia*, *S. borealis*, and *S. rosea*. *Swiftia phaeton* sp. nov. differs from them. *Swiftia borealis* and *S. dubia* have a sparse distribution of polyps in their colonies (Grasshoff 1977). However, one might wrongly identify *S. phaeton* sp. nov. as *S. rosea* based on the dense distribution of polyps around the branches. Nonetheless, *S. rosea* is endemic to the boreal NE Atlantic Ocean and, after observation of museum specimens of this species, the morphological differences between both species are clear. *Swiftia phaeton* sp. nov. colonies and polyps (including anthocodiae) are of a darker red than *S. rosea* colonies, which are rose with white anthocodiae. Besides, *S. phaeton* sp. nov. has thicker branches and polyps and a clear division between polyp mound and anthocodiae (Fig. 2D–F). Long spindles from the inner layer of the coenenchyme of the new species are compacted and slightly thinner than the outer layer of capstans of the coenenchyme, while the coenenchyme inner layer of sclerites in *S. rosea* is thick compared to its outer layer (Fig. 3;

Grasshoff 1977). At the sclerome level, *S. phaeton* sp. nov. differs from *S. borealis*, which has no capstans but flattened sclerites (Grasshoff 1977). Despite having similarly long, sharp spindles like *S. dubia* and *S. rosea*, *S. phaeton* sp. nov. has more rounded capstans in the outer layer of the coenenchyme. Its capstans resemble double-headed sclerites (see Bayer et al. 1983: fig. 159), but with more warts on their tips (Fig. 4C).

A unique morphological feature of *S. phaeton* sp. nov. is the presence of bar-like rods on top of the polyp mound, observed clearly with the micro-CT (Figs 4C, 5). “Finger-biscuit” rods were considered a definitive characteristic of the genus, based on the observation of specimens from the Pacific Ocean (Horvath 2019) yet, the species from the Atlantic Ocean do not have rods. The presence of rods in *Swiftia* was proposed to be related with northern latitudes of the eastern Pacific (Horvath 2019). Nonetheless, these sclerites occur neither in colonies from the eastern Atlantic temperate *S. dubia* collected from the Azores archipelago, nor in the boreal *S. borealis* and *S. rosea* that we studied. Also, *S. phaeton* sp. nov. rods are different from the common round-ended finger-biscuit rods, having instead pointed ends and prominent warts (Figs 4C, 5).

We applied micro-CT for the first time in the observation of morphological features of a new octocoral species. Similarly, Bayer (1973) used the scanning electron microscope (SEM) for the first time to photograph sclerites of octocorals that used to be drawn in previous taxonomic papers (e.g., Cairns 2009). The 3D image based on micro-CT of a polyp of *S. phaeton* sp. nov. with its sclerites (Fig. 5) is shown for the first time in a taxonomic work on octocorals (Fig. 5). Stereo pairs of polyps of Primnoidae species scanned by SEM were already used with the purpose of showing the 3D position of the sclerites (Cairns 2016). However, this technique is not as effective in octocorals with smaller and more complex sclerites, like those of the family Plexauridae, where the tissue in-between sclerites hinders the total visualisation of the calcareous structures. The micro-CT of *S. phaeton* sp. nov. has endorsed the observation of characters previously not shown but used to describe and differentiate species of plexaurid octocorals. This technique has the advantages of being non-destructive and of building a virtual 3D model that allows the observation of sclerites from distinct perspectives, including their relationships to each other and also the measurement of morphometric data. As already proven for bryozoans (Matsuyama et al. 2015), this technique has potential for future taxonomic studies of benthic marine invertebrates.

Taxonomic studies are essential for scientific and conservation endeavours. This is particularly true considering the unexplored deep-sea areas, such as off northwest Africa, and taxa as Octocorallia, both of which lack taxonomical expertise. In Mauritania, the natural and human impact has already occurred in the form of depleted oxygen levels, sedimentation, demersal fisheries, and local oil exploration (Colman et al. 2005; Ramos et al. 2017c; Wienberg et al. 2018). Therefore, it is crucial to describe its diversity before it becomes extinct.

## Conclusions

The genus *Swiftia* now includes four species inhabiting the NE Atlantic Ocean. *Swiftia phaeton* sp. nov., an inhabitant of the upper bathyal off Mauritania, is the

southernmost species. Micro-CT images of morphological details of gorgonians have the potential to show important diagnostic features, allowing us to visualise and compare them with other species. It is of fundamental importance in the description of new Octocorallia, which has only a handful of expert taxonomists around the globe. At the same time, in order to assess the consequences of the natural and anthropogenic impacts that are currently taking place on unexplored areas, such as NW Africa and the Mauritanian deep sea, it is very important to know, describe, and conserve the fauna of this geographical area. Discoveries of additional new octocoral species are foreseen for the coral framework off Mauritania during future deep-sea research.

## Acknowledgements

The authors are thankful to the crew and scientific team of MSM 16/3 ‘PHAETON’ cruise onboard RV Maria S. Merian for collecting images, specimens, and data that made this work possible. Special thanks are given to the ROV Pilot Thomas Lundälv from the Sven Lovén Center for Marine Infrastructure at Tjärnö, Sweden, for his skilful work. We also thank Prof. Dr. Bert Hoeksema, Mr. Koos van Egmond, and Ms. Karen van Dorp for facilitating access to specimens at Naturalis. We thank Dr. Alexander Kieneke for his guidance with the critical point dryer and Nicol Mahnken for her patience while taking sclerite and polyp SEM images. Thanks are due to the referees for their constructive comments on the manuscript. ÍS was funded by Fundação para a Ciência e a Tecnologia (FCT) Doctoral grant SFRH/BD/101113/2014 and has received a Marine and Environmental Sciences Centre (MARE) travel grant to visit Naturalis. This research received support from the SYNTHESYS Project <http://www.synthesys.info/> which is financed by European Community Research Infrastructure Action under the FP7 “Capacities” Program. This publication is supported by the Deutsche Gesellschaft für Internationale Zusammenarbeit (GIZ) through the WASP (West African Biodiversity under Pressure) Project, Contract 81248171, to AF.

## References

- Bayer FM (1956) Octocorallia. In: Moore RC (Ed.) Treatise on invertebrate paleontology. University of Kansas Press, Lawrence, KS, F166–F189, 192–231.
- Bayer FM (1961) The shallow-water Octocorallia of the west Indian region. Studies on the fauna of Curaçao and other Caribbean Islands 12(1): 1–373. <http://www.repository.naturalis.nl/document/549850>
- Bayer FM (1973) A new gorgonacean octocoral from Jamaica. Bulletin of Marine Science 23(2): 387–398. <https://repository.si.edu/bitstream/handle/10088/886/Bayer-063-1973-pg-387-398.pdf>

- Bayer FM (1981) Key to the genera of Octocorallia exclusive of Pennatulacea (Coelenterata: Anthozoa), with descriptions of new taxa. *Proceedings of the Biological Society of Washington* 94(3): 902–947. <https://repository.si.edu/handle/10088/978>
- Bayer FM, Weinheimer AJ (1974) Prostaglandins from *Plexaura homomalla*: Ecology, utilization and conservation of a major medical marine resource. *Studies in Tropical Oceanography* 12: 1–165. <https://repository.si.edu/handle/10088/6191>
- Bayer FM, Grasshoff M, Verseveldt J (1983) Illustrated trilingual glossary of morphological and anatomical terms applied to Octocorallia. E.J. Brill Archive/Dr. W. Backhuys, Leiden, 75 pp.
- Bigelow HB (1911) The Work of the 'Michael Sars' in the north Atlantic in 1910. *Science* 34(862): 7–10. <https://doi.org/10.1126/science.34.862.7>
- Breedy O, Cairns SD, Häussermann V (2015) A new alcyonacean octocoral (Cnidaria, Anthozoa, Octocorallia) from Chilean fjords. *Zootaxa* 3919(2): 327–334. <https://doi.org/10.11646/zootaxa.3919.2.5>
- Breedy O, Rouse GW, Stabbins A, Cortés J, Cordes EE (2019) New records of *Swiftia* (Cnidaria, Anthozoa, Octocorallia) from off the Pacific Costa Rican margin, including a new species from methane seeps. *Zootaxa* 4671(3): 407–419. <https://doi.org/10.11646/zootaxa.4671.3.6>
- Brito A, Ocaña O (2004) Corales de las islas Canarias. Editorial Lemus, La Laguna, 477 pp.
- Buschewski U (2016) Die Gattung *Acanthogorgia* (Anthozoa: Octocorallia) in Kaltwasserriffen des europäischen Kontinentalrandes – Charakterisierung der Arten anhand der funktionalen Ordnung des Skleroms mittels verschiedener morphologischer Methoden. Master's thesis, University of Greifswald, Greifswald.
- Cairns SD (2009) Influence of Frederick (Ted) M. Bayer on deep-water octocoral research. *Marine Ecology Progress Series* 97: 7–10. <https://doi.org/10.3354/meps08066>
- Cairns SD (2016) The marine fauna of New Zealand: Primnoid octocorals (Anthozoa, Alcyonacea) - Part 2. *Primnoella*, *Callozostrom*, *Metafannyella*, *Callogorgia*, *Fanellia* and other genera. NIWA Biodiversity Memoir, 129. NIWA: Wellington, 129 pp. [ISBN 978-0-473-36056-6]
- Colman JG, Gordon DM, Lane AP, Forde MJ, Fitzpatrick JJ (2005) Carbonate mounds off Mauritania, northwest Africa: status of deep-water corals and implications for management of fishing and oil exploration activities. In: Freiwald A, Roberts MJ (Eds) *Cold-water corals and ecosystems*. Springer, Berlin, Heidelberg, 417–441. [https://doi.org/10.1007/3-540-27673-4\\_21](https://doi.org/10.1007/3-540-27673-4_21)
- Deichmann E (1936) The Alcyonaria of the western part of the Atlantic Ocean. *Memoirs of the Museum of Comparative Zoology*, Harvard, Cambridge, USA, 317 pp. <https://doi.org/10.5962/bhl.title.49348>
- Den Hartog JC (1984) An introduction to the CANCAP-project of the Dutch Rijksmuseum von natuurlijke historie (RMNH), with special reference to the CANCAP-VI expedition (1982) to the Cape Verde islands. *Courier Forschungsinstitut Senckenberg* 68: 5–15. <https://www.repository.naturalis.nl/document/148941>
- Duchassaing P, Michelotti J (1864) Supplément au mémoire sur les coralliaires des Antilles. *Mémoires de l'Académie des Sciences de Turin* 2(23): 97–206.
- Ehrenberg CG (1834) Beiträge zur physiologischen Kenntniss der Corallenthiere im Allgemeinen, und besonders des rothen Meeres, nebst einem Versuche zur physiologischen Systematik derselben. *Abhandlungen der Königlichen Akademie der Wissenschaften zu*

- Berlin 1: 225–380. <http://bibliothek.bbaw.de/bibliothek-digital/digitalequellen/schriften/anzeige?band=07-abh/1832-1&seite:int=00000243>
- Ellis J, Solander D (1786) The natural history of many curious and uncommon Zoophytes collected from various parts of the globe. Printed for Benjamin White and Son, at Horace's Head, Fleet-Street, and Peter Elmsly, in the Strand, London, 206 pp. <https://doi.org/10.5962/bhl.title.64985>
- ESRI Ocean Basemap (2019) ESRI Ocean Basemap. <https://www.arcgis.com/home/item.html?id=6348e67824504fc9a62976434bf0d8d5>
- GEBCO Compilation Group (2019) GEBCO 2019 Grid. <https://doi.org/10.5285/836f016a-33be-6ddc-e053-6c86abc0788e>
- Goldberg WM (2001) The sclerites and geographic distribution of the gorgonian *Swiftia exserta*. Bulletin of the Biological Society of Washington 10: 100–109.
- Grasshoff M (1977) Die Gorgonarien des östlichen Nordatlantik und des Mittelmeeres. III Die Familie Paramuriceidae (Cnidaria, Anthozoa). Meteor Forschungsergebnisse 27: 5–76.
- Grasshoff M (1981) Polypen und Kolonien der Blumentiere (Anthozoa); I, Der Bau der Polypen. Natur und Museum 111(5): 1–8.
- Grasshoff M (1982) Die Gorgonaria, Pennatularia und Antipatharia des Tiefwassers der Biskaya (Cnidaria, Anthozoa). Ergebnisse der französischen Expeditionen BioGas, PolyGas, Geomanche, Incal, Noratlante und Fahrten der „Thalassa“. II. Taxonomischer Teil. Bulletin du Muséum National d'Histoire Naturelle Paris 4(3): 731–766. <https://archive.org/details/biostor-251401>
- Grasshoff M (1985) Die Gorgonaria und Antipatharia der Großen Meteor-Bank und der Josephine Bank (Cnidaria: Anthozoa). Senckenbergiana Maritima 17: 65–87.
- Grasshoff M (1986) Die Gorgonaria der Expeditionen von “Travailleur” 1880–1882 und “Talisman” 1883 (Cnidaria, Anthozoa). Bulletin du Muséum National d'Histoire Naturelle Paris 4(8): [A1.] 9–38. <http://bionames.org/bionames-archive/issn/0181-0626/8/9.pdf>
- Grasshoff M (1988) The genus *Leptogorgia* (Octocorallia: Gorgoniidae) in West Africa. Atlantide Report 14: 91–147.
- Grasshoff M (1989) Die Meerenge von Gibraltar als Faunen-Barriere: Die Gorgonaria, Pennatularia und Antipatharia der Balgim-Expedition (Cnidaria: Anthozoa). Senckenbergiana Maritima 20: 201–223.
- Grasshoff M (1992) Die Flachwasser-Gorgonarien von Europa und Westafrika (Cnidaria, Anthozoa). Courier Forschungsinstitut Senckenberg 149: 1–135.
- Gray JE (1859) On the arrangement of zoophytes with pinnated tentacles. Annals & Magazine of Natural History 4(24): 439–444. <https://doi.org/10.1080/00222935908697159>
- Grieg JA (1887) Bidrag til de norske Alcyonariet. Bergens Museums Aarsberetning 1886: 1–26.
- Haeckel E (1866) Generelle Morphologie der Organismen. Georg Reimer, Berlin, 574 pp. <https://doi.org/10.1515/9783110848281>
- Hagen E (2001) Northwest African upwelling scenario. Oceanologica Acta 24(1): 113–128. [https://doi.org/10.1016/S0399-1784\(00\)01110-5](https://doi.org/10.1016/S0399-1784(00)01110-5)
- Horvath EA (2019) A review of gorgonian coral species (Cnidaria, Octocorallia, Alcyonacea) held in the Santa Barbara Museum of natural History research collection: focus on species from Scleraxonia, Holaxonia, Calcaxonia—Part III: Suborder Holaxonia continued, and suborder Calcaxonia. ZooKeys 860: 183–306. <https://doi.org/10.3897/zookeys.860.34317>

- Kükenthal W (1924) *Gorgonaria*. Das Tierreich, Vol. 47. Walter de Gruyter & Company, Berlin, 478 pp.
- Lamouroux JVF (1812) Extrait d'un mémoire sur la classification des polypiers coralligènes non entièrement pierreux. *Nouveau Bulletin des Sciences Société Philomatique de Paris Ser. 3* 63: 181–188.
- Linnaeus C (1758) *Systema naturae* (Editio Decima). Holmiae: Impensis Direct. Laurentii Salvii, Stockholm, 824 pp. <https://doi.org/10.5962/bhl.title.542>
- López-González PJ (2006) A new gorgonian genus from deep-sea Antarctic waters (Octocorallia, Alcyonacea, Plexauridae). *Helgoland Marine Research* 60(1): 1–6. <https://doi.org/10.1007/s10152-005-0008-1>
- Madsen FJ (1970) Remarks on *Swiftia rosea* (Grieg) and related species (Coelenterata, Gorgonaria). *Steenstrupia* (Copenhagen) 1: 1–10.
- Manuel RL (1981) *British Anthozoa*. Academic Press, London, 241 pp.
- Marañón E, Holligan PM (1999) Photosynthetic parameters of phytoplankton from 50°N to 50°S in the Atlantic Ocean. *Marine Ecology Progress Series* 176: 191–203. <https://doi.org/10.3354/meps176191>
- Matsuyama K, Titschack J, Baum D, Freiwald A (2015) Two new species of erect Bryozoa (Gymnolaemata: Cheilostomata) and the application of non-destructive imaging methods for quantitative taxonomy. *Zootaxa* 4020(1): 81–100. <https://doi.org/10.11646/zootaxa.4020.1.3>
- Oñate SC (2017) Marine molluscs (Gastropoda and Bivalvia) from northwest Africa. PhD thesis. Universidade de Vigo, Vigo.
- Ramos A, Ramil F, Sanz JL (2017a) Deep-sea ecosystems off Mauritania: an Introduction. In: Ramos A, Ramil F, Sanz JL (Eds) *Deep-Sea Ecosystems Off Mauritania*. Springer, Dordrecht, 1–51. [https://doi.org/10.1007/978-94-024-1023-5\\_1](https://doi.org/10.1007/978-94-024-1023-5_1)
- Ramos A, Ramil F, Sanz JL (2017b) Deep-sea ecosystems off Mauritania. Research of marine biodiversity and habitats in the northwest African margin. Springer, The Netherlands, 683 pp. <https://doi.org/10.1007/978-94-024-1023-5>
- Ramos A, Sanz JL, Ramil F, Agudo LM, Presas-Navarro C (2017c) The giant cold-water coral mounds barrier off Mauritania. In: Ramos A, Ramil F, Sanz JL (Eds) *Deep-Sea Ecosystems Off Mauritania*. Springer, Dordrecht, 481–525. [https://doi.org/10.1007/978-94-024-1023-5\\_13](https://doi.org/10.1007/978-94-024-1023-5_13)
- Sampaio Í, Carreiro-Silva M, Freiwald A, Menezes G, Grasshoff M (2019) Natural history collections as a basis for sound biodiversity assessments: Plexauridae (Octocorallia, Holaxonia) of the Naturalis CANCAP and Tyro Mauritania II expeditions. *ZooKeys* 870: 1–32. <https://doi.org/10.3897/zookeys.870.35285>
- Sampaio Í, Beuck L, Menezes G, Freiwald A (in press) The Mauritanian Slope (NE Atlantic) has no desert: *Swiftia phaeton* (Holaxonia: Plexauridae) shaping coral gardens. In: Chimienti G (Ed.) *Corals – Habitat formers from the shallow to the deep*. IntechOpen, London.
- Sanz JL, Maestro A, Agudo LM (2017) The Mauritanian margin. Bathymetric and geomorphological characteristics. In: Ramos A, Ramil F, Sanz JL (Eds) *Deep-Sea Ecosystems Off Mauritania*. Springer, Dordrecht, 53–117. [https://doi.org/10.1007/978-94-024-1023-5\\_2](https://doi.org/10.1007/978-94-024-1023-5_2)
- Spalding MD, Fox HE, Allen GR, Davidson N, Ferdaña ZA, Finlayson M, Halpern BS, Jorge MA, Lombana A, Lourie SA, Martin KD, McManus E, Molnar J, Recchia CA, Robertson J (2007) Marine ecoregions of the world: A bioregionalization of coastal and shelf areas. *Bioscience* 57(7): 573–583. <https://doi.org/10.1641/B570707>

- Studer T (1887) Versuch eines Systemes der Alcyonaria. Archiv für Naturgeschichte 53(1): 1–74[, pl. 1].
- Studer T (1901) Alcyonaires provenant des campagnes de l'Hirondelle (1886–88). Résultats des campagnes scientifiques du Prince Albert I<sup>er</sup> de Monaco 20: 1–64. <https://doi.org/10.5962/bhl.title.58246>
- Tixier-Durivault A, d'Hondt MJ (1974) Les octocoralliaires de la campagne Biacores. Bulletin du Muséum National d'Histoire Naturelle 3(252): 1361–1433. <https://www.biodiversitylibrary.org/page/57268681>
- Van der Land J (1988) *Tyro* Mauritania-II Expedition List of Stations: 1–9. Rijksmuseum van Natuurlijke Historie, Leiden. [mimeographed]
- Verrill AE (1883) Report on the Anthozoa, and on some additional species dredged by the “Blake” in 1877–1879, and by the U.S. Fish steamer “Fish Hawk” in 1880–82. Bulletin of the Museum of Comparative Zoology 11: 1–72. <https://biodiversitylibrary.org/page/6587690>
- Verrill AE (1928) Hawaiian shallow-water Anthozoa. Bernice P. Bishop Museum Bulletin 49: 1–30. <https://doi.org/10.5962/bhl.title.58574>
- Westphal H, Beuck L, Braun S, Freiwald A, Hanebuth T, Hetzinger S, Klicpera A, Kudrass H, Lantusch H, Lundälv T, Vicens GM, Preto N, Reumont J, Schilling S, Taviani M, Wienberg C (2012) Phaeton — Paleoceanographic and paleo-climatic record on the Mauritanian shelf. Cruise No. MSM16/3 in Maria S. Merian-Berichte. Hamburg: Leitstelle Deutsche Forschungsschiffe Institut für Meereskunde der Universität Hamburg, Hamburg. DFG-Senatskommission für Ozeanographie, 57 pp. [https://doi.org/10.2312/cr\\_msm16\\_3](https://doi.org/10.2312/cr_msm16_3)
- Wien K, Kölling M, Schulz HD (2007) Age models for the Cape Blanc Debris Flow and the Mauritania Slide Complex in the Atlantic Ocean off NW Africa. Quaternary Science Reviews 26(19–21): 2558–2573. <https://doi.org/10.1016/j.quascirev.2007.06.018>
- Wienberg C, Titschack J, Freiwald A, Frank N, Lundälv T, Taviani M, Beuck L, Schröder-Ritzau A, Kregel T, Hebbeln D (2018) The giant Mauritanian cold-water coral mound province: Oxygen control on coral mound formation. Quaternary Science Reviews 185: 135–152. <https://doi.org/10.1016/j.quascirev.2018.02.012>
- Williams GC, Breedy O (2016) A new species of whip-like gorgonian coral in the genus *Swiftia* from the Gulf of the Farallones in Central California, with a key to Eastern Pacific species in California (Cnidaria, Octocorallia, Plexauridae). Proceedings of the California Academy of Sciences 4(63): 1–13. <https://biostor.org/reference/249101>
- Wirshing HH, Messing CG, Douady CJ, Reed J, Stanhope MJ, Shivji MS (2005) Molecular evidence for multiple lineages in the gorgonian family Plexauridae (Anthozoa: Octocorallia). Marine Biology 147(2): 497–508. <https://doi.org/10.1007/s00227-005-1592-y>
- Wright EP, Studer T (1889) Report on the Alcyonaria collected by H.M.S. Challenger during the years 1873–76. Report on the Scientific Results of the Voyage of H.M.S. Challenger during the years 1873–76, 314 pp. <https://doi.org/10.5962/bhl.title.6513>

# Phylogenetic review of the millipede genus *Cherokia* Chamberlin, 1949 (Polydesmida, Xystodesmidae)

Luisa Fernanda Vasquez-Valverde<sup>1</sup>, Paul E. Marek<sup>1</sup>

<sup>1</sup> *Virginia Tech, Department of Entomology, 170 Drillfield Drive, Blacksburg, Virginia 24061, USA*

Corresponding author: Luisa Fernanda Vasquez-Valverde ([luisafvv@vt.edu](mailto:luisafvv@vt.edu))

---

Academic editor: Dragan Antić | Received 28 January 2022 | Accepted 5 May 2022 | Published 20 June 2022

<http://zoobank.org/856382C3-0061-465D-899A-704EF7797CF9>

---

**Citation:** Vasquez-Valverde LF, Marek PE (2022) Phylogenetic review of the millipede genus *Cherokia* Chamberlin, 1949 (Polydesmida, Xystodesmidae). ZooKeys 1106: 141–163. <https://doi.org/10.3897/zookeys.1106.81386>

---

## Abstract

The millipede genus *Cherokia* Chamberlin, 1949 is a monospecific taxon, with the type species *Cherokia georgiana* (Bollman, 1889). The last revision of the genus was made by Hoffman (1960) where he established three subspecies. Here we used molecular phylogenetics to assess the genus and evaluate whether it is a monophyletic group, and if the subspecies are each monophyletic. We included material from literature records and three natural history collections. Newly collected samples were obtained through a citizen science project. Morphological characters underlying subspecies groups—the shape of the paranota, body size, and coloration—were evaluated. A molecular phylogeny of the genus was estimated based on DNA sequences for seven gene loci, and a species delimitation analysis was used to evaluate the status of the subspecies. The documented geographical range of *Cherokia* in the United States was expanded to include a newly reported state record (Virginia) and about 160 new localities compared to the previously known range. Morphological characters, which included the shape of the paranota and body size that had been historically used to establish subspecies, showed clinal variation with a direct relationship with geographical distribution and elevation, but not with phylogeny. Coloration was highly variable and did not accord with geography or phylogeny. The phylogeny recovered *Cherokia* as a monophyletic lineage, and the species delimitation test supported the existence of a single species. The subspecies *Cherokia georgiana ducilla* (Chamberlin, 1939) and *Cherokia georgiana latassa* Hoffman, 1960 have been synonymized with *Cherokia georgiana*. The molecular and morphological evidence showed that *Cherokia* is a monospecific genus with the sole species, *Cherokia georgiana*, being geographically widespread and highly variable in its morphology.

## Keywords

Citizen science, DNA barcoding, morphology, phylogenetics, subspecies

## Introduction

The family Xystodesmidae (Polydesmida) includes 539 species with a center of diversity concentrated in the Appalachian Mountains (Means et al. 2021a, b; Hennen et al. 2022). Within the family Xystodesmidae, the Appalachian genus *Cherokia* Chamberlin, 1949 (Fig. 1) was named after the Cherokee, an indigenous group of peoples in the southeastern United States. This monospecific genus in the xystodesmid tribe Rhysodesmini was erected by Chamberlin (1949) for the species *Fontaria georgiana* Bollman, 1889 as its type species. After its description, various authors proposed multiple species that were all subsequently synonymized with the type species *Cherokia georgiana* (Bollman, 1889) based on gonopod morphology (Causey 1950; Hoffman 1950; Chamberlin and Hoffman 1958). However, all the above-mentioned authors pointed out the considerable color, body size, and shape variation in millipedes of the genus *Cherokia*.

Prior to Hoffman's (1960) revision, no one had carried out a comprehensive synthesis of this genus. He (Hoffman 1960) proposed *Cherokia* as a monospecific genus, with the sole species *Cherokia georgiana* divided into three subspecies: *Cherokia georgiana georgiana* (Bollman, 1889), *Cherokia georgiana ducilla* (Chamberlin, 1939), and *Cherokia georgiana latassa* Hoffman, 1960. Hoffman (1960) described in detail



**Figure 1.** *Cherokia georgiana* (Bollman, 1889), the wrinkled flat-backed millipede. Dorsal view of the whole body of specimen MPE04539 (Male, GA – White Co.) deposited in the Virginia Tech Insect Collection (VTEC). The image shows the more common coloration for the species and the prominent wrinkles of the cuticle.

the morphological variation and geographical distribution of *Cherokia*. He also differentiated the three subspecies from each other based on morphological features that included the position of the scapulora and the ratio of the body length versus its width. The scapulora is a term defined by Hoffman (1960: 231) as: “from the Latin “*scapula*,” a shoulder, and “*ora*,” the rim of a shield”. The scapulora in *C. g. latassa* is found in a marginal position, which separates it from *C. g. georgiana* and *C. g. ducilla* that have a submarginally located scapulora (Fig. 2A, B). The subspecies, *C. g. georgiana* and *C. g. ducilla*, were differentiated from each other based on the ratio of the previously mentioned body measurements (i.e., body length versus its width) (Hoffman 1960).

Hoffman (1960) confronted various problems during his revision of the genus *Cherokia*. The first one, he explained, was the fact that “despite the diversity of body form, color pattern, and morphological details which occurs in the genus, the male gonopods remain essentially similar” (Hoffman 1960: 227). Although some variation in the solenomere shape in specimens in the North Carolina mountains was observed by Hoffman (1960), the character was not consistent and did not correlate with geographical distribution or subspecies differentiation. Additionally, the same author expressed a struggle with confidently assigning all individuals to one of the subspecies. For this reason, Hoffman (1960) proposed an intermediate form, termed an “intergrade” between *C. g. georgiana* and *C. g. ducilla*. These intergrades were documented within a wide geographical band (~30 km) in western North Carolina between the distributions of *C. g. georgiana* and *C. g. ducilla*.

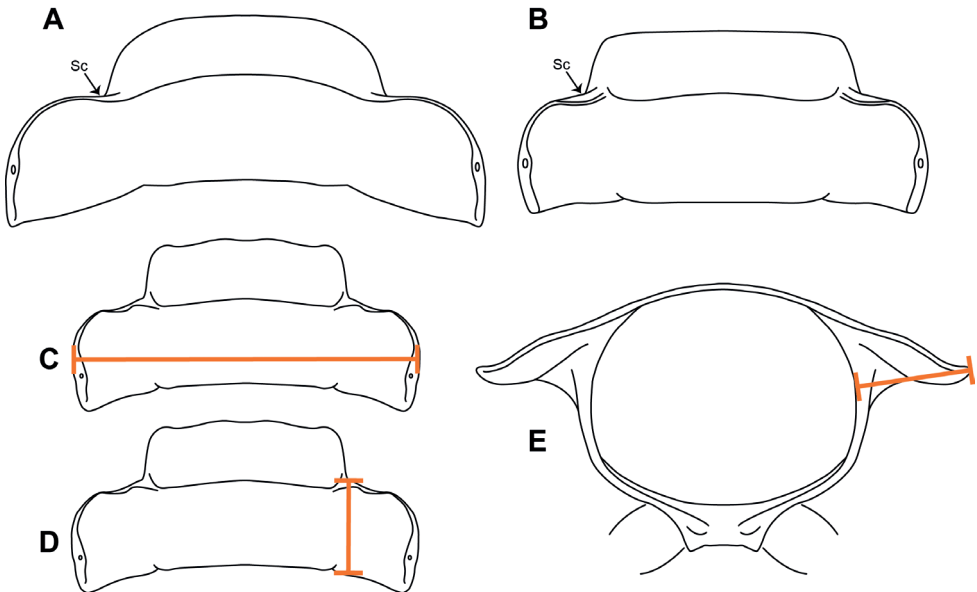


**Figure 2.** Position of the scapulae (Sc) **A** strictly marginal **B** submarginal. Measurements of the 12<sup>th</sup> body ring **C** metazonite width **D** metazonite length **E** paranota extension. Adapted from Hoffman (1960).

After 1960, some authors have indirectly mentioned *Cherokia* in tribal revisions (Hoffman 1978) and checklists (Shelley 1980, 2000; Marek et al. 2014). More recent research on the family Xystodesmidae, using a synthesis of morphological and molecular characteristics, has confidently placed the genus *Cherokia* within the family Xystodesmidae and subfamily Rhysodesminae Brolemann, 1916 as sister to the genus *Pleurolooma* Rafinesque, 1820 (Means and Marek 2017; Means et al. 2021b). As a result of field collections for this recent work, a large number of *Cherokia* individuals were collected from throughout the eastern United States, and within its range. These recent results combined with materials from natural history collections from the mid-1900s up to now, point to an even greater diversity than initially uncovered.

Here we used natural history collections in combination with new material sampled from nearly 200 locations within the range of *Cherokia*. These new samples, specially prepared for preservation of DNA, provided the basis to estimate an evolutionary history using molecular phylogenetics and address the status of the three subspecies within *Cherokia georgiana*.

## Materials and methods

### Selection of samples and Citizen science project

Specimens of the genus *Cherokia* preserved in the Virginia Tech Insect Collection were selected based on the availability to score both morphological and molecular characters from them. Individual live millipede specimens or their tissues were fixed in either 100% ethanol or Qiagen RNAlater thereby preserving DNA and other genetic material. Whole body specimens (minus tissue preserved for DNA) were then preserved in 70% isopropanol for subsequent morphological evaluation.

New samples were needed from some localities that had not previously been sampled; these localities were in the periphery of the known distribution of *Cherokia* or in areas where DNA-grade specimens were unavailable. A season of fieldwork was planned for the Summer 2020, however, due to the SARS-CoV-2/COVID-19 pandemic, and state restrictions, travel was not feasible. In response, and with the objective of obtaining these required samples, a citizen science project was developed. This enabled the general public to participate in the collection of millipedes of the genus *Cherokia*, and to learn about biodiversity.

For the citizen science project, collection kits and information pamphlets were designed with step-by-step instructions and other information for the public to obtain samples in an accurate and lawful way (Fig. 3B). Citizen scientists were recruited with social media through Facebook and Twitter, and the kits were shipped to interested participants. A small plastic keychain of *Cherokia* was included in the kit as a token of participation (Fig. 3E). Once the participants received the kit and collected millipedes, they were instructed to ship the millipedes to the lab at Virginia Tech, so we could identify, process and preserve them following methodology described by Means et al. (2015).

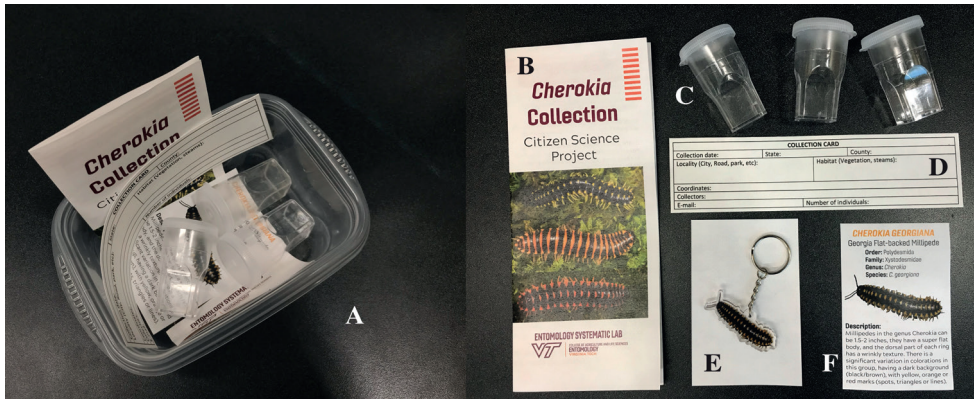


**Figure 3.** Citizen science collection kit **A** plastic food container (32 FL OZ) **B** instruction flyer: with step-by-step instructions of collecting and shipping **C** clear plastic collection vials **D** collection card **E** token for the participant: millipede keychain and **F** *Cherokia* identification card.

### DNA extraction, phylogenetics analysis and species delimitation

Preserved tissue (legs or head) from each individual was used for DNA extraction with a Qiagen DNeasy kit. The DNA obtained from the extraction was amplified via polymerase chain reaction (PCR) for seven gene regions: cytochrome oxidase subunit I (COI), small subunit RNA (12S), tRNA-Valine (tRNA-Val), large subunit RNA (16S), elongation factor- $\alpha$  (EF1 $\alpha$ ), RNA polymerase II largest subunit (RNAPol2), and F-box (fBox). The mitochondrial 12S, tRNA-Val, and 16S regions were amplified as a single contiguous stretch. Amplification of DNA was carried out according to Means et al. (2021a, b). These PCR amplicons were cleaned, quantified, normalized, and sequenced on an Applied Biosystems ABI 3730 capillary sequencer at the University of Arizona Genetics Core.

The sequences were analyzed in Mesquite (Version 3.61) (Maddison and Maddison 2019) using the sequence analysis module Chromaseq (Version 1.52) that implements phred and phrap (Ewing et al. 1998; Maddison and Maddison 2020) for chromatogram base calling, trimming, quality control and generation and curation of matrices. The outgroups were selected based on the phylogeny inferred by Means et al. (2021b) and included a single individual of: *Pleuroloma flavipes* Rafinesque, 1820, *Pleuroloma plana* Shelley, 1980 and *Pleuroloma cala* (Chamberlin, 1939). Sequences were aligned with the progressive sequence alignment program MAFFT (Version 7) using the model L-INS-I (Katoh and Standley 2013). A nucleotide base composition homogeneity chi-square test in IQ-TREE 2 (Version 2.0.4; Minh et al. 2020) was run with the aligned sequences for each of the genes to test the heterogeneity of the sequences ( $H_{\text{alternative}}$  = homogeneity) and excluding the sequences of the outgroup taxa. The sequences that failed the heterogeneity test were excluded from the phylogeny. Afterwards, each locus was partitioned by gene, intron/exon location, and codon position. The seven loci were concatenated into a single matrix. The partitioned matrix

was analyzed using ModelFinder to test alternative nucleotide evolution models and to infer the model of best-fit for the data (Kalyaanamoorthy et al. 2017). The selected model was then used to estimate a phylogenetic tree for the genus with the maximum likelihood-based phylogenetics software IQ-TREE 2. Single gene alignments were then analyzed separately to estimate gene trees with the same methods and software as above.

To determine whether the subspecies of *Cherokia georgiana* represent distinct genetic groups, Automatic Barcode Gap Discovery (ABGD) species delimitation analysis was used. This method uses an alignment of sequences of a single locus (COI) to make a pairwise distance matrix and determine if a barcode gap exists. A barcode gap is observed when the intraspecific distance among unique sequences is smaller than the interspecific distance (Puillandre et al. 2012). This analysis was run in the ABGD online server using the alignment of *Cherokia* sequences for the locus COI, excluding the outgroup sequences.

### Distribution mapping and morphological characters analysis

To infer a detailed geographical range of the genus *Cherokia*, records in the literature, natural history collections, and new collections from the citizen science project were included. All the localities of specimens of *Cherokia* documented in Hoffman (1960) and from the Virginia Tech Insect Collection, Virginia Museum of Natural History (VMNH), and Florida State Collection of Arthropods (FSCA) were digitized. Digitization involved transcribing the label data of specimens in a spreadsheet using the Darwin Core data standard (Wieczorek et al. 2012). Text-based details of the label including state, county, and any other locality information were manually entered in a spreadsheet. In cases where precise geographical coordinates (e.g., latitude and longitude) were not provided, the text of the localities from the labels was transcribed, georeferenced and geographical coordinates automatically estimated using the software GEOLocate (Rios and Bart 2010) to retrospectively obtain decimal degree coordinates and an error radius based on precision of the text locality. To supplement this data set, localities from *Cherokia* specimens from the Virginia Tech Insect Collection (VTEC) that were already digitized and with geographical coordinates recorded at the time of collection were downloaded from the online database SCAN (Barkworth et al. 2019). This data set of coordinates (from collections and literature), was the basis to produce a comprehensive map of the geographical range of *Cherokia*. The map was constructed in the online GIS application SimpleMapper (Shorthouse 2010).

For the analysis of morphological features, the traits described in Hoffman (1960) were revisited: width-to-length ratio, color (hue and pattern), gonopods, and the position of the scapulora (Fig. 2A, B). Hoffman (1960) measured the entire length of the trunk of the millipedes; however, due to the flexibility of the trunk and the rings that make up the trunk—causing accordion-like compression and extension—these overall length measurements typically have a large error. With the idea of evaluating size variation more accurately, the 12<sup>th</sup> body ring only was dissected from each specimen and measured for: (1) width (Fig. 2C) and (2) length (Fig. 2D) of the metazonite in dorsal

view; and (3) the paranota lateral extension from a posterior view (Fig. 2E). Measurement of a single ring reduces the error, because a single diplosegmental ring is rigid and inflexible, and hypothetically linearly correlated to overall length. To control for a non-normal body size distribution, a natural logarithm to transform the raw measurements was used. Linear regressions were then used to evaluate potential correlations between the measurements and elevation.

*Cherokia georgiana* exhibits a considerable diversity in coloration patterns throughout its geographical distribution. To evaluate this variation, pictures of the species taken from the specimens selected for the analysis and those observed on iNaturalist (available from <https://www.inaturalist.org>; accessed May, 2020) were included. Before including pictures from iNaturalist, identifications of the observations of *Cherokia* were confirmed by the authors (accessed on 18 May 2020). Afterwards the pictures were coded based on selection of one of three hue (red, orange, and yellow) and pattern groups (bimaculate, trimaculate, and striped), and scored. These pattern codes were then mapped onto the distribution of *Cherokia* to test if there is a correspondence with geographical areas and phylogenetic relationships.

## Results

### Selection of samples and Citizen science project

The citizen science campaign on social media received more than 100 responses from a Facebook and Twitter post. This resulted in 68 people who completed a Google form expressing their interest to participate in the project. Fifty people were then selected based on their location and proximity to areas previously not surveyed. Due to the limited number of kits available, sampling efforts were focused on the collection of millipedes in targeted localities in Georgia, Alabama and Tennessee. A total of 41 kits (Fig. 3) were shipped between the months of July and August of 2020 to participants who provided all the required information in the online form. From October 2020 to March 2021, a total of 23 live millipedes were received as a result of this project, and 13 of them were identified as *Cherokia* and included in the morphological and molecular analysis.

A total of 106 individuals from the genus *Cherokia* were included in the molecular phylogenetic analysis: 74 males, 31 females and one juvenile. Of these, 88% of the selected samples were previously deposited at the VTEC, and the remaining 12% corresponded to new samples obtained from the citizen science project.

### DNA extraction, phylogenetics analysis and species delimitation

The amplification and sequencing of DNA for the loci, COI, 12S, tRNA-Val and 16S, had a high rate of success, and only one specimen did not amplify (Suppl. material 1). For the locus fBox, the rate of success in amplification and sequencing was 96%, and for the

loci EF1 $\alpha$  and RNAPol2 that rate was considerably lower with 75% and 55% of the total sequences obtained. When amplifications and/or sequencing failed, amplifications were repeated up to three times using the same DNA extraction before discontinuing attempts.

The multiple sequence alignment in MAFFT and inference of nucleotide evolution models in ModelFinder resulted in a 3865 bp concatenated matrix divided into six partitions and composed of 142 bp of 12S (TIM+F+G4 nucleotide evolution model), 82 bp of tRNA-Val (TIM+F+G4), 1081 bp of 16S (TIM+F+G4), 600 bp of COI (pos 1 TN+I+G4, pos 2 TIM3+F+R2 and pos 3 TIM3+F+G4), 585 bp of EF1 $\alpha$  (pos 1 & 2 TN+I+G4, pos 3 TIM3+F+R2 and intron GTR+F+I+G4), 978 bp of RNAPol2 (pos 1, 2, 3 & intron 1 TN+F+R2 and intron 2 TIM+F+G4), and 397 bp of fBox (pos 1 & 2 TN+I+G4 and pos 3 TIM3+F+R2). Of the 3865 nucleotide characters, 2726 corresponded to constant sites, 738 were parsimony-informative, and 401 were singleton sites. The average uncorrected pairwise distance for COI sequences between individuals from the same locality was 0.00470 (max. = 0.01644, min. = 0,  $\sigma$  = 0.005), and in total 0.07704 (max. = 0.12105, min. = 0,  $\sigma$  = 0.02742). The maximum uncorrected pairwise distance (COI) between *Cherokia* and *Pleurolooma* was 0.14740. The estimated phylogeny for *Cherokia* using the seven loci and the above-mentioned partitions and models is shown in Fig. 4.

The ABGD analysis included high-quality COI sequences for 105 specimens of *Cherokia* and excluded the sequences from the outgroup taxon *Pleurolooma*. The analysis was carried out on the ABGD web server using the Jukes-Cantor (JC69) substitution model and a relative gap width of 1.5X. The results of this analysis showed that a barcode gap does not exist in the COI sequences of *Cherokia* (Fig. 5A), and supports the model that all the individuals belong to the same group. Fig. 5B depicts what an expected histogram with a barcode gap present would look like; the dotted line marks the separation between the two groups and represents the likelihood of two species.

## Distribution mapping and morphological character analysis

A total of 201 reports were digitized and georeferenced from Hoffman (1960) ( $N$  = 103), the VMNH ( $N$  = 31) and FSCA ( $N$  = 67) natural history collections. Localities from the VTEC were obtained (already databased), thereby adding 222 *Cherokia* records to the database. The map for the geographical distribution of the genus *Cherokia* (Fig. 6) was constructed using 253 coordinates from localities representing 848 individuals. The geographical distribution includes seven states: Alabama, Georgia, Kentucky, North Carolina, South Carolina, Tennessee and Virginia. Ninety-six counties from throughout the aforementioned states have records of *Cherokia* individuals.

All of the adult individuals used for the phylogeny were included in the morphological analysis. The juvenile (Fig. 4; GA-TIF-MPE03692) was excluded due to lack of development in its morphological characters, which could have introduced unwanted outliers and substantial error in the data set. The measurement from the metazonal width had the greatest variation range (range = 6.0–9.3 mm,  $\sigma$  = 0.74,  $N$  = 105), followed by the paranotal extension (range = 1.25–2.17 mm,  $\sigma$  = 0.24,  $N$  = 105), and lastly by the metazonal length (range = 1.54–2.60 mm,  $\sigma$  = 0.20,  $N$  = 105).



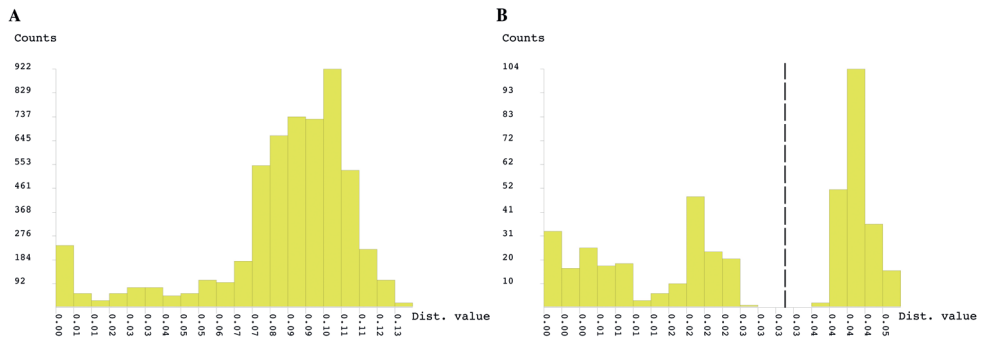


**Figure 5.** ABGD analysis results **A** *Cherokia* Chamberlin, 1949 sequences, no barcode gap observed **B** simulated sequences, barcode gap marked by the dotted line.

Once all the measurements were log-transformed, a linear regression analyzing the correlation between elevation and body dimensions were conducted for each of the respective measurements (Fig. 8). These analyses suggest that, in general, there is a negative correlation between the body measurements and the elevation; millipedes with smaller body sizes tended to be present in a higher elevation than those with a larger size.

The position of the scapulora as described in Hoffman (1960) (Fig. 2) could not be consistently discerned and objectively scored and was not included in this analysis. Nevertheless, a qualitative difference in the shape of the anterior border of the paranota was observed and generally showed two phenotypes for this character. The first phenotypic group includes a distinct sinuous curvature on the anterior border of the paranota, while the posterior paranotal corner protrudes backwards posteriorly beyond the margin of the posteromedial margin of the metazonite (Fig. 9A–C, blue lines). The second phenotypic group includes an almost straight anterior border, and the posterior corner is nearly aligned with the posteromedial margin of the metazonite (Fig. 9D, E, red lines).

The coloration analysis of *Cherokia* included a total of 124 images of individuals identified as *Cherokia* on iNaturalist. The identifications of *Cherokia* observations on iNaturalist were confirmed by the authors based on the diagnosis below. The pictures were coded using the three colors (red, orange and yellow), and three patterns (bimaculate, trimaculate, and striped). Most of the individuals exhibited only one of the colors, and a smaller proportion of them exhibited two. The color white was only observed present while in combination with another color (i.e., white and orange), while the other colors were present by themselves or with another.

In the bimaculate pattern, a spot of color was present laterally on each paranota (there are two paranota per ring) with the center lacking pigmentation (Fig. 10A–C). The trimaculate pattern, is characterized by a coloration spot on each paranota in addition to a middorsal spot on the ring. The middorsal or paranotal spots had different sizes and could be one of three shapes: a circle, oval, or a triangle (Fig. 10D–F). The striped pattern is where a color band is on the posterior margin of the body ring that runs from one paranota to the other. The band could have

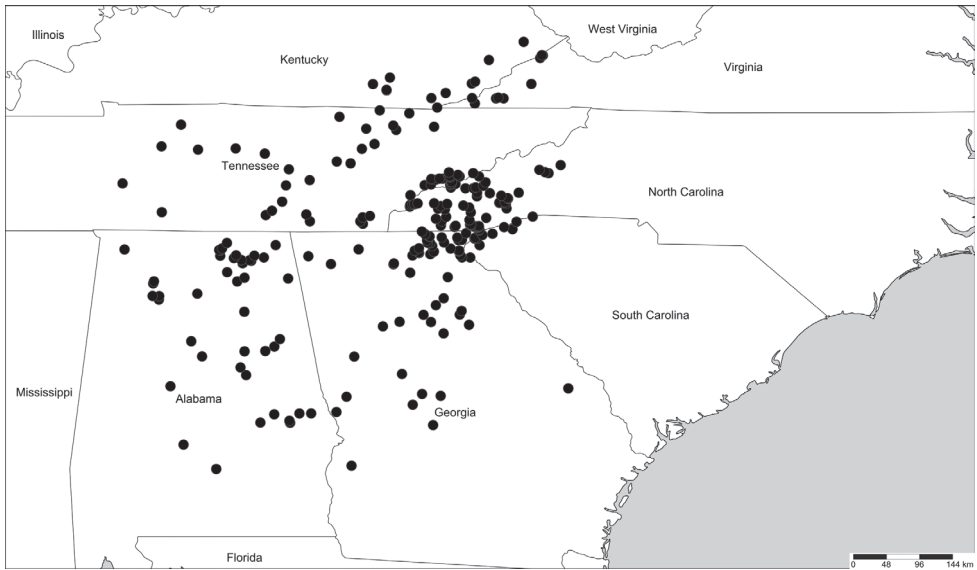


**Figure 6.** Geographical distribution of the genus *Cherokia* Chamberlin, 1949. Mapped using a set of 235 coordinates, from 848 individual records from Hoffman (1960), and natural history collections (VMNH, FSCA, VTEC).

various thicknesses, and in some cases an apparent superposition of the trimaculate pattern was evident atop the banded pattern (Fig. 10G–I). There was no clear relationship between geographical distribution and the color or patterns; in some cases, syntopic individuals of *Cherokia* from the same locality exhibited different coloration patterns.

## Taxonomy

**Family Xystodesmidae Cook, 1895**

**Subfamily Rhysodesminae Brolemann, 1916**

**Tribe Rhysodesmini Brolemann, 1916**

**Genus *Cherokia* Chamberlin, 1949**

**Type species.** *Cherokia georgiana* (Bollman, 1889)

***Cherokia georgiana* (Bollman, 1889)**

**Vernacular name:** Wrinkled Flat-backed Millipede

*Fontaria georgiana* Bollman, 1889a: 344. MALE HT (United States National Museum, USNM). United States: Georgia, Bibb County.

*Fontaria tallulah* Bollman, 1889a: 344. FEMALE HT (USNM). United States: Georgia, Habersham County. Synonymized by Hoffman, 1950b: 23.

*Mimuloria furcifer* Chamberlin, 1940a: 282, fig. 1. MALE HT (USNM). United States: North Carolina, Buncombe County. Synonymized by Hoffman, 1950b: 23.

*Mimuloria georgiana* – Loomis 1943: 402.

*Dynoria parvior* Chamberlin, 1947: 10, fig. 4. MALE HT (USNM). United States: Georgia, Union County. Synonymized by Hoffman, 1950b: 23.

*Cherokia georgiana* – Chamberlin 1949a: 3.

*Cherokia georgiana georgiana* Hoffman 1960: 240, figs 3d, 4e, 5a, 6, 7. syn. nov.

*Mimuloria ducilla* Chamberlin, 1939: 7, fig. 12. MALE HT (USNM). United States: North Carolina, Jackson County.

*Mimuloria georgiana* (nec Bollman, 1889) – sensu Loomis, 1943: 402.

*Cherokia georgiana ducilla* Hoffman 1960: 255, figs 3b–e, 4f, 5b, 6, 7. syn. nov.

*Cherokia georgiana latassa* Hoffman, 1960: 257, figs 3a, c, 4a–e, 5c, d, 7. MALE HT (USNM). United States: Tennessee, Warren County. syn. nov.

**Note.** For a complete taxonomic listing, see Means et al. (2021b), Suppl. material 1.

**Diagnosis.** Adults in the genus *Cherokia* are distinct from other rhysoedesmiline genera based on the following combination of characters: **Body rings:** dorsal surface of the metazonites with a noticeably wrinkly texture. Paranota horizontal and wide, with little downwards curvature, making the body appear flatter than other rhysoedesmiline. **Gonopods:** Telopodite sublinear in shape (Fig. 7), not distinctly curved or twisted as in the Apheloriini. Telopodite with a cingulum. Acropodite with its apex appearing flat and truncated. Telopodite with a long acicular prefemoral process; not a stout, curved prefemoral process nor wholly lacking as in the Apheloriini. **Cyphopods:** receptacle absent. **Coloration:** yellow to red hues in bimaculate, trimaculate and striped patterns (Fig. 10). Yellow trimaculate is the most frequent color morph (Fig. 1).

## Discussion

The previously reported geographical range of *Cherokia* sensu Hoffman (1960), included six states, 43 counties and 93 localities. Here we report the presence of *Cherokia* in a seventh state (Virginia) and 53 new counties, for a total of 160 new localities where specimens of the genus have been collected. In prior systematic analyses of the millipede family Xystodesmidae, *Cherokia* was represented by three individuals, sequenced for six genes (Means et al. 2021b). Here, to address species boundaries in greater detail, we increased this number to 106 individuals sequenced for seven genes, for a total of 450 sequences and 3865 base pairs of DNA. These sequences were used to infer a phylogeny (Fig. 4). Of the seven loci amplified and sequenced for the phylogenetic reconstruction of the genus *Cherokia*, RNAPol2 was less successful than others in terms of amplification (presence of bands on electrophoretic gels) and sequencing (low quality reads: phred scores > 20). The presence of stop codons in RNAPol2 sequences,

despite viewing in six alternative reading frames, is unexpected and may indicate that it is a recent pseudogene. However, the relatively lower success in sequencing of this locus does not appear to affect the general topology of the phylogeny.

Based on the molecular phylogeny, *Cherokia* is a monophyletic taxon (Fig. 4) sister to *Pleurolooma*. There is a clade formed by two individuals from the same locality (Monte Sano State Park, Madison Co., Alabama) that is sister to the remaining ones. Three statistically well-supported clades are present and subtended by long branches; however, the other individuals in the phylogeny are paraphyletic with respect to these clades and are not reciprocally monophyletic with them. In general, individuals from the same locality or nearby localities grouped together. Individuals from Kentucky and Virginia occur together with some individuals from Tennessee in a clade with very short branches. This block of individuals corresponds with the northeastern limit of the geographical range of the genus, and to the Cumberland Mountain Thrust Block region, a mountainous and complex region lying between the dissected Appalachian



**Figure 7.** Scanning electron micrograph of a *Cherokia georgiana* male gonopod. Medial view of specimen MPE04252 (VTEC).

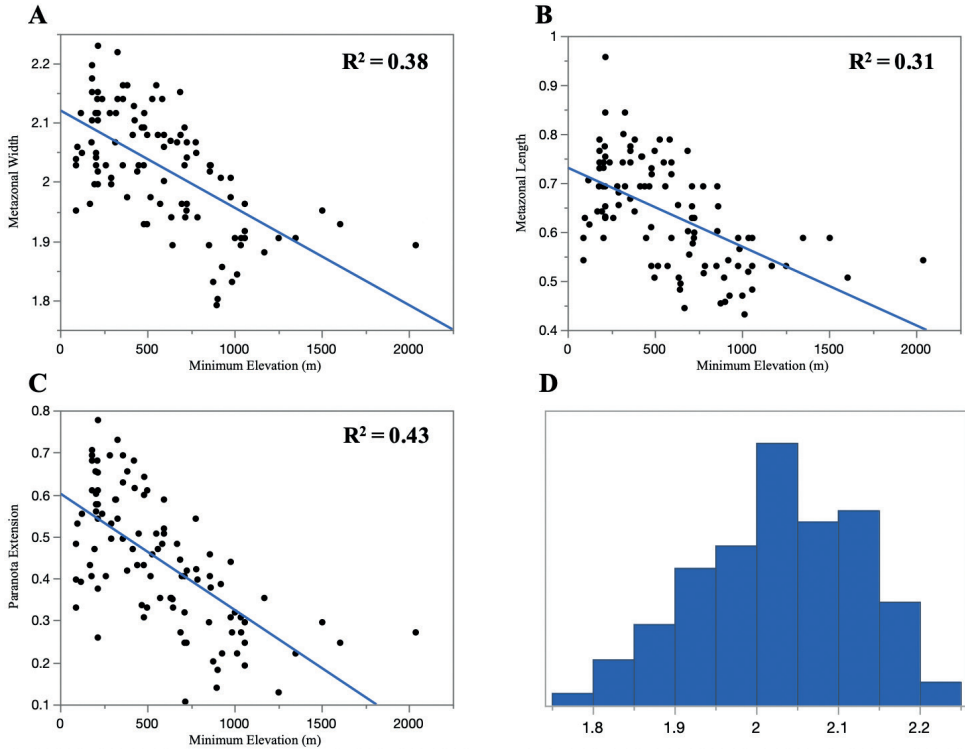


**Figure 8.** Linear regression of the elevation and body measurements **A** metazonal width **B** metazonal length **C** paranota extension and **D** Ln-transformed metazonal width distribution.

Plateau to the west and the Valley and Ridges to the east. This region also houses a clade of millipedes in the genus *Brachoria* Chamberlin, 1939 with similarly very shallow genetic divergences as *Cherokia* (Marek 2010). These shallow branches in *Cherokia*, as in *Brachoria* (Marek 2010), may represent relatively more recent and/or rapid diversification in the area, and may be due to shared mechanisms of regional diversity, or be associated with mimicry evolution in the area. *Cherokia* is a known participant of Müllerian mimicry in the region (Marek and Bond 2009; Marek 2010).

The morphological characters evaluated by Hoffman (1960) were reexamined with new measurements and compared to geographical variables (i.e., elevation) and the phylogeny. The measurements taken from the 12<sup>th</sup> body ring and its inverse linear correlation with elevation showed that, in general, individuals of *Cherokia* with smaller body size and shorter paranota tend to be present at higher elevations than those with a larger size and longer paranota (Fig. 8). While the new measurements showed the same distribution as Hoffman (1960), the variation appears to be clinal, and not discordant variation with abrupt changes that would be expected to correspond to species boundaries. Many terrestrial invertebrate taxa show smaller body sizes at higher eleva-

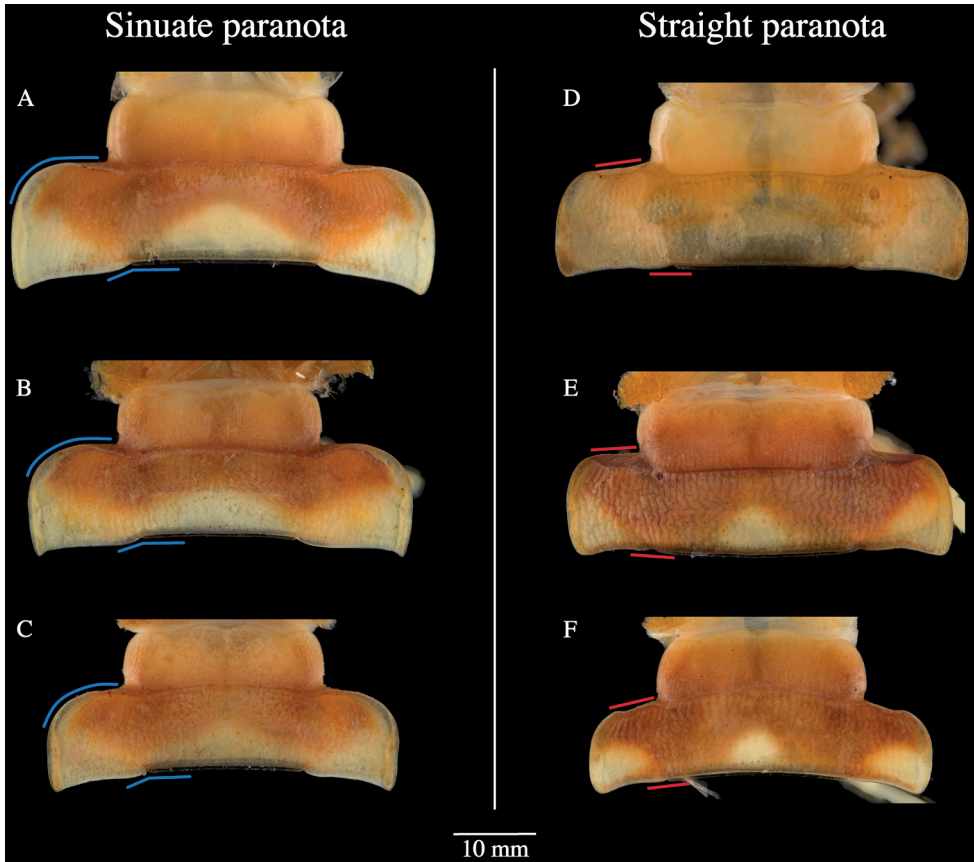


**Figure 9.** Variation in the paranota shape in *Cherokia* Chamberlin, 1949. Images of the 12th body ring of males (VTEC) showing sinuate paranota **A** SPC000060 (AL-MAR) **B** MPE01272 (AL-MAD) **C** MPE01336 (AL-WIN) or straight paranota **D** MPE02360 (GA-FLO) **E** MPE01308 (GA-DAW) **F** MPE01822 (GA-RAB). Blue and red lines denote the differences between the paranota shape.

tions, but the converse has also been observed (Hodkinson 2005). Smaller *Cherokia* at higher elevations may be associated with resource limitation as has been implicated in other terrestrial invertebrate groups (Hodkinson 2005). Alternatively, the smaller body sizes may be associated with body shape differences linked to burrowing efficiency in different leaf-litter substrates at higher elevations (e.g., there is a greater diversity and abundance of evergreen trees at higher elevations).

The results of the ABGD analysis showed a congruent pattern where genetic distances are continuously distributed and no barcode gap exists (Fig. 5A). This shows that there are no clear genetic clusters indicative of a barcode gap for distinct species or subspecies (Fig. 5B). While sampling effort may affect ABGD analyses, our dataset of 106 specimens uniformly sampled from across the distribution of the genus supports the hypothesis of a single, widespread species.

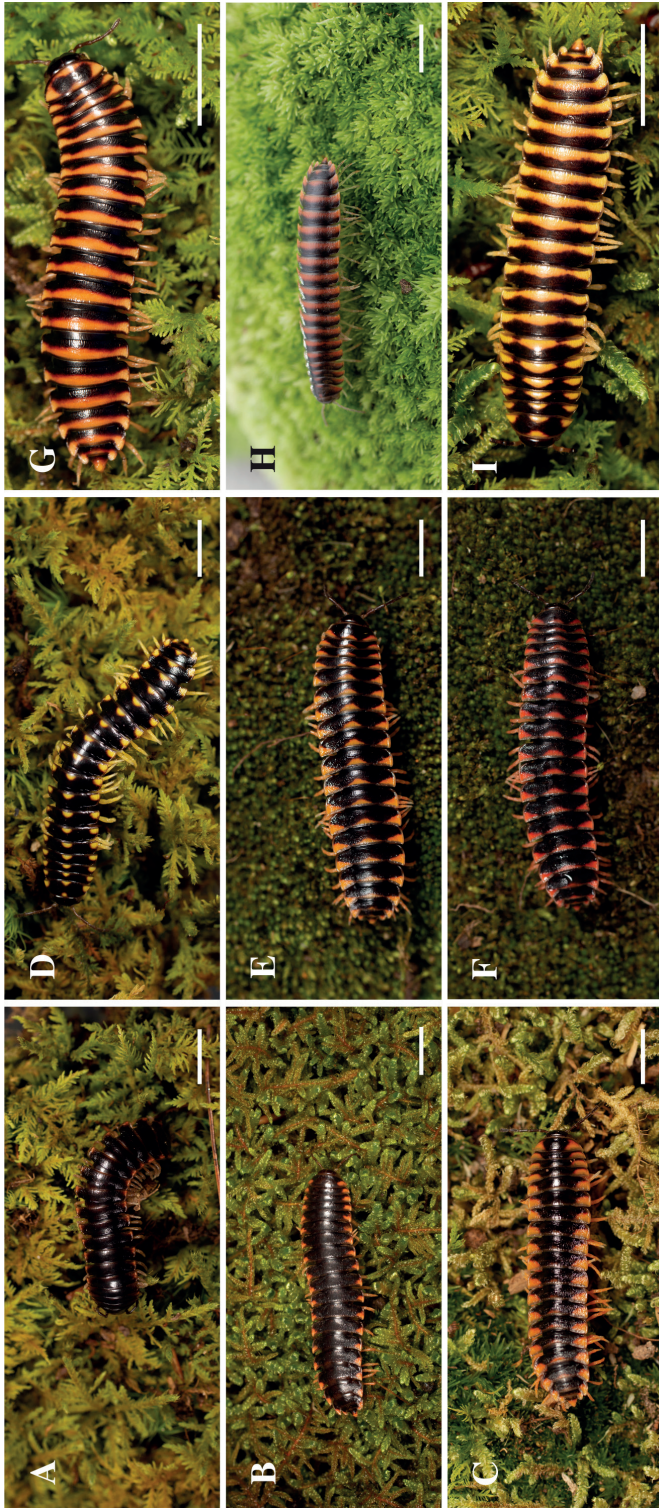


**Figure 10.** Coloration patterns observed in *Cherokia* Chamberlin, 1949. Bimaculate **A** MPE01512 (NC-MAC) **B** MPE04252 (GA-JAC) **C** MPE02181 (TN-MOR), trimaculate **D** MPE01508 (TN-SEV) **E** MPE01225 (TN-VBU) **F** MPE01227 (TN-VBU), and striped **G** MPE00505 (NC-HIG) **H** MPE04515 (SC-OCO) **I** MPE00501 (NC-HIG). All specimens are from the VTEC. Scale bars 10 mm.

The position of the scapulora (sensu Hoffman 1960) was not a useful character, due to the difficulty of distinguishing its two states from each other (marginal and submarginal); perhaps this is due to its continuous nature, as is the case with the body size characters above (Fig. 8). During the examination of this character, we observed that the two states (marginal and submarginal) were not phylogenetically or geographically concordant. As described above (Fig. 9), the anterior margin of the paranota roughly grouped into two distinguishable shapes: sinuate or straight. To evaluate the relevance of this newly discovered character, its geographical distribution was mapped (Fig. 11).

The geographical distribution shows that the individuals with sinuate paranota generally tend to be located in the western part of the Appalachian region, while the individuals with a straight paranota are located in the eastern part. This separation appears to correspond to the Tennessee River Valley and the geological barrier that it represents for the genus, and other co-distributed taxa (e.g. *Nannaria wilsoni* species group; Hennen et al. 2022). However, in the southern part of the geographical distribution of *Cherokia*, especially in the state of Alabama, both shapes of the paranota overlap and no clear geographical separation was observed (Fig. 11). When this character was traced on the phylogeny of the genus, most individuals in one clade exhibited straight paranota (Fig. 4, blue), while the other clade (and two individuals from Monte Sano State Park, Alabama) possessed sinuate paranota (Fig. 4, red). One individual in the phylogeny and geographical distribution appears as an outlier for the general trend of this character (Fig. 4, GA-FLO-MPE03260\*). Although a qualitative character and correlated with metazonite width ( $p = 0.0001$ ), in some cases it is difficult to distinguish straight versus sinuate, and the variation appears to be clinal. In contrast with the scapulora and color characteristics, this character is largely concordant with the phylogeny, but in itself as a single character, insufficient for species or subspecies delimitation.

The coloration patterns were plotted on a map to assess concordance with the geographical distribution. Fig. 12 shows the distribution of the patterns (bimaculate, trimaculate, or striped), and the colors (red, orange or yellow). Some localities have all three types of patterns and/or colors—in contrast with Hoffman's (1960) supposition that each coloration is geographically isolated. Nearly all possible combinations of colors and patterns were observed, but the trimaculate yellow color morph was the most common (both in frequency of individuals and geographical area). The bimaculate pattern was only observed with an orange hue (the bimaculate orange color morph, Fig. 10A–C). Fig. 12 shows that neither the pattern (bimaculate, trimaculate, striped) nor the colors (red, orange, yellow), have any clear geographical association. [Note that the number of geographical data points that were used for these maps (Fig. 11) were greater ( $N = 124$ ) than the one used for the phylogenetic analysis ( $N = 106$ ). Because the number of images available for the specimens actually used in the phylogeny was relatively small ( $N = 26$ ) and limited the scope of inference, iNaturalist reports for *Cherokia* were also included in this section.] Perception of color can be affected by the observer, lighting conditions, veiling conditions, and distance, thereby adding error to

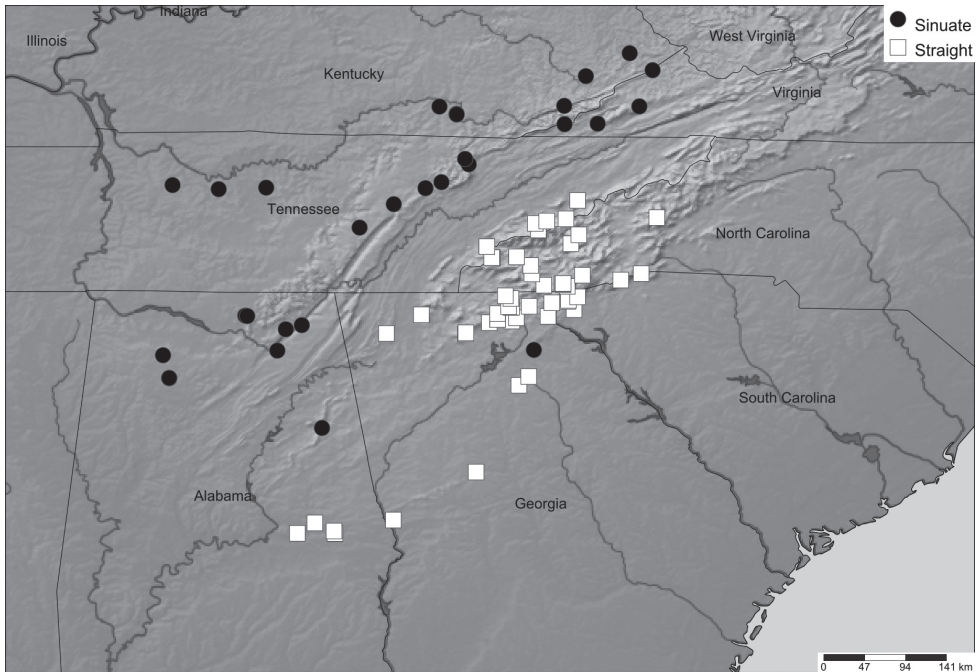


**Figure 11.** Geographical distribution of *Cherokia* Chamberlin, 1949, showing the two types of paranota shape. Map includes specimens used for the morphological analysis and deposited at VTEC ( $N = 105$ ).

the evaluation of this character (Endler 1990). In the future, a less error-prone and less human-centric technique should be implemented to obtain more accurate coloration data such as using a spectrometer and incorporating the visual systems of the predators of *Cherokia* (likely avian) to evaluate the coloration according to the perceivers' eyes.

The use of citizen science as a tool for obtaining and analyzing data has been successfully demonstrated by various research groups. The Cornell Lab of Ornithology, for example, has developed multiple projects involving amateur ornithologists and the general public for around two decades. Data obtained from those initiatives have been published in several peer-reviewed research papers in various journals (Bonney et al. 2009). The small-scale citizen science project that was made as part of this research demonstrated that it is an effective method to obtain samples from remote and inaccessible localities, or in special situations such as the SARS-CoV-2 pandemic. Although the first response to the initiative was highly positive, follow-up contact with the interested participants was more difficult and less successful. The number of people who shipped samples back to us ( $N = 12$ ) corresponds to around the 30% of the kits shipped to selected participants ( $N = 41$ ). Improved communication with the participants, and a more structured timeline will be needed to increase the overall success of this initiative in future projects. Nonetheless the citizen science project offered an impactful opportunity to share the research with a broader community.

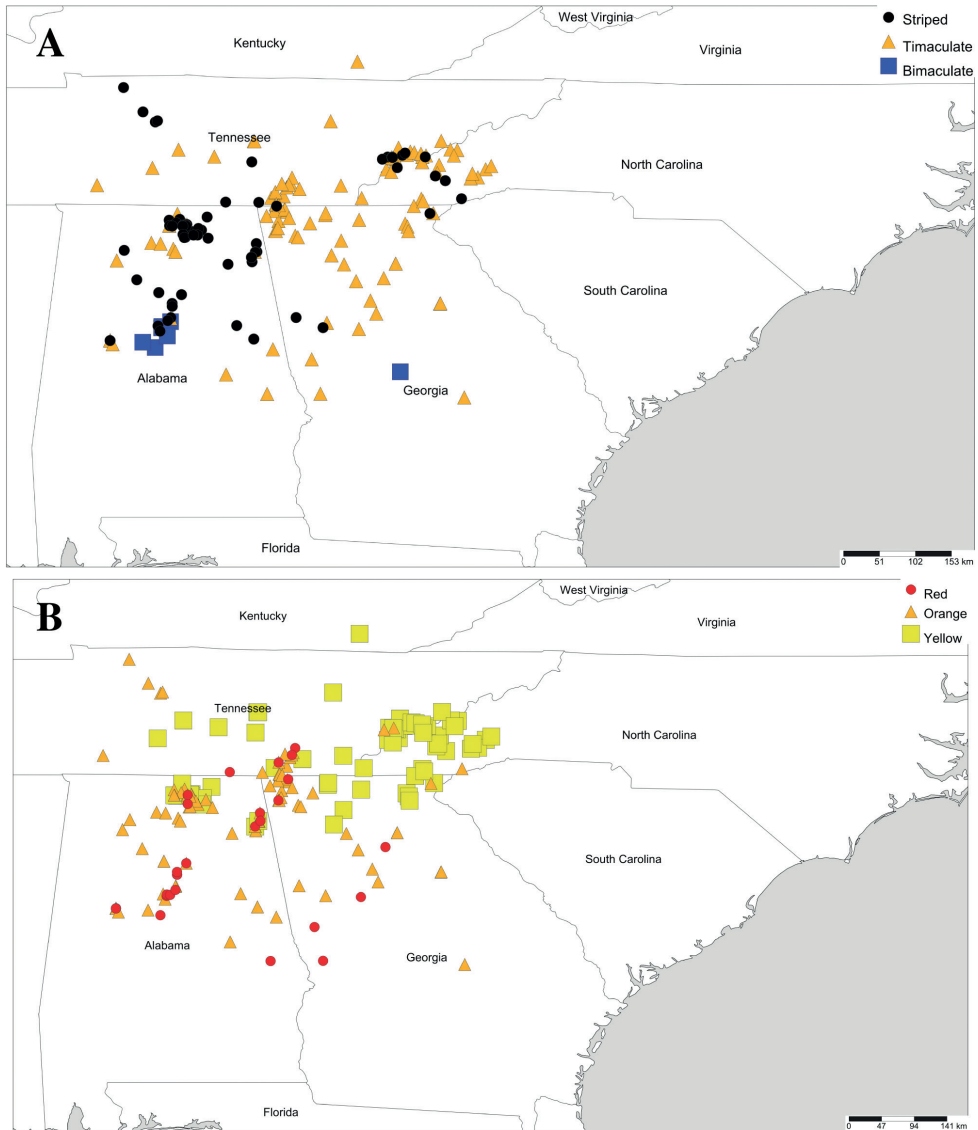


**Figure 12.** Geographical distribution of *Cherokia* Chamberlin, 1949 vs. coloration patterns **A** patterns **B** colors. Mapped using iNaturalist pictures reported for *Cherokia* ( $N = 124$ ).

## Conclusions

Morphological characters showed clinal variation and a direct relationship with geographical distribution and elevation, but not with the phylogeny. Coloration was highly variable and did not accord with neither geography nor phylogeny. The phylogeny recovered *Cherokia* as a monophyletic taxon, and the ABGD species

delimitation test showed no barcode gap supporting the existence of multiple species. The molecular and morphological evidence showed that *Cherokia* is a monospecific genus with the sole species *Cherokia georgiana* being geographically widespread and highly variable in its morphology.

## Acknowledgements

This research was supported by a National Science Foundation grant to P. Marek (Division of Environmental Biology, Systematics and Biodiversity Sciences # 1916368). Derek Hennen and Jackson Means helped confirm identifications of *Cherokia* observations on iNaturalist. We thank those who provided specimens: Roger Birkhead, Sawyer Birkhead, Chris Eaton, Barbara Graham, Christina Fizer, Sherrie White, Jessica Clay, Tracey Muise and Raegan Rainey. Robin Andrews and Bill Shear served on FVV's thesis committee, and provided suggestions for earlier versions of the manuscript. Nesrine Akkari, Weixin Liu and Dragan Antić were reviewers who provided comments on previous versions of this paper.

## References

- Barkworth M, Brandt B, Dyreson C, Cobb N, Pearse W (2019) Symbiota2: Enabling greater collaboration and flexibility in mobilizing biodiversity data. *Biodiversity Information Science and Standards* 3: e37208. <https://doi.org/10.3897/biss.3.37208>
- Bollman CH (1889) Notes upon some myriapods belonging to the U. S. National Museum. *Proceedings of the United States National Museum* 11(722): 343–350. <https://doi.org/10.5479/si.00963801.11-722.343>
- Bonney R, Cooper CB, Dickinson J, Kelling S, Phillips T, Rosenberg KV, Shirk J (2009) Citizen Science: A Developing Tool for Expanding Science Knowledge and Scientific Literacy. *Bioscience* 59(11): 977–984. <https://doi.org/10.1525/bio.2009.59.11.9>
- Causey NB (1950) A collection of Xystodesmid millipeds from Kentucky and Tennessee. *Entomological News* 61: 5–7.
- Chamberlin RV (1949) A new genus and four new species in the diplopod family Xystodesmidae. *Proceedings of the Biological Society of Washington* 62: 3–6.
- Chamberlin RV, Hoffman RL (1958) Checklist of the Millipeds of North America, 236 pp. <http://repository.si.edu/xmlui/handle/10088/10042> [May 26, 2021]
- Endler JA (1990) On the measurement and classification of colour in studies of animal colour patterns. *Biological Journal of the Linnean Society. Linnean Society of London* 41(4): 315–352. <https://doi.org/10.1111/j.1095-8312.1990.tb00839.x>
- Ewing B, Hillier L, Wendl MC, Green P (1998) Base-calling of automated sequencer traces using phred. I. Accuracy assessment. *Genome Research* 8(3): 175–185. <https://doi.org/10.1101/gr.8.3.175>

- Hennen DA, Means JC, Marek PE (2022) A revision of the *wilsoni* species group in the millipede genus *Nannaria* Chamberlin, 1918 (Diplopoda, Polydesmida, Xystodesmidae). *ZooKeys* 1096: 17–118. <https://doi.org/10.3897/zookeys.1096.73485>
- Hodkinson ID (2005) Terrestrial insects along elevation gradients: Species and community responses to altitude. *Biological Reviews of the Cambridge Philosophical Society* 80(3): 489–513. <https://doi.org/10.1017/S1464793105006767>
- Hoffman RL (1950) Records and descriptions of diplopods from the Southern Appalachians. *Journal of the Elisha Mitchell Scientific Society* 66: 11–33.
- Hoffman RL (1960) Revision of the Millipede Genus *Cherokia* (Polydesmida: Xystodesmidae). *Proceedings of the United States National Museum* 112(3436): 227–264 <http://repository.si.edu/xmlui/handle/10088/16695> (May 26, 2021).
- Hoffman RL (1978) A new genus and species of Rhysodesmine millipede from southern Georgia (Polydesmida: Xystodesmidae). *Proceedings of the Biological Society of Washington (USA)* 91: 365–373.
- Kalyaanamoorthy S, Minh BQ, Wong TKF, von Haeseler A, Jermiin LS (2017) ModelFinder: Fast model selection for accurate phylogenetic estimates. *Nature Methods* 14(6): 587–589. <https://doi.org/10.1038/nmeth.4285>
- Katoh K, Standley DM (2013) MAFFT Multiple Sequence Alignment Software Version 7: Improvements in Performance and Usability. *Molecular Biology and Evolution* 30(4): 772–780. <https://doi.org/10.1093/molbev/mst010>
- Loomis HF (1943) New cave and epigeal millipedes of the United States, with notes on established species. *Bulletin of the Museum of Comparative Zoology* 92: 373–410.
- Maddison WP, Maddison DR (2019) Mesquite: A modular system for evolutionary analysis. Version 3.61. <http://www.mesquiteproject.org>
- Maddison DR, Maddison WP (2020) Chromaseq: a Mesquite package for analyzing sequence chromatograms. Version 1.52. <http://chromaseq.mesquiteproject.org>
- Marek PE (2010) A revision of the Appalachian millipede genus *Brachoria* Chamberlin, 1939 (Polydesmida: Xystodesmidae: Apheloriini). *Zoological Journal of the Linnean Society* 159(4): 817–889. <https://doi.org/10.1111/j.1096-3642.2010.00633.x>
- Marek PE, Bond JE (2009) A Müllerian mimicry ring in Appalachian millipedes. *Proceedings of the National Academy of Sciences of the United States of America* 106(24): 9755–9760. <https://doi.org/10.1073/pnas.0810408106>
- Marek PE, Tanabe T, Sierwald P (2014) A species catalog of the millipede family Xystodesmidae (Diplopoda: Polydesmida). *Virginia Museum of Natural History, Special Publication* 17.
- Means JC, Marek PE (2017) Is geography an accurate predictor of evolutionary history in the millipede family Xystodesmidae? *PeerJ* 5: e3854. <https://doi.org/10.7717/peerj.3854>
- Means JC, Francis EA, Lane AA, Marek PE (2015) A general methodology for collecting and preserving xystodesmid and other large millipedes for biodiversity research. *Biodiversity Data Journal* 3: e5665. <https://doi.org/10.3897/BDJ.3.e5665>
- Means JC, Hennen DA, Marek PE (2021a) A revision of the minor species group in the millipede genus *Nannaria* Chamberlin, 1918 (Diplopoda, Polydesmida, Xystodesmidae). *ZooKeys* 1030: 1–180. <https://doi.org/10.3897/zookeys.1030.62544>

- Means JC, Hennen DA, Tanabe T, Marek PE (2021b) Phylogenetic Systematics of the Millipede Family Xystodesmidae. *Insect Systematics and Diversity* 5(2): e1. <https://doi.org/10.1093/isd/ixab003>
- Minh BQ, Schmidt HA, Chernomor O, Schrempf D, Woodhams MD, von Haeseler A, Lanfear R (2020) IQ-TREE 2: New Models and Efficient Methods for Phylogenetic Inference in the Genomic Era. *Molecular Biology and Evolution* 37(5): 1530–1534. <https://doi.org/10.1093/molbev/msaa015>
- Puillandre N, Lambert A, Brouillet S, Achaz G (2012) ABGD, Automatic Barcode Gap Discovery for primary species delimitation. *Molecular Ecology* 21(8): 1864–1877. <https://doi.org/10.1111/j.1365-294X.2011.05239.x>
- Rios NE, Bart HL (2010) GEOLocate Version 3.22. Belle Chasse, LA: Tulane University Museum of Natural History. <https://www.geo-locate.org>
- Shelley RM (1980) Revision of the millipede genus *Pleurolooma* (Polydesmida: Xystodesmidae). *Canadian Journal of Zoology* 58(2): 129–168. <https://doi.org/10.1139/z80-017>
- Shelley RM (2000) Annotated checklist of the millipeds of North Carolina (Arthropoda: Diplopoda), with remarks on the genus *Sigmoria* Chamberlin (Polydesmida: Xystodesmidae). *Journal of the Elisha Mitchell Scientific Society* 116: 177–205.
- Shorthouse DP (2010) SimpleMappr, an online tool to produce publication-quality point maps. <https://www.simplemappr.net> [Accessed April 30, 2021]
- Wieczorek J, Bloom D, Guralnick R, Blum S, Döring M, Giovanni R, Robertson T, Vieglais D (2012) Darwin Core: An Evolving Community-Developed Biodiversity Data Standard. *PLoS ONE* 7(1): e29715. <https://doi.org/10.1371/journal.pone.0029715>

## Supplementary material I

### Specimens used in the phylogenetic analysis

Authors: Luisa Fernanda Vasquez-Valverde, Paul E. Marek

Data type: List of taxa and NCBI accession numbers

Explanation note: List of specimens used in the phylogenetic analysis, with their localities and NCBI accession numbers.

Copyright notice: This dataset is made available under the Open Database License (<http://opendatacommons.org/licenses/odbl/1.0/>). The Open Database License (ODbL) is a license agreement intended to allow users to freely share, modify, and use this Dataset while maintaining this same freedom for others, provided that the original source and author(s) are credited.

Link: <https://doi.org/10.3897/zookeys.1106.81386.suppl1>

## Supplementary material 2

### *Cherokia georgiana* specimens examined

Authors: Luisa Fernanda Vasquez-Valverde, Paul E. Marek

Data type: List of taxa

Explanation note: List of *Cherokia georgiana* specimens examined from literature and natural collections.

Copyright notice: This dataset is made available under the Open Database License (<http://opendatacommons.org/licenses/odbl/1.0/>). The Open Database License (ODbL) is a license agreement intended to allow users to freely share, modify, and use this Dataset while maintaining this same freedom for others, provided that the original source and author(s) are credited.

Link: <https://doi.org/10.3897/zookeys.1106.81386.suppl2>

## Supplementary material 3

### Individual gen trees

Authors: Luisa Fernanda Vasquez-Valverde, Paul E. Marek

Data type: Phylogenetic

Explanation note: Individual gene phylogenies of *Cherokia georgiana*.

Copyright notice: This dataset is made available under the Open Database License (<http://opendatacommons.org/licenses/odbl/1.0/>). The Open Database License (ODbL) is a license agreement intended to allow users to freely share, modify, and use this Dataset while maintaining this same freedom for others, provided that the original source and author(s) are credited.

Link: <https://doi.org/10.3897/zookeys.1106.81386.suppl3>



# Taxonomic reassessment of chaetognaths (Chaetognatha, Sagittoidea, Aphragmophora) from Korean waters

Seohwi Choo<sup>1</sup>, Man-Ki Jeong<sup>2</sup>, Ho Young Soh<sup>1,3</sup>

**1** Big data Fishery Resource Management Interdisciplinary Program, Chonnam University, Yeosu 59626, Republic of Korea **2** Department of Smart Fisheries Resources Management, Chonnam National University, Yeosu 59626, Republic of Korea **3** Department of Ocean Integrated Science, Chonnam National University, Yeosu 59626, Republic of Korea

Corresponding authors: Ho Young Soh ([hysoh@jnu.ac.kr](mailto:hysoh@jnu.ac.kr)), Man-Ki Jeong ([jmgdeux@gmail.com](mailto:jmgdeux@gmail.com))

---

Academic editor: Pavel Stoev | Received 7 January 2022 | Accepted 30 May 2022 | Published 21 June 2022

---

<http://zoobank.org/EFA7EF37-2B83-458D-931D-9A53DB311472>

---

**Citation:** Choo S, Jeong M-K, Soh HY (2022) Taxonomic reassessment of chaetognaths (Chaetognatha, Sagittoidea, Aphragmophora) from Korean waters. ZooKeys 1106: 165–211. <https://doi.org/10.3897/zookeys.1106.80184>

---

## Abstract

Since the first record of chaetognaths (arrow worms) reported from Korean waters by Molchanov in 1907, three families, 12 genera and 21 species have been additionally described. Eighteen of the 21 recorded species have been reported under scientific names different from the latest taxonomic system. This study aimed to address this issue by conducting a taxonomic re-evaluation of chaetognaths collected from Korean waters. Furthermore, the taxonomic usefulness of morphological differences in corona ciliata and distribution of ciliary sense receptors were re-examined using specimens stained with 1% Chlorazol black E (CBE) solution. This study includes taxonomically-validated voucher specimens of 18 species from Korean waters. Based on the specimens, re-description including image data and CBE staining pattern, distribution, ecological information and improved key were provided for each species. However, *Decipisagitta decipiens*, *Serratosagitta serratodentata* and *Sagitta pseudoserratodentata* from Korean waters is still questioned because of the paucity of the voucher specimen and scientific literature.

## Keywords

Arrow worms, chaetognaths, East China Sea, key, staining solution, taxonomy, voucher specimens

## Introduction

The chaetognaths are marine mesoplanktonic carnivores present in most marine habitats and play an important role in the food web of pelagic ecosystems comprising connecting planktonic organisms of higher trophic levels. They have two sets of retractable chitinous grasping spines flanking a ventral mouth. They mostly feed on copepods, cladocerans, amphipods, krill and fish larvae depending on their size and developmental stage (Vega-Pérez 1995; Kruse et al. 2010). Occasionally, they also feed on organic debris (Grigor et al. 2020). These arrow-like creatures are of great ecological value, especially as a major food source for commercial fish, such as sardines and mackerel (Chacko 1949; Park 1970). Chaetognath species are distributed worldwide, including the Pacific, Atlantic, Indian and Antarctic Oceans. They are found in most of the vertical realms spanning from the surface to the bottom of the ocean (Müller et al. 2019; WoRMS 2022). As many species of arrow worm have different distributions depending on water mass, they have been historically used as research subjects to evaluate the marine environment (Russell 1936; Tokioka 1940; Bone et al. 1991; Terazaki 1992; Nagai et al. 2006). Their geographic distribution patterns have been used as important biological indicators to explain environmental physicochemical properties, such as cold current, warm current and oceanic frontal area (Park 1967; Park et al. 1990, 1991, 1992).

The phylum Chaetognatha was first mentioned as “arrow-shaped worms” by Slabber M (1769) and Krohn (1844) reported valuable anatomical features to characterise their internal organisation, nervous system, testes and chitinous cephalic armature. A comprehensive and detailed description of their morphology has been presented by Müller et al. (2019). The foundation of modern systematics of Chaetognatha was established by Ritter-Záhony (1911), who classified 27 species into six genera. Subsequently, the taxonomic categories from family to class were defined by Tokioka (1965a, b), who proposed an advanced classification system. He classified 58 species into two classes, two orders, five families and 15 genera. Of the two classes, Archisagittoidea comprises only fossil species, while Sagittoidea contains all the present chaetognaths existing today. The latter was subdivided into two orders, Phragmophora and Apheragmophora, based on the presence or absence of transversal musculature (i.e. phragms) in the body, respectively. Bieri (1991) proposed a comprehensive classification system for 114 species belonging to 22 genera and eight families. To date, the phylum Chaetognatha includes 133 species allocated to 26 genera and eight valid families (including Heterokrohniidae) (Müller et al. 2019). The taxonomic categories proposed by Tokioka (1965a, b) and Bieri (1991) are still mostly valid (WoRMS 2022), although recent molecular analyses have invalidated Pterosagittidae family (Gasmi et al. 2014; Nair et al. 2015; Müller et al. 2019; Peter et al. 2020).

Despite the long taxonomic history of Chaetognatha and its ecological importance, taxonomic research on Korean species is extremely limited. The first record of chaetognaths in Korean waters was presented by Molchanov (1907). Subsequently, Tokioka (1940) reported the geographical distribution of 13 species of order Apheragmophora. Including these 13 species, Park (1967, 1970, 1973) reported brief taxonomic and ecological features of 19 species. The number of chaetognath species in Korea was finally expanded to 21 by including two species described by Kim (1987).

For the past 20 years, only ecological studies of chaetognaths in Korean waters have been carried out, based on these 21 species as indicators of various water masses and currents near the Korean Peninsula (Park et al. 1990, 1991, 1992; Yoo 1991; Yoo and Kim 1996, 1997; Nagai et al. 2006). The original descriptions and drawings by Park (1970) and Kim (1987) are the only studies available on Korean waters; however, both of them are theses for Doctoral and Master's degrees, respectively, written only in Korean and are yet to be published. Furthermore, because none of the voucher specimens of 21 species used for description by Park (1970) and Kim (1987) are available and the accessible records of five species contain very short descriptions and sketches, it is difficult to confirm their presence in Korean waters. More importantly, these species have been reported under scientific names that are different from the latest taxonomic system. These taxonomic limitations regarding the Korean chaetognath taxa result in misidentification and low reliability of ecological research using indicator species.

Therefore, in this study, we aimed to accomplish the following: 1) to secure the first taxonomically verified voucher specimens of chaetognath from Korean waters and disclose them to public institutions; 2) to create the first comprehensive report of taxonomic features, including morphology, ecology and image information on Korean chaetognath species, based on newly-obtained voucher specimens; and 3) to provide an updated key to species for chaetognath taxa in Korea.

## Materials and methods

### Analysis of previous literature in Korea

To understand the current status of Korean record on chaetognaths, a total of 14 taxonomic and ecological papers published since 1940 to date were investigated (Tokioka 1940, 1951; Park 1967, 1970, 1973; Park et al. 1990, 1991, 1992; Yoo 1991; Yoo and Kim 1996, 1997; Terazaki 1998; Nagai et al. 2006; Lee et al. 2016). The distribution of Korean chaetognath taxa mentioned in literature has been divided into four groups (the East Sea, Korea Strait, northern East China Sea and Yellow Sea) according to the physical characteristics of each sea near Korea (Fig. 1). All the mentioned species in literature (21 species of three genera, most belong to genus *Sagitta*) belong to order Aphragmophora, of which, three families, 12 genera and 21 species have been identified according to the traditional taxonomy conventions (Table 1). We performed a taxonomical comparative analysis of descriptions in previous literature and the newly-obtained specimens from Korean waters to confirm the existence of the 21 mentioned species in Korea, which were recorded in literature without voucher specimens.

### Morphological examination

Field surveys were conducted at 20 stations in Korean waters from May 2019 to August 2020. Zooplankton collection was carried out from the bottom layer to the surface layer using a conical net (diameter: 0.6 m, mesh size: 200  $\mu\text{m}$ ) and MOCNESS

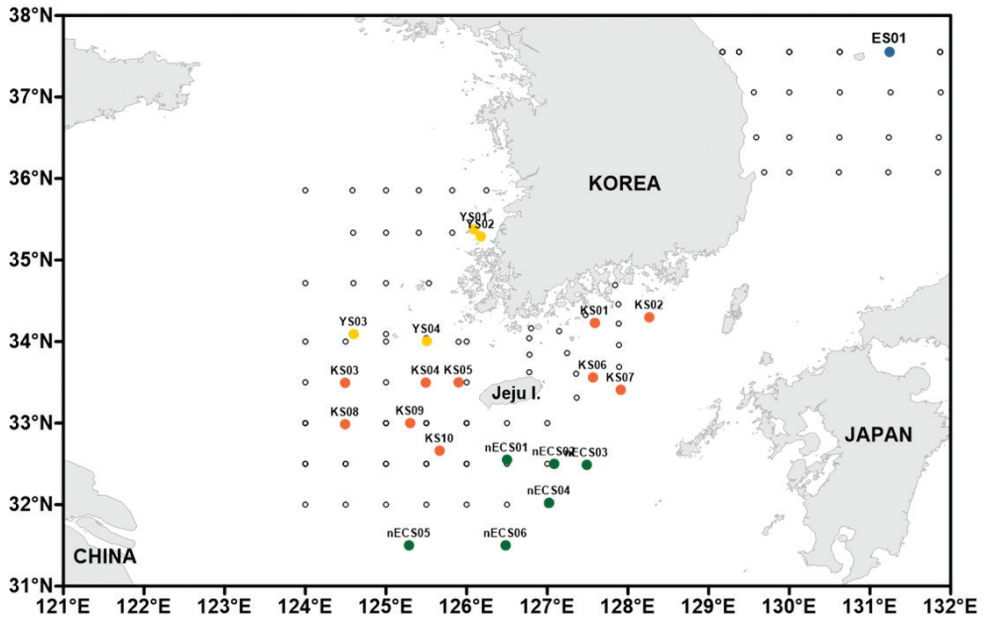


**Figure 1.** Sampling stations in Korean waters. Empty circles, sampling stations; filled circles, the stations where the chaetognaths were secured.

(area of mouth: 1 m<sup>2</sup>, mesh size: 200 μm). Samples were fixed with 5% formalin and the morphological features were observed using a stereo-optical microscope (DS-Fi3, Nikon, Japan). Furthermore, chaetognath specimens were identified at the species level by referring to the taxonomic terms suggested by Kapp (1991) and adults were isolated from the identified specimens according to Alvारीño (1967). The quantitative and qualitative characteristics, based on Gasmi et al. (2014) (Table 2), were photographed using an optical light microscope equipped with a camera (DS-Fi3, Nikon, Japan) and analysed using the in-built software (NIS-Elements BR, version: 5.11.00, Nikon, Japan). Any features that were difficult to observe under the light microscope (including shape and location of corona ciliata rings, structure of fins and morphological patterns on the body surface) were confirmed by staining with Chlorazol black E (CBE) solution (1% in 95% ethanol and diluted in 3:7 ratio with distilled water prior to staining). The CBE pattern has been described as per Müller et al. (2014) (Fig. 2). To supplement the field specimens obtained in this study, 50 samples (eight genera, nine species) stored at the National Institute of Biological Resources (NIBR) were used for taxonomic re-examination. Based on the study by Kapp (1991), the taxonomic terminology and their abbreviations for chaetognath species identification used in this study are as follows: **AN**, anus; **AF**, anterior fin; **AT**, anterior teeth; **CC**, corona ciliata; **CF**, caudal fin; **COL**, collarette; **CL**, caudal length; **EP**, eye pigments; **GS**, grasping spine; **IN**, intestine; **ID**, intestinal diverticula; **LF**, lateral fin; **MO**, mouth; **OL**, ovary length; **O**, ovary; **PF**, posterior fin; **PT**, posterior teeth; **RLZ**, rayless zone; **SV**, seminal vesicle; **TL**, total length; **TM**, transverse muscle; and **VG**, ventral ganglion.

**Table 1.** Korean chaetognath species list reported in previous studies. The species list consists of Tokioka (1940), Tokioka (1951), Park (1967), Park (1970), Park (1973), Park et al. (1990, 1992), Park et al. (1991), Yoo (1991), Yoo and Kim (1996), Terazaki (1998), Yoo and Kim (1997), Nagai et al. (2006). Abbreviation: ES = East Sea; KS = Korea strait; nECS = northern East China Sea; YS = Yellow Sea.

Taxa	ES	KS	nECS	YS	ES, KS, YS and nECS
Class Sagittoidae					
Order Aphragmophora					
Family Krohnittidae					
<b>Genus <i>Krohnitta</i> Ritter-Zahony, 1910</b>					
<i>Krohnitta pacifica</i> (Aida, 1897)	•	•		•	•
<i>Krohnitta subtilis</i> (Grassi, 1881)	•	•			•
Family Pterosagittidae (not valid)					
<b>Genus <i>Pterosagitta</i> Costa, 1869</b>					
<i>Pterosagitta draco</i> (Krohn, 1853)	•	•			•
Family Sagittidae					
<b>Genus <i>Aidanosagitta</i> Tokioka, 1965</b>					
<i>Aidanosagitta crassa</i> (Tokioka, 1938)	•	•	•	•	•
<i>Aidanosagitta neglecta</i> (Aida, 1897)	•	•			•
<i>Aidanosagitta regularis</i> (Aida, 1897)	•	•		•	•
<b>Genus <i>Decipisagitta</i> Tokioka, 1965</b>					
<i>Decipisagitta decipiens</i> (Fowler, 1905)	•	•			•
<b>Genus <i>Ferosagitta</i> Kassatkina, 1971</b>					
<i>Ferosagitta ferox</i> (Doncaster, 1902)	•	•			•
<i>Ferosagitta robusta</i> (Doncaster, 1902)	•	•			•
<b>Genus <i>Flaccisagitta</i> Tokioka, 1965</b>					
<i>Flaccisagitta enflata</i> (Grassi, 1881)	•	•	•	•	•
<i>Flaccisagitta hexaptera</i> (D'Orbigny, 1902)	•	•			•
<b>Genus <i>Mesosagitta</i> Tokioka, 1965</b>					
<i>Mesosagitta minima</i> (Grassi, 1881)	•	•			•
<b>Genus <i>Parasagitta</i> Tokioka, 1965</b>					
<i>Parasagitta elegans</i> (Verrill, 1873)	•	•	•		•
<b>Genus <i>Pseudosagitta</i> Germain &amp; Joubin, 1912</b>					
<i>Pseudosagitta lyra</i> (Krohn, 1853)	•	•			•
<b>Genus <i>Sagitta</i> Guoy &amp; Gaimard, 1827</b>					
<i>Sagitta bipunctata</i> Quoy & Gaimard, 1827	•	•			•
<b>Genus <i>Serratosagitta</i> Tokioka, 1965</b>					
<i>Serratosagitta pacifica</i> (Tokioka, 1940)	•	•		•	•
<i>Serratosagitta pseudoserratodentata</i> (Tokioka, 1940)	•	•			•
<i>Serratosagitta serratodentata</i>	•	•	•		•
<b>Genus <i>Zonosagitta</i> Tokioka, 1827</b>					
<i>Zonosagitta bedoti</i> (Beraneck, 1895)	•	•	•		•
<i>Zonosagitta pulchra</i> (Doncaster, 1902)		•			•
<i>Zonosagitta nagae</i> Alvarino, 1967	•	•		•	•

## Results

### General taxonomical characteristics

The size of the chaetognaths belonging to the order Aphragmophora ranged between 5 and 80 mm. Aphragmophora had no transverse muscles in the body. In general, species diagnosis in Aphragmophora was mostly based on the size and body appearance, the morphology of the intestine, the chitinous cephalic armature (shape and number of grasping spines and teeth) and the shape and position of the corona ciliata, lateral fins and seminal vesicles.



**Figure 2.** Schematic drawing showing the distribution of the ciliary sense organs (modified from Müller et al. 2014) **A** *Ferosagitta robusta* **B** *Pterosagitta draco*. Colour indicated dorsomedian line (red); dorsolateral line (green); lateral line (blue); receptors on the lateral fin (purple); anterolateral receptors on the tail fin (yellow); posterior receptors on the tail fin (orange).

**Table 2.** Quantitative and qualitative characters of the chaetognaths used in this study (modified after Gasami et al. 2014).

Quantitative characters		Qualitative characters
C1	Transverse muscles (absent/ present)	Q1 Total length (min/max)
C2	Body firmness (flaccid/ rigid)	Q2 Body/ tail ratio
C3	Body transparency (transparent, opaque, translucent)	Q3 Number of anterior teeth
C4	Collarette (absent/ present)	Q4 Number of posterior teeth
C5	Number of lateral fins (one pair/ two pairs)	Q5 Number of hooks (min/max)
C6	Fin positions. Anterior fins can be present on anterior part of ventral ganglion, middle of ventral ganglion, end of ventral ganglion, long distance behind the end of the ventral ganglion.	
C7	Comparison of anterior fins and posterior fins size	
C8	Rayless zone in the lateral fins (absent/ present)	
C9	Intestinal diverticula (absent/ present)	
C10	Type of hooks (gently curved/ gently curved and serrated/ abruptly curved)	
C11	Type of seminal vesicle (elongated, oval, spherical, conical)	
C12	Positions of seminal vesicle	
C13	Type of eye pigment (E, T, star, H, +, B shaped)	
C14	Type of corona ciliata (following Tokioka (1965))	
C15	Type of teeth row	
C16	Number of teeth row (only anterior row/ only posterior row/ presented both anterior and posterior)	

## Transparency of the body

The transparency of the body is related to the development of longitudinal muscles in the trunk and tail and is a distinguishing characteristic at the generic level (Bieri 1991). However, the criteria for classifying the transparency of the body were not clear in previous studies. In this study, body transparency was classified into three types: first, the transparent type, which has weak and flexible muscles; second, the translucent type, where the internal organs can be observed from the dorsal side (e.g. digestive apparatus and ovaries), but the ventral ganglion is not visible; and third, the opaque type with strong, rigid muscles, with internal organs and ventral ganglion being invisible from the dorsal side. Representative genera of these categories were *Flaccisagitta* (Fig. 3A), *Pterosagitta* (Fig. 3B) and *Aidanosagitta* (Fig. 3C), respectively.

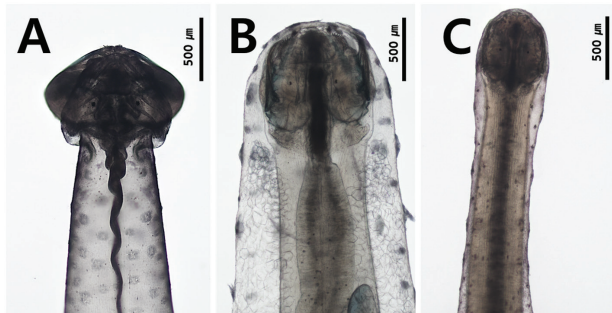


**Figure 3.** Appearance of body **A** transparent and flaccid body (*Flaccisagitta enflata*) **B** translucent body (*Pterosagitta draco*) **C** opaque and rigid body (*Aidanosagitta crassa*).

## Fins

The fins are used for floating and balancing (Hyman 1959). The parts of the body between the fins and the distribution of the fins on the body are morphological features of all the species (Duvert and Salat 1990); however, each species has its characteristic fin size and position. Although fins are easily damaged during the collection and fixation process, they are conspicuous characteristics of chaetognaths. They are located on the lateral and terminal parts of the body and their size, location and starting point are key characteristics. In this study, the number of fins was used as a feature to distinguish families; specimens with one pair of fins on the lateral sides of the body belonged to the families Krohnittidae and genus *Pterosagitta* and those with two pairs of fins belonged to families Sagittidae (Fig. 4A–C).

Another diagnostic character at the genus and species level is the presence of a rayless zone in the lateral fins. For example, *Zonosagitta* has a long rayless zone on the anterior fins, but *Aidanosagitta* does not have a rayless zone on either anterior or posterior fins (Fig. 5A, B). The starting and ending points of the fins are also important taxonomic features. In general, the anterior fins begin at the anterior, middle or tip of the ventral ganglion. For instance, the anterior fins of *Pseudosagitta* and *Zonosagitta* begin at the anterior position to the ventral ganglion, while those of *Ferosagitta* and *Aidanosagitta* reach the ventral ganglion. On the contrary, the anterior fins of *Flaccisagitta* are located on the posterior part of the body far from the ventral ganglion.

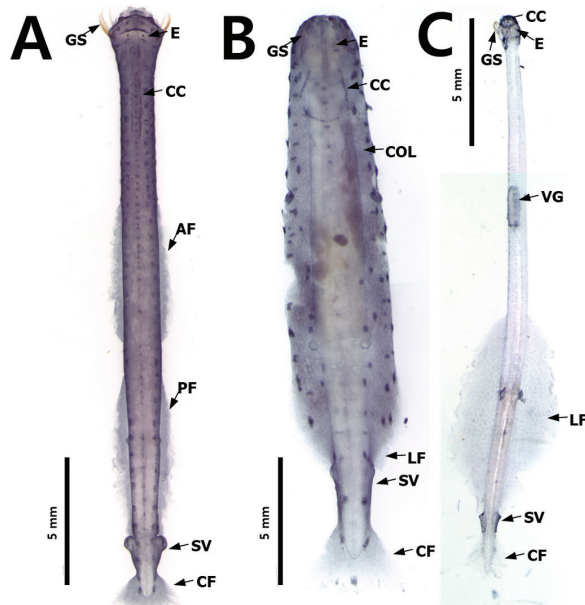


**Figure 4.** Three families inhabiting Korean waters **A** *Ferosagitta robusta* (Sagittidae) **B** *Pterosagitta draco*; **C** *Krohnitta subtilis* (Krohnittidae). Abbreviations: AF = anterior fin; CC = corona ciliata; COL = collette; CF = caudal fin; E = eye; GS = grasping spine; LF = lateral fin; PF = posterior fin; SV = seminal vesicle; VG = ventral ganglion.

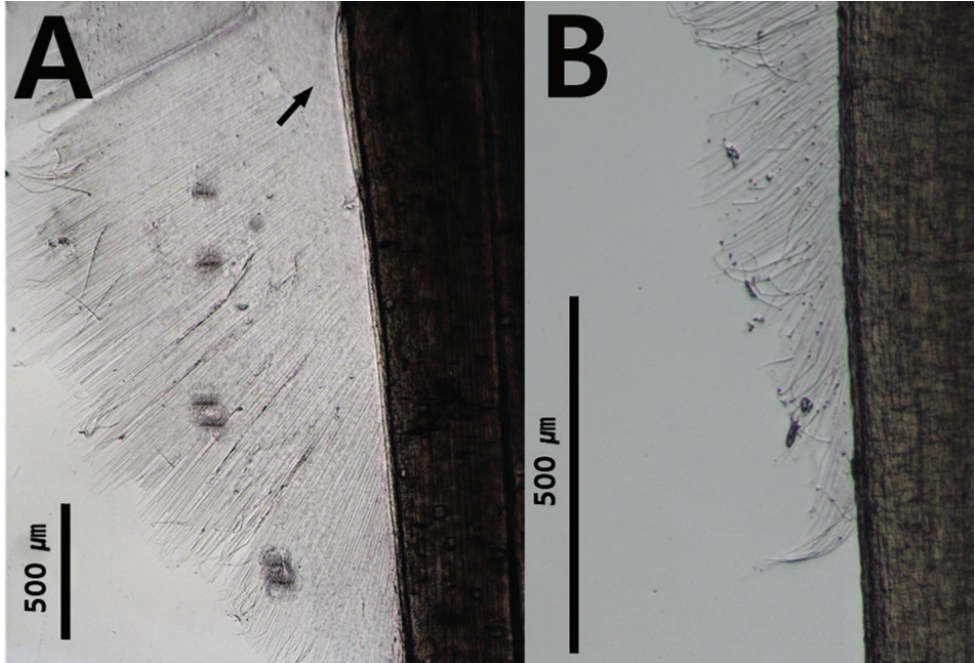


**Figure 5.** Presence and absence of rayless zone on lateral fins **A** black arrow shows rayless zone on posterior fin (*Zonosagitta naga*) **B** completely rayed fin (*Aidanosagitta crassa*).

### Seminal vesicles

All chaetognaths are hermaphroditic and have both female and male organs. In particular, the shape and location of seminal vesicles are distinct in different species. Seminal vesicles can be elongated along the lateral side of the tail (Fig. 6A) or have a pear, spherical or conical shape (Fig. 6B–E). *Serratosagitta pacifica* has a distinct elongated knob with lateral protuberances. The chaetognath species can also be classified according to the location of seminal vesicles between the end of the posterior lateral fin and the caudal fin. The species can be classified, based on the vesicles that touch both posterior and caudal fins (Fig. 6A, D), those close to one of the two fins (Fig. 6B, E, F) and those well-separated from the two fins (Fig. 6C).

### Intestinal diverticula

The digestive apparatus of the chaetognath is in a single line from the mouth to the anus located just anterior to the posterior septum; the intestine extends in the trunk, but is not present in the tail. Classification can be done, based on the presence or absence of two intestinal diverticula located in the most anterior part of the intestine. They are clearly observed in the genera *Aidanosagitta* (Fig. 7A) and *Ferosagitta* (Fig. 7B), but not in *Pterosagitta* (Fig. 3B) and *Zonosagitta* (Fig. 7C, D).

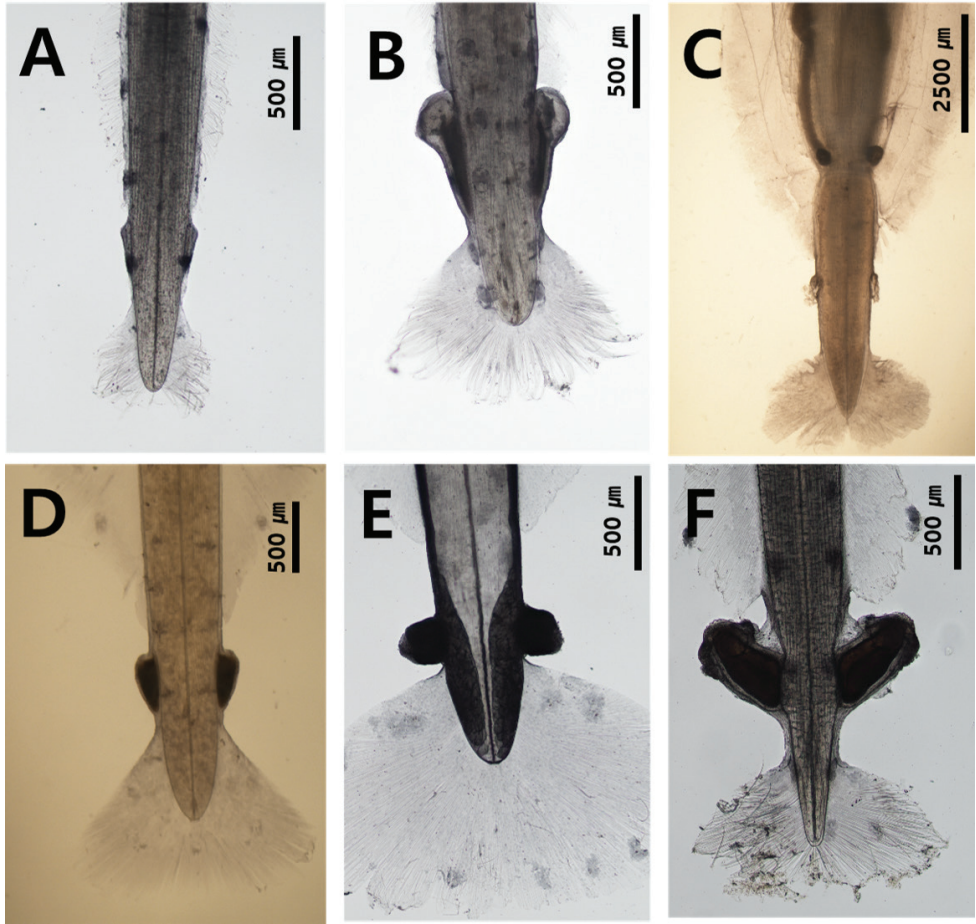


**Figure 6.** Shape and position of seminal vesicles **A** *Aidanosagitta regularis* (elongated) **B** *Ferosagitta robusta* (pear shape) **C** *Pseudosagitta lyra* (spherical shape) **D** *Zonosagitta nagae* (conical shape) **E** *Flaccisagitta enflata* (spherical shape) **F** *Serratosagitta pacifica* (seminal shape with chitinous teeth).



**Figure 7.** Intestinal diverticular (shown by white arrow) **A** *Aidanosagitta regularis* (present) **B** *Ferosagitta robusta* (present) **C** *Zonosagitta nagae* (absent) **D** *Zonosagitta bedoti* (absent).

## Grasping spines

The grasping spines are laterally attached to the head of chaetognaths and are used for capturing and swallowing prey. The grasping spines of the family Krohnittidae are sharply curved, while those of Sagittidae are gently curved (Fig. 8A–C; Tokioka 1965a). The grasping spines of the genus *Serratosagitta* belonging to Sagittidae are serrated (Fig. 8C; Tokioka and Pathansali 1963).

## Anterior and posterior teeth

The number of teeth rows is an important key to distinguish families (Tokioka 1965 a, b). Sagittidae (including *Pterosagitta draco*) has two rows of teeth arranged in a comb shape (Fig. 9A), while Krohnittidae has only one row of anterior teeth arranged in a fan shape (Fig. 9B).

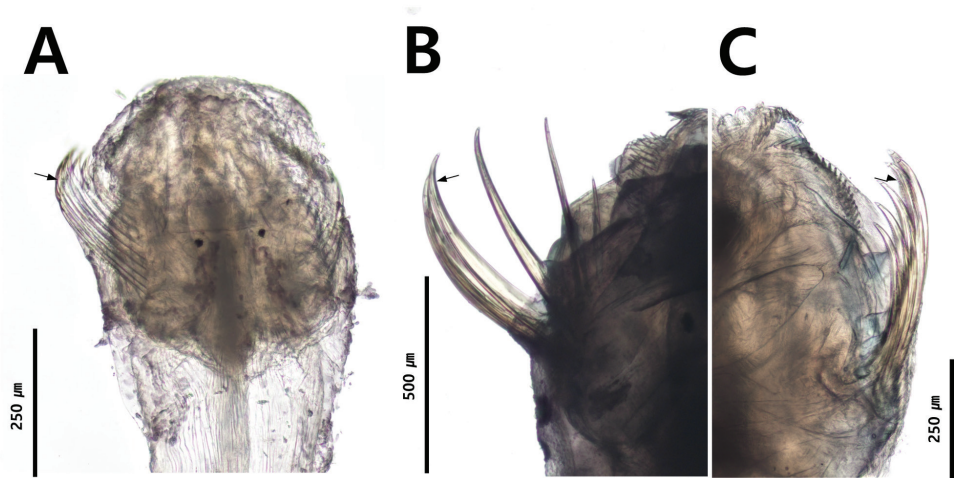


**Figure 8.** Grasping spine **A** abruptly curved hooks (*Krohnitta subtilis*, Krohnittidae) **B** gently curved and not serrated hooks (*Ferosagitta robusta*, Sagittidae) **C** gently curved and serrated hooks (*Serratosagitta pacifica*, Sagittidae).

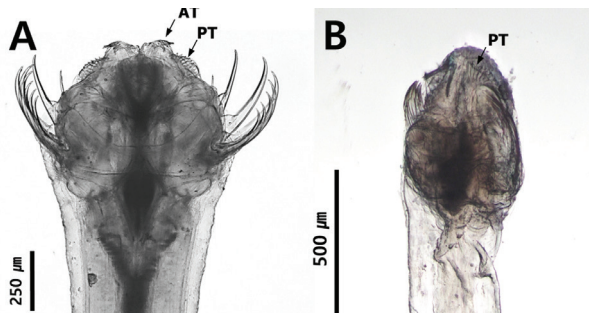


**Figure 9.** Number and shape of dentition **A** *Ferosagitta robusta* (two rows) **B** *Krohnitta subtilis* (one row).

**Corona ciliata**

The corona ciliata is related to the sensory organs, presumably involved in chemoreception (Bleich et al. 2017) and is observed on the dorsal side of the specimen (Kapp 1991). It begins behind the eyes in *Aidanosagitta regularis* and *Pterosagitta draco* (Fig. 10A, B) or in front of the eyes in *Serratosagitta pacifica* and *Flaccisagitta enflata* (Fig. 10C, D). The corona ciliata may also extend behind the neck, a short distance in the anterior trunk region (Fig. 10A, C) or does not exceed the head (Fig. 10D).



**Figure 10.** Position and shape of corona ciliata **A** *Aidanosagitta regularis* **B** *Pterosagitta draco* **C** *Serratosagitta pacifica* **D** *Flaccisagitta enflata*.

**Systematics**

**Order Aphragmophora Tokioka, 1965a**

**Diagnosis.** Ventral transverse musculature absent, less glandular structures on body surface. Grasping spines gently or abruptly curved (Tokioka 1965a). Collarette absent, present or small that is almost absent. Intestinal diverticula absent or present. One or two rows of teeth, teeth-rows arranged in comb or fan shape. One paired or two paired lateral fins with or without rayless zone (Alvariño 1967).

**Key to family of Aphragmophora**

- 1 One pair of lateral fins ..... 2
- Two pairs of lateral fins ..... 4
- 2 One row of teeth, collarette absent..... **Krohnittidae (present in Korea)**
- Two rows of teeth ..... 3

- 3 One pair of lateral fins on the tail, Collarette remarkably thick .....  
 ..... *Pterosagitta draco* (present in Korea)  
 – One pair of lateral fins on the trunk..... *Pterokrohniidae*  
 4 Two rows of teeth, neck contraction ..... *Bathybelidae*  
 – Two rows of teeth ..... *Sagittidae* (present in Korea)

### Family Krohnittidae Tokioka, 1965

**Diagnosis.** Small head. Grasping spines abruptly curved. One row of teeth. Collarette either short or absent. One pair of lateral fins arranged on the posterior trunk and tail.

### Genus *Krohnitta* Ritter-Záhony, 1910

**Diagnosis.** Slender and transparent body. Lateral fins on the body and tail with rayless zone or partially rayed. Intestinal diverticula absent. Seminal vesicles oval or elongated touching both lateral fins and caudal fins.

### Key to species of *Krohnitta*

- 1 One pair of fins with rayless zone. Seminal vesicles oval shaped and elongated, touching both paired fins and caudal fins..... *K. subtilis*  
 – One pair of rayed fins. Seminal vesicles oval shaped and placed dorsally at the point where lateral fins meet caudal fins..... *K. pacifica*

### *Krohnitta subtilis* (Grassi, 1881)

Figs 3C, 4C, 8A, 9B, 11A–D

*Spadella subtilis*: Grassi, 1883: 16 p., table 1.

*Krohnia subtilis*: Fowler, 1906: 25–26 p., figs 86–88; Michael 1908: 269–270 p.

*Krohnitta subtilis*: Burfield & Harvey, 1926: 117 p., figs 45–50.; Thomson 1947: 22 p.; Tokioka 1965: 352–353 p.; Alvarino 1967: 18–20 p., fig. 9 A–D; Srinivasan 1979: 37–39 p., fig. 21 A–D; Michel 1984: 30 p., fig. 41; McLelland 1989: 158 p., fig. 5A–D; Park et al. 1990: 74–76 p., fig. 52.; Nair et al. 2008: 210 p., table 1.

**Material examined.** Korea Strait (33°30.000'N, 125°54.000'E), 0–90 m depth, oblique towing with conical net, Feb 2020, NIBRIV0000895313 (one specimen); northern East China Sea (33°00.000'N, 127°4.098'E), 0–110 m depth, oblique towing with conical net, Feb 2020, NIBRIV0000895312 (one specimen).

**Description.** Total body length ranged between 10.8 and 11.5 mm and tail 27.3–33.7% of body length. Hooks 8–10. Anterior teeth 14. Slender and transparent body

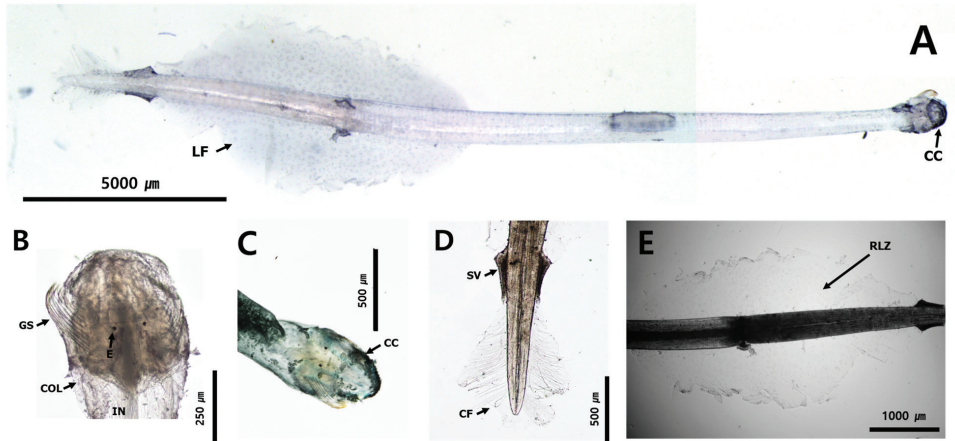


**Figure 11.** **A** *Krohnitta subtilis* (dorsal view) **B** head **C** tail **D** lateral fin. Abbreviations: CC = corona ciliata; CF = caudal fin; COL = collarette; E = eye; GS = grasping spine; IN = intestine; LF = lateral fin; RLZ = Ray less zone; SV = seminal vesicle.

(Fig. 11A). Small head. One row of stout teeth arranged in fan shape (Fig. 9B). Collarette and intestinal diverticula absent (Fig. 11B). Grasping spine abruptly curved (Fig. 8A). Round eyes with eye pigments in “E” shape (Fig. 11B). Corona ciliata beginning in front of eyes with round shape (Fig. 11C). Lateral fins 29.4% of body length. Starting points of lateral fins 54.3% and ending points of lateral fins 82.2% of body length, respectively. One pair of lateral fins only rayed on outer edge, with forward ends equidistant from caudal septum (Fig. 11A, E). Caudal fin roughly round in shape (Fig. 11D). Seminal vesicles elongated with anterolateral-edge-opening touching both lateral fins and caudal fin (Fig. 11D).

**Distribution.** This species is found in the epipelagic (0–200 m depth) and mesopelagic zones (200–500 m depth) of the Pacific, Indian and Atlantic Oceans (Pierrot-Bults and Nair 1991), the Indian water (George 1952) and the Tosa Bay in Japan (Ohnishi et al. 2014), while in this study, it was found in the epipelagic zone (0–110 m depth) of the Korea Strait and northern East China Sea (Fig. 1: stations KS05 and nECS04).

**Ecology.** This cosmopolitan species can be found in tropical to temperate waters (Alvariño 1967). The temperature ranged between 16.40 and 16.41 °C and salinity was 34.58 psu at the sampling stations of this study.

**Remarks.** This species is clearly distinguished from *K. pacifica* by the presence of a rayless zone in the lateral fin. Furthermore, the presence of a pair of lateral fins with a wide rayless zone and a fan-shaped dentition in *K. subtilis* collected from Korean waters are consistent with the records of Alvariño (1967) and Bieri (1991). However, the location of the corona ciliata (in front of the eyes, Fig 11C) of the species found in Korean waters was different from that of the previous records (located behind the eye). No specific pattern was observed through CBE staining on the body surface.

***Krohnitta pacifica* (Aida, 1897)**

*Krohnitta pacifica*: Tokioka, 1965: 352–353 p.; Alvariño 1967: 15–17 p., fig. 7A–E; Michel 1984: 29 p., fig. 40; Kim 1987: 35–36 p., plate 13; Park et al. 1990: 73 p., fig. 51.

**Material examined.** Northern East China Sea (32°29.420'N, 127°29.654' E), 20–100 m depth, oblique towing with MOCNESS, Aug 2020 (one specimen).

**Description.** Slender and transparent body. Small head. Grasping spines abruptly curved. One row of stout teeth arranged in fan shape. One pair of lateral fins partially rayed, forward and equidistant from caudal septum. Lateral fins positioned at anterior end, at level of caudal septum with rayed lateral fins. Caudal fin damaged. Collarette and intestinal diverticula absent. No seminal vesicle visible.

**Distribution.** This species is found in the epipelagic zone (0–200 m depth) of the northern Indian Ocean (Pierrot-Bults and Nair 1991), the Gulf of Mexico (Pierce 1951) and the Japanese coast (Tosa Bay, Sagami and Suruga) (Nagasawa and Marumo 1972; Ohnishi et al. 2014) and, in this study, it was found in the epipelagic zone (20–100 m depth) of the northern East China Sea (Fig. 1: station nECS03).

**Ecology.** An inhabitant of the surface layer of the warm oceanic waters (Tokioka 1940). Mature specimen was reported to be 6–8 mm in length (Alvariño 1967). The temperature range in the sampling stations of this study was 18.49–28.84 °C and salinity range was 30.71–34.59 psu.

**Remarks.** Only immature individuals could be collected in this study. The specimens of *K. pacifica* we observed had one pair of fins and the structure of the fin was rayed, except for the base part close to the body. These were distinct characteristics of *K. pacifica* that differentiated it from *K. subtilis*. Since seminal vesicles were not observed in all observed Korean specimens, they were classified as immature stage (Alvariño 1967).

**Family Pterosagittidae Tokioka, 1965a**

**Diagnosis.** Wide head. Two rows of teeth. Collarette wide and extending through full body. One pair of rayed lateral fins located on the tail. Intestinal diverticula absent. Only one genus has been described within this family: *Pterosagitta* (Costa, 1869).

**Remarks.** A previous phylogenetic study reported that Pterosagittidae is genetically quite close to Sagittidae (Gasmi et al. 2014; Nair et al. 2015; Peter et al. 2020; Müller et al. 2019). In this study, a recent research paper was reviewed and Pterosagittidae was marked as invalid (Table 1).

**Key to the species of *Pterosagitta***

- 1 One pair of rayed lateral fins on the tail. Collarette extremely thick and extends from head to seminal vesicles. Seminal vesicles oval-shaped and elongated, touching both lateral fins and caudal fin ..... ***P. draco***

***Pterosagitta draco* (Krohn, 1853)**

Figs 3B, 4B, 10B and 12A–D

*Spadella draco*: Grassi, 1883: 15 p.; Beraneck 1895: 154 p.; Aida 1897: 20 p., fig. 12; Doncaster 1902: 214–215 p.

*Pterosagitta draco*: Michael, 1919: 264–265 p., table 18; Thomson 1947: 22–23 p.; Tokioka 1965: 351–352 p.; Alvariño 1967: 21–22 p., fig. 11A–D; Srinivasan 1979: 34–35 p., fig. 19A–E; Michel 1984: 29 p., fig. 5; Kim 1987: 33–34 p., plate 12; Park et al. 1990: 71–73 p., fig. 50.

**Material examined.** Northern East China Sea (32°30.000'N, 127°5.100'E), 0–120 m depth, oblique towing with conical net, Feb 2020, NIBRIV0000895299 (one specimen).

**Description.** Total body length ranged between 6.5 and 9.1 mm and tail 38.4–40.1% of body length. Hooks 8. Anterior teeth 10 and posterior teeth 12. Rigid and translucent body (Fig. 12). Wide and angular head (Fig. 12). Wide collarette extending over entire body and reaching anterior of seminal vesicles (Fig. 12A, C). Rectangular eyes with “T” shaped eye pigments (Fig. 12B). Intestinal diverticula absent (Fig. 3B). Lateral fins 20.7% of body length. Starting point of lateral fins 65.2% and ending points of lateral fins 86.3% of body length, respectively. One pair of lateral fins triangular-shaped and completely rayed, with forward ends at level of caudal septum (Fig. 12A, D). Seminal vesicles posteriorly elongated with anterior knob touching lateral fins (Fig. 12C–D). Eggs reaching middle of body. Corona ciliata anteriorly opened with horseshoe shape beginning in neck region and ending just behind eyes (Figs 10B, 12A).

**Distribution.** This species is located in the epipelagic (0–200 m depth) and mesopelagic zones (200–500 m depth) of the Pacific, Indian and Atlantic Oceans (Pierrot-Bults and Nair 1991), the epipelagic zone (0–200 m depth) of the Caribbean Sea (Michel, 1984), the coastal waters surrounding India (George 1952) and the Tosa Bay in Japan (Ohnishi et al. 2014). In this study, it was found in the epipelagic zone (0–120 m depth) of the northern East China Sea (Fig. 1: station nECS02).

**Ecology.** This species is widely distributed in warm water masses and appears all year round in Korean waters, except in the Yellow Sea (Kim 1987). The temperature range of the Caribbean Sea was reported as 22–29 °C, and salinity range was 33–38 psu (Michel 1984). At the sampling stations of this study, the temperature ranged between 15.83–28.80 °C and salinity ranged between 31.38–34.60 psu.

**Remarks.** The largest specimen collected in this study was 9.1 mm in length, which was at stage 4 maturity. It was smaller than the specimen from New Zealand (16 mm) reported by Lutschinger (1993). It had characteristics consistent with the *Pterosagitta draco* reported from the Pacific (Alvariño 1967; Michel 1984), such as the presence of two rows of teeth, one pair of lateral fins, a corona ciliata located between the back of the eye and the neck and a broad collarette extending from the head to seminal vesicles. We observed one specimen for CBE staining pattern: dorsomedian

line, 8 dots; dorsolateral line, 25 dots; lateral line, 10 dots; receptors on the lateral fin, 2 dots; anterolateral receptors on the caudal fin, 3 dots; posterior receptors on the caudal fin, 6 dots.

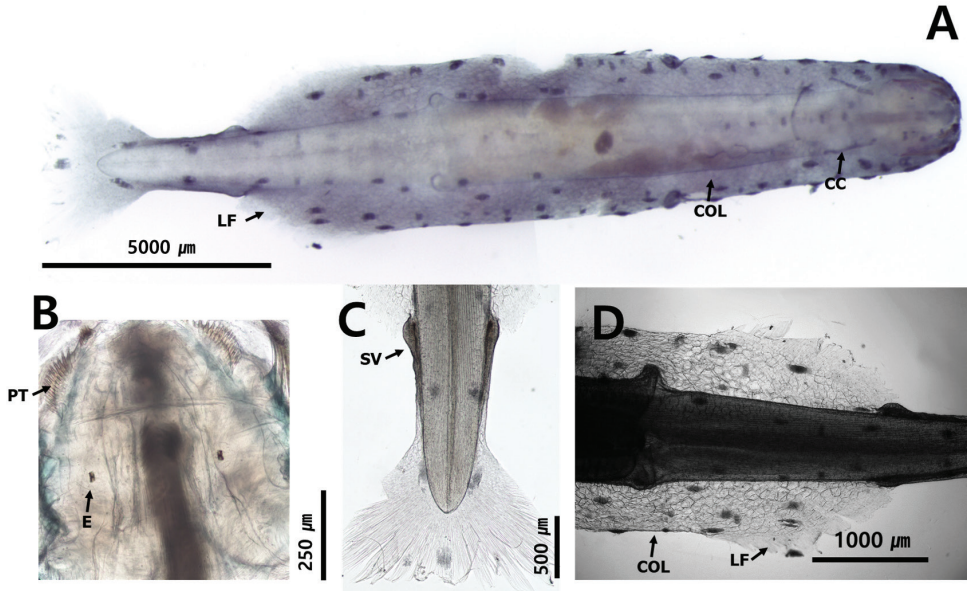


**Figure 12.** **A** *Pterosagitta draco* (dorsal view) **B** head **C** tail **D** lateral fin. Abbreviations: CC = corona ciliata; COL = collarette; E = eye; LF = lateral fin; PT = posterior teeth; SV = seminal vesicle.

**Family Sagittidae (Claus & Grobben, 1905)**

**Diagnosis.** Two rows of stout teeth arranged in comb shape. Two pairs of lateral fins on the trunk and tail.

**Key to genus of Sagittidae**

- 1 Serrated grasping spines ..... *Serratosagitta* (present in Korea)
- Non-serrated grasping spines ..... 2
- 2 Flaccid body ..... 3
- Rigid body ..... 6
- 3 Intestinal diverticula present ..... 4
- Intestinal diverticula absent ..... 5
- 4 Anterior fins beginning at the middle of ventral ganglion, the seminal vesicle closer to lateral fins than caudal fin ..... *Decipisagitta*
- Anterior fins beginning between ventral ganglion and caudal septum, the seminal vesicle well-separated from lateral fins, but touching caudal fins ..... *Mesosagitta* (present in Korea)

- 5 Anterior fins beginning far behind the end of the ventral ganglion.....  
 ..... *Flaccisagitta* (present in Korea)
- Anterior fins beginning at the end of ventral ganglion .....  
 ..... *Pseudosagitta* (present in Korea)
- 6 Intestinal diverticula present .....7
- Intestinal diverticula absent .....9
- 7 Collarette present.....8
- Collarette and rayless zone on lateral fins absent .....  
 ..... *Parasagitta* (present in Korea)
- 8 The head width greater than body width, short collarette, the rayless zone on  
 lateral fins present, the corona ciliata beginning before the eye.....  
 ..... *Ferosagitta* (present in Korea)
- The head width smaller than body width, well-developed collarette, com-  
 pletely rayed lateral fins, the corona ciliata beginning behind the eye .....  
 ..... *Aidanosagitta* (present in Korea)
- 9 Anterior part of lateral fins with rayless zone.....  
 ..... *Zonosagitta* (present in Korea)
- Rayless zone on lateral fins absent ..... *Sagitta* (present in Korea)

### Genus *Serratosagitta* Tokioka & Pathansali, 1963

**Diagnosis.** Intestinal diverticula either absent or present. Grasping spines serrated. Two rows of teeth. Two pairs of lateral fins either with rayless zone or completely rayed.

#### Key to species of *Serratosagitta*

- 1 Intestinal diverticula absent .....2
- Intestinal diverticula present .....3
- 2 Seminal vesicles with forward elongated knob and teeth-like appendages  
 forming 5–10 distal protrusions anteriorly, well-separated from caudal fin  
 but touching posterior fins, the posterior fins and anterior fins of almost same  
 length ..... *S. pacifica*
- Seminal vesicles touching the posterior fins and caudal fin, the posterior fins  
 longer than anterior fins..... *S. serratodentata*
- 3 Seminal vesicles well-separated from caudal fin, but touching posterior fins, pos-  
 terior fins and anterior fins of almost same length ..... *S. pseudoserratodentata*

### *Serratosagitta pacifica* (Tokioka, 1940)

Figs 6F, 8C, 10C, 13A–E

*Sagitta serratodentata pacifica*: Tokioka, 1959: 72–80 p., fig. 10, table 10; Park et al. 1990: 52–54 p. figs 31, 32.

*Sagitta pacifica*: Alvariño, 1961: 71 p., fig. A, B, table 2; Alvariño 1967: 36–39 p., fig. 22A–D; Pierrot-Bults 1974: 221–222 p., fig. 6; Francisco 1977: 226–229 p., plate 1; Srinivasan 1979: 27–29 p., fig. 15A–G; Kim 1987: 18–20 p., plate 3.  
*Serratosagitta pacifica*: Tokioka, 1965: 345–346 p.; Lutschinger 1993: 30–31 p., fig. 15 A–B.

**Material examined.** Korea Strait (33°24.504'N, 127°54.600'E), 0–50 m depth, oblique towing with MOCNESS, May 2019, NIBRIV0000895311 (two specimens); Korea Strait (33°33.600'N, 127°34.002'E), 0–96 m depth, oblique towing with conical net, Feb 2020 (one specimen); northern East China Sea (32°33.000'N, 126°30.000 E), 0–100 m depth, oblique towing with conical net, Feb 2020, NIBRIV0000895310 (three specimens); northern East China Sea (32°00.000'N, 127°4.098'E), 0–120 m depth, oblique towing with conical net, Feb 2020, two specimens.

**Description.** Total body length ranged within 11.8 and 13.7 mm. Tail 23.4–24.9% of body length. Hooks 6–7. Anterior 10–13 and posterior teeth 16–25. Rigid and opaque body (Fig. 13A). Small head (Fig. 13A, B). Grasping spines serrated on edge (Fig. 8C). Collar absent (Fig. 10C, 13A). Rectangular eyes with “T” shaped eye pigments (Fig. 13B). Intestinal diverticula absent (Fig. 10C). Anterior fins spanned 21.9% of body length. Anterior fins completely rayed beginning between ventral ganglion and caudal septum. Starting point of anterior fins 34.6% and ending points of anterior fins 55.1% of body length, respectively (Fig. 13A, D). Posterior fins 26.2% of body length and 1.2 times longer than anterior fins. Starting points of posterior fins 63.7% and ending points of posterior fins 89.7% of body length, respectively. Posterior fins well-separated from anterior fins (Fig. 13A, E). Caudal fin triangular shaped (Fig. 13A, C). Seminal vesicles touched or closed to lateral fins and well-separated from tail fin (Fig. 13C) with elongated knob facing obliquely forward and teeth-like appendages forming 5–10 distal protrusions. Eggs reached anterior of anterior fins. Collar beginning in front of eyes and extended over neck (Fig. 10C, 13A).

**Distribution.** This species is found in the epipelagic (0–200 m depth) and mesopelagic zones (200–500 m depth) of the Pacific and Indian Oceans (Alvariño 1967; Pierrot-Bults and Nair 1991), the epipelagic zone of Red Sea, Californian waters (Pierrot-Bults 1976) and the Tosa Bay in Japan (Ohnishi et al. 2014). In this study, it was distributed in the epipelagic zone (0–50 m depth) of the Korea Strait and northern East China Sea (Fig. 1: stations KS06, KS07, nECS01 and nECS04).

**Ecology.** This species mainly inhabits Indo-pacific warm-water masses (Bieri 1959). In the Pacific Ocean, it is a known indicator species of the Kuroshio Water Mass (Kim 1987). In this study, the temperature range of sampling locations was 16.37–20.57 °C and salinity ranged between 34.48–34.61 psu.

**Remarks.** The seminal vesicles are used as an important morphological feature to identify the genus *Serratosagitta*. *S. serratodentata* has thick collar tissue in front of the seminal vesicles and two projections at the anterior-lateral corner. The seminal vesicles touch the end of posterior fins (Alvariño 1961). The seminal vesicles of *S. pseudoserratodentata* have one projection at the front corner, with small teeth at the anterior end. The seminal

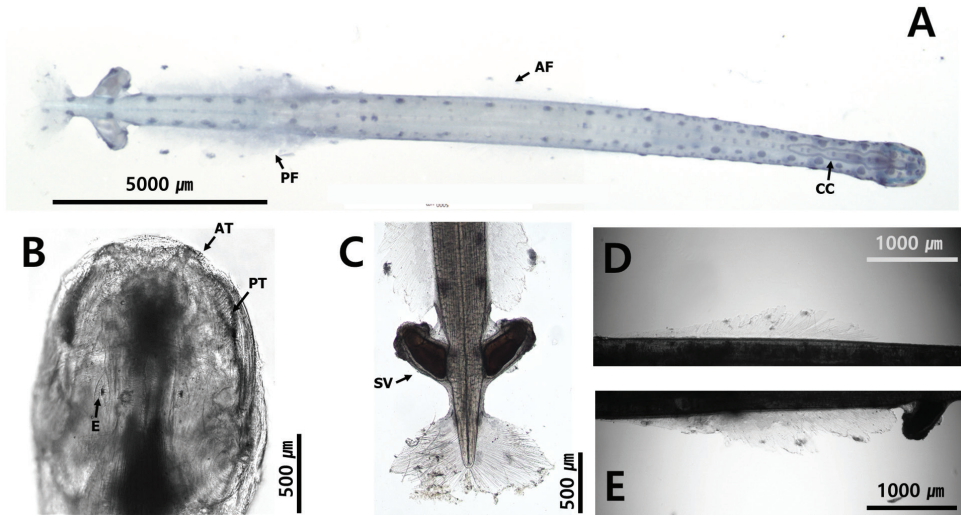


**Figure 13.** **A** *Serratosagitta pacifica* (dorsal view) **B** head **C** tail **D** anterior fin **E** posterior fin. Abbreviations: AF = anterior fin; AT = anterior teeth; CC = corona ciliata; COL = collarette; E = eye; PF = posterior fin; PT = posterior teeth; SV = seminal vesicle.

vesicles are well-separated from the posterior fins and caudal fin (Alvariño 1961). In the *S. pacifica* (nine specimens), the number of protrusions vary between 5 and 10. The inner serrated row of the grasping spine and the “teeth cells” forming protrusions at the anterior margin of the seminal vesicles were consistent with previous records (Alvariño 1967; Pierrot-Bults 1976). We observed three specimens for CBE staining pattern: dorsomedian line 43 dots; dorsolateral line, 54–69 dots; lateral line, 24 dots; receptors on the lateral fin, 10 dots; anterolateral receptors on the caudal fin, 2 dots; posterior receptors on the caudal fin, 3–4 dots. The dorsomedian dots are patterned as small spots that cross the centre of the body and larger symmetrical spots on dorsolateral line dots.

### Genus *Mesosagitta* Tokioka, 1965a

**Diagnosis.** Flaccid and opaque body. Collarette absent. Intestinal diverticula present. Grasping spine gently curved and not serrated. Intestinal diverticula present. The anterior fins begin between ventral ganglion and caudal fin and are shorter than posterior fins.

### *Mesosagitta minima* (Grassi, 1881)

*Spadella minima*: Grassi, 1883: 15 p.

*Sagitta minima*: Aida, 1897: 15 p., fig. 5; Michael 1908: 74 p.; Michael 1919: 248–249 p.; Tokioka 1940: 5 p.; Thomson 1947: 19 p.; Prado 1961: 39–41 p.; Alvariño

1967: 59–61 p., figs 36, 37; Ducret 1974: 166 p., table.1; Srinivasan 1979: 24–26 p., fig. 13; Michel 1984: 25–26 p., fig. 34; McLelland 1989: 163 p., table.1, figs 8D, 12D.

**Material examined.** Northern East China Sea (32°29.420'N, 127°29.654'E), 20–100 m depth, oblique towing with MOCNESS, Aug 2020 (one specimen).

**Description.** Small head. Two pairs of lateral fins with rayless zone. Intestinal diverticula small. Seminal vesicles divided into a small anterior knob and elongated posterior part and well-separated from posterior fins, but touching caudal fin. Corona ciliata elongated oval-shaped beginning in neck.

**Distribution.** This cosmopolitan species is found in the epipelagic zone (0–200 m depth) of the Pacific, Indian and Atlantic Oceans (Pierrot-Bults and Nair 1991) and the epipelagic zone (0–200 m depth) of the Japan coast (Sagami Bay and Suruga Bay) (Nagasawa and Marumo 1972). In this study, it was found in the epipelagic zone (20–100 m depth) of the northern East China Sea (Fig.1, station nECS03).

**Ecology.** *Mesosagitta minima* is abundant in mixed waters of the western North Atlantic Ocean (Pierce 1951). Mature specimens ranged within the size of 7–8 mm (Park 1970). The temperature range measured in the sampling stations was 18.49–28.84 °C and salinity range was 30.71–34.59 psu.

**Remarks.** Only immature individuals could be collected in this study. We easily distinguished *M. minima* amongst the collected specimens by the relatively small head and unique body shape that thickens towards the tail. These Korean specimens were classified as immature because seminal vesicles and ovaries were absent and undeveloped short eggs (mentioned in description of Alvariño (1967) as a feature of the second stage of development) were observed in the body.

### Genus *Flaccisagitta* Tokioka, 1965a

**Diagnosis.** Transparent or translucent body. Collarlet absent. Intestinal diverticula absent. The anterior fins begin at a far distance behind the end of the ventral ganglion. Seminal vesicles spherical shaped.

#### Key to species of *Flaccisagitta*

- |   |  |                     |
|---|--|---------------------|
| 1 | Large body (> 40 mm), small eggs reaching the neck .....                               | <i>F. hexaptera</i> |
| – | Small body (< 20 mm), large eggs reaching the anterior part of posterior fins<br>..... | <i>F. enflata</i>   |

### *Flaccisagitta enflata* (Grassi, 1881)

Figs 3A, 6E, 10D and 14A–E

*Spadella enflata*: Grassi, 1883: 13 p., fig. 7.

*Sagitta inflata*: Ritter-Záhony, 1908: 13–15 p., fig. 4A–D; Srinivasan 1979: 18–19 p., fig. 9.

*Sagitta enflata*: Aida, 1897: 15–16 p., fig. 6; Fowler 1906: 69 p., figs 9–17; Ritter-Záhony 1909: 791–792 p.; Michael 1919: 242–244 p., fig. 28, table 1; Burfield and Harvey 1926: 95–96 p., fig. 5; Pierce 1951: 221–222 p., fig. 4, table 12; Alvaríño 1967: 29–34 p., fig. 17A–G; Michel 1984: 18–19 p., figs 2, 20.

*Sagitta enflata* f. *gardineri*: Tokioka, 1959: 91–92 p., table 19

*Flaccisagitta enflata*: McLelland, 1989: 159 p., figs 7A and 12B

**Material examined.** Korea Strait (32°59.175'N, 124°29.595'E), 20–25 m depth, oblique towing with MOCNESS, Nov 2019, NIBRIV0000895309 (three specimens); northern East China Sea (32°0.000'N, 127°4.098'E), 0–110 m depth, oblique towing with conical net, Feb 2020, NIBRIV0000895308 (four specimens); northern East China Sea (32°30.000'N, 126°30.000'E), 0–100 m depth, oblique towing with conical net, Feb 2020 (one specimen).

**Description.** Total body length ranged between 12.7 and 15.4 mm. Tail 14.1–17.6% of body length. Hooks 8–10. Anterior teeth 6–10 and posterior teeth 10–17, respectively. Transparent body, inflated towards middle (Fig. 14). Triangular-shaped head (Fig. 14A). Collarette absent (Figs 3A, 10D). Blunt teeth (Fig. 14B). Round eyes with star-shaped eye pigments (Fig. 14B). Intestinal diverticula absent (Fig. 10D). Anterior fins 17.0% of body length. Anterior fins began at middle of body at far distance back of ventral ganglion and partially rayed. Starting points of anterior fins 43.7% and ending

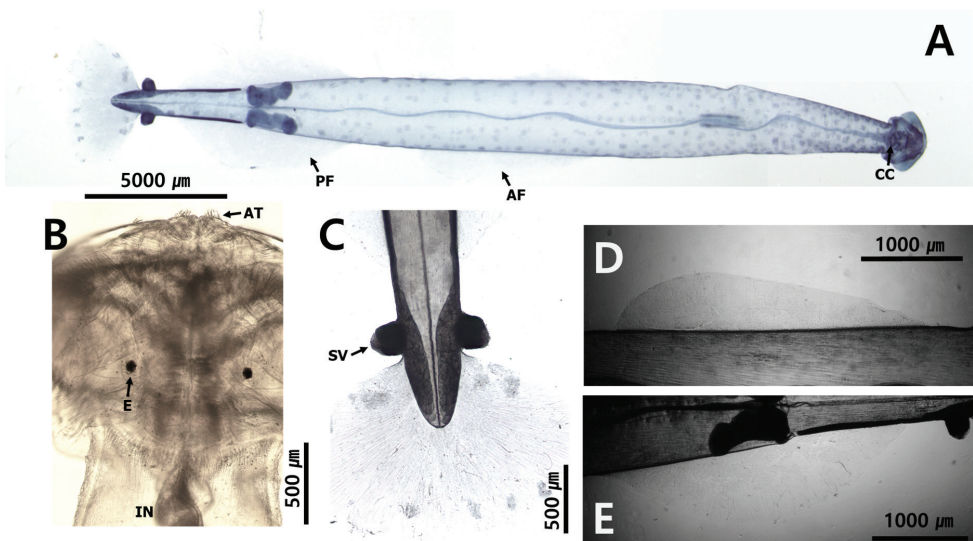


**Figure 14.** **A** *Flaccisagitta enflata* (dorsal view) **B** head **C** tail **D** anterior fin **E** posterior fin. Abbreviations: AF = anterior fin; AT = anterior teeth; CC = corona ciliata; E = eye; IN = intestine; PF = posterior fin; SV = seminal vesicle.

points of anterior fins 64.4% of body length, respectively (Fig. 14A, D). Posterior fins 20.5% of body length and 1.2 times longer than anterior fins. Starting points of posterior fins 71.9% and end points of posterior fins 92.5% of body length, respectively. Posterior fins well-separated from anterior fins (Fig. 14A, E). Caudal fin roundish, fan-shaped and fully rayed (Fig. 14C). Seminal vesicles touching caudal fin, but separated from posterior fins, spherical in shape with rupture in middle in mature specimen (Fig. 14C). Corona ciliata beginning in front of eyes and reaching neck (Figs 10D, 14A, 14B).

**Distribution.** This cosmopolitan species is found in the epipelagic (0–200 m depth) and mesopelagic zones (200–500 m depth) of the Pacific, Indian and Atlantic Oceans (Pierrot-Bults and Nair 1991), the coastal area of Japan (Tosa Bay; Ohnishi et al. 2014) and the epipelagic zone (0–150 m depth) of the Korea Strait (Park 1970). In this study, it was found in the epipelagic zone (0–110 m depth) of the northern East China Sea (Fig. 1: stations KS08, nECS01 and nECS04).

**Ecology.** This is used as an indicator species of warm currents in water surrounding Korea (Park 1970). The temperature range in the sampling stations was 16.52–28.80 °C and the salinity range was 28.96–33.22 psu.

**Remarks.** The transparent and flaccid body, star-shaped eye pigments and seminal vesicle morphology were consistent with those recorded in previous studies by Alvariño (1967) and Nagasawa (1976). Two types of Korean *Flaccisagitta enflata* have been reported, a small type: 10–20 mm long and a large type: 20–28 mm long (Park 1970). In this study, only the small type (< 20 mm) of *F. enflata* was collected. We observed seven specimens for CBE staining pattern: dorsomedian line, 12 dots; dorsolateral line, > 150 dots; ambiguous lateral line, receptors on the lateral fin, 2 dots (easily damaged); anterolateral receptors on the caudal fin, 4 dots; posterior receptors on the caudal fin, 7 dots. The pattern of dorsomedian dots lined up behind the ventral ganglion and the pattern of dorsolateral dots intensively scattered ahead of ventral ganglion.

### *Flaccisagitta hexaptera* (d'Orbigny, 1836)

Fig. 15A–E

*Sagitta hexaptera*: Conant, 1896: 213 p.; Aida 1897: 14 p., fig. 3; Fowler 1906: 70 p., figs 30–33; Ritter-Záhony 1908: 9–10 p., figs 3, 3A, 3B; Ritter-Záhony 1909: 789–790 p.; Ritter-Záhony 1911: 2–3 p.; Burfield and Harvey 1926: 95–96 p., figs 6–9; Tokioka 1959: 382–383 p., fig. 21; Alvariño 1967: 27–29 p., fig. 16A–I; Srinivasan 1979: 14–16 p., fig. 7A–G; Michel 1984: 21p., fig. 25.

*Flaccisagitta hexaptera*: McLelland, 1989: 159–160 p., figs 7B, C and 12A.

**Material examined.** Korea Strait (33°24.504'N, 127°54.600'E), 0–50 m depth, oblique towing with MOCNESS, Nov 2019, NIBRIV0000895298 (one specimen).

**Description.** Total body length ranged between 15 and 49 mm. Tail 19–24% of body length. Hooks 4–11. Anterior teeth 2–4 and posterior teeth 2–9, respectively.

Large and translucent body (Fig. 15). Intestinal diverticula absent (Fig. 15B). Collarlet absent (Fig. 15A). Eyes “D” shaped with “T” shaped eye pigments (Fig. 15B). Anterior fins short, beginning at middle of body between ventral ganglion and caudal septum, round-shaped and partially rayed (Fig. 15A, D). Posterior fins well-separated from anterior fins and partially rayed (Fig. 15A, E). Caudal fin roundish triangular-shaped and completely rayed (Fig. 15A, C). Seminal vesicles spherical with anterolateral edge opening (Fig. 15C). Seminal vesicle touching or close to tail fin and well-separated from lateral fins (Fig. 15C). Eggs reaching forward end of anterior fins. Corona ciliata beginning in front of eyes and reaching neck (Fig. 15B).

**Distribution.** This cosmopolitan species is found in the epipelagic (0–200 m depth) and mesopelagic zones (200–500 m depth) of the Pacific, Indian and Atlantic Oceans (Pierrot-Bults and Nair 1991), in the Indian coast (George 1952), the Tosa Bay in Japan (Ohnishi et al. 2014), the Korea Strait and south of East Sea (Park 1970). In this study, it was found in the epipelagic zone (0–50 m depth) of the Korea Strait (Fig. 1: station KS07).

**Ecology.** This species is considered as an indicator species of the Kuroshio warm current and fully-grown adults inhabit depths of < 200 m (Park 1970). In this study, individuals under Stage 3 were mainly found between the Jeju Straits (0–100 m depth). The temperature range in the sampling stations was 16.52–20.57 °C and salinity range was 34.48–34.61 psu.

**Remarks.** Though mainly immature individuals were reported in previous studies from Korea, in this study, adults longer than 40 mm were collected for the first time. The Korean species was consistent with those found in previous studies by Alvariño (1967) and Michel (1984) in terms of body size, length and shape of the egg, presence of small and round anterior fins in the middle of the body and the absence of bridge connecting the anterior and posterior fins. As the adult *Flaccisagitta hexaptera* is large

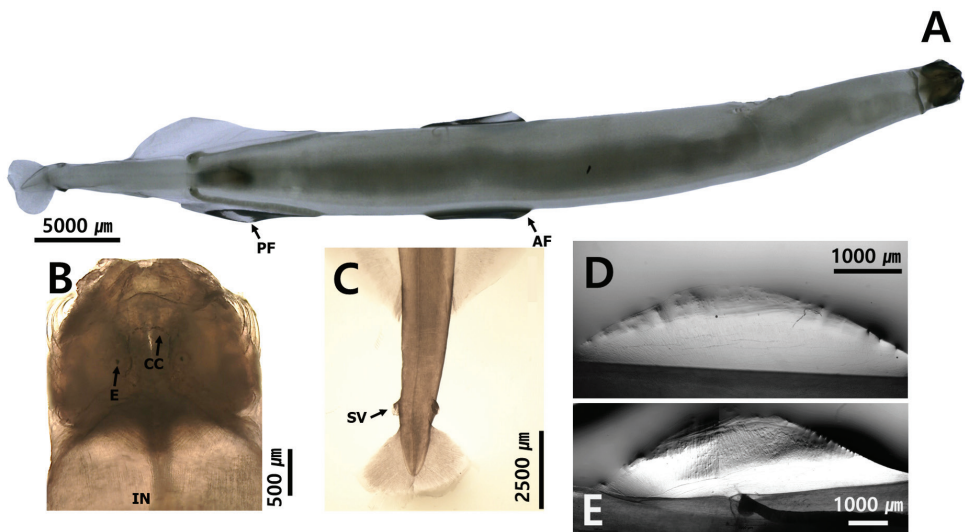


**Figure 15.** **A** *Flaccisagitta hexaptera* (dorsal view) **B** head **C** tail **D** anterior fin **E** posterior fin. Abbreviations: AF = anterior fin; CC = corona ciliata; E = eye; IN = intestine; PF = posterior fin; SV = seminal vesicle.

(> 20 mm), it can be difficult to distinguish the adult *Flaccisagitta enflata* from the immature *F. hexaptera*. However, it is possible when noting that the eggs of *F. hexaptera* are long and thin, whereas those of *F. enflata* are large and short. Another feature relevant for the diagnosis of *F. hexaptera* is the number of conspicuous anterior teeth which never exceed four, while it is eight in *F. enflata*. No specific pattern was observed through CBE staining on the body surface.

### Genus *Pseudosagitta* Germain & Joubin, 1912

**Diagnosis.** Flaccid and transparent body (but more opaque than *Flaccisagitta*). Collarette absent. Intestinal diverticula absent. Two pairs of lateral fins partially rayed and connected with a tegumentary bridge. Anterior fins beginning at the rear end of ventral ganglion and longer than posterior fins.

#### *Pseudosagitta lyra* (Krohn, 1853)

Figs 6C, 16A–E

*Sagitta lyra*: Aida, 1897: 15 p., fig. 4; Fowler 1906: 33 p.; Ritter-Záhony 1908: 10–13 p., fig. 1A–E; Burfield and Harvey 1926: 98 p., figs 18–24; Thomson 1947: 10–11 p.; Alvarino 1967: 23–26 p., fig. 14A–O; Lea 1955: 28–30 p., plate 3; Srinivasan 1979: 20–21 p., fig. 10A–F; Michel 1984: 22–23 p., fig. 27.

*Flaccisagitta lyra*: McLelland, 1989: 162 p., figs 7D, 7E and 12C.

**Material examined.** Korea Strait (33°48.924'N, 126°48.666'E), 40–70 m depth, oblique towing with MOCNESS, May 2019, NIBRIV0000895307 (one specimen).

**Description.** Total body length ranged between 16.0 and 60.0 mm. Tail 14–20% of body length. Hooks 8–9. Anterior teeth 4–9 and posterior 8–10, respectively. Large, flaccid and opaque body (Fig. 16). Intestinal diverticula absent (Fig. 16B). Collarette absent (Fig. 16A and B). Eyes square shaped with “H” shaped eye pigments (Fig. 16B). Anterior fins beginning at ventral ganglion, anterior of anterior fins with ray less zone and angular shape, conspicuously longer than posterior fins (Fig. 16A, D). Posterior fins with rayless zone connected with anterior fins by tegumentary bridge (Fig. 16A, E). Caudal fin roundish and completely rayed (Fig. 16C). Eggs reaching middle of posterior fins (Fig. 16A). Corona ciliata not clear (Fig. 16B). Seminal vesicles spherical and opening in middle of edge (Fig. 16C). Seminal vesicles touching neither of posterior or caudal fins, located closer to posterior fins (Fig. 16C).

**Distribution.** This species is found in the mesopelagic (500–1,000 m depth) and bathypelagic zones (1,000–2,000 m depth) of the Pacific, Indian and Atlantic Oceans (Pierrot-Bults and Nair 1991) and the Tosa Bay in Japan (Ohnishi et al. 2014). In this study, it was distributed in the epipelagic zone (40–70 m depth) of the Korea Strait (Fig. 1, station KS06).

**Ecology.** This species has a high prevalence in warm waters (Park 1970). In this study, specimens collected around Jeju Island were mainly distributed at water

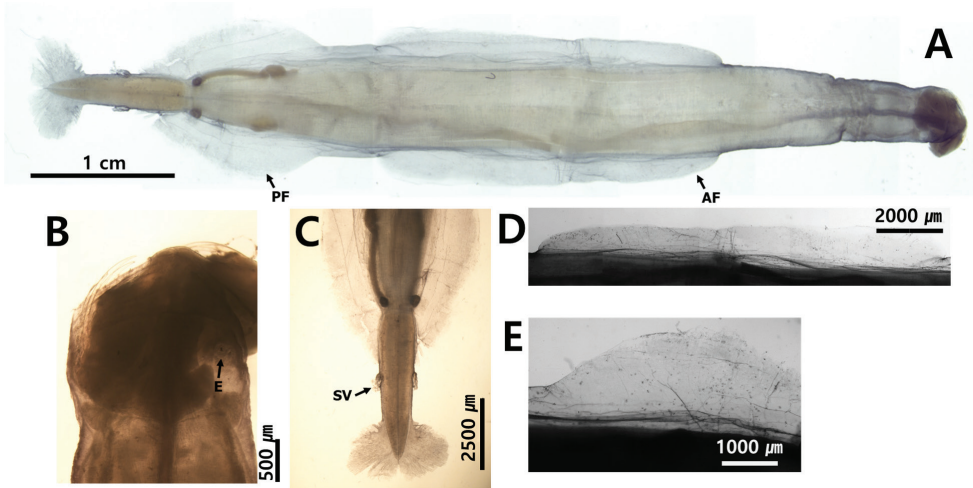


**Figure 16.** **A** *Pseudosagitta lyra* (dorsal view) **B** head **C** tail **D** anterior fin **E** posterior fin. Abbreviations: AF = anterior fin; E = eye; PF = posterior fin; SV = seminal vesicle.

depths > 50 m. The temperature range in the sampling stations was 16.47–21.34 °C and the salinity range was 34.17–34.52 psu.

**Remarks.** In Korean specimens, the position and length of the fins, distance between the anterior and posterior fins and shape of the seminal vesicles were morphologically consistent with the previous records of *Pseudosagitta lyra* (Alvariño 1967; Michel 1984; Lutschinger 1993). As one of the larger species of arrow worm, *P. lyra* reaches a maximum size of 42 mm (Michel 1984; Lutschinger 1993). However, the largest of the Korean specimens collected in this study was 60 mm in length. *Pseudosagitta scrippsae* can be easily confused with *P. lyra*, with similar size and position and shape of the fins and seminal vesicles. However, *P. scrippsae* can be differentiated by the presence of a distinct collarette around the neck (Chihara and Murano 1997). No specific pattern was observed through CBE staining on the body surface.

### Genus *Parasagitta* Tokioka, 1965a

**Diagnosis.** Slender and either opaque or translucent body. Collarette absent or small (almost absent). Intestinal diverticula present or absent. Grasping spines not serrated. Two rows of teeth. Two pairs of lateral fins completely rayed.

#### *Parasagitta elegans* (Verrill, 1873)

Fig. 17A–E

*Sagitta elegans*: Verrill, 1873: 332–333 p.; Conant 1896: 211–212 p.; Fowler 1906: 31–32 p.; Lea 1955: 22–28 p., plate 3.

**Material examined.** East Sea (37°33.198'N, 131°14.598'E), 0–100 m depth, oblique towing with conical net, Feb 2020, NIBRIV0000895306 (five specimens).

**Description.** Total body length ranged between 32.5 and 37.0 mm. Tail 14.7–20.6% of body. Hooks 11–12. Anterior teeth 9–10 and posterior teeth 22–29, respectively. Rigid and opaque body (Fig. 17). Collarette absent (Fig. 17A). Intestinal diverticula present, but not obvious. Anterior fins 18.8% of body length. Anterior fins beginning at middle of ventral ganglion and partially rayed. Starting points of anterior fins 38.5% and ending points of anterior fins 57.5% of body length, respectively (Fig. 17D). Posterior fins 22.3% of body length and 1.2 times longer than anterior fins. Starting points of posterior fins 67.7% and ending points of posterior fins 88.7% of body length, respectively. Posterior fins well-separated from anterior fins (Fig. 17E). Seminal vesicles elongated (Fig. 17C). Caudal fin roundish triangular-shaped (Fig. 17C). Square eyes “+” shaped eye pigments (Fig 17B). Corona ciliata beginning in front of eyes and expanding to anterior trunk (Fig. 17B).

**Distribution.** This species is found in the Epipelagic (0–200 m depth), mesopelagic (200–500 m depth) and bathypelagic zones (1000–2000 m depth) of the Pacific, Indian and Atlantic Oceans (Terazaki 1998; Choe and Deibel 2000) and the epipelagic and mesopelagic zones of the East Sea (Park 1970). In this study, it was found in the epipelagic zone (0–100 m depth) of the East Sea.

**Ecology.** A cold-water species, *P. elegans* is mainly found in the northern part of the Pacific Ocean (Bieri 1959). The spawning season is winter and fully mature individuals are  $\geq 30$  mm in length (Park 1970). The temperature range in the sampling stations of this study was 8.20–11.97 °C and the salinity range was 34.11–34.20 psu.

**Remarks.** The absence of a rayless zone in the anterior and posterior fins and a collarette in anterior body and the presence of small seminal vesicles extending along

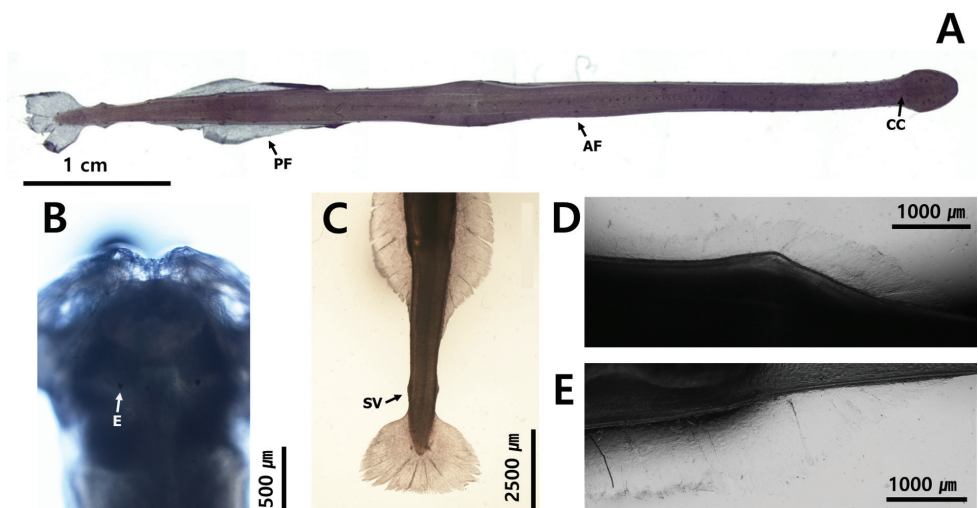


**Figure 17.** **A** *Parasagitta elegans* (dorsal view) **B** head **C** tail **D** anterior fin **E** posterior fin. Abbreviations: AF = anterior fin; E = eye; PF = posterior fin; SV = seminal vesicle.



**Remarks.** Only immature individual was collected in this study. We easily distinguished *F. ferox* amongst the collected specimens by the presence of distinct head as wide as the trunk and the presence of elongated ovoid seminal vesicles on the body. The Korean specimen was classified as immature because the boundary of the seminal vesicles was not obvious and the inside was mostly empty. This characteristic is consistent with Alvaríño's (1967) description regarding the immaturity of this species.

***Ferosagitta robusta* (Doncaster, 1902)**

Figs 3A, 6B, 8B, 9A, 18A–E

*Sagitta robusta*: Fowler, 1906: 19–20 p., figs 59–64; Ritter-Záhony 1908: 792 p.; Burfield and Harvey 1926: 100–101 p., figs 33–37; Thomson 1947: 13–15 p.; Alvaríño 1962: 187–198 p., figs 1–5; Alvaríño 1967: 66–71 p., figs 42A–D; Srinivasan 1979: 32–34 p., fig. 18A–G.

**Material examined.** Yellow Sea (34°5.502'N, 124°36.000'E), 0–75 m depth, oblique towing with conical net, Aug 2019, NIBRIV0000895305, (one specimen).

**Description.** Total body length ranged between 10.0 and 11.5 mm. Tail 27.8–35.0% of body length. Hooks 6–8. Anterior teeth 9–10 and posterior teeth 12–20, respectively. Rigid and opaque body (Fig. 18). Head wide as neck, roughly round or square shaped (Fig. 18A). Grasping spines gently curved and not serrated edge of hooks (Figs 8B, 9A). Teeth short and firm (Fig. 9A). “B” shaped eyes had “T” shaped eye pigments (Fig. 18B). Collarlet on neck (Figs 9A, 18A). Anterior fins 22.4% of body length. Anterior fins beginning just at posterior of ventral ganglion. Starting points of anterior fins 33.1% and ending points of anterior fins 56.5% of body length, respectively (Fig. 18A, D). Posterior fins 25.8% of body length and 1.2 times longer than anterior fins. Starting points of posterior fins 62.6% and ending points of posterior fins 88.4% of body length, respectively. Posterior fins separated from anterior fins and partially rayed. Caudal fin roughly round-triangle shaped, completely rayed (Fig. 18C). Seminal vesicles pear-shaped with elongated posterior trunk and anterior roundish knob and touching both posterior and caudal fins. (Fig. 18A, C). Conspicuous intestinal diverticula present (Fig. 9A). Eggs reached anterior of ventral ganglion. Corona ciliata beginning behind eyes and expanding to anterior of trunk (Fig. 18A).

**Distribution.** This species is found in the epipelagic zone (0–200 m depth) of Pacific and Indian Oceans (Pierrot-Bults and Nair 1991), the west coast of Florida (Pierce 1951), Indian coast (George 1952) and the Tosa Bay in Japan (Ohnishi et al. 2014). In this study, specimens were found in the epipelagic zone (0–75 m depth) of the Yellow Sea (Fig. 1: station YS03). *Ferosagitta robusta* is a typical Indo-pacific warm-water species (George 1952). The horizontal distribution range is wider than the vertical range and many individuals are mainly found in the surface layer (Park 1970). In this study, this species rarely appeared under low temperature conditions and their presence was predominant in the sea area affected by warm currents. The temperature range in the sampling stations was within 25.87–28.70 °C and salinity range was 32.72–33.11 psu.

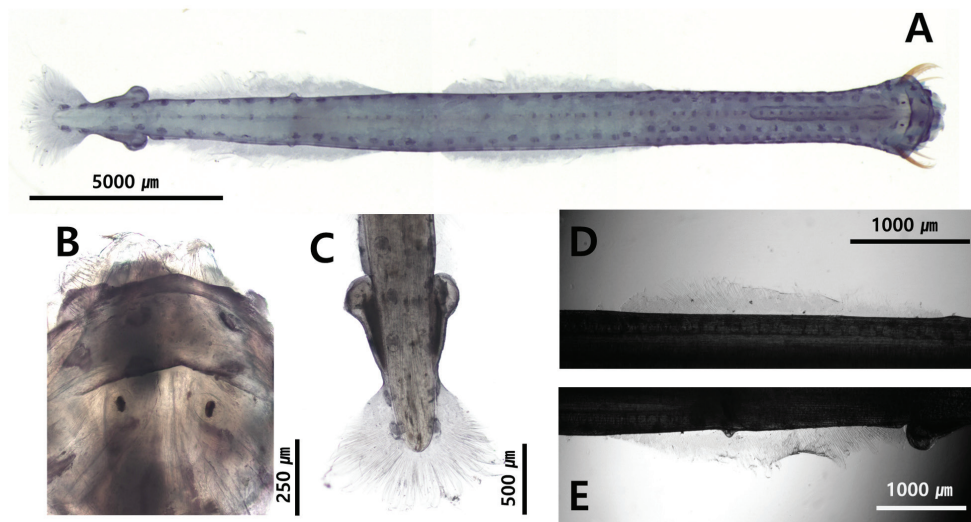


**Figure 18.** *A* *Ferosagitta robusta* (dorsal view) *B* head *C* tail *D* anterior fin *E* posterior fin. Abbreviations: AF = anterior fin; AT = anterior teeth; CC = corona ciliata; E = eye; PF = posterior fin; PT = posterior teeth; SV = seminal vesicle.

**Remarks.** Characteristics of the species in Korean waters, such as the conspicuous intestinal diverticula, head and body width and the seminal vesicles shape, are consistent with previous records (Alvariño 1967; Chihara and Murano 1997). The main difference between this species and another congeneric species of Korea, *F. ferox*, is the shape of the seminal vesicles. Seminal vesicles of *F. robusta* are very conspicuous, touching both posterior end of posterior fins, while that in *F. ferox* are not so conspicuous and are close to both posterior fins and caudal fin (Alvariño 1962). We observed one specimen for CBE staining pattern: dorsomedian line, 49 dots; dorsolateral line, 38 dots; lateral line, 30 dots; receptors on the lateral fin, 6 dots; anterolateral receptors on the caudal fin, 4 dots; posterior receptors on the caudal fin not observed due to damage.

**Genus *Aidanosagitta* Tokioka & Pathansali, 1963**

**Diagnosis.** Rigid and opaque body. Intestinal diverticula present. Collarette present or absent. Grasping spine gently curved and not serrated. Two rows of stout teeth arranged in a comb shape. Two pairs of lateral fins completely rayed.

**Key to species of *Aidanosagitta***

- 1 Seminal vesicles large and oval shaped, well-separated from caudal fins but touching posterior fins ..... *A. neglecta*
- Seminal vesicles small and elongated ..... 2

- 2 Seminal vesicles touching both posterior fins and caudal fin and opening at the anterolateral edge. Collarette covered on ventral ganglion (N type) from head to body (C type) or on the partial body (I type).....*A. crassa*
- Seminal vesicles well-separated from caudal fins, but touching the posterior fins. Thick collarette covered head to tail. Small sized body (< 10 mm).....  
..... *A. regularis*

### *Aidanosagitta neglecta* (Aida, 1897)

*Sagitta neglecta*: Aida, 1897: 16–17 p., fig. 7; Fowler 1906: 15–17 p., fig. 8; Michael 1919: 258 p., table 13, fig. 9; Burfield and Harvey 1926: 99 p, fig. 27; Thomson 1947: 17–18 p.; Tokioka 1959: 373–375 p., table 12, figs 103, 104; Sund 1961: 110 p., table 1; Alvariño 1967: 74 p., table 12, figs 46, 47; Srinivasan 1979: 26–27 p., fig. 14; Nair et al. 2008: 210 p., table 2.

**Material examined.** Korea Strait (34°41.577'N, 127°50.460'E), 0–20 m depth, oblique towing with conical net, Feb 2021 (one specimen).

**Description.** Rigid and opaque body. Narrow collarette and extending to half distance from neck to ventral ganglion. Intestinal diverticula present. Grasping spine gently curved. Two rows of stout teeth arranged in comb shape. Two pairs of lateral fins completely rayed, anterior fins beginning at end of ventral ganglion. Seminal vesicles oval-shaped with opening at anterolateral edge, position of seminal vesicles well separated from caudal fin, but touching posterior fins.

**Distribution.** This species is found in the epipelagic zone (0–200 m depth) of the Pacific and Indian Oceans (Pierrot-Bults and Nair 1991) and the coastal waters of the Philippines, India and Hong Kong (George 1952; Tse et al. 2007; Noblezada and Campos 2008; Lie et al. 2012).

**Ecology.** A mature specimen has been reported to be 8 mm in size (Alvariño 1967). This species shows a diurnal vertical migration in the summer off the Hong Kong coast (Lie et al. 2012). The temperature range in the sampling stations of this study was 16.40–16.41 °C and the salinity was 34.58 psu.

**Remarks.** Only one immature individual was collected in this study. *Aidanosagitta neglecta* is similar to *A. regularis* in morphological characteristics including collarette. However, the former had much larger seminal vesicles, thus they can be easily distinguished from each other. *Aidanosagitta neglecta* collected from Korean waters was smaller than the previously reported adult specimens, but seminal vesicles were obviously swollen in an oval shape. Despite the presence of swollen seminal vesicles, the Korean specimen was considered as immature because its size was smaller than the known record of the adult (Alvariño 1967).

### *Aidanosagitta crassa* (Tokioka, 1939)

Figs 3C, 5B, 19A–F

*Aidanosagitta crassa* f. *naikaiensis*: Tokioka, 1959: 376–377 p., fig. 16, table 15.

*Sagitta crassa*: Tokioka, 1939: 349–352 p., figs 1–8

**Material examined. Type C (collarette type):** East Sea (37°33.198'N, 131°14.598'E), 0–100 m depth, oblique towing with conical net, Feb 2020, NIBRIV0000895304 (one specimen); Yellow Sea (35°22.550'N, 126°5.366'E), 0–16.5 m depth, oblique towing with conical net, Jul 2020, five specimens; Korea Strait (34°13.698'N, 127°35.400'E), 0–28 m depth, oblique towing with conical net, Feb 2020 (one specimen). **Type N (naked type):** Yellow Sea (35°17.316'N, 126°10.483'E), 0–6.4 m depth, oblique towing with conical net, Jul 2020, NIBRIV0000895303 (three specimens).

**Description. Type C:** total body length ranged within 9.9 and 11.2 mm. Tail 26.6–29.8% of body length. Rigid and opaque body (Fig. 19). Head small. Collarette beginning at neck and reaching middle of body (Fig. 19A). Round eyes star-shaped eye pigments. Corona ciliata beginning from neck, elongated to anterior of ventral ganglion (Fig. 19A, B). Intestinal diverticula present (Fig. 19C). Two pairs of lateral fins completely rayed (Fig. 19E, F). Anterior fins 18.1% of body length. Anterior fins beginning at posterior of ventral ganglion. Starting points of anterior fins 29.6% and ending points of anterior fins 46.6% of body length, respectively (Fig. 19D). Posterior fins 23.0% of body length and 1.3 times longer than anterior fins. Starting of posterior fins 62.0% and ending points of posterior fins 86.9% of body length, respectively. Posterior fins well separated from anterior fins beginning at middle of body (Fig. 19A, D). Seminal vesicles longitudinally elongated (Fig. 19D). Eggs reaching posterior of ventral ganglion.

**Type N:** total body length ranged between 8.1 and 8.2 mm. Tail 27.0–30.0% of body length (Fig. 19B). Collarette beginning at anterior of ventral ganglion and reaching posterior of ventral ganglion (Fig. 19B). Anterior fins 19.1% of body length. Anterior fins beginning at posterior of ventral ganglion. Starting points of anterior fins 34.0% and end points of anterior fins 54.6% of body length, respectively (Fig. 19B). Posterior fins 24.6% of body length and 1.3 times longer than anterior fins. Starting points of posterior head 60.9% and ending points of posterior fins 88.2% of body length, respectively. Posterior fins well-separated from anterior fins beginning at middle of body (Fig. 19A, B).

**Distribution.** This species is found in the neritic water of the Pacific Ocean (Pierrot-Bults and Nair 1991), the neritic coastal water of Hong Kong (Tse et al. 2007) and the Tosa Bay of Japan (Ohnishi et al. 2014). In this study, it was found in the epipelagic zone (0–100 m depth) of the East Sea, Korea Strait and Yellow Sea (Fig. 1, stations ES01, YS01, YS02 and KS01).

**Ecology.** *Aidanosagitta crassa* appears in high abundance throughout the year in the relatively low saline waters of the Yellow Sea and coast of Jeju (Park 1970). This species rarely appears in the summer warm waters of southern Korea. The body length varies according to the season and it has been reported that they are large (type C) in winter and small in summer (type N) (Park 1970). Specimens of type C die after spawning and those of type N dominate the new generation (Park 1970). We obtained specimens from the East Sea in winter and the Yellow Sea in summer.

**Remarks.** Previous researchers classified *Aidanosagitta crassa* into three types according to the distribution of the collarette: C type, covers from the neck to the body; N type,

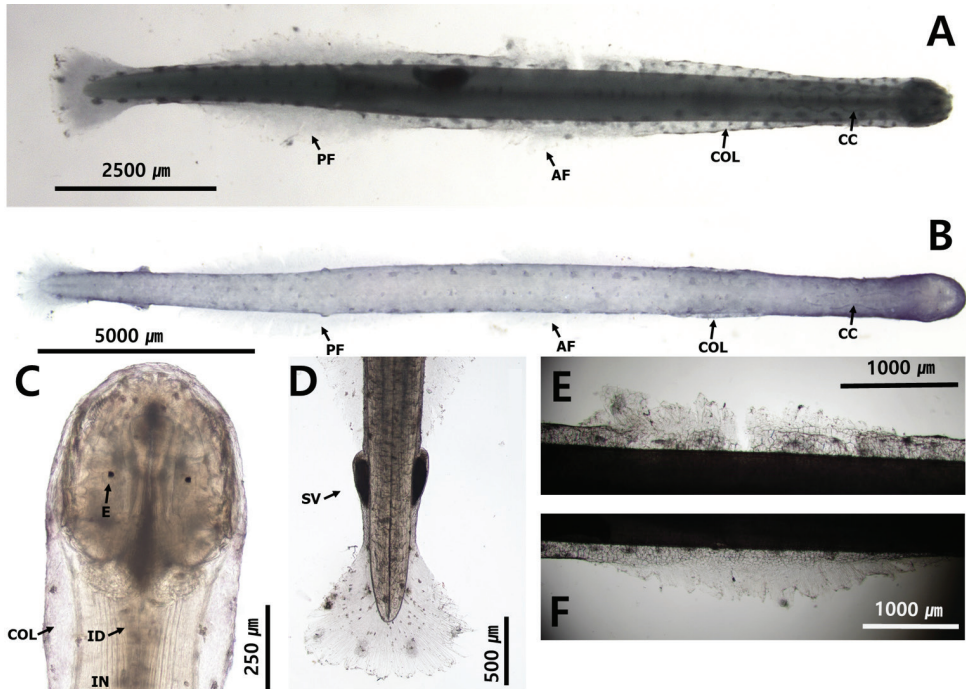


**Figure 19.** **A** *Aidanosagitta crassa* Type C (dorsal view) **B** *Aidanosagitta crassa* Type N (dorsal view) **C** head and neck **D** tail **E** anterior fin **F** posterior fin. Abbreviations: AF = anterior fin; CC = corona ciliata; COL = collarette; E = eye; IN = intestine; ID = intestine diverticula; PF = posterior fin; SV = seminal vesicle.

covers only the ventral ganglion; and I type, covers the ventral ganglion and partially covers the body (Park 1970). In this study, specimens of types C and N were collected and the Korean type C from the Yellow Sea had the same morphological characteristics of the collarette as the original description of this species reported by Tokioka (1939). Similarly, type N, which appeared together with type C at other stations of the Yellow Sea, was consistent with the morphological characteristics of the collarette of *A. crassa* and *f. naikaiensis* (Tokioka 1939). It has been reported that the three types of *A. crassa* appear at different periods depending on environmental factors (water temperature and salinity) of the specific sea area; however, in this study, both types appeared simultaneously in the Yellow Sea. A more detailed ecological investigation of the impact of environment factors on the succession of the three types of *A. crassa* is necessary. We observed four specimens for type C of *A. crassa* CBE staining pattern: dorsomedian line, 14 dots; dorsolateral line, > 100 dots; lateral line, 8 dots; receptors on the lateral fin, 8 dots; anterolateral receptors on the caudal fin, 4 dots; posterior receptors on the caudal fin, 6 dots. The pattern of dorsomedian dots was small spots that crossed the centre of the body and larger symmetrical spots on dorsolateral line dots. In addition, we observed three specimens for type N of *A. crassa* CBE staining pattern: dorsomedian line, 35 dots; dorsolateral line, 34 dots; lateral line, 12 dots; receptors on the lateral fin, not observed; anterolateral receptors on the caudal fin, 2 dots; posterior receptors on the caudal fin, 4 dots.

***Aidanosagitta regularis* (Aida, 1897)**

Figs 6A, 7A, 10A, 20A–E

*Sagitta regularis*: Aida, 1897: 17–18 p., fig. 8; Doncaster 1902: 211 p., fig. 7; Burfield and Harvey 1926: 100 p., figs 31–32; Thomson 1947: 18–19 p.; Alvarino 1967: 72–75 p., fig. 48A–D; Srinivasan 1979: 31–32 p., fig. 17A–F; Nair et al. 2008: 110 p., table 2.

**Material examined.** Korea Strait (33°33.600'N, 127°34.002'E), 0–96 m depth, oblique towing with conical net, Feb 2020, NIBRIV0000895302 (one specimen); northern East China Sea (32°33.000'N, 126°30.000'E), 0–100 m depth, oblique towing with conical net, Feb 2020, NIBRIV0000895301 (one specimen); northern East China Sea (32°30.000'N, 127°5.100'E), 0–120 m depth, oblique towing with conical net, Feb 2020 (one specimen).

Description. Total body length ranged within 6.1 and 6.7 mm. Tail 30.5–31.7% of body length. Hooks 6. Anterior teeth 3–4 and posterior teeth 5–6, respectively. Rigid and opaque body (Fig. 20). Head small, triangular shaped (Fig. 20B). Round eyes with “B”-shaped eye pigments (Fig. 20B). Collarette expanding to seminal vesicles (Fig. 20A). Corona ciliata beginning from neck to anterior of ventral ganglion (Fig. 10A). Anterior fins 12.3% of body length. Anterior fins beginning at posterior of ventral ganglion. Starting points of anterior fins 37.3% and ending points of anterior fins 50.9% of body length, respectively (Fig. 20D). Posterior fins 22.0% of body length and 1.8 times longer than anterior fins. Starting points of posterior fins 62.9% and ending points of posterior fins 84.7% of body length, respectively. Posterior fins not connected to anterior fins, beginning in front of caudal septum and both anterior fins and posterior fins completely rayed (Fig. 20D, E). Caudal fin fully rayed and roughly round or triangle-shaped (Fig. 20C). Intestinal diverticula present (Figs 7A, 20B). Seminal vesicles longitudinally elongated along body (Fig. 20C). Eggs reaching posterior of ventral ganglion.

**Distribution.** This species is found in the epipelagic (0–200 m depth) and mesopelagic zones (200–500 m depth) of Pacific and Indian Oceans (Pierrot-Bults and Nair 1991) and the epipelagic zone (0–100 m depth) of the Tosa Bay in Japan (Ohnishi et al. 2014). In this study, it was found in the epipelagic zone (0–120 m depth) of the Korea Strait and northern East China Sea (Fig. 1, stations KS06, nECS01 and nECS02).

**Ecology.** This species is considered a warm-water Indo-Pacific indicator species because many individuals appear in high-temperature and high-salinity water and the distribution range is limited to the areas affected by warm currents (Park 1970).

**Remarks.** Amongst the Korean specimens, the collarette was differently inflated, thick and covered the body surface. However, the position and shape of the corona ciliata and fins were consistent with the original description (Aida 1897). *Aidanosagitta regularis* is similar to *A. bedfordii*; however, these two species can be distinguished by the morphological difference in the eye pigments (elongated vs. roundish). We observed two specimens for CBE staining pattern: dorsomedian line, 28 dots; dorsolateral line, 34 dots; lateral line, 44 dots; receptors on the lateral fin, 3 dots; anterolateral receptors on the caudal fin, 2 dots; posterior receptors on the caudal fin, not observed due to damage.

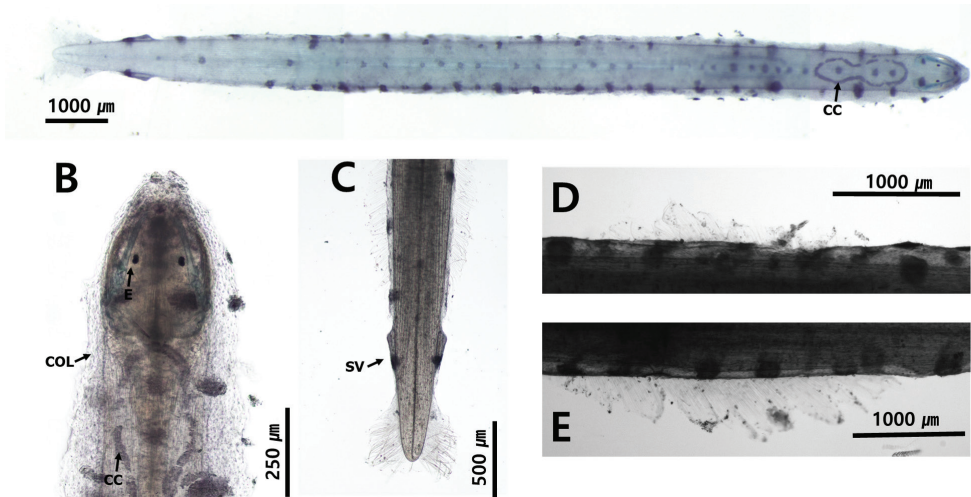


**Figure 20.** **A** *Aidanosagitta regularis* (dorsal view) **B** head **C** tail **D** anterior fin **E** posterior fin. Abbreviations: CC = corona ciliata; COL = collarette; E = eye; SV = seminal vesicle.

### Genus *Sagitta* Quoy & Gaimard, 1827

**Diagnosis.** Rigid and opaque body. Collarette almost absent. Intestinal diverticula absent or present. Grasping spines not serrated. Two pairs of lateral fins completely rayed.

### *Sagitta bipunctata* Quoy & Gaimard, 1827

*Sagitta bipunctata*: Quoy & Gaimard, 1827: 232–233 p., figs 1, 2, 6, 7; Aida 1897: 13–14 p., fig. 1; Ritter-Záhony 1908: 15 p., figs 2, 2A; Ritter-Záhony 1910: 2 p., Fowler 1906: 68 p.; Sund 1961: 110 p., table 1; Alvariño 1967: 44–49 p., fig. 26A–D; Dallot and Ducret 1969: 19 p., table 1; Srinivasan 1979: 8–9 p., fig. 3A–F; Michel 1984: 17–18 p., fig. 18; McLelland 1989: 163–164 p., figs 9A, 12I; Villenas and Palma 2006: 105 p., table 1

**Material examined.** Yellow sea (33°0.111'N, 125°29.581'E), 0–86 m depth, oblique towing, July 2020.

**Description.** Small, rigid and opaque body. Small head. Collarette almost absent (thin on neck). Eyes square-shaped with no eye pigments observed in this study. Intestinal diverticula absent. Forward end of anterior fins not visible. Posterior fins beginning in front of caudal septum and closing to seminal vesicles, completely rayed. Seminal vesicles elongated with small indentations and touching both lateral and caudal fins.

**Distribution.** This species is found in the epipelagic (0–200 m depth) and mesopelagic zones (200–500 m depth) of Pacific, Indian and Atlantic Oceans (Pierrot-Bults and Nair 1991). This species appears in most of the seas across Korean waters.

**Ecology.** *Sagitta bipunctata* is known as a cosmopolitan species, appearing in temperate and tropical seas; it is an indicator species of high salinity and the presence of oceanic water (Pierce 1953). The temperature range in sampling stations of this study was 15.08–22.17 °C and the salinity range was 31.77–34.01 psu.

**Remarks.** Only one immature individual was collected in this study. *Sagitta bipunctata* can be distinguished from other Korean species by the following characteristics: absence of intestinal diverticular, presence of completely rayed lateral fins and the restricted position of collarette on the posterior part of the body. The seminal vesicles of Korean specimen were not sufficiently mature compared to the description of Alvariño (1967).

### *Zonosagitta Tokioka, 1965a*

**Diagnosis.** Rigid or flaccid and transparent or opaque body. Collarette small (almost absent). Intestinal diverticula absent. Grasping spines not serrated. Two pairs of lateral fins partially rayed. Anterior part of anterior fins elongated and rayless. Anterior fins longer than posterior fins.

#### Key to species of *Zonosagitta*

- 1 The anterior fins beginning at the middle of ventral ganglion, the seminal vesicles oval shaped touching neither the posterior fins nor caudal fin, small eyes with star-shaped eye pigments ..... *Z. bedoti*
- The anterior fins beginning at the end of ventral ganglion, the seminal vesicles conical-shaped and touching both lateral fins and caudal fin, small eyes with “E” shaped eye pigments..... *Z. nagae*
- The anterior fins beginning at the middle of ventral ganglion, the seminal vesicles elongated with a roundish anterior protruding part, small eyes with star shaped eye pigments..... *Z. pulchra*

### *Zonosagitta bedoti* (Béraneck, 1895)

Figs 7D, 21A–E

*Sagitta bedoti* f. *minor*: Tokioka, 1959: 89–90 p., table 18.

*Sagitta bedoti*: Béraneck, 1895: 147–152 p.; Fowler 1906: 6–8 p., figs 1–8; Michael 1919: 255–257 p., figs 6, 20, 24, 30; Burfield and Harvey 1926: 94–95p., figs 1–2; Thomson 1947: 18 p.; Kitou 1966: 239 p., table 1; Alvariño 1967: 53–55 p., fig. 32A–D; Francisco 1977: 229–231 p., plate 2; Srinivasan 1979: 6–7 p., fig. 2A–G.

**Material examined.** Korea Strait (33°0.000'N, 125°18.000'E), 0–75 m depth, oblique towing with conical net, Feb 2020, NIBRIV0000895300 (one specimen); northern

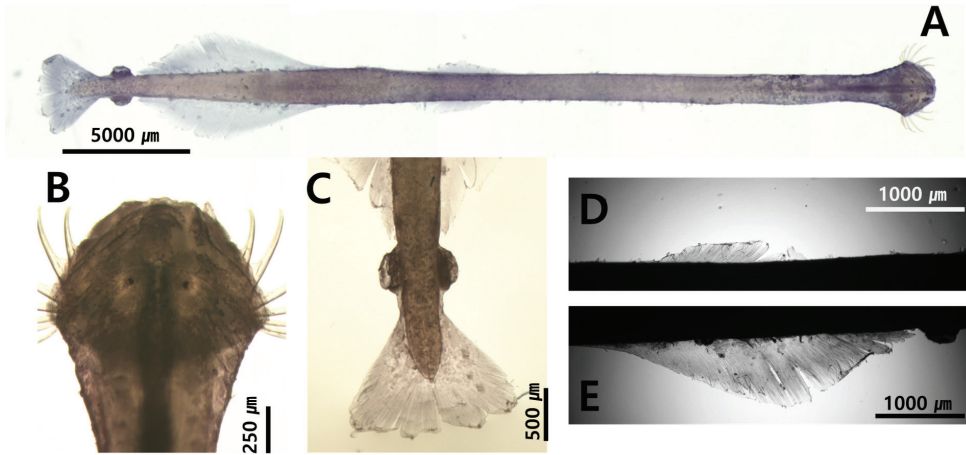


**Figure 21.** **A** *Zonosagitta bedoti* (dorsal view) **B** head **C** tail **D** anterior fin **E** posterior fin. Abbreviations: AF = anterior fin; E = eye; PF = posterior fin; SV = seminal vesicle.

East China Sea (31°30.000'N, 126°28.998'E), 0–82 m depth, oblique towing with conical net, Feb 2020 (one specimen).

**Description.** Total body length ranged from 16–17 mm. Tail 3.71% of body length. Hooks 7. Anterior teeth 27–28 and posterior teeth 30–35, respectively. Opaque and rigid body (Fig. 21). Head wider than body (Figs 7D, 21A). Short and dense teeth. Intestinal diverticula absent (Figs 7D, 21B). “D”-shaped eyes with star-shaped eye pigments (Fig. 21B). Corona ciliata beginning behind eyes and elongated over neck (Fig. 21B). Anterior fins 26.5% of body length. Anterior fins beginning at middle of ventral ganglion, anterior of anterior fins narrow with rayless zone and posterior of anterior fins partially rayed. Anterior fins 1.3 times longer than posterior fins. Starting points of anterior fins 34.3% and ending points of anterior fins 60.0% of body length, respectively (Fig. 21A, D). Posterior fins 19.8% of body LENGTH. Starting points of posterior fins 63.7% and ending points of posterior fins 89.7% of body length, respectively. Posterior fins connected with anterior fins (Fig. 21A). Caudal fin triangular-shaped and completely rayed (Fig. 21C). Seminal vesicles spherical in shape with lateral rupture in mature specimen (Fig. 21C).

**Distribution.** This species is found in the epipelagic zone (0–200 m depth) of the Pacific and Indian Oceans (Pierrot-Bults and Nair 1991) and the Tosa Bay in Japan (Ohnishi et al. 2014). In this study, it was found in the epipelagic zone (0–100 m depth) of the Korea Strait and northern East China Sea (Fig. 1: stations KS09 and nECS06).

**Ecology.** *Zonosagitta bedoti* is used as an indicator species in the front area where warm and cold water meet (Park 1970). The temperature range in the sampling location in this study was between 14.62 and 15.01 °C and the salinity range was 33.67–33.81 psu.

**Remarks.** *Zonosagitta bedoti* and *Z. nageae* are similar in morphology at the immature stage. However, because adult *Z. nageae* are relatively larger, immature *Z. nageae*

may be misidentified as *Z. bedoti*. Adults of both species can be distinguished from each other by the shape of seminal vesicles and eye pigments. *Zonosagitta nageae* has an “E”-shaped eye pigment, while *Z. bedoti* has a star-shaped eye pigment. The spot pattern on the body surface found through CBE staining is as follows: irregular spot pattern which continued from the head to the ventral ganglion and six spots along the outside of the body were symmetrical around the tail.

### *Zonosagitta nageae* (Alvariño, 1967)

Figs 6D, 7C, 22A–E

*Sagitta nageae*: Alvariño, 1967: 55–58 p., fig. 34A–D.

**Material examined.** Korea Strait (33°29.662'N, 125°30.881'E), oblique towing with MOCNESS, 32–58 m depth, July 2020, NIBRIV0000895297 (two specimens); Korea Strait (33°24.504'N, 127°54.600'E), 0–50 m depth, oblique towing with conical net, May 2019, two specimens; northern East China Sea (31°30.000'N, 125°17.100'E), 0–50 m depth, oblique towing with conical net, Feb 2020, NIBRIV0000895296 (one specimen).

**Description.** Total body length ranged from 11–15 mm. Hooks 6–8. Anterior teeth 11–15 and posterior teeth 15–35, respectively. Rigid and opaque body (Fig. 22A). Long and dense teeth. Collarete present on neck (Fig. 22B). Intestinal diverticula absent (Fig. 7C). Eyes “D”-shaped with “E”-shaped eye pigments (Fig. 22B). Anterior fins 27.7% of body length and 1.5 times longer than posterior fins. Anterior fins beginning in front of ventral ganglion and partially rayed. Starting points of anterior fins 28.6% and ending points of anterior fins 59.8% of body length, respectively (Fig. 22A, D). Posterior fins 18.0% of body length. Starting points of posterior fins 67.8% and ending points of posterior fins 91.9% of body length, respectively. Posterior fins connecting with anterior fins partially rayed (Fig. 22A, E). Seminal vesicles conical-shaped with small indentations and well separated from posterior fins (Fig. 22C). Eggs reached posterior of anterior fins. Corona ciliata beginning behind eyes and elongated over neck (Fig. 22C).

**Distribution.** This species is found in the epipelagic zone (0–200 m depth) of the Pacific and Indian Oceans (Pierrot-Bults and Nair 1991). In this study, the species was found in the epipelagic zone (0–120 m depth) of the northern East China Sea, the Korea Strait and the Yellow Sea (Fig. 1: stations KS03, KS07 and nECS05).

**Ecology.** This species appears year-round in most of the seas around Korea, predominantly in the southern and western seas and shows high abundance in areas where warm and cold currents meet (Park 1970). In summer, the temperature range was 15.49–28.70 °C and the salinity was 30.92–34.01 psu. In winter, the temperature range was 11.47–11.58 °C and the salinity was 32.44–32.49 psu.

**Remarks.** The anterior fin of *Zonosagitta nageae* had a longer rayless zone than the posterior fin, clearly distinguishing it from *Z. bedoti*. CBE staining showed the follow-

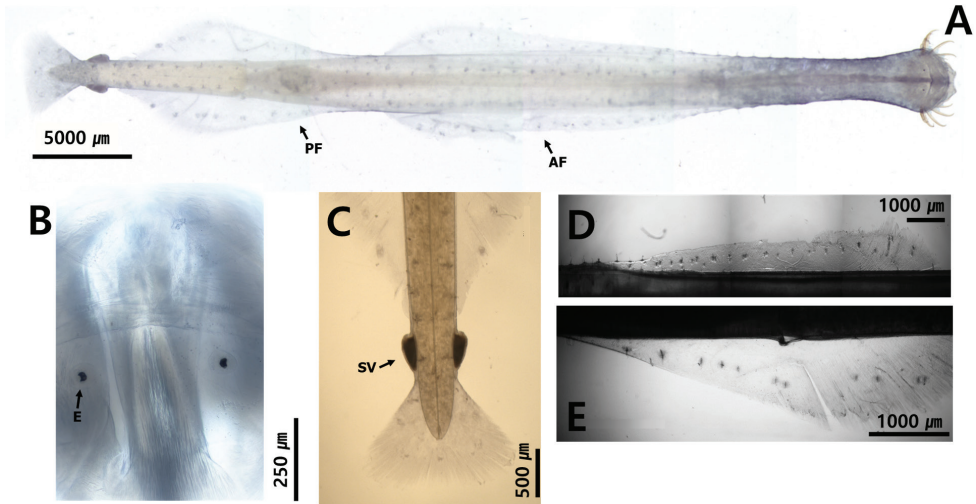


**Figure 22.** **A** *Zonosagitta nagee* (dorsal view) **B** head **C** tail **D** anterior fin **E** posterior fin. Abbreviations: AF = anterior fin; E = eye; PF = posterior fin; SV = seminal vesicle.

ing spot pattern on the body surface: an irregular spot pattern continued from the head to the middle of the ventral ganglion; symmetrical dots appeared near the rayless zone of each fin (13 spots on anterior fin, 6 spots on posterior fin).

### *Zonosagitta pulchra* (Doncaster, 1902)

*Sagitta pulchra*: Doncaster, 1902: 213 p.; Fowler 1906: 72 p.; Michael 1919: 251–253 p., tables 7, 8; Burfield and Harvey 1926: 100 p., fig. 30; Thomson 1947: 19–20 p.; Kitou 1966: 239 p., table 1; Alvariño 1967: 34–35 p., figs 20–21; Francisco 1977: 231–233 p.; Srinivasan 1979: 29–30 p., fig. 16.

**Material examined.** Korea Strait (34°17.868'N, 128°15.854'E), 0–60 m depth, oblique towing with MOCNESS, Feb 2020 (one specimen).

**Description.** Rigid and transparent body. Collarette present. Intestinal diverticula absent. Grasping spine gently curved. Two rows of stout teeth arranged in comb shape. Two pairs of lateral fins partially rayed, anterior fins begin at the end of ventral ganglion. Seminal vesicles elongated with an anterior protruding part usually roughly round and touching both lateral fins and caudal fin.

**Distribution.** The species is found in the epipelagic zone (0–200 m depth) of the Pacific and Indian Oceans (Pierrot-Bults and Nair 1991) and off the coast of Philippines (Noblezada and Campos 2008). In this study, it was found in the epipelagic zone (0–120 m depth) of the northern East China Sea, the Korea Strait and the Yellow Sea (Fig. 1: station KS02).

**Ecology.** *Z. pulchra* is considered to be a neritic species (Bieri 1959; Pierrot-Bults and van der Spoel 2003). The temperature range in the sampling stations of this study was 11.95–14.79 °C and the salinity range was 33.59–34.00 psu.

**Remarks.** Only one immature individual was collected in this study. The examined Korean specimen belongs to the genus *Zonosagitta* by the absence of intestinal diverticular and the presence of rayless zone in the anterior part of anterior fins. This Korean specimen was identified as *Z. pulchra* because its anterior fins were more angled than those of *Z. bedoti* or *Z. nageae*. The seminal vesicles of Korean specimen were not sufficiently mature compared to description of Alvarino (1967).

## Discussion

Based on a taxonomic review of newly obtained specimens from Korea, we confirmed the appearance of chaetognath taxa in Korean waters corresponding to one order, three families, 11 genera and 18 species. Taxonomically identified voucher specimens (*Krohntitta subtilis*, *K. pacifica*, *Pterosagitta draco*, *Aidanosagitta crassa*, *A. neglecta*, *A. regularis*, *Ferosagitta ferox*, *F. robusta*, *Flaccisagitta enflata*, *F. hexaptera*, *Mesosagitta minima*, *Parasagitta elegans*, *Pseudosagitta lyra*, *Sagitta bipunctata*, *Serratosagitta pacifica*, *Zonosagitta bedoti*, *Z. nageae* and *Z. pulchra*) were obtained for the first time in Korea and their taxonomic and ecological features were reported. Although the overall morphological characteristics of the six species (*A. neglecta*, *F. ferox*, *K. pacifica*, *M. minima*, *S. bipunctata* and *Z. pulchra*) were mostly consistent with the previously-reported species, their essential characteristics have been briefly described in this study because only immature individuals of these six species were collected. On the contrary, the three species (*Decipisagitta decipiens*, *Serratosagitta serratodentata*, *S. pseudoserratodentata*) mentioned in literature have very poor taxonomic basis for their academic report (drawings, descriptions and voucher specimens), which can result in possible misidentification and their presence in Korean waters is questionable. Most of the samples in this study were collected in summer and winter. Extension of the investigation period to spring and autumn in future studies can facilitate identification of adult specimens of the above-mentioned six species or clarification of the presence or absence of the three suspicious species.

The detailed characteristics of the corona ciliata and fins of chaetognaths are important as taxonomic keys to distinguish genera, but they are difficult to observe under a stereomicroscope. In order to address this problem, we stained the surface of the specimens with CBE, which has rarely been used in the past for observing chaetognaths. The CBE staining of the Korean specimens clearly revealed the features of the corona ciliata, fins and body surface. The corona ciliata of *Aidanosagitta* is located from behind the eyes to the anterior part of the trunk, whereas that of *Sagitta*, *Serratosagitta*, *Ferosagitta*, *Parasagitta* and *Zonosagitta* extends from the front of the eyes to the neck; hence, the two groups could be clearly distinguished. *Flaccisagitta* is also distinctly differentiable from other genera as the corona ciliata

extends from the front of the eyes to the anterior part of the neck. We propose the location and shape of these corona ciliata as additional taxonomic keys to distinguish Korean taxa at the genus level. On the contrary, *Krohnitta subtilis* had a circular corona ciliata located in front of the eyes, unlike other congeneric species, in which a circular corona ciliata appeared behind the eyes. Bieri (1974) has suggested the artificial position change of the corona ciliata due to damaged specimens. Therefore, the differences in corona ciliata between *Krohnitta subtilis* found in Korea and other known congeneric species need to be confirmed by examining more specimens.

The distribution of dots on the body surface was easily confirmed through microscopic observation after CBE staining. The dots pattern is expressed by a regular arrangement of tactile cilia distributed on the body surface of the chaetognaths (Aida 1897). The tactile cilia are reported to have two types of hair (Aida 1897; Feigenbaum 1978). One is transversally orientated ciliary fence organs and the other is longitudinally orientated ciliary tuft organs (Aida 1897; Bone and Pulsford 1978; Müller et al. 2014). The tactile cilia are capable of responding to water movement on the surface of the body or of detecting prey (Horridge and Boulton 1967). Recent studies have established the role of tactile cilia as nerve receptors (Müller et al. 2014). In this study, *Aidanosagitta*, *Serratosagitta* and *Ferosagitta* have similar round dots of symmetry based on the dorsal median line from the head to the tail, but their size and location are different for each genus. *Zonosagitta nageae* and *Z. bedoti* also showed a marked difference from other genera by showing irregular spot patterns from the head to the ventral ganglion.

On the contrary, *Flaccisagitta* did not have similar spot patterns on the body surface between the two Korean species. Irregular spots on the body surface of the *Flaccisagitta enflata* were observed; however, *F. hexaptera* did not exhibit any spot patterns, similar to *Pseudosagitta lyra*. Since the fully-grown body of this species is usually large with a size of 50 mm and more, it is presumed that the relatively thick epidermis prevented effective staining. The regularity of these patterns has also been observed in species such as *Sagitta hispida*, *S. enflata*, *S. elegans*, *Spadella schizoptera* and *Spadella cephaloptera* (Feigenbaum, 1977); however, evidence for establishing a connection with genealogy is lacking. Moreover, basic data obtained from a complete individual pattern will be valuable to explain the commonalities at genus levels. Further application of the CBE staining method to other taxa of Aphragmophora will clarify whether new features, such as the location and shape of the corona ciliata and the spot patterns on the body surface, are effective as genus or species grouping features.

## Acknowledgements

We would like to thank Dr. Kasatkina, Dr. Perez and Dr. P Stoev who made constructive and invaluable suggestions and comments. This work was supported by a grant from the National Institute of Biological Resources (NIBR), funded by the Ministry of

Environment (MOE) of the Republic of Korea (NIBR202130203) and project titled “Research center for fishery resource management based on the information and communication technology” (2022, Grant number 20180384), funded by the Ministry of Oceans and Fisheries, Korea.

## References

- Aida T (1897) Chaetognaths of Misaki Harbor. *Annotationes Zoologicae Japonenses* 1: 13–21.
- Alvariño A (1961) Two new chaetognaths from the Pacific. *Pacific Science* 15(1): 67–77.
- Alvariño A (1962) Taxonomic revision of *Sagitta robusta* and *Sagitta ferox* Doncaster, and notes on their distribution in the Pacific. *Pacific Science* 16: 186–201.
- Alvariño A (1967) The Chaetognatha of the NAGA Expedition (1959–1961): In the South China Sea and the Gulf of Thailand (Vol. 4). University of California, Scripps Institution of Oceanography, 197 pp.
- Beraneck E (1895) Les chétognathes de la baie d’Amboine (voyage de MM. M. Bedot et C. Pictet dans l’archipel Malais). *Revue Suisse de Zoologie et Annales du Musée d’Histoire naturelle de Genève* 3: 137–159. <https://doi.org/10.5962/bhl.part.75137>
- Bieri R (1959) The Distribution of the Planktonic Chaetognatha in the Pacific and their Relationship to the Water Masses 1. *Limnology and Oceanography* 4(1): 1–28. <https://doi.org/10.4319/lo.1959.4.1.0001>
- Bieri R (1974) A new species of *Spadella* (Chaetognatha) from California. *Publications of the Seto Marine Biological Laboratory* 21(3–4): 281–286. <https://doi.org/10.5134/175863>
- Bieri R (1991) Systematics of the Chaetognatha. In: Bone Q, Kapp H, Pierrot-Bults AC (Eds) *The Biology of the Chaetognaths*. Oxford Science Publications, New York, 122–136.
- Bleich S, Müller CH, Graf G, Hanke W (2017) Flow generation by the corona ciliata in Chaetognatha – quantification and implications for current functional hypotheses. *Zoology (Jena, Germany)* 125: 79–86. <https://doi.org/10.1016/j.zool.2017.09.001>
- Bone Q, Pulsford A (1978) The arrangement of ciliated sensory cells in *Spadella* (Chaetognatha). *Journal of the Marine Biological Association of the United Kingdom* 58(3): 565–570. <https://doi.org/10.1017/S0025315400041229>
- Bone Q, Pulsford A (1984) The sense organs and ventral ganglion of *Sagitta* (Chaetognatha). *Acta Zoologica* 65(4): 209–220. <https://doi.org/10.1111/j.1463-6395.1984.tb01042.x>
- Bone Q, Kapp H, Pierrot-Bults AC (1991) Biology of chaetognaths. Distribution patterns in chaetognatha. In: Bone Q, Kapp H, Pierrot-Bults AC (Eds) *The Biology of the Chaetognaths*. Oxford Science Publications, New York, 86–116.
- Burfield ST, Harvey EJW (1926) No. V.-The Chaetognatha of the “Sealark” Expedition. *Transactions of the Linnean Society of London. 2<sup>nd</sup> Series. Zoology (Jena, Germany)* 19(1): 93–119. <https://doi.org/10.1111/j.1096-3642.1926.tb00543.x>
- Chacko PI (1949) Food and feeding habits of the fishes of the Gulf of Manaar. *Proceedings of the Indiana Academy of Sciences* 29(3): 83–97. <https://doi.org/10.1007/BF03049962>
- Chihara M, Murano M (1997) *An Illustrated Guide to Marine Plankton in Japan*. Tokai University Press, 1571 pp.

- Choe N, Deibel D (2000) Seasonal vertical distribution and population dynamics of the chaetognath *Parasagitta elegans* in the water column and hyperbenthic zone of Conception Bay, Newfoundland. *Marine Biology* 137(5): 847–856. <https://doi.org/10.1007/s002270000413>
- Claus C, Grobben K (1905) *Lehrbuch der Zoologie*. Elwert'sche Verlagsbuchhandlung, Marburg, Hessen, 955 pp.
- Conant FS (1896) XXXII. – Notes on the Chaetognaths. *Journal of Natural History* 18(105): 201–214. <https://doi.org/10.1080/00222939608680443>
- Costa A (1869) Di un nuovo genere di Chaetognati. *Annuario del Museo Zoologico della Università di Napoli* 5: e54.
- Dallot S, Ducret F (1969) Un chaetognathe mésoplanctonique nouveau: *Sagitta megalophthalma* sp. n. *Beaufortia* 17(224): 13–20.
- Doncaster L (1902) Chaetognatha, with a note on the variation and distribution of the group. The fauna and geography of the Maldive and Laccadive Archipelagoes 1: 209–218.
- Ducret F (1974) Sur un chaetognathe voisin de *Sagitta tropica* observe en Mer Rouge. *Journal of the Marine Biological Association of India* 16: 161–168.
- Duvert M, Salat C (1990) Ultrastructural studies on the fins of chaetognaths. *Tissue & Cell* 22(6): 853–863. [https://doi.org/10.1016/0040-8166\(90\)90048-E](https://doi.org/10.1016/0040-8166(90)90048-E)
- Feigenbaum DL (1978) Hair-fan patterns in the Chaetognatha. *Canadian Journal of Zoology* 56(4): 536–546. <https://doi.org/10.1139/z78-077>
- Fowler GH (1906) The Chaetognatha of the Siboga Expedition. *Siboga-Esped., Mon.* xxi. 1907. Chaetognatha. *National Antarctic Expedition Natural History* 3: 991–996.
- Francisco PP (1977) Taxonomy of the chaetognaths of the bight of panama. *Anales del Instituto de Investigaciones Marinas de Punta Betín* 9: 225–240.
- Gasmi S, Néve G, Pech N, Tekaya S, Gilles A, Perez Y (2014) Evolutionary history of Chaetognatha inferred from molecular and morphological data: A case study for body plan simplification. *Frontiers in Zoology* 11(1): 1–25. <https://doi.org/10.1186/s12983-014-0084-7>
- George PC (1952) A systematic account of the chaetognatha of the Indian coastal waters, with observations on their seasonal fluctuations along the Malabar Coast. *Proceedings of the National Institute of Sciences of India* 18(6): 657–689.
- Germain L, Joubin L (1912) Note sur quelques Chétognathes nouveaux des croisières de SAS le Prince de Monaco. *Bulletin de l'Institut Océanographique* 228: 1–14.
- Grassi BC (1883) I Chaetognati. *Fauna und Flora des Golfes von Neapel Monograph* 5: 1–126.
- Grigor JJ, Schmid MS, Caouette M, Onge VS, Brown TA, Barthélémy RM (2020) Non-carnivorous feeding in Arctic chaetognaths. *Progress in Oceanography* 186: e102388. <https://doi.org/10.1016/j.pocean.2020.102388>
- Horridge GA, Boulton PS (1967) Prey detection by Chaetognatha via a vibration sense. *Proceedings of the Royal Society of London: Series B, Biological Sciences* 168(1013): 413–419. <https://doi.org/10.1098/rspb.1967.0072>
- Hyman L (1959) The enterocoelous coelomates-phylum Chaetognatha. *The invertebrates: smaller coelomate groups* 5: 1–71.
- Kapp H (1991) Morphology and anatomy. In: Bone Q, Kapp H, Pierrot-Bults AC (Eds) *The Biology of the Chaetognaths*. Oxford Science Publications, New York, 5–17.

- Kassatkina AP (1971) New neritic species of chaetognaths from the Possjet Bay in the Sea of Japan. Zoological Institute Academy of Sciences of the U.S.S.R 8(16): 265–294.
- Kim WR (1987) Taxonomical study on the chaetognaths in Korean waters. Master Thesis, University of Hanyang, Seoul, South Korea.
- Kitou M (1966) A new species of *Sagitta* (Chaetognatha) collected off the Izu Peninsula. La mer: Bulletin de la Société franco-japonaise d'Océanographie 4: 238–240.
- Krohn A (1844) Anatomisch physiologische Beobachtungen über die *Sagitta bipunctata*. Nessler and Melle, Hamburg, Germany, 16 pp. <https://doi.org/10.1080/037454809496523>
- Krohn A (1853) Nachträgliche Bemerkungen über den Bau der Gattung Sagitta, nebst der Beschreibung einiger neuen Arten. Archiv für Naturgeschichte 19: 266–281.
- Kruse S, Brey T, Bathmann U (2010) Role of midwater chaetognaths in Southern Ocean pelagic energy flow. Marine Ecology Progress Series 416: 105–113. <https://doi.org/10.3354/meps08773>
- Lea HE (1955) The chaetognaths of western Canadian coastal waters. Journal of the Fisheries Board of Canada 12(4): 593–617. <https://doi.org/10.1139/f55-031>
- Lee BR, Kim HW, Park W (2016) Distribution of chaetognaths (Aphragmophora: Sagittidae) in Korean waters. Ocean Science Journal 51(3): 447–454. <https://doi.org/10.1007/s12601-016-0040-x>
- Liang TH, Vega-Pérez LA (1995) Studies on chaetognaths off Ubatuba region, Brazil. II. Feeding habits. Boletim do Instituto Oceanográfico 43(1): 35–48. <https://doi.org/10.1590/S0373-55241995000100003>
- Lie AA, Tse P, Wong CK (2012) Diel vertical migration and feeding of three species of chaetognaths (*Flaccisagitta enflata*, *Aidanosagitta delicata* and *Aidanosagitta neglecta*) in two shallow, subtropical bays in Hong Kong. Journal of Plankton Research 34(8): 670–684. <https://doi.org/10.1093/plankt/fbs041>
- Lutschinger S (1993) The marine fauna of New Zealand: Chaetognatha (arrow worms). New Zealand Oceanographic Institute Memoir 101.
- McLelland JA (1989) An illustrated key to the Chaetognatha of the northern Gulf of Mexico with notes on their distribution. Gulf and Caribbean Research 8(2): 145–172. <https://doi.org/10.18785/gr.0802.07>
- Michael E (1908) Notes on the Identification of the Chaetognatha. The Biological Bulletin 15(2): 67–84. <https://doi.org/10.2307/1536091>
- Michael E (1919) Report on the Chaetognatha collected by the United States fisheries steamer “Albatross” during the Philippine expedition, 1907–1910 (Vol. 1). Bulletin - United States National Museum 1(4): 235–277. <https://doi.org/10.5962/bhl.title.17878>
- Michel HB (1984) Chaetognatha of the Caribbean Sea and adjacent areas (Vol. 15). National Oceanic and Atmospheric Administration. Technical Report of National Marine Fisheries Service 15: e25.
- Molchanov LA (1907) Ein Beitrag zur Klassifikation der Chaetognathen. Zoologischer Anzeiger Leipzig 31: 220–222.
- Müller CH, Rieger V, Perez Y, Harzsch S (2014) Immunohistochemical and ultrastructural studies on ciliary sense organs of arrow worms (Chaetognatha). Zoomorphology 133(2): 167–189. <https://doi.org/10.1007/s00435-013-0211-6>

- Müller CH, Harzsch S, Perez Y (2019) 7. Chaetognatha (Handbook of Zoology). Miscellaneous Invertebrates, De Gruyter, Germany, 282 pp. <https://doi.org/10.1515/9783110489279-007>
- Nagai N, Tadokoro K, Kuroda K, Sugimoto T (2006) Occurrence characteristics of chaetognath species along the PM transect in the Japan Sea during 1972–2002. *Journal of Oceanography* 62(5): 597–606. <https://doi.org/10.1007/s10872-006-0079-x>
- Nagasawa S (1976) Identification of young chaetognaths based on the characteristics of eyes and pigmented regions. *Bulletin of the Plankton Society of Japan* 23: 96–106.
- Nagasawa S, Marumo R (1972) Feeding of a pelagic chaetognath, *Sagitta nagae* Alvaríño in Suruga Bay, central Japan. *Journal of the Oceanographical Society of Japan* 28(5): 181–186. <https://doi.org/10.1007/BF02108551>
- Nair VR, Panampunnayil SU, Pillai HU, Gireesh R (2008) Two new species of Chaetognatha from the Andaman Sea, Indian Ocean. *Marine Biology Research* 4(3): 208–214. <https://doi.org/10.1080/17451000701696260>
- Nair VR, Kidangan FX, Prabhu RG, Bucklin A, Nair S (2015) DNA barcode of Chaetognatha from Indian Waters. *Indian journal of Geo-Marine Science* 44(9): 1366–1376.
- Noblezada MMP, Campos WL (2008) Spatial distribution of chaetognaths off the northern Bicol Shelf, Philippines (Pacific coast). *ICES Journal of Marine Science* 65(3): 484–494. <https://doi.org/10.1093/icesjms/fsn027>
- Ohnishi T, Ueda H, Kuroda K (2014) Community structure and spatial distribution of chaetognaths in Tosa Bay on the temperate Kuroshio coast of Japan. *Plankton & Benthos Research* 9(3): 176–187. <https://doi.org/10.3800/pbr.9.176>
- Park JS (1967) Note Sur Les Chaetognathes Indicateurs Planctoniques Dans La Mer Coreenne En Hiver 1967. *The Korean Society of Oceanography* 2(1–2): 34–41.
- Park JS (1970) The chaetognaths of Korean waters. PhD Thesis, Pukyong National University, Busan, South Korea.
- Park JS (1973) The distribution of chaetognaths in the Korea strait and their relation to the character of water masses. *The Korean Society of Oceanography* 8(1): 22–32.
- Park JS, Lee SS, Kang YS, Lee BD, Hun SH (1990) The distributions of copepods and chaetognaths in the southern waters of Korea and their relationship to the characteristics of water masses. *Korean Journal of Fisheries and Aquatic Sciences* 23(3): 245–252.
- Park JS, Lee SS, Kang YS, Huh SH (1991) Distribution of indicator species of copepods and chaetognaths in the middle East Sea of Korea and their relationships to the characteristics of water masses. *Korean Journal of Fisheries and Aquatic Sciences* 24(3): 203–213.
- Park JS, Lee SS, Kang YS, Lee BD, Huh SH (1992) Distribution of indicator species of copepods and chaetognaths in the southeastern area of the Yellow Sea and their relationship to the characteristics of water masses. *Korean Journal of Fisheries and Aquatic Sciences* 25(4): 251–264.
- Peter S, Nair MB, Pillai D (2020) Evolutionary analyses of phylum Chaetognatha based on mitochondrial cytochrome oxidase I gene. *Turkish Journal of Zoology* 44(6): 508–518. <https://doi.org/10.3906/zoo-2004-18>
- Pierce EL (1951) The Chaetognatha of the west coast of Florida. *The Biological Bulletin* 100(3): 206–228. <https://doi.org/10.2307/1538532>

- Pierrot-Bults AC (1974) Taxonomy and zoogeography of certain members of the “*Sagitta serratodentata*-group” (Chaetognatha). *Bijdragen tot de Dierkunde* 44(2): 215–234. <https://doi.org/10.1163/26660644-04402002>
- Pierrot-Bults AC (1976) Histology of the seminal vesicles in the “*Sagitta serratodentata*-group” (Chaetognatha). *Bulletin Zoologisch Museum* 5(4): 19–30.
- Pierrot-Bults AC, Nair VR (1991) Distribution patterns in Chaetognatha. In: Bone Q, Kapp H, Pierrot-Bults AC (Eds) *The Biology of the Chaetognaths*. Oxford Science Publications, New York, 86–116.
- Pierrot-Bults AC, van der Spoel S (2003) Macro zooplankton diversity: How much do we really know? *Zoologische Verhandelingen* 345: 297–312.
- Prado MS (1961) Chaetognatha encontrados em águas brasileiras. *Boletim do Instituto Oceanográfico* 11(2): 31–55. <https://doi.org/10.1590/S0373-55241961000100002>
- Quoy JRC, Gaimard JP (1827) Observations zoologiques faites à bord de l’Astrolabe, en mai 1826, dans le Détroit de Gibraltar. *Annales des Sciences naturelles* 10(1): 5–239.
- Ritter-Záhony R (1908) Chätognathen (Vol. 14). *Denkschriften der Kaiserlichen Akademie der Wissenschaften* 84: 1–18.
- Ritter-Záhony R (1909) Die Chaetognathen der Gazelle-Expedition. *Zoologischer Anzeiger* 34(26): e5.
- Ritter-Záhony R (1910) Die Chatognathen. *Fauna Arctica* 5(1): 249–288.
- Ritter-Záhony R (1911) Revision der Chaetognathan. *Deutsche Sudpolar Expedition 1901–1903*. Band 13, Zoologie 5. Hft. 1: 1–72.
- Russell FS (1936) Observations on the distribution of plankton animal indicators made on Col. ET Peel’s yacht “St. George” in the mouth of the English Channel, July, 1935. *Journal of the Marine Biological Association of the United Kingdom* 20(3): 507–522. <https://doi.org/10.1017/S0025315400058094>
- Slabber M (1769) Natuurkundige verlustigingen, behelzende microscopise waarneemingen van de in-en uitlandse water-en land-dieren. In: J. Bosch (Ed.) *Haarlem*, 1–18.
- Srinivasan M (1979) Taxonomy and Ecology of Chaetognatha of the west coast of India in relation to their role as indicator organisms of water masses. *Zoological Survey of India. Technical Monograph* 3: 1–47.
- Sund PN (1961) Two new species of Chaetognatha from the waters off Peru. *Pacific Science* 15: 105–111.
- Terazaki M (1992) Horizontal and vertical distribution of chaetognaths in a Kuroshio warm-core ring. *Deep-Sea Research. Part A, Oceanographic Research Papers* 39: 231–245. [https://doi.org/10.1016/S0198-0149\(11\)80014-2](https://doi.org/10.1016/S0198-0149(11)80014-2)
- Terazaki M (1998) Life history, distribution, seasonal variability and feeding of the pelagic chaetognath *Sagitta elegans* in the Subarctic Pacific: A review. *Plankton Biology and Ecology* 45(1): 1–17.
- Thomson JM (1947) The chaetognaths of Southeastern Australia. *Bulletin of the Council for Scientific and Industrial Research Melbourne* 222(14): 1–43.
- Tokioka T (1939) Chaetognaths collected chiefly from the Bays of Sagami and Suruga with some notes on the shape and structure of the seminal vesicles. *Records of Oceanographic Works in Japan* 10: 122–150.

- Tokioka T (1940) The chaetognath fauna of the waters of western Japan. *Records of Oceanographic Works in Japan* 12(22): e940.
- Tokioka T (1951) Pelagic tunicates and chaetognaths collected during the cruises to the New Yamato Bank in the Sea of Japan. *Publications of the Seto Marine Biological Laboratory* 2(1): 1–25. <https://doi.org/10.5134/174451>
- Tokioka T (1959) Observations on the taxonomy and distribution of chaetognaths of the North Pacific. *Publications of the Seto Marine Biological Laboratory* 7(3): 349–456. <https://doi.org/10.5134/174631>
- Tokioka T (1965a) The taxonomical outline of Chaetognatha. *Publications of the Seto Marine Biological Laboratory* 12(5): 335–357. <https://doi.org/10.5134/175381>
- Tokioka T (1965b) Supplementary notes on the systematics of Chaetognatha. *Publications of the Seto Marine Biological Laboratory* 13(3): 231–242. <https://doi.org/10.5134/175405>
- Tokioka T, Pathansali D (1963) A new form of *Sagitta bedoti* Beraneck found in the littoral waters near Penang. *Bulletin of the National Science Museum* 33: 1–5.
- Tse P, Hui SY, Wong CK (2007) Species composition and seasonal abundance of Chaetognatha in the subtropical coastal waters of Hong Kong. *Estuarine, Coastal and Shelf Science* 73(1–2): 290–298. <https://doi.org/10.1016/j.ecss.2007.01.011>
- Verrill AE (1873) Report upon the invertebrate animals of Vineyard Sound and the adjacent waters, with an account of the physical characters of the region. United States Commission of Fish and Fisheries, Government Printing Office, Washington, 295–778. <https://doi.org/10.5962/bhl.title.11688>
- Villenas F, Palma S (2006) *Sagitta chilensis* nueva especie de chaetognato en fiordos australes chilenos (Chaetognatha, Aphragmophora, Sagittidae). *Investigaciones Marinas* 34(1): 101–108. <https://doi.org/10.4067/S0717-71782006000100009>
- WoRMS Editorial Board (2022) World Register of Marine Species. <https://www.marinespecies.org> [at VLIZ] [Accessed 2021-12-24] <https://doi.org/10.14284/170>
- Yoo KI (1991) Zooplankton studies of Yellow Sea in Korea. *Yellow Sea Research* (4): 31–37.
- Yoo KI, Kim WR (1996) Spatial distribution of Chaetognaths in the Yellow Sea in the summer. *Korean Journal of Environmental Biology* 14(2): 155–160.
- Yoo KI, Kim WR (1997) Seasonal variation of Chaetognaths off Kori, Korea. *Korean Journal of Environmental Biology* 15(1): 9–17.

